International Atomic Energy Agency

INDC(CPR)-011/GI

INDC

INTERNATIONAL NUCLEAR DATA COMMITTEE

NUCLEAR DATA RESEARCH

IN THE PEOPLE'S REPUBLIC OF CHINA

CONTRIBUTED PAPERS PRESENTED AT THE TOPICAL MEETING DURING THE

16TH INTERNATIONAL NUCLEAR DATA COMMITTEE MEETING

19-23 OCTOBER 1987, BEIJING, PEOPLE'S REPUBLIC OF CHINA

Compiled by
Zhou Delin and Liu Tingjin
CNDC, Institute of Atomic Energy, Beijing, China

March 1988

IAEA NUCLEAR DATA SECTION, WAGRAMERSTRASSE 5, A-1400 VIENNA

INDC(CPR)-011/GI

NUCLEAR DATA RESEARCH

IN THE PEOPLE'S REPUBLIC OF CHINA

CONTRIBUTED PAPERS PRESENTED AT THE TOPICAL MEETING DURING THE

16TH INTERNATIONAL NUCLEAR DATA COMMITTEE MEETING

19-23 OCTOBER 1987, BEIJING, PEOPLE'S REPUBLIC OF CHINA

Compiled by
Zhou Delin and Liu Tingjin
CNDC, Institute of Atomic Energy, Beijing, China

March 1988

Reproduced by the IAEA in Austria
March 1988

88-01186

PREFACE

These proceedings comprise the reports presented orally or distributed in written form during the time of topical discussion on nuclear data activities in China, held at the occasion of the sixteenth INDC Meeting in Beijing. The majority of these reports described the progress of neutron nuclear data measurements in various Institutions except the two comprehensive papers of CNDC and A+M data working groups of CNDC respectively on the nuclear data and A+M data activities in China.

The authers of these reports have been asked to give their measurement results numerically and in more detail than usual as far as possible. It is nice to see that most of them have done so and they have paid more attention to provide the numerical results of their measurements for communication. Thus the space of these proceedings has been extended, in spite of the fact that some reports and even those which have been presented or distributed during the meeting have not been included. And some groups engaged in neutron or charged particle nuclear data measurement or research in IAE and other Institutions have failed to submit report to the meeting.

Zhou Delin

Member of INDC

CONTENTS

Nuclear Data Activities in China

Cai Dunjiu Shi Xiangjun* Yuan Hanrong
Chinese Nuclear Data Center P.O.Box 275(41), Beijing, China

1. Introduction

In China, the scientific research on nuclear physics started in the late 1950's. At that time a research reactor and some accelerators were built in the Institute of Atomic Energy, Beijing, and some nuclear data measurements were carried out. As to the nuclear data compilation and evaluation, it started systematically just in 1975, when the Chinese Nuclear Data Center (CNDC) and the Chinese Nuclear Data Coordination Network (CNDCN) were set up in order to meet the requirements of development of nuclear energy, nuclear science and engineering technology. Since China was non IAEA member at that time, we could get only very few evaluated data from abroad publications, we had to do evaluation ourselves to serve our users, many experimental and theoretical nuclear scientists were involved in the related work, including developing theoretical models, writing calculation codes and performing nuclear data evaluation, etc.

This situation has been changed since the CNDC started to make contacts with IAEA/NDS, JAERI/NDC and BNL/NNDC in 1980. Especially, since the People's Republic of China became an IAEA member in 1984, the international cooperation and exchange have obviously increased between the CNDC and other nuclear data centres. For example, we have participated in the evaluation and compilation of neutron data, structure and decay data, fission product yields and charged particle data under international cooperation, and some coordinated research programmes under the IAEA contracts. We have got whole sets of evaluated neutron data of ENDF/B-4, ENDL, JENDL-2, INDL/V and quite a lot of EXFOR experimental data as well as some programmes from IAEA/NDS and OECD/NEADB. We have also sent some neutron data evaluated or measured in China to IAEA/NDS and several codes to NEA Data Bank. It is clear that the international cooperation and exchange have promoted the

*The report was presented by Dr. Shi Xiangjun, one of the authors, in the 16-th INDC Meeting in Beijing on 19, Oct. 1987.

nuclear data activities in Cnina and also become a proper approach for us to make contributions to the international nuclear data activities.

Afterwards, according to the needs of nuclear data for both home and abroad we will do our best in nuclear data activities to make more contributions.

2. Organizations and Objectives

2.1 Chinese Nuclear Data Center (CNDC)

As mentioned above, the Chinese Nuclear Data Center was founded in 1975 by the Ministry of Nuclear Industry. At present, the CNDC has about 30 scientists and a number of support staff, and is equipped with a PDP 11/70 computer.

The principal task of the CNDC is to function as a national center for generating, collecting, processing and disseminating nuclear data, to provide services to all nuclear data users in China, and to coordinate nuclear data activities on a national scale.

So far the CNDC's activities have mainly involved the following respects:

- working out a countrywide, long-term plan on nuclear data measurement and evaluation; arranging and coordinating nuclear data activities of the CNDCN;
- studying and developing nuclear data evaluation methods; coordinating and supervising data evaluators; compiling and evaluating nuclear data;
- collecting and validating data processing programmes, reports and recommended data from the network;
- maintaining and developing the Chinese Evaluated Nuclear Data Library (CENDL);
- performing benchmark testing of CENDL and generating multigroup constants for users;
- maintaining the data base of internationally available nuclear data files; providing selective retrievals and data processing to users;
- providing nuclear data and computer program services; publishing nuclear data reports and other publications;

____ convening national nuclear data meetings;

____ coordinating cooperation and exchange in the nuclear data field with other national and international nuclear data organizations.

2.2 Chinese Nuclear Data Coordination Network (CNDCN)

The CNDCN is composed of the institutes and universities which are taking up nuclear data measurement and evaluation. It is organized and coordinated by the CNDC. At present, the network has about 20 members. The following list shows the main 12 institutions in the network which have participated in the nuclear data activities for many years.

Institution	City
Beijing University	Beijing
Qinghua University	Beijing
Beijing Normal University	Beijing
Sichuan University	Chengdu
Fudan University	Shanghai
Jilin University	Changchun
Nankai University	Tianjin
Wuhan University	Wuhan
Lanzhou University	Lanzhou
Institute of Nuclear Research	Shanghai
Institute of Applied Physics and Computational Mathematics	Beijing
Institute of Atomic Energy	Beijing

All the network members undertake their projects according to the nuclear data plan and their own capacity and conditions under the guidance of the CNDC. The measured or evaluated data are provided to the CNDC. Of course, all the members of the CNDCN get some financial support from the Ministry of Nuclear Industry.

2.3 Working Groups

In order to assist the CNDC in its primary task on a national scale, some working groups on the following specialities were organized.

- Nuclear Data Measurement
- Theoretical Calculation of Nuclear Data
- Neutron Nuclear Data Evaluation
- γ-Production Data
- Construction of Chinese Nuclear Data Library (CENDL)
- Group Constant Generation and Benchmark Testing
- Nuclear Data processing and computational program
- Nuclear Structure and Decay Data
- Charged particle Nuclear Data
- Fission Product Yield Data
- Neutron Resonance Parameter and level Density
- Atomic and Molecular Data (1986)

The members of these groups come from CNDC and network institutions.

The function of working groups is as follows:

- To search the proper way or method to perform the given task;
- To hold symposiums in order to exchange experiences or discuss common problems appearing in the activities;
- To examine, review and recommend the data from the network.

2.4 China Committee of Nuclear Data (CCND)

In order to strengthen the guidance of nuclear data activities in China, the China Committee of Nuclear Data was established at the end of 1986.

- It is a professional consultative organization under the leadership of the leading body responsible for nuclear data research work in China.
- It attaches importance to the investigation of the urgent demands for nuclear data in atomic energy, nuclear science

and nuclear engineering technology development, and to the better understanding of the progress and achievements made in the field of international nuclear data activities.

- It is responsible for the examination of the nuclear data longterm programme and phase plans, and offers key task projects and proposals of different kinds to the leading body for consideration.
- It helps the leading body to examine and approve the important progress and achievements made in nuclear data research.
- It plays its own role in such fields as external relations, nuclear technical and academic exchange at home and abroad, and takes vigorous action to promote the mutual relation, intercourse and cooperation with the organizations of the same occupation, at home and abroad.

3. Progress in nuclear data measurements

Nuclear data measurements have been carried out since early 1960's in China. Now, some equipments for nuclear data measurement have been built. The main facilities are listed in table 1.

The measurement program is focussed on the nuclear data of key importance for nuclear energy and nuclear technology applications, such as neutron induced nuclear fission (including fission cross section, fission neutron number, fission neutron spectra, fission product yields), fast neutron spectroscopy (including angular distribution of scattered neutrons, double differential cross sections and secondary neutron energy spectra from neutron induced reactions), fast neutron reaction(including (n,n'), (n,2n), (n,p), (n,d), (n,α) reaction cross section, radiative capture γ and γ-ray production cross sections), charged particle nuclear reaction and nuclear decay etc.

Recently, we have participated in the International Fluence-Rate Intercomparison and the following CRP organized by IAEA:

- Measurement and analysis of 14 MeV neutron nuclear data needed for fission and fusion reactor technology.
- Measurement and analysis of double-differential neutron emission spectra in (p,n) and (α,n) reactions.

Table 1.

Unit	Main Facilities	Research Subjects
IAE	600KV Cockcroft-Walton(200-500KV) 2.5 MV Van de Graaff (0.3-2.5MV) AVF Cyclotron (E_p~3-15MeV, E_d~4-14MeV, E_α ~ 8-28MeV) HI-13 Tandem (HVEC, 3-13MV, ±1KV, provide p,d,α .....heavy ion) Heavy Water Reactor (15MW, 2.8×10^{14}n/sec, cm^2) Swimming Pool Reactor (4000 KW)	Fission Process study Fast neutron spectroscopy Fast neutron reaction Nuclear structure and decay A+M Light and heavy ion nuclear reaction Application of nuclear technique
Institute of Nuclear Science and Technology of Sichuan University	Cockcroft-Walton (400KV; 200KV, ~5ns) 2.5MV Van de Graaff (~1ns) Cyclotron (ϕ1.2M, E_d ~12MeV)	Fast neutron scat. angular distr. Neutron capture γ-ray Charged particle reaction, A+M
Peking University	4.5MV VDG (1-2ns, 0.3-4.5MV, provide p,d,α ,.....Ar, will be operated in 1988) Tandem 2x7MV (EN-18, 0.5-6.5MV, will be operated in 1988) 2x1.7MV (NEC, 5SDH-2)	Nuclear reaction & nuclear structure Nuclear fission Material Science, Atomic collision Heavy ion reaction

Unit	Main Facilities	Research Subjects
Qinghua University	200KV Cockcroft-Walton	Fast neutron scat. & reactions
Beijing Normal University	400KVC-W with post helix acceleration	Fast neutron spectra & γ production
Institute of Nuclear Research in Shanghai	4MV VDG(NEC, $E_p \sim 0.3$-4MV, ± 1KV) Tandem 2x6MV (indigenously designed, under construction) AVF Cyclotron (ϕ1.2M, $E_p \sim 3$-30 MeV, d, α, ...heavy ion)	Application of nuclear technique In-beam γ-spectroscopy Light ion & charged particle nuclear reaction
Fudan University	2.5 MV VDG Tandem 2x3 MV (NEC, is being installed)	Application of Nuclear technique Fast neutron reaction, A+M

3.1 Fission Neutron Spectrum

— The prompt neutron spectrum from the spontaneous fission of ^{252}Cf has been measured in the 0.9 MeV to 14.5 MeV region using the time-of-flight method. The data were fitted with the Maxwellian distribution and the result of T=1.418±0.15 MeV was obtained.[1,2]

Recently we concentrate our attention on the study on low energy part of the spectrum. A flight path of 35 cm was used for the experiment. The neutron detector was a thick lithium glass scintillator (9 mm). A low-mass, fast ionization chamber (1.65 g) was used as fragment detector. The detection efficiency for fission fragments was approximately 98.2%. The final result will be given after calibrating of the neutron detector efficiency.[2]

— The neutron spectrum of thermal neutron induced fission of ^{235}U has been measured for the 0.6 MeV to 16 MeV neutrons using the time-of-flight method at heavy water research reactor. We found that the experimental data over the full energy range could not be described by a Maxwellian distribution.

— We are also preparing the measurement about the neutron spectra from fission of ^{238}U induced by about 9 MeV neutrons at HI-13 tandem accelerator.

Fission Neutron Number

The neutron emission probabilities for long range alpha(LRA), helium-3, triton and proton accompanied fission of ^{252}Cf were measured in a three parameter experiment in which a liquid scintillation detector and a semiconductor telescope were used to record the number of prompt neutrons and the energy of light charged particles. The average number of neutrons per fission for LRA, He-3, triton and proton are equal to 3.13±0.02, 3.09±0.09, 2.95±0.05 and 3.24±0.07, respectively. The $p(\nu)$ distribution for binary fission and triton and LRA accompanied fission and the dependences of $\bar{\nu}$ on light particle's energy E_α and E_t were obtained.

3.2 Fission Cross Sections

For past years, the fission cross sections for several actinide nuclides, such as $^{233,235,238}U$, ^{237}Np and ^{239}Pu, have been

measured for some neutron energy regions including thermal neutron, 0.03 -1.5 MeV, 3-6 MeV and 14-18 MeV neutrons which are available at IAE. The relative and absolute measurement techniques have been developed. An accuracy of 2% for absolute measurements has been achieved.

Recently, we have measured fission cross sections of ^{235}U and ^{239}Pu as well as fission cross section ratio of ^{238}U to ^{235}U around 14 MeV neutron energy by means of the time correlated associated particle (TCAP) technique and using T(d,n) ^{4}He reaction.[3] In this method, the neutron flux was precisely determined by counting the associated alpha particle; the background of fission events coming from scattered and thermal neutrons could be minimized. So the uncertainties of the measured fission cross sections may be reduced to about 1%.

The measured results are listed as follows:

En, MeV	$\sigma_f(^{235}U)$	$\sigma_f(^{238}U)/ f(^{235}U)$
14.2	2.078±0.04 b	
14.7	2.098±0.04	0.565±0.014

3.3 Fission Product Yields

Some measurements for fission yields were performed at the IAE.[4] Radiochemistry method and γ-ray spectrum method were set up for these measurements successively. The fission rate was determined accurately with double fission chamber, so we can obtain absolute fission yield data. However, for Cf-252 measurement, the absolute fission rate was obtained with catcher foil technique for the first time. Most products can be determined by γ-ray spectrum method, but some yields of two wings and valley region were measured by radiochemistry method. Then we are able to obtain more absolute yields, more complete mass distribution curve and some mass distribution characteristics. The precision of yield data is 3 % to 10 % for peak yields, and 5 % to 25 % for valley yields.

Following fission systems have been determined for several years: the fission of U-235 induced by thermal neutrons, fission

spectrum neutrons and 14.9 MeV neutrons; the fission of U-238 induced by 3.0, 5.0, 8.3 and 14.9 MeV neutrons; and Cf-252 spontaneous fission. Some of the mass-yield curves obtained are shown in Fig.

3.4 Differential and double differential neutron cross sections

— IAE Three fast neutron TOF spectrometers for this purpose have been built at the cyclotron, cockcroft-walton and tandem accelerators respectively.[1]

Neutron scattering angular distributions of D, Li, Be, B, C and ^{238}U and neutron emission spectra of D and ^{238}U have been measured at 14 MeV, using the α-particle associated TOF spectrometer.[5]

At the cyclotron, a deuterium target was built and the D + D reaction neutron source and other reactions were studied. Neutron scattering angular distribution measurement was carried out on C, D, ^{6}Li, ^{7}Li etc.

At HI-13 tandem accelerator, we plan to measure double differential neutron emission cross sections in the neutron energy range 8-13 MeV and of the (p,n) reactions.

— INST (Institute of Nuclear Science and Technology, Sichuan University) Measurements of differential elastic scattering cross sections (including small-angle elastic scattering) of fast neutrons on some nuclides have been carried out using 400 kV Cockcroft-Walton and 2.5 MV VDG accelerators.[6]

- The 14.7 MeV neutron elastic scattering differential cross sections of U, Pb, Fe, Al, C and Be have been measured in the angular range 2.7-9.9 degrees using a fast neutron position-sensitive spectrometer and associated particle TOF method. The detector consisted of a ST-1701 liquid scintillator, with both end-faces in optical contact with two photomultiplier tubes. The position of incident neutrons is determined by time difference between signals from the photomultiplier tubes. The time resolution of the system is 0.87 ns. From the experimental results no evidence for the "anomalies" has been found at the smallangle range.

Similar conclusion was obtained in measurements of 14.2 MeV neutron scattering from Al, Ti, Fe, Cu, Mo, Cd, W, Pb, Bi and

U at small-angle range, using a usual neutron detector and associated particle TOF method.

- Differential elastic scattering cross sections of the fast neutrons from Molybdenum, Niobium (En = 14.2 MeV, $\theta = 5^{o}-150^{o}$), Tungsten (En=14.7 MeV, $\theta=45^{o}-150^{o}$) and Nickel (En=1 MeV, $\theta=20^{o}-150^{o}$) have been measured also.

3.5 Neutron Reaction Cross Sections Measured with Activation Method

The reaction cross section measurements with activation method for (n,γ), (n,n'), (n,p), (n,2n) processes on more than 30 nuclides have been performed[1]. The measurements of the radioactivity were carried out with a calibrated 80x80 mm NaI(Tl), or a 136 cm^3 Ge(Li) detector. The main points of measurement are summarized as follows:

Reaction	Neutron energy, MeV	Measured nuclides
n,r	0.1-1.5	^{139}La, ^{152}Sm, ^{180}Hf, ^{193}Ir, ^{194}Pt, ^{197}Au
n,n'	threshold-5.5	^{87}Sr, $^{113,115}In$, ^{195}Pt
n,p	threshold-18	^{24}Mg, $^{46,48}Ti$, $^{54,56}Fe$, ^{58}Ni, $^{85,87}Rb$, ^{115}In, ^{140}Ce, ^{181}Ta
n,d	threshold-18	^{58}Ni
n,α	threshold-18	^{27}Al, ^{51}V, ^{54}Fe, ^{59}Co, ^{85}Rb, ^{93}Nb, ^{115}In
n,2n	threshold-18	^{45}Sc, ^{55}Mn, ^{59}Co, ^{58}Ni, $^{85,87}Rb$, ^{89}Y, ^{90}Zr, ^{93}Nb, $^{113,115}In$, ^{126}I, $^{136,138,140,142}Ce$, ^{169}Tm, ^{181}Ta, ^{196}Pt, ^{197}Au

Reaction	Neutron energy, MeV	Measured nuclides
n,3n	threshold-18	^{169}Tm, ^{197}Au
σ_m/σ_g	threshold-18	^{44}Sc, ^{112}In, ^{133}Cs

As examples, the isomeric cross sections for ^{115}In (n,n') ^{115m}In and ^{115}In (n,2n) ^{114m}In reactions around 14 MeV neutron energy are shown in Fig.[7]

3.6 Neutron Radiative Capture γ and γ-ray Production Data

In recent years, IAE, ILENP (Institute of Low Energy Nuclear Physics, Beijing Normal University) and INST (Institute of Nuclear Science and Technology, Sichuan University, Chengdu) are engaged in the measurements of the neutron radiative capture γ and γ production data, including discrete and high energy γ-rays from (nth, γ) and (n,xγ), (n, γ) processes at the neutron energy of $\sim$14 MeV.

— γ-ray production data

• IAE The γ-rays of some nuclides (n,xγ) reactions at 55° were measured at the cockcroft-walton accelerator by a complete shielded 70 cc Ge(Li) and 67.5 cc HPGe(n) detector using the associated particle gated timing method.[8] The integrated cross sections which are listed in the following are deduced by $4\pi\frac{d\sigma}{d\Omega}(55^{\circ})$

Nuclides	^{56}Fe	^{58}Ni	^{60}Ni	^{63}Cu	^{65}Cu	^{209}Bi
$\sigma_{n,n'r}$,mb	613±48	320±30	766±72	596±64	463±46	295±30

• ILENP The pulsed fast neutron time of flight facility at Cockcroft-Walton accelerator is used to discriminate the scattering neutron events. Discrete γ-ray spectra and production cross sections for 14.9 MeV neutrons with ^{12}C, ^{27}Al, ^{51}V, ^{56}Fe, ^{59}Co, ^{93}Nb at 90° have been measured, and angular distributions of the discrete γ-ray spectra are being measured.[9]

— Neutron radiative capture γ

. IAE The γ-ray spectra from ^{23}Na, ^{27}Al, ^{31}P, ^{32}S (nth, γ) reactions have been measured with the reactor thermal neutron source, high-pure thermal neutron beam filter and a three crystal pair spectrometer. The cross sections are 529±26 mb for ^{32}S(nth,γ) and 180±6 mb for ^{31}P (nth, γ), respectively.

The radiative capture γ-ray data (Er > 14.2 MeV) from ^{56}Fe, $^{238}U(n,\gamma)$ at E_n = 14.2 MeV are measured with a ϕ20x10 cm NaI (Tl) detector. The cross section are 790±130 μb for $^{56}Fe(n,\gamma)$ and 1080±180 μb for $^{238}U(n,\gamma)$, respectively.

. INST The neutron caputure cross sections of Nb, Tm, and Ta at 120° were measured in the 10-100 KeV neutron energy range, (at 2.5 MV VDG pulsed accelerater, by two Moxon-Rae detectors with graphite converters).[10]

The neutron capture cross sections for Nd, Sm, Gd, Tb, Dy, Tm, Yb, Hf, Ta and W have been measured using a large liquid scintillator and TOF technique in the 0.34-1.68 MeV neutron energy range.[10]

— We have built up a γ-ray goniometer at HI-13 accelerator. The anticoincidence shielded large NaI(Tl) γ-spectrometer has a good energy resolution (less than 5% at E_r = 20 MeV) and high efficiency, and a 130 cc HPGe(n) detector will be used.

3.7 Absolute Measurement of Neutron Fluence and Energy

The accurate measurements of fast neutron fluence and neutron source emission rate are of importance for absolute nuclear data measurement. Some methods for that, such as proportional counter, proton recoil telescope, associated particle method, standard long counter and activation foil have been developed. In recent years, we have participated in the international intercomparisons of neutron fluence (at 144 KeV, 565 KeV and 14 MeV), neutron source emission rate and neutron energy which were organized by BIPM.[11] The results are listed as follows:

Neutron energy MeV	Method	Uncertainty %	Deviation between our result & international average value %	
0.1-0.5	H_2 proportional counter	±1.8	~ 0	(1985)
0.5-1.5	CH_4 proportional counter	±1.8	< +1.8	(1985)
1.5-5	Semiconductor telescope	±1.9	~ -0.3	(1985)
14	associated particle proton recoil telescope	±1 ±1.9	< -0.6	(1982)
12-18	Relative to ^{27}Al (n, α), ^{56}Fe (n,p)			
Neutron source $5x10^4$-$1x10^8$ n/s	circulating manganese bath	±1	-0.585	(1984)

4. Activities on Nuclear Data Evaluation

4.1 Nuclear Data Evaluation

According to the long-term plan on nuclear data evaluation many experimenters from the network institutions, such as Sichuan University, Qinghua University, Beijing University, Beijing Normal University, Lanzhou University and the IAE, have been engaged in the compilations and evaluations of neutron data for general purpose, nuclear data for special purposes and the studies on the evaluation methods.

4.1.1 Neutron Data for general purpose

Up to now, the neutron data including file-1 to file-5 for 36 nuclides (or elements) have been evaluated in the ENDF/B-4 format. All evaluated data make up the first version of the Chinese Evaluated Nuclear Data Library (CENDL-1)[12] and are stored on magnetic tapes. The evaluated nuclides include H, D, T, ^{3,4}He, ^{6,7}Li, ^{9}Be, ^{10,11}B, N, O, ^{19}F, ^{23}Na, Mg, ^{27}Al, Si, V, Cr, Fe, Ni, Cu, Zn, Zr, Nb, Mo, Sn, Hf, Ta, W, Au, Pb, ^{235,238}U and ^{239,240}Pu. The incident neutron energy range of the evaluated data is from 10^{-5} to 2×10^{7}eV.

The evaluations for some other structural material elements, such as P, S, Ca, Ti, Mn, Co, Ag, Cd, In and Sb have also been finished. The data will be included in the new version of CENDL.

Besides, under the cooperation with a Japanese Scientist a CNDC's staff evaluated the neutron data of ^{107,109,Nat}Ag (file 1-5, 13-15) for JENDL-3 at the beginning of 1987 at JAERI.

4.1.2 Nuclear Data for Special Purposes

a) Charged Particle Nuclear Data (CPND)

The evaluation of the CPND was started in 1975. In 1983, a CPND group was organized. Its members are from the IAE, the Institute of Applied Physics and Computational Mathematics, Sichuan University and the Institute of Nuclear Research in Shanghai. By July of 1986, this group had collected the measured data for about 16 reactions performed in China and compiled them in the EXFOR format. The group has also developed a simple program for checking the EXFOR entries. In order to develop international cooperation this group has joined the activities of the IAEA/NDS coordinated network of CPND centres since 1985.

b) Actinide Nuclear Data (AND)

Some transplutonium nuclear data had been evaluated and compiled before 1985 and a report of CNDC-85012 was published. Since 1985, the CNDC has participated the IAEA/NDS coordinated research program on the "Validation and Benchmark Testing of Actinide Nuclear Data". The neutron data evaluation for ^{249}Bk and ^{249}Cf have been finished. The evaluation of the neutron capture cross sections of ^{241}Am is being undertaken.

c) Fission Product Yield Data (FPYD)

A group at IAE is engaged in FPYD measurement and evaluation. Before 1981, three versions of "Evaluated Fission-Product Yield" had been issued.

On the basis of IAEA/NDS' suggestion, this group has continued to develop the Rider and Crouch FPYD libraries, abiding by the IAEA/NDS suggestions to issue a compilation of recommended values similar to the well-known Meek and Rider file at regular intervals.

Since 1985, this group has been devoting itself to the project of setting up a fission product yield library. In the first phase of the project, top priority was given to the following 10 fission systems: U235T, U235F, U235HE, U238F, U238HE, Pu239T, Pu239F, Pu241T, U233T, Th232F.

Up to now, the 10 sets of fission yield data evaluation have been completed. The recommended values have been edited in the ENDF/B-5 format and in a "people-readable" format. The first set of recommended FPYD values has been transmitted to the IAEA/NDS.

The recommended values of the thermal fission of ^{235}U and ^{239}Pu have been tested and compared with ENDF/B-VE by Dr. T. R. England (LASL) through calculating the decay powers. The results are satisfactory.

d) Nuclear Structure and Decay Data (NSDD)

Initiated by the visit of Dr. S. Pearlstein, Director of the Brookhaven Nuclear Data Center, USA, in 1981, the CNDC has participated in the international effort on NSDD evaluation. Accordingly, ten mass chains were permanently assinged to China (A=51-56, 195-198). The Chinese NSDD evaluation group was formed

in 1983 and the members are from IAE, Jilin University, Changchun, and the Institute of Nuclear Research in Shanghai.

Up to now, the evaluation for mass chains of A=51, 54, 55, 56, 170, 172 has been finished and published with the help of the NNDC; work on the evaluation of mass chains of A=52, 195 and 196 is in progress.

4.1.3 Evaluation Methods

To improve evaluation, some evaluation methods have been developed or are being developed, such as

a) Data processing methods

- Curve fitting:a spline fitting program for multi-sets of data has been written, with which the knots can be optimized and spline order number can be chosen;
- "Union adjusting" (to make all cross sections consistence for one nuclide or material):
  * single energy point union adjusting based on Bayes principle;
  * spline fitting for multi-curves;
- Simultaneous evaluation for several nuclides (materials) based on spline fitting for multi-curves.

b) Covariance processing methods

- Calculation of covariance matrix for experimental data using the information about errors in experiments given by authors. The program is being coded.
- Covariance propagation in data evaluation processing, including curve fitting, union adjusting. The programs have been finished. Some primary results have been got. Now the programs are being improved and will be used in more realistic case;
- Simplification of the methods to deal with experimental data with covariance. Some primary results have been got;
- Calculation of covariance matrix between different nuclides (which are relative to each other in experimental measurements). The study in physics has been finished. The program is being written.

In fact, our efforts in this field have been made for years. But so far only some primary results have been got, we still have a lot of work to do and a long way to go.

c) Systematics Studies

Systematics studies on the excitation functions of the (n,2n), (n,3n) as well as (n,x) (x=p,d,t and ^{3,4}He) reactions have been performed. The parameterized formulae and all the parameters related have been obtained on the basis of the evaporation model with preequilibrium mechanism and the collected data for A=25-200 in the neutron energy range of from threshold to 25 MeV.

With the formulae and parameters, the excitation function could be predicted more reliable than before for the energy regions or nuclides not measured heretofore.

Recently, the systematics study on the (n,γ) reaction cross sections has also been performed.

4.2 Theory Research and Nuclear Data Calculation

As we know, in nuclear data evaluation the theoretical calculation plays an important role. Since the CNDCN was formed many theorists in the CNDCN have been engaged in the study of applications of various kinds of nuclear reaction theories and models, developing computer codes and performing theoretical calculations of nuclear data.

The main theories and methods applied for calculations of neutron nuclear data are shown in the following list:

In statistical theory calculations, the calculated results are very sensitive to the level density and its parameters, so that some efforts were made in this field and a new set of level density parameters in the Gilbert-Cameron formula has been gained based on more accurate data which were obtained in recent years.

To improve the agreement between calculated results and experimental data of double differential cross sections the effects of the Fermi Motion and the Pauli Principle were first taken into account in the exciton model by our theorists. This physical consideration has been accepted by some colleagues in the world.

At present, an unified preequilibrium and equilibrium model with conservation of angular momentum is being developed under an IAEA contract.

Apart from these, some studies on underlying theory have also been carried out in the CNDCN. For instance, some encouraging results have been reached in the study on the microscopic theory

Theory	Target	Institution
Phase Shift Analysis	H, D	Fudan Univ.
Faddeev Equation	D	CNDC
Resonance Group Theory	^{3}H, ^{3}He	Inst. of Nucl. Resea.
R-Matrix Theory Optical Model Hauser-Feshbach Theory DWBA	^{6}Li, ^{7}Li	Jilin Univ.
Quasifree Scattering	^{9}Be	Inst. of Appl. Phys. and Comput. Math.
Optical Model Hauser-Feshbach Theory with WFC Evaporation Model Preequilibrium Exciton Model DWBA Couple Channel Calculation	structural and fissionable nuclei	CNDC Nankai Univ. Wuhan Univ. Beijing Univ.

of the nuclear optical potential and the study on the fission mechanism. The study on new sets of nucleon-nucleon interaction of rank-1 and rank-2 separable types through fitting 2-body and 3-body data is in progress in order to improve calculations of few-body reaction data.

On the basis of theory research mentioned above many computer codes for data calculations have been developed. Three of them have been sent to NEA Data Bank. Now some important codes are being revised or standardized.

4.3 Multigroup Constant Generation and Benchmark Testing of Nuclear Data

A group responsible for the generation of multi-group constants and benchmark testing of nuclear data was formed in 1978. Since then, the main efforts of this group have been made in developing computer programmes.

Up to now, the group has developed or implemented the following programs for multigroup cross section generation:

— RQCS, a program to calculate multigroup constants for thermal fission reactors. It generates group constants for MUFT and GAM. (1980)

— KQCS, a fast reactor multigroup constant program based on the Bondarenko method, which adjusts group constants to temperature and composition of the reactor. (1982)

— NGCPS, a group constant generation system for fast reactor and shielding calculation;

— LEK, a format transform program to match the ENDF/B-4 data file with the KQCS program;

— AMPX-2, a large modular nuclear data processing program, which was obtained from ORNL/RSIC. It has been implemented on the IBM-3031 computer (1986);

— NJOY, another large modular nuclear data processing program, which was obtained from NESC at ANL(USA). It has been implemented on the CYBER 170/825 at the IAE(1986).

With these programs the CNDC can provide various types of input data for nuclear power reactor design calculations and shielding analysis. The calculations of multigroup cross sections for nuclear power reactor, fast reactor and fusion research already started.

As to the benchmark testing, the following programs have been written or implemented:

— FEONAN, which can be applied to calculate the uncollided transmitted neutron spectra and check total cross sections using the Broomstick experiments performed at ORNL;

— NDP, one-dimensional diffusion program, which can be applied to calculate effective multiplication factors, spectrum indexes, and critical dimensions for reactors;

— TDBDC, two-dimensional diffusion and burnup program, which can be used for fast reactor analysis;

— PETRC, a pertubation reactivity coefficient program, which can be applied to calculate one-dimensional or two-dimentional systems;

— DTF4C, one-dimensional discrete ordinate Sn program, which is a version of the US DTF4 program;

— ONEDANT, one-dimensional discrete ordinate Sn program, which uses the Synthetic Diffusion Method (SDM) allowing for effective accelerated convergence (1986).

The checks of total cross sections for Fe, O, Na and N elements of CENDL-1 have been performed using programm FEONAN.

4.4 Nuclear Data and Program Library

In the CNDC there is a library group, which is responsible for the nuclear data library and the associated computer program library.

At present the group has the following main tasks:

— to prepare and maintain the Chinese Nuclear Data Library (CENDL);

— to collect evaluated nuclear data and computer programs prepared by other centers;

— to improve or develop the library management program system, data processing programs and evaluation system; to make complete evaluations of specific nuclides;

— to collect, compile and evaluate A+M data and establish an A+M data library under cooperation with the A+M data working group;

— to issue nuclear data publications;

— to provide nuclear data and program services to Chinese Users and exchange them with IAEA/NDS and other centers;

— to operate, maintain and manage the computer PDP 11/70.

5. Development for future

As concerns the nuclear data activities in China in future the first important objective is still to satisfy the requirement of the development of nuclear energy as well as the application of nuclear technology in our country.

As a matter of fact, in the early 1970's our country had a research project on fast breeder reactor and fusion research. However, the project was not made an expected progress for some reasons. Recently the fast reactor and fusion research project has been resumed and reinforced, and a plan for developing hybrid reactor has also been worked out.

In order to meet the needs of nuclear data and A+M data for the plans mentioned above, the nuclear data activities must be further developed in our country. Under the CCND's suggestion, the future project of the CNDC's activities is mainly as follows:

a) to update the evaluated neutron data library for general purpose through:

— reevaluating some important nuclides,

— adding some other selected nuclides after analysing and reviewing the existing evaluations made by other centres, etc;

b) to extend the evaluation of nuclear data for special purposes, such as charged particle nuclear data, neutron dosimetry and activation reaction data;

c) to collect and compile A+M data and build up a corresponding A+M data library. The first step is to collect and compile the existing bibliographic and numerical data as well as calculate and measure some of A+M data;

d) to make benchmark testing on some important evaluated nuclear data;

e) to improve and complete theoretical calculation codes, evaluation and data processing systems to improve the quality of evaluated data.

Apart from these, our center and network would like to develop international cooperation and exchange activities more actively. At present we are participating in some CRP activities as mentioned at the beginning. It is expected that we shall make more contributions to the existing and new CRP activities. On the other hand, we wish to strengthen bilateral cooperations with other centres or foreign institutions. It is planned to evaluate neutron data of O and F elements for ENDF/B-6 under the cooperation between the CNDC and the NNDC (actually, the LASL and ORNL). We are sure that this kind of cooperation activities is profitable for both participating sides.

Finally, on behalf of CNDC we wish to take this opportunity to express our gratitude to IAEA and other centers as well as all old and new foreign friends for their contributions to promote their cooperations with the CNDC in nuclear data activities.

Reference

(1) Tang Hongqing, Neutron Nuclear Data Measurement in IAE, This Proceedings.

(2) Meng Jiangchen, Li Anli et al., Chinese Journal of Nuclear Physics 2,163(1981) and 4, 145(1982);

Meng Jiangchen et al., Chinese Journal of Nuclear Physics, 4, (1987);
Han Hongyin et al., Chinese Journal Nuclear Physics, 4, 289(1985).

(3) Li Jingwen et al., Fission Cross Section Measurements Around 14 MeV, INDC(CPR)-009/L, August 1986.

(4) Li Ze et al., Measurement of fission product yields, This Proceedings;
Li Ze et al., Chinese Journal of Nuclear Physics, 5, 226(1983);
Li Ze et al., Chinese Journal of Nuclear Physics, 7, 97(1985).

(5) Shen Guanren et al., Chinese Journal of Nuclear Physics, 8, 289(1986) and 6, 193(1984).

(6) Cao Jianhua et al., Neutron Nuclear Data Measurement in Sichuan University, This Proceedings.

(7) Lu Hanlin et al., This Proceedings;
Fan Peiguo et al., Chinese J. Nucl. Phys. 2, 337(1980);
Lu Hanlin et al., A. E.Sci.and Technol., 2, 113(1975). (in Chinese)

(8) Shi Xiamin, Wu Yongshun et al., Proceedings of the International Conference 6-10 September 1982 Antwerp, p373, Chinese Jounal of Nuclear Physics, 4, 121 and 299(1982).

(9) Zhou Hongyu et al., INDC (CPR)-010/L, November 1986;
Yan Yiming et al., On Some Results of the Measurements of the Angular Distributions of Separated γ-ray Production Cross Sections from Reactions (n,xr) for ^{51}V Induced by 14.9 MeV Neutrons, This Proceedings.

(10) Xu Haishan et al., Fast Neutron Capture Cross Sections of Tm-169 and Ta-181 from 1.0 to 1.5 MeV, This Proceedings;
Xia Yijun et al., The Neutron Capture Cross Sections of ^{93}Nb, ^{169}Tm and ^{181}Ta in the energy range from 10 to 100 keV, This Proceedings.

(11) V. E. Lewis, International Intercomparison of T+d Neutron Fluence and Energy Using Niobium and Zirconium Activation (NPL, UK);
T. B. Ryves, International Fluence-rate Intercomparison for 144 and 565 keV Neutrons (NPL, UK);
E. J. Axton, Results of an Intercomparison of Neutron source Emission Rates (1979-1984) CCEMR1 (III)/85-2.

(12) Cai Dunjiu et al., Chinese Evaluated Nuclear Data Library, Version 1 (CENDL-1), CNDC-85010, 1986.

NEUTRON NUCLEAR DATA MEASUREMENT IN IAE

Tang Hongqing

Institute of Atomic Energy, P.O.Box 275, Beijing

1. Introduction

For the purpose of nuclear energy development program and nuclear applications, accelerators and reactors have been built in the Institute of Atomic Energy and mono- or quasimono-energetic neutron sources from thermal energy to 40 MeV can be obtained. The neutron source energy range for main experimental devices is shown in fig.1.

Following neutron nuclear data have been measured

- fission cross sections
- average fission neutron number and fission neutron number distributions
- fission product yields
- prompt fission neutron spectra
- cross sections of fast neutron induced reactions, such as (n,n'), (n,2n), (n,p), (n,d), (n,alpha).....
- radiative capture and (n,n'γ) cross sections
- fast neutron scattering angular distributions and double differential neutron emission spectra
- neutron spectra and cross sections of charged particle induced reactions.

In addition, the properties of neutron sources have been studied and neutron source and neutron flux standard has been established.

2. Neutron nuclear data measurement

A. Fission data

In late 1950's, nuclear fission was studied. Later on, fission neutron number and its distributions were measured using Cd-loaded or Gd-loaded liquid scintillator with a diameter of 60 cm. In 1980's, the neutron emission probability in the long range alpha, ^{3}He, T and P accompanied fission of ^{252}Cf has been measured in a three-parameter experiment. In this experiment, the liquid scintillator was used for neutron detection and a telescope was used for the detection of light charged particles. The results were given at the International Conference on Nuclear Data for Basic and Applied Science, Santa Fe, 1985.

Fission cross sections were measured for ^{235}u, ^{238}U, ^{237}Np and ^{239}Pu at 14 MeV and other incident neutron energies. An accuracy of 1.9% was achieved for ^{235}U at 14 MeV, using a time correlated associated particle technique. Some recently-measured results were published in INDC(CPR)-009/L, Aug. 1986.

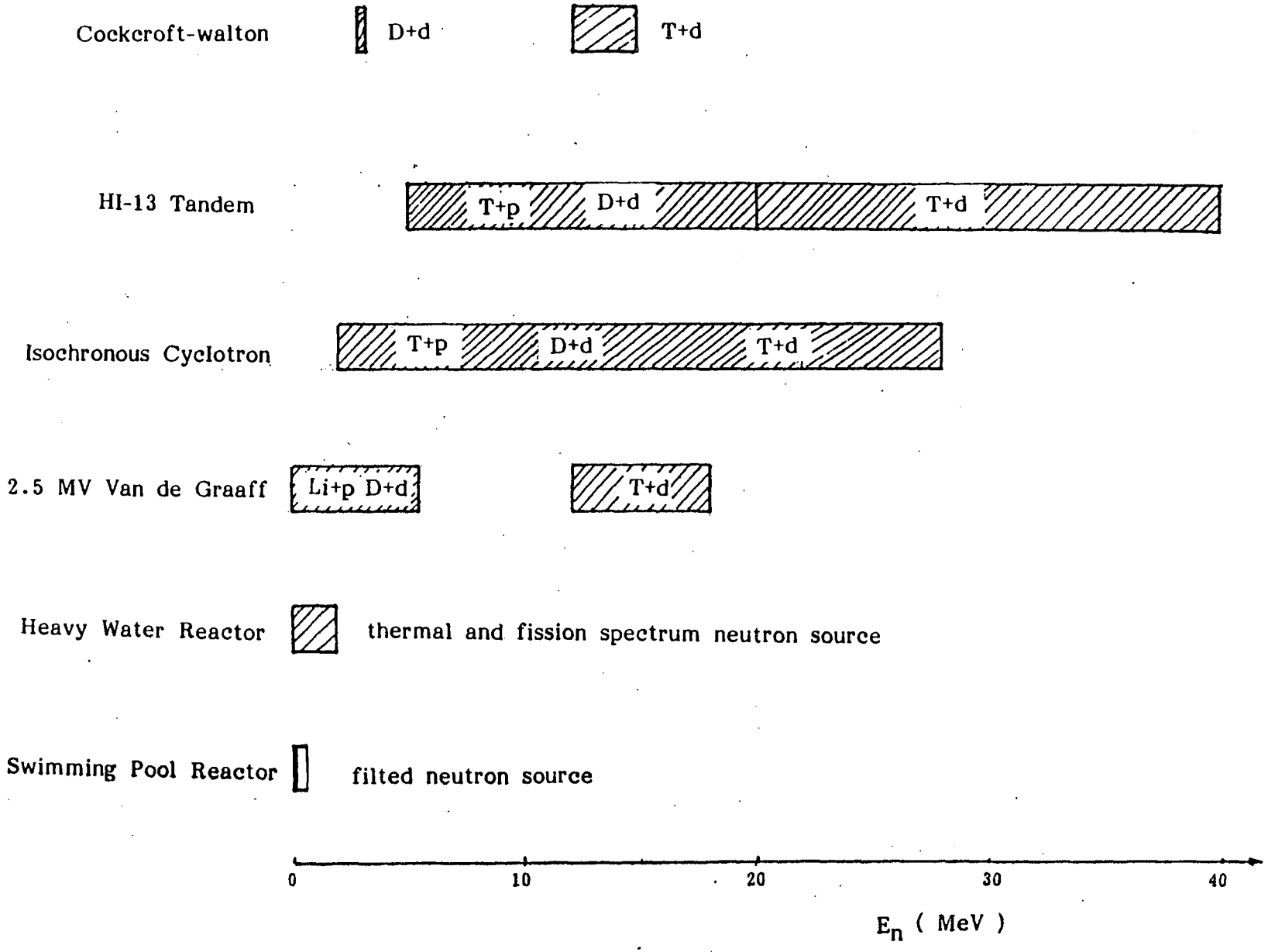

Fig.1 Neutron source energy range at IAE

For the fission product yield measurement, two methods—radiochemistry technique and Ge(Li) gamma-ray spectrum technique were established. The fission rate is determined with a double fission chamber. For ^{252}Cf measurement, the absolute fission rate was obtained with a catcher foil technique. The accuracy of the yield data is 3—10% for peak yields and 5—25% for valley yields. Mass distributions for ^{235}U induced by thermal and 14.9 MeV neutrons and for ^{238}U induced by 3, 5, 8.3 and 14.9 MeV neutrons have been published in Chinese Journal of Nuclear Physics. Fig.2 shows the product mass distribution of the ^{252}Cf spontaneous fission. The mass distribution of the fission spectrum neutron induced fission of ^{235}U is shown in fig.3.

Prompt fission neutron spectrum measurement was made of ^{252}Cf and ^{235}U using a TOF technique. The neutron spectrum energy range in the ^{252}Cf spontaneous fission measurement is 0.9 to 14.5 MeV. The data was fitted with the Maxwellian distribution and a result of T=1.418 $\pm$0.015 MeV was obtained(see fig.4). Recently, the attention has been focused on the study of the lower energy part of the spectrum. A new measurement was performed using a lithium glass scintillator as the neutron detector and a fast ionization chamber with low mass (1.65 grams) as the fission fragment detector. The flight path is 35 cm. The final result will be given after calibration of neutron detector efficiency. The neutron spectrum of thermal neutron induced fission of ^{235}U was measured in the neutron spectrum energy range 0.6 to 16 MeV at the heavy water research reactor. The result is shown in fig.5. The experimental data can not be fitted satisfactorily by the Maxwellian distribution in the measured spectrum energy range. In the spectrum energy region below 6 MeV, the spectrum approaches Maxwellian distribution. However, in the energy range beyond 6 MeV, the spectrum deviates down from Maxwellian distribution by 50% at about 14 MeV. The data are preliminarily compared with Madland-Nix model calculation (with a constant cross section). In the energy range 1 to 15 MeV, the experimental data agree with Madland-Nix modelcalculation approximately. However, the experimental data are 20% higher than the calculations in the lower energy range.

B. Fast neutron reaction cross sections

The cross sections of the (n,γ), (n,p), (n,d), (n,α), (n,n'), (n,2n) and (n,3n) reactions on more than 30 nuclides have been measured by means of an activation method in the incident neutron energy range 0.1 to 18 MeV. Radioactivity of the residuals were measured with a calibrated NaI (ϕ 80x80mm) or a Ge(Li) detector with a volume of 136 cm^3. Table 1 lists most of measured nuclear reactions. In recent years, the investigation is focused on the measurement of isomeric cross sections of the $^{115}In(n,2n)^{114m}In$, $^{115}In(n,n')^{115m}In$ and $^{113}In(n,n')^{113m}In$ reactions. Because of the low threshold and high cross sections in the (n,n') reactions, the

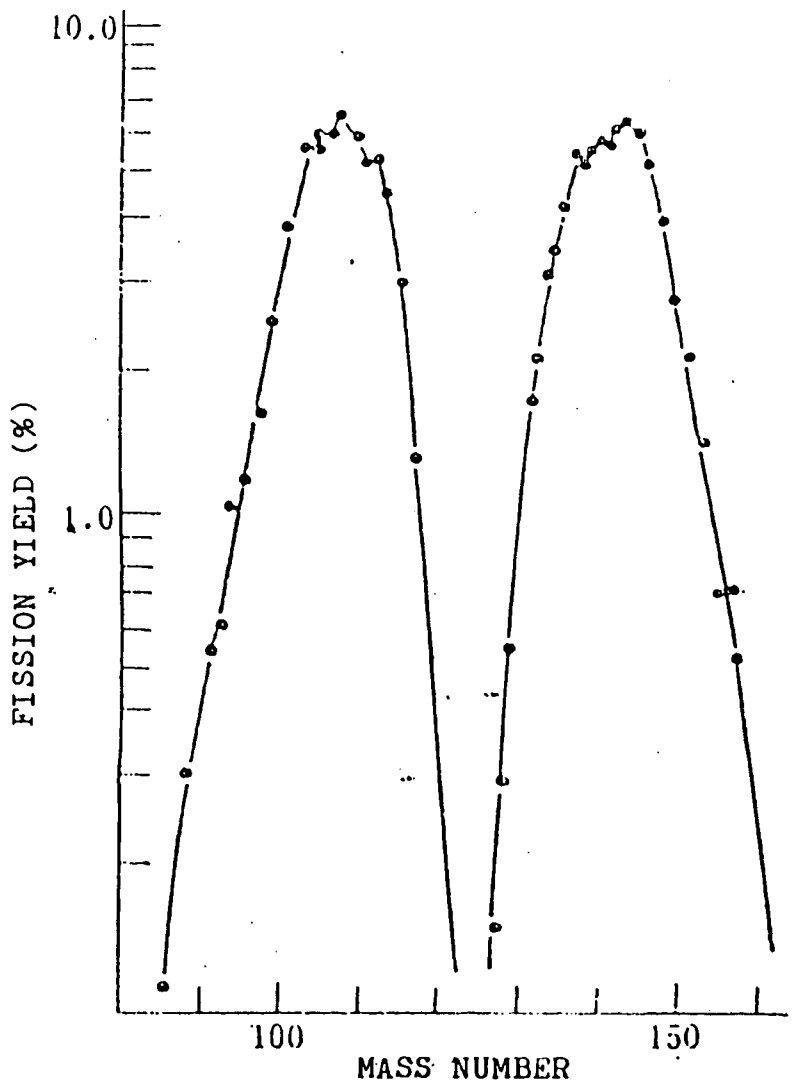

Fig. 2 Fission fragment mass distribution in the ^{252}Cf spontaneous fission

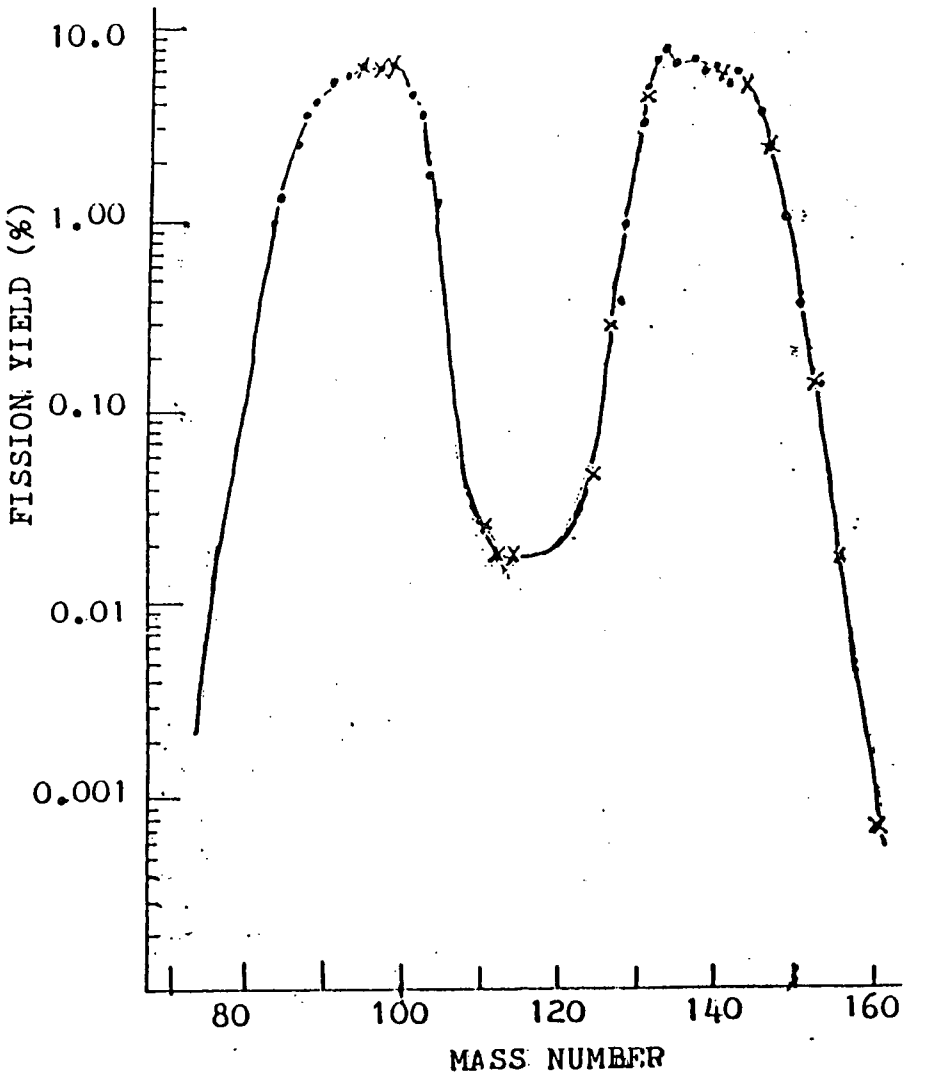

Fig.3 Fission fragment mass distribution of ^{235}U induced by fission spectrum neutrons

• -- γ-ray spectrum method

X -- Radiochemistry method

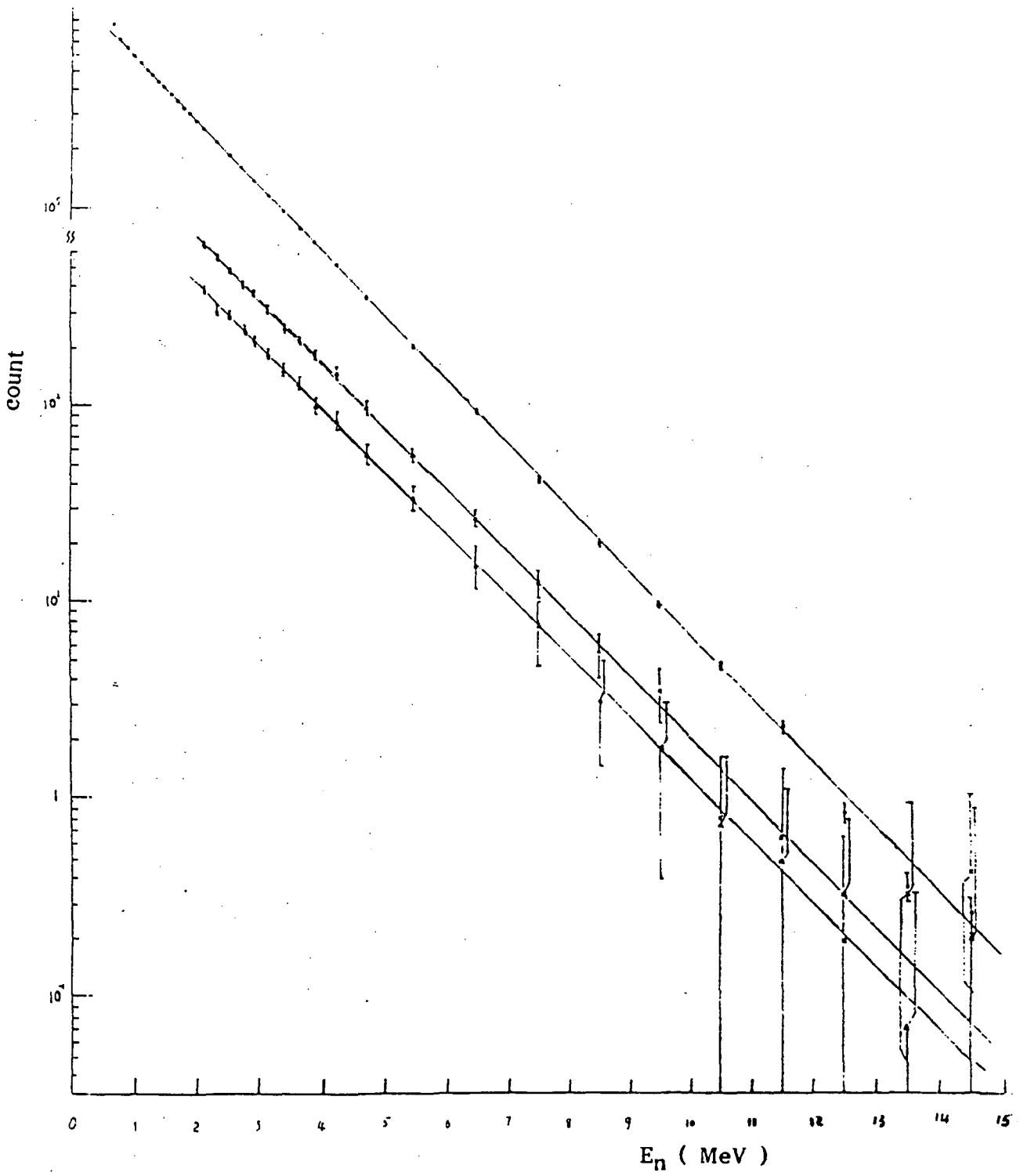

Fig.4 Fission neutron spectrum of the ^{252}Cf spontaneous fission
---detection bias is 0.5 MeV, flight path is 2.05 m,
---detection bias is 1.75 MeV, flight path is 3.02 m,
---detection bias is 1.75 MeV, flight path is 2.53 m.
solid line---Maxwellian distribution fitted curve

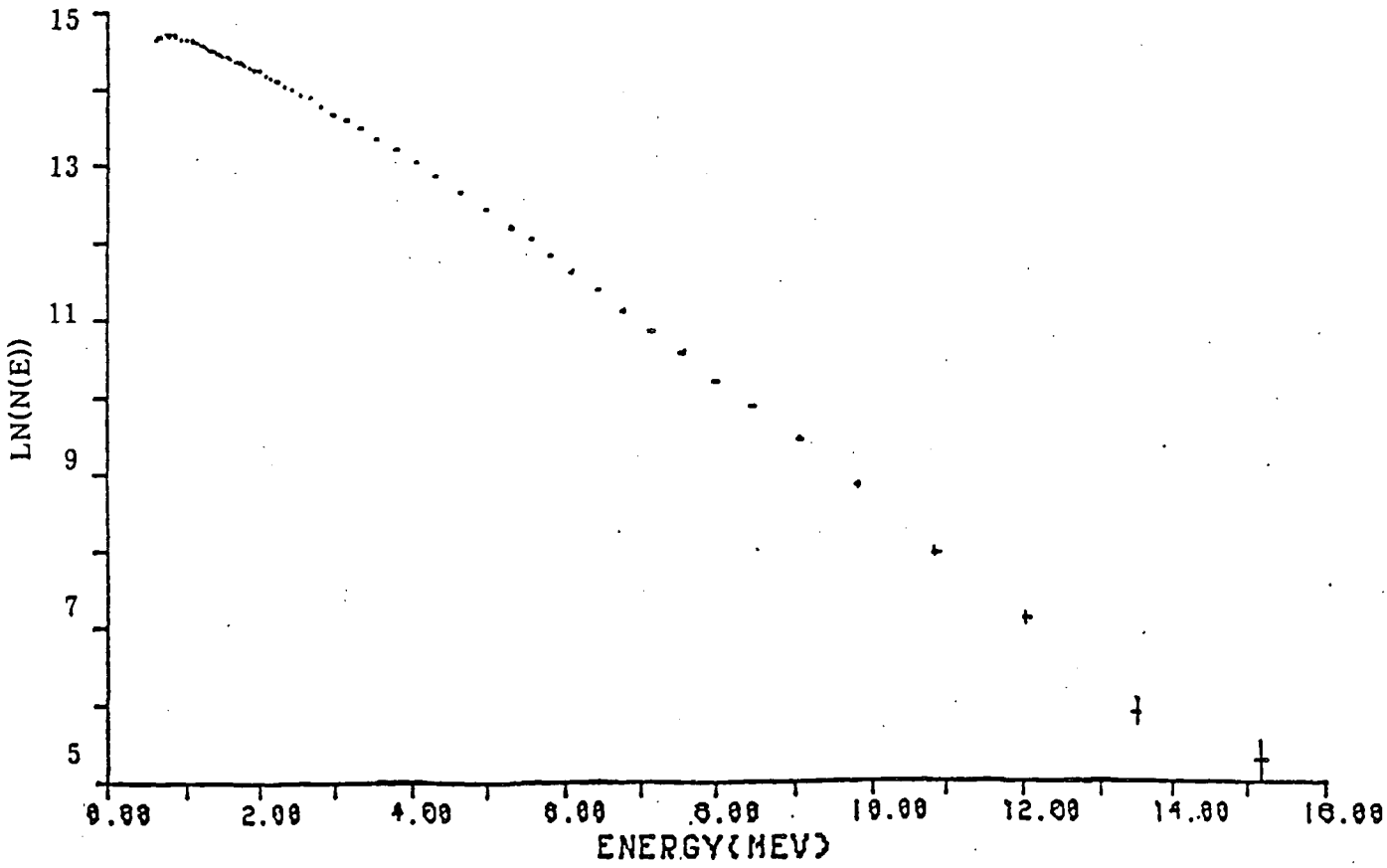

Fig.5 Fission neutron spectrum of ^{235}U induced by thermal neutrons

Table 1. Reaction cross sections measured by activation technique

reaction type	incident neutron energy range (MeV)	nuclides
(n,γ)	0.1-1.5	^{139}La, ^{152}Sm, ^{180}Hf, ^{193}Ir, ^{194}Pt, ^{197}Au
(n,n')	threshold--5.5	^{87}Sr, $^{113,115}In$*, ^{195}Pt
(n,p)	threshold--18	^{24}Mg, $^{46,48}Ti$, $^{54,56}Fe$, ^{58}Ni, $^{85,87}Rb$*, ^{115}In, ^{140}Ce*, ^{181}Ta
(n,d)	threshold--18	^{58}Ni
(n,α)	threshold--18	^{27}Al, ^{51}V, ^{54}Fe, ^{59}Co, ^{85}Rb*, ^{93}Nb, ^{115}In
(n,2n)	threshold--18	^{45}Sc, ^{55}Mn, ^{58}Ni, ^{59}Co, $^{85,87}Rb$*, ^{89}Y, ^{90}Zr, ^{93}Nb, $^{113,115}In$*, ^{126}I, $^{136,138}Ce$*, $^{140,142}Ce$*, ^{169}Tm, ^{181}Ta, ^{196}Pt, ^{197}Au
(n,3n)	threshold--18	^{169}Tm, ^{197}Au

* results measured in the past two years

corrections for low energy neutron effects should be carefully considered. Table 2 lists the corrections and their uncertainties. The measured excitation functions are shown in figs. 6—8.

C. Differential and double differential cross sections

Three fast neutron TOF spectrometers for angular distribution and neutron spectrum measurement have been built at the cyclotron, Cockcroft-Walton and tandem accelerators respectively.

At the cyclotron, a deuterium gas target was built and the D+D reaction neutron source and other reactions were studied. Neutron scattering angular distribution measurement was carried out on C, D, ^{6}Li, ^{7}Li, etc.

At the Cockcroft-walton generator, neutron scattering angular distributions of D, ^{6,7}Li, Be, B, C and ^{238}U and neutron emission spectrum of D and ^{238}U have been measured at 14 MeV neutron energy, using the alpha-particle associated TOF spectrometer. Some recently-measured results on ^{238}U induced by 14.2 MeV neutrons are shown in figs. 9—12.

At the HI-13 tandem accelerator, we tested pulsed proton and deuteron beam, and performed a preliminary measurement on neutron scattering and (p,n) neutron emission spectrum. Fig.13 show the properties of the pulsed deuteron beam and D+D neutron source. The ^{59}Co(p,n)^{59}Ni reaction neutron TOF spectrum at bombarding energy of 15 MeV and the TOF spectrum of 13 MeV neurtons scattered from ^{12}C are shown in figs.14—15.

D. Neutron induced gamma-ray data

Gamma-rays of the (n,n'γ) reactions on ^{56}Fe, ^{58}Ni, ^{60}Ni, ^{63}Cu, ^{65}Cu and ^{209}Bi were measured at 55 degrees by a complete shielded 70 cm^3 Ge(Li) or 67.5 cm^3 HP Ge(n) detector at the Cockcroft-walton generator, using the associated particle gated timing method. The integrated gamma-ray production cross sections are deduced by the following expression

$$\sigma_{n,n'} = 4\pi \frac{d\sigma}{d\Omega}(55^{o}) .$$

The gamma-ray spectrum from ^{27}Al, ^{31}P and ^{32}S induced by thermal neutrons have been measured by a three crystal pair spectrometer. The cross sections are 529±26 mb for the ^{32}S(n_{th},γ) reaction and 180±6 mb for the ^{31}P(n_{th},γ) reaction.

Radiative capture gamma-ray data from ^{56}Fe and ^{238}U at 14.2 MeV neutron energy were measured by a Φ 20x10 cm NaI(Tl) detector. The cross sections are 790±130 μb for the ^{56}Fe(n,γ) reaction and 1080±180 μb for ^{238}U(n,γ) reaction. The gamma-ray angular distributions of the ^{12}C(n,γ) reaction at 14 MeV neutron energy is shown in fig.16.

Table 2 : Corrections and Uncertainties

Source	Correction (%)			Uncertainty (%)		
	^{115m}In	^{114m}In	^{113m}In	^{115m}In	^{114m}In	^{113m}In
1, Neutron from $D(d,n)^3He$ reaction	0.25		0.2	0.05		0.05
2, Neutron scattering effects due to target system	7.2	1.2	5.5	2.2	0.3	1.8
3, Neutron scattering by sample	0.8	0.3	0.6	0.4	0.1	0.3
4, Neutron absorption in the target backing		1.6			0.2	
5, Gamma ray self-absorption in sample	4.0	7.2	3.4	0.4	1.0	0.4
6, Sample area effect	0.6	1.0	0.6	0.1	0.3	0.1
7, Variation of neutron yield		0.1----3.5		0.2	0.1	0.2
8, Detector efficiency or activity ratio				1.5	1.7	1.5
9, Neutron fluence or standard cross section				2.4	1.2	2.4
10, Angular distribution of neutron				1.0	1--3	1.0
Total				3.6	2.4	3.4
Excitation curve				3.7	3.8	3.6

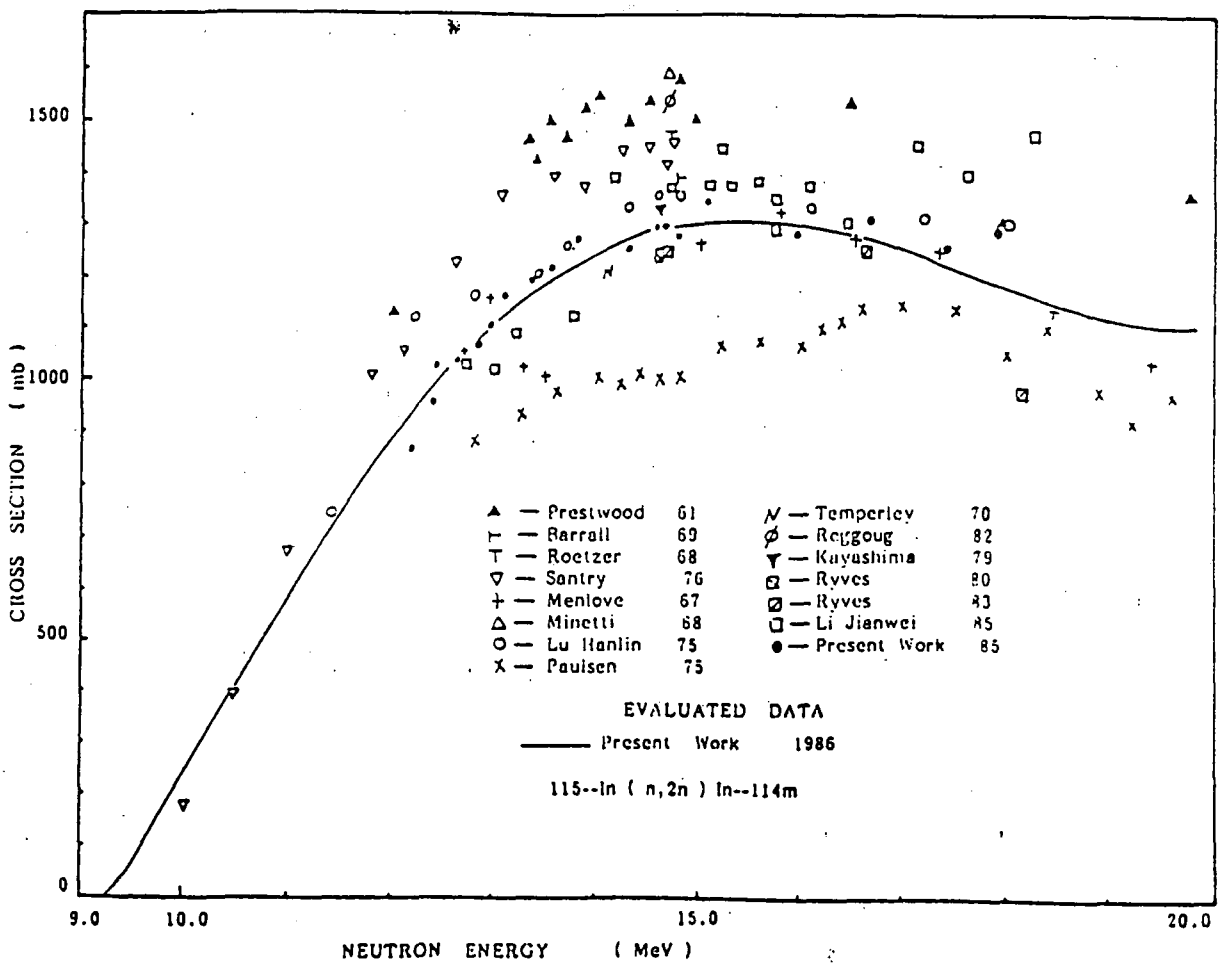

Fig.6 Cross sections of the $^{115}In(n,2n)^{114m}In$ reaction

3. Plan in coming years

In the past years, we spent much time to prepare experimental facilities at tandem. Up to now, the three-detector fast neutron TOF spectrometer and the gamma-ray goniometer have been set up. The TOF facility can be rotated in the angular range -30 to 165 degrees and moved forward or backward from about 1.5 meters to 6 meters. The neutron detectors are ST-451 liquid scintillators with a diameter of 18 cm and thickness of 5 cm. The TOF experimental setup is shown in fig.17. The gamma-ray device consists of an anticoicident, completely shielded NaI(Tl) detector (Φ 240x250 mm) and a Ge(Li) detector, which can be rotated about the center of the sample. The system is shown in fig.18.

The pulsed proton and deuteron beams with FWHM of 1 to 1.5 ns and a peak current of 1 ma have been obtained, as metioned above. From now on, some neutron nuclear data measurements and neutron physics study will shift to the tandem accelerator. In the coming few years, we plan to do following neutron xeperiments at the tandem

a. measurement of fission product yields and prompt fission neutron spectra at about 10 MeV neutron energy.

b. studying gas production reactions in the structure material and measuring fast neutron reaction cross sections in the incident neutron energy range 6 to 12 MeV.

c. measurement of differential and double differential cross sections on fuel, blanket and structural elements in the incident neutron energy range 7 to 13 MeV.

d. investigating double differential neutron emission spectra of the (p,n) reactions on some isotopes, such as ^{59}Co, ^{95}Mo, ^{96}Mo, etc.

e. measuring (n,n'γ) cross sections and fast neutron radiative capture gamma-ray spectrum and cross sections.

f. performing neutron polarization experiment.

In addition, atomic and molecular physics experiment will be carried out at the tandem. The measurement on double differential neutron emission spectrum, fast neutron radiative capture and fast neutron induced reaction cross sections at the Cockcroft- walton and othor accelerators will be continued.

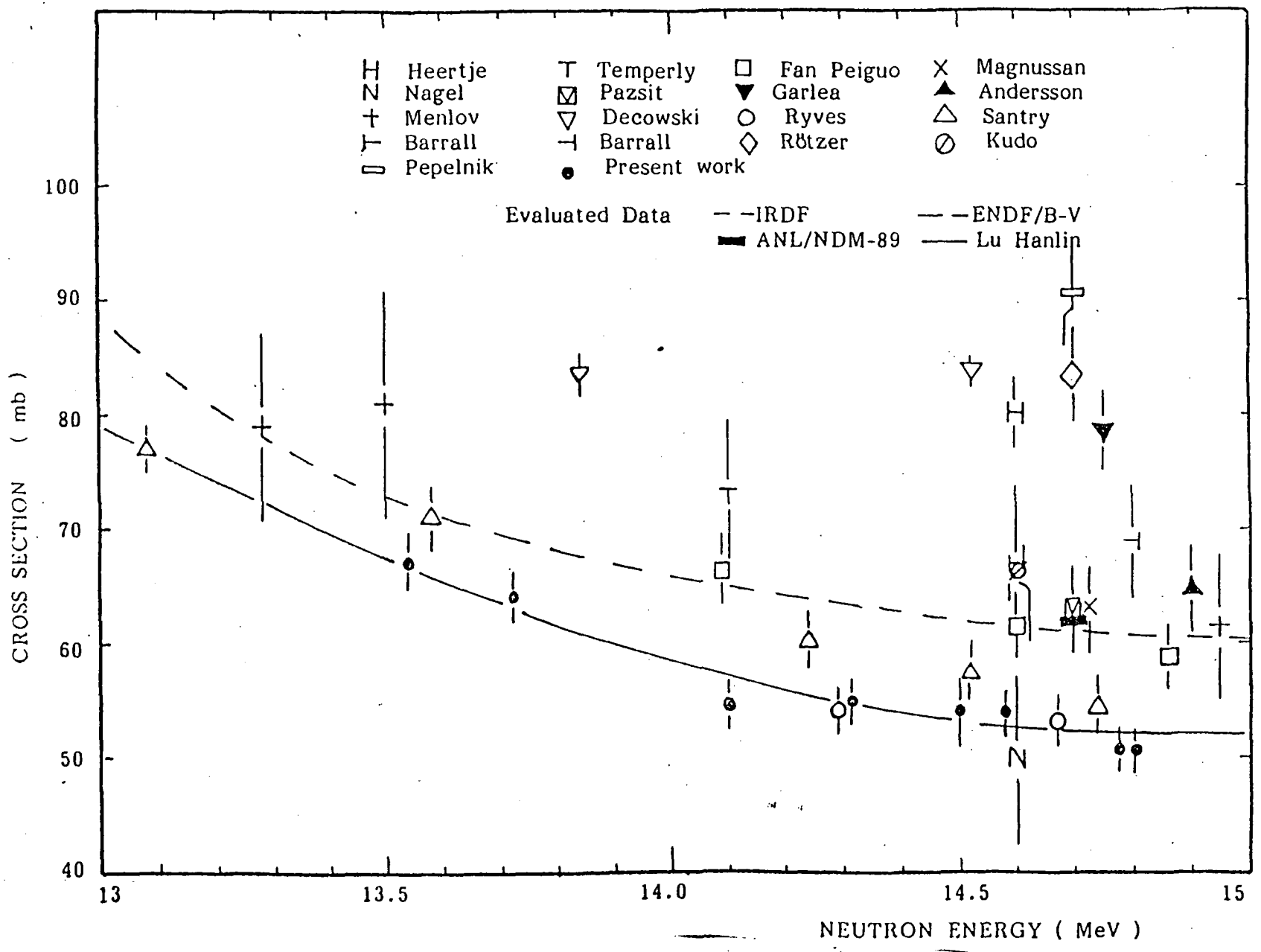

Fig.7 Cross sections of the $^{115}In(n,n')^{115m}In$ reaction

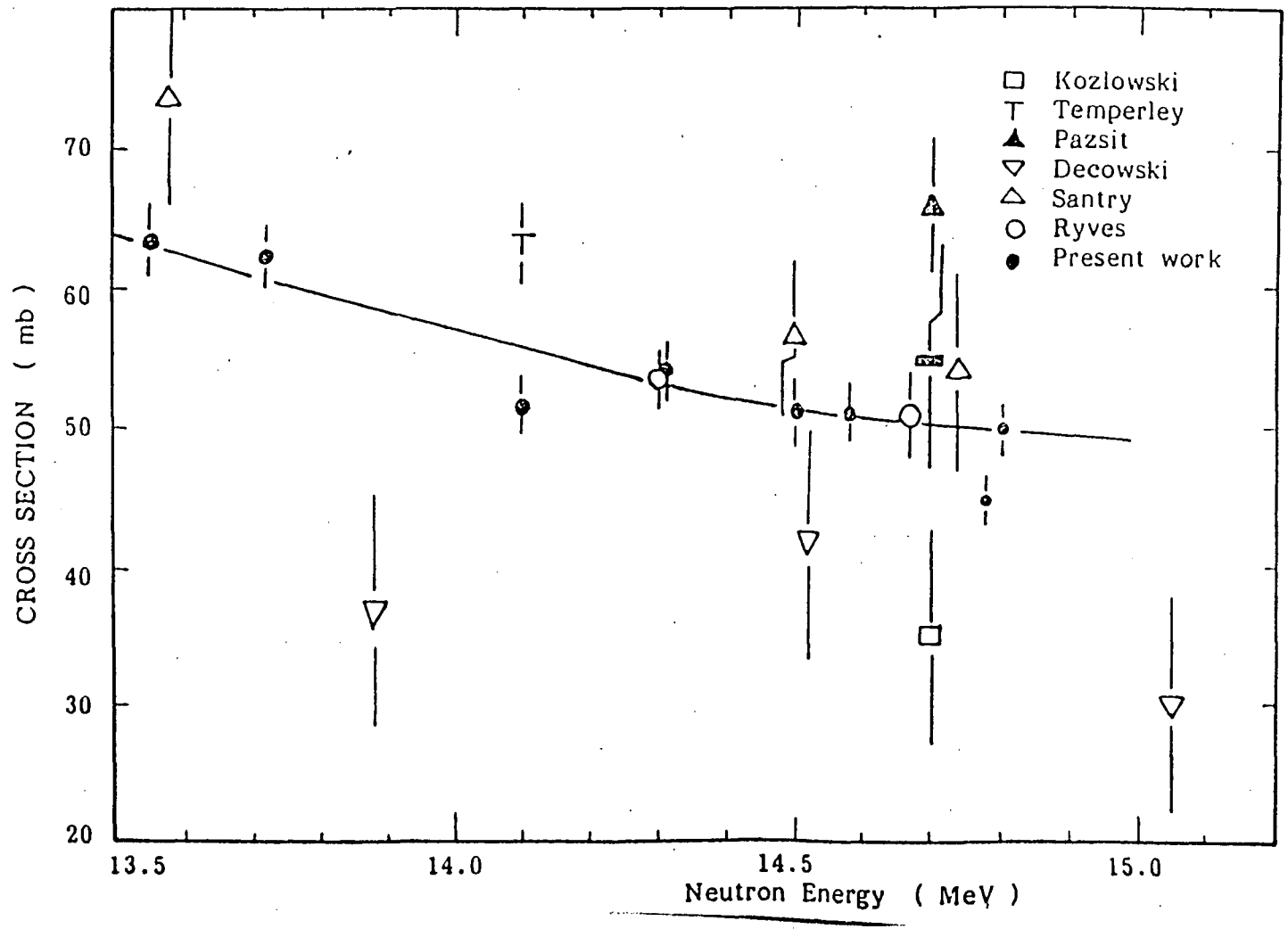

Fig.8 Cross sections of the $^{113}In(n,n')^{113m}In$ reaction

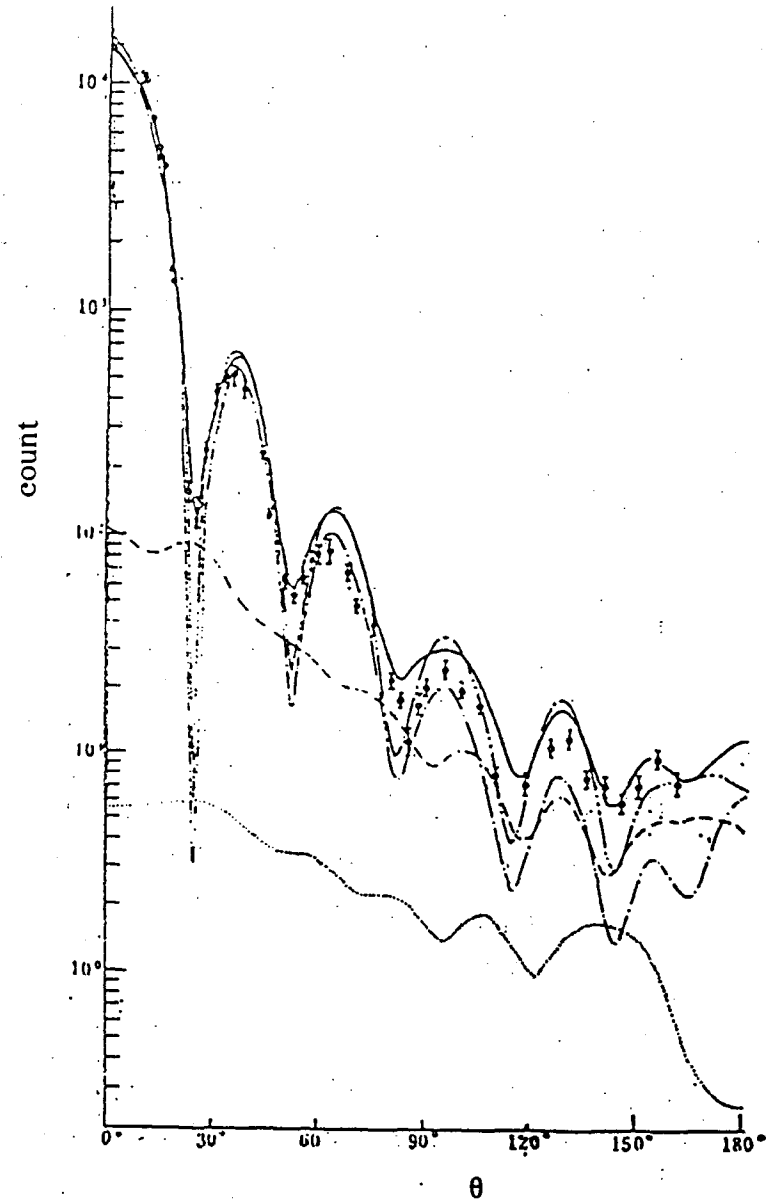

Fig.9 Angular distribution of 14.2 MeV neutrons elastically scattered from ^{238}U

● ---experimental result, —··— spherical optical model calculation,

—·—coupled channel theory calculation for the ground state,

----- coupled channel theory calculation forthe first excited state

..... coupled channel theory calculation for the second excited state

solid curve is the sum of the coupled channel theory calculation for the ground, first and second excited states

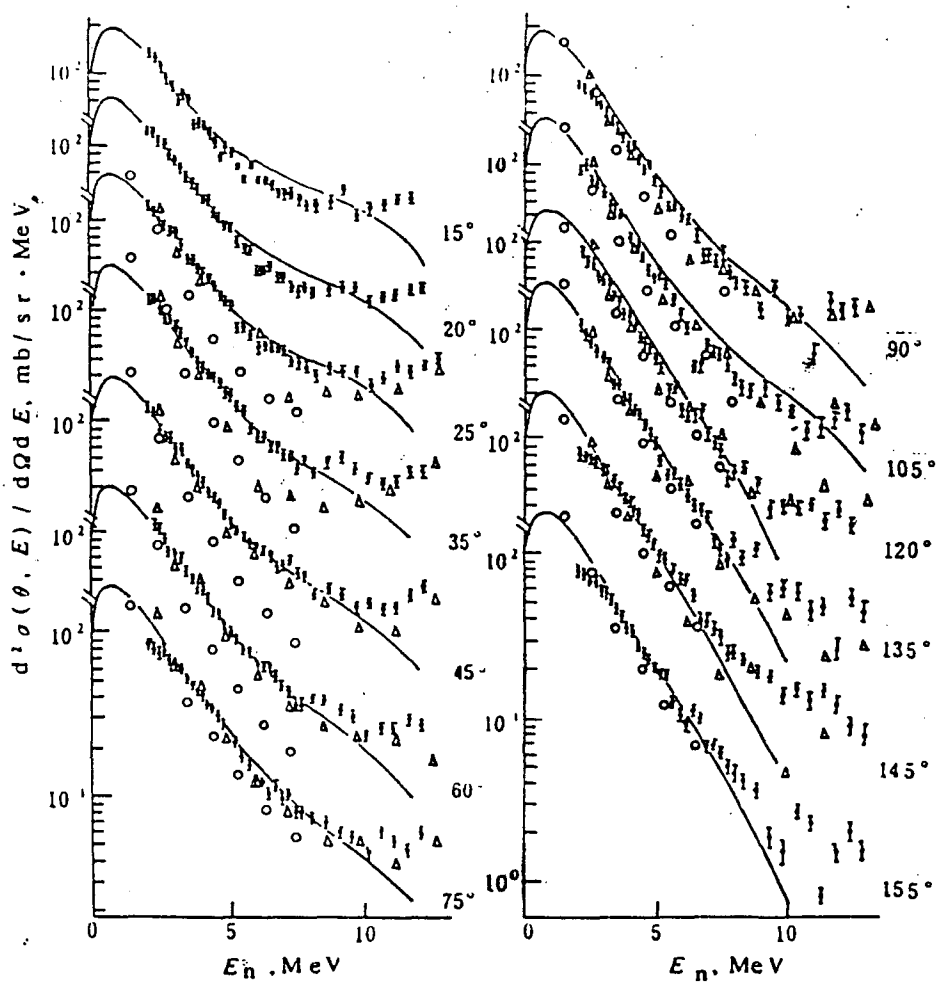

Fig.10 double differential neutron emission spectra of ^{238}U induced by 14.2 MeV neutrons

●—present work, △—Kammerdiener,

○—Voignier, solid curve—evaporation model calculation

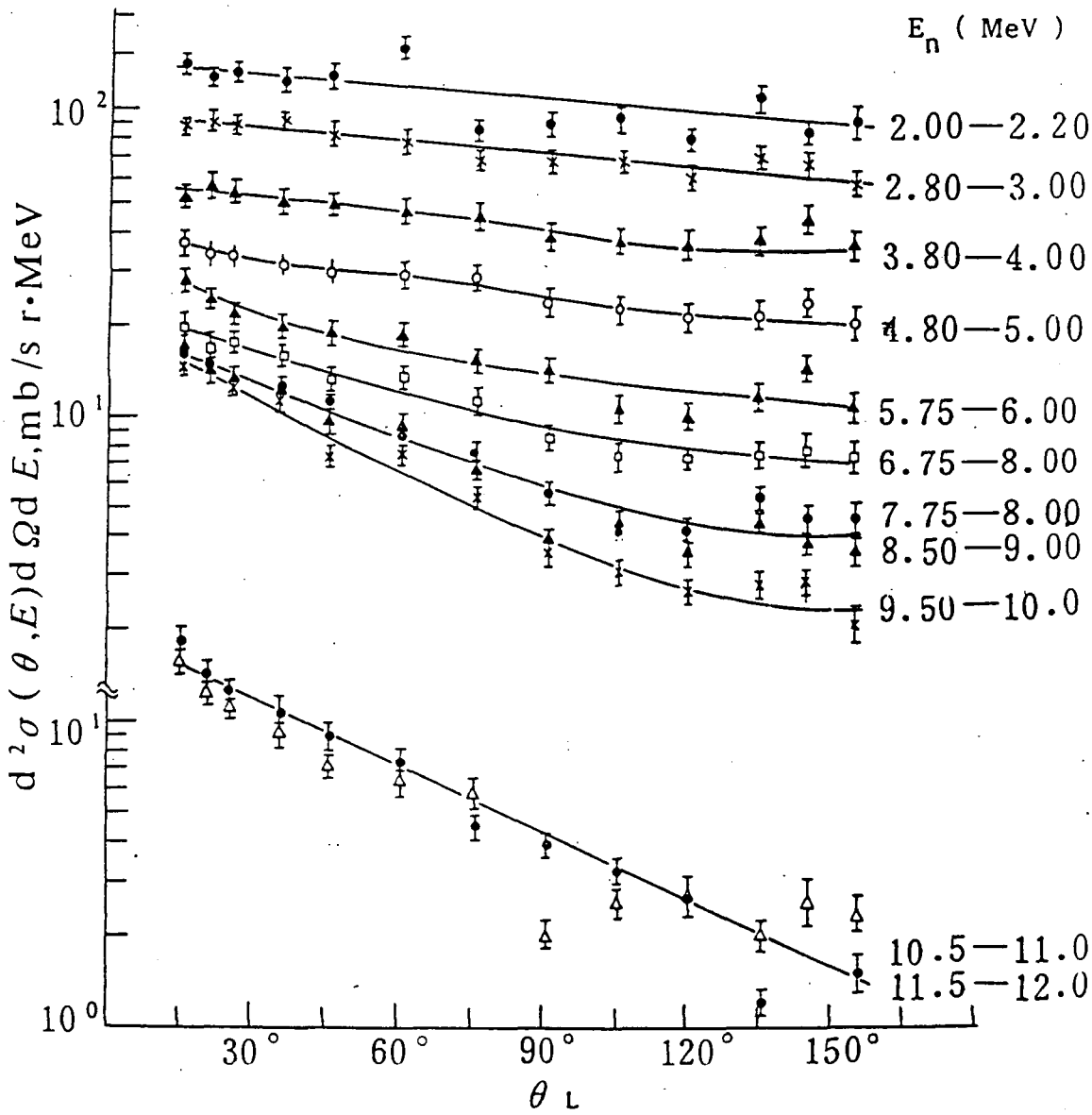

Fig.11 Double differential cross section angular distributions of ^{238}U measured by present work

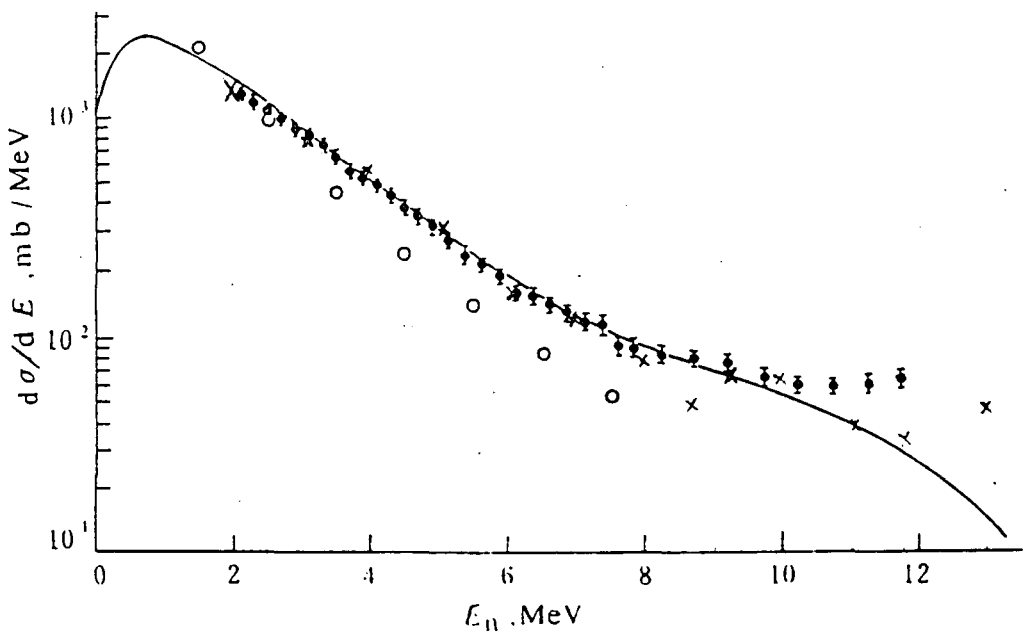

Fig.12 The integral spectrum over the whole space
● --present work, O-- Voignier's data
solid curve --calculations of the evaporation model with preequilibrium emission mechanism
x -- Degtyarev's data, obtained by averaging over the emission angles in the forward semisphere.

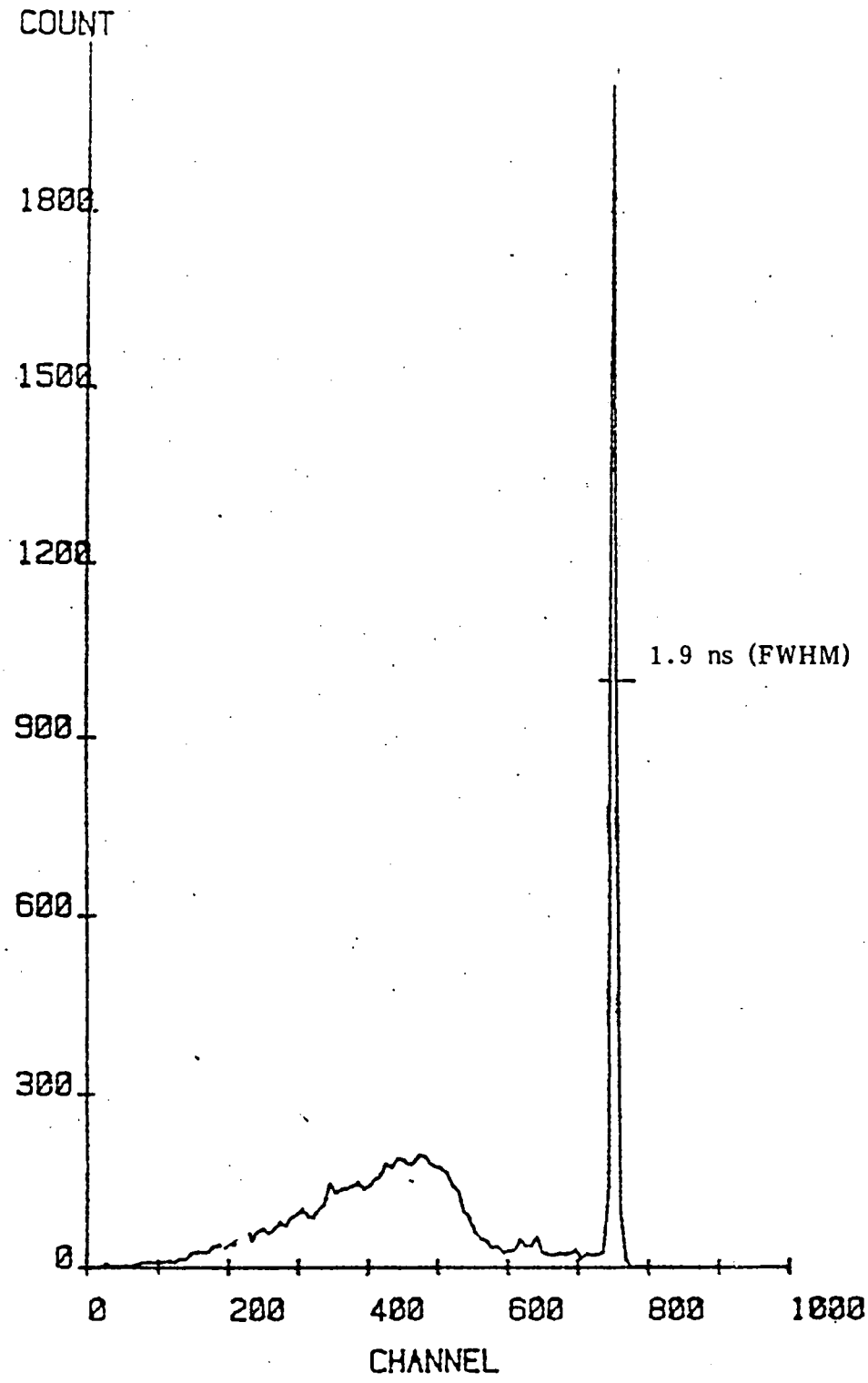

Fig.13 Neutron TOF spectrum of the D(d,n) reaction, E_d=10 MeV channel width is 0.435 ns , $\theta = 0^{o}$.

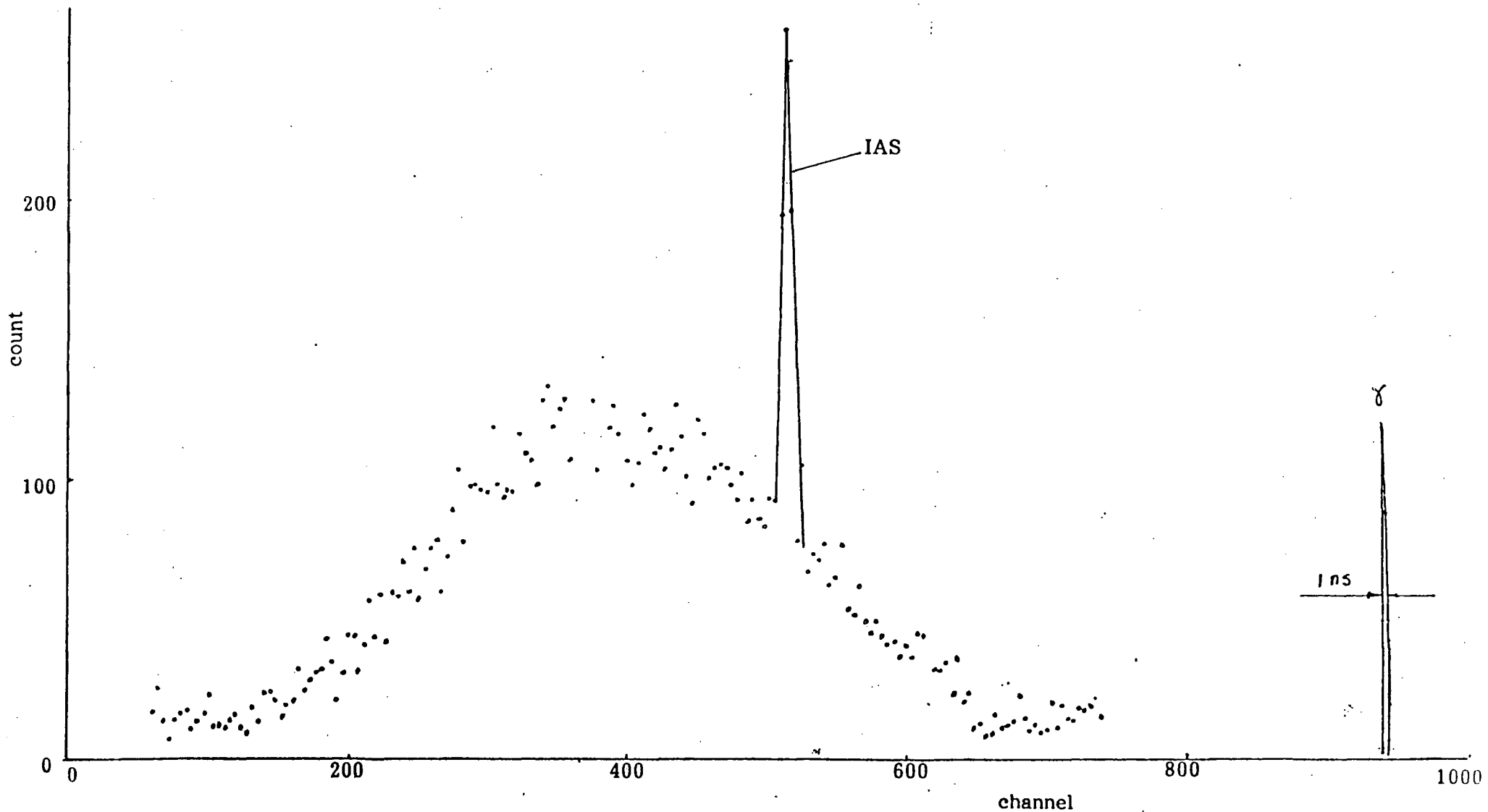

Fig.14 Neutron TOF spectrum of the $^{59}Co(p,n)^{59}Ni$ reaction $\theta=45^{o}$, E_p = 15 MeV flight path is 6.81 m., channel width is 0.435 ns.

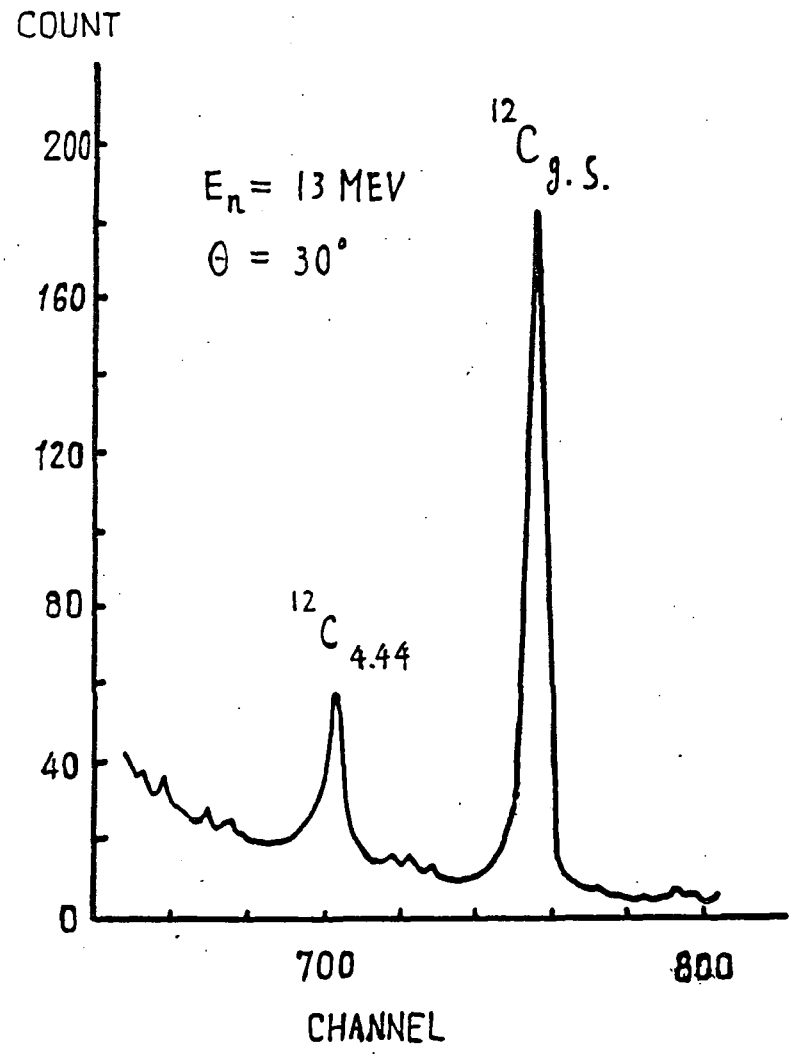

Fig.15 TOF spectrum of 13 MeV neutrons scattered from ^{12}C, $\theta = 30^{o}$

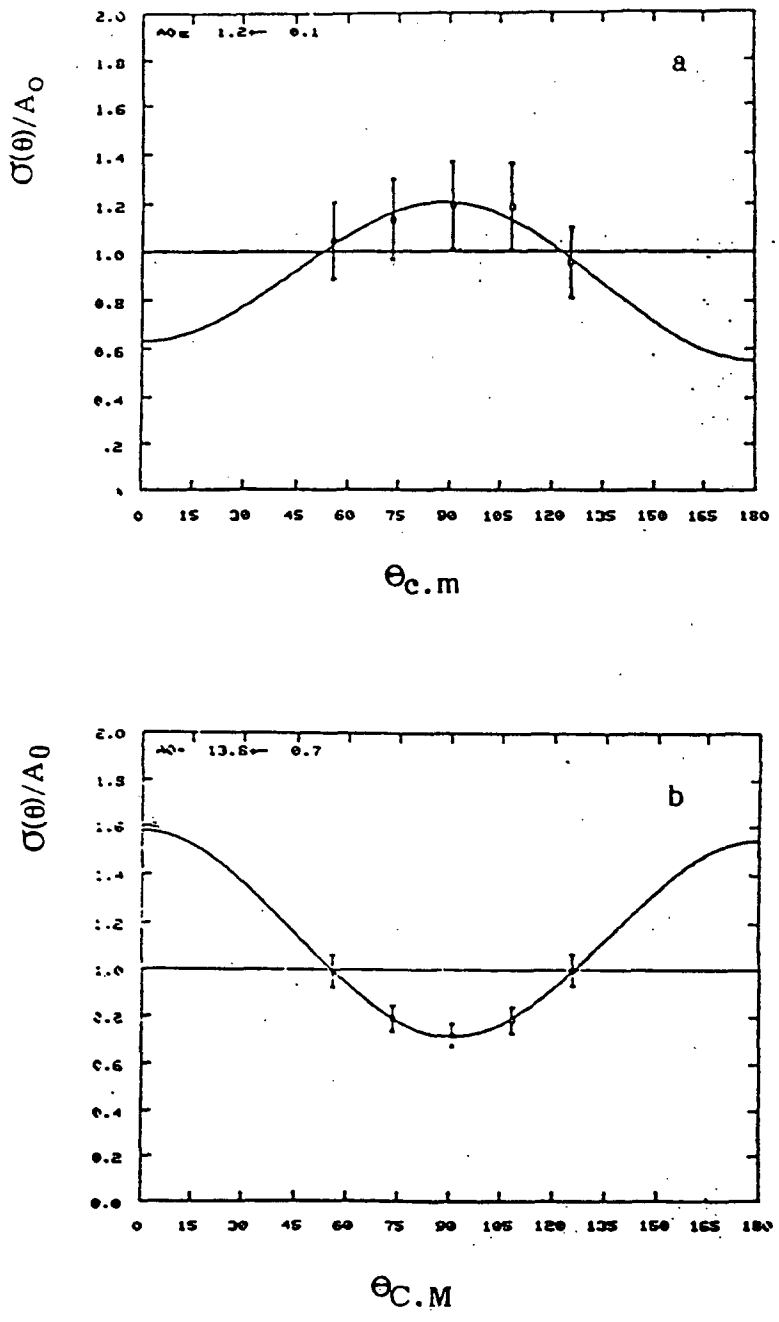

Fig.16 Gamma-ray angular distributions of the $^{12}C(n,\gamma)$ reaction
a. transition to the ground state of ^{12}C,
b. transition to the first excited state of ^{12}C

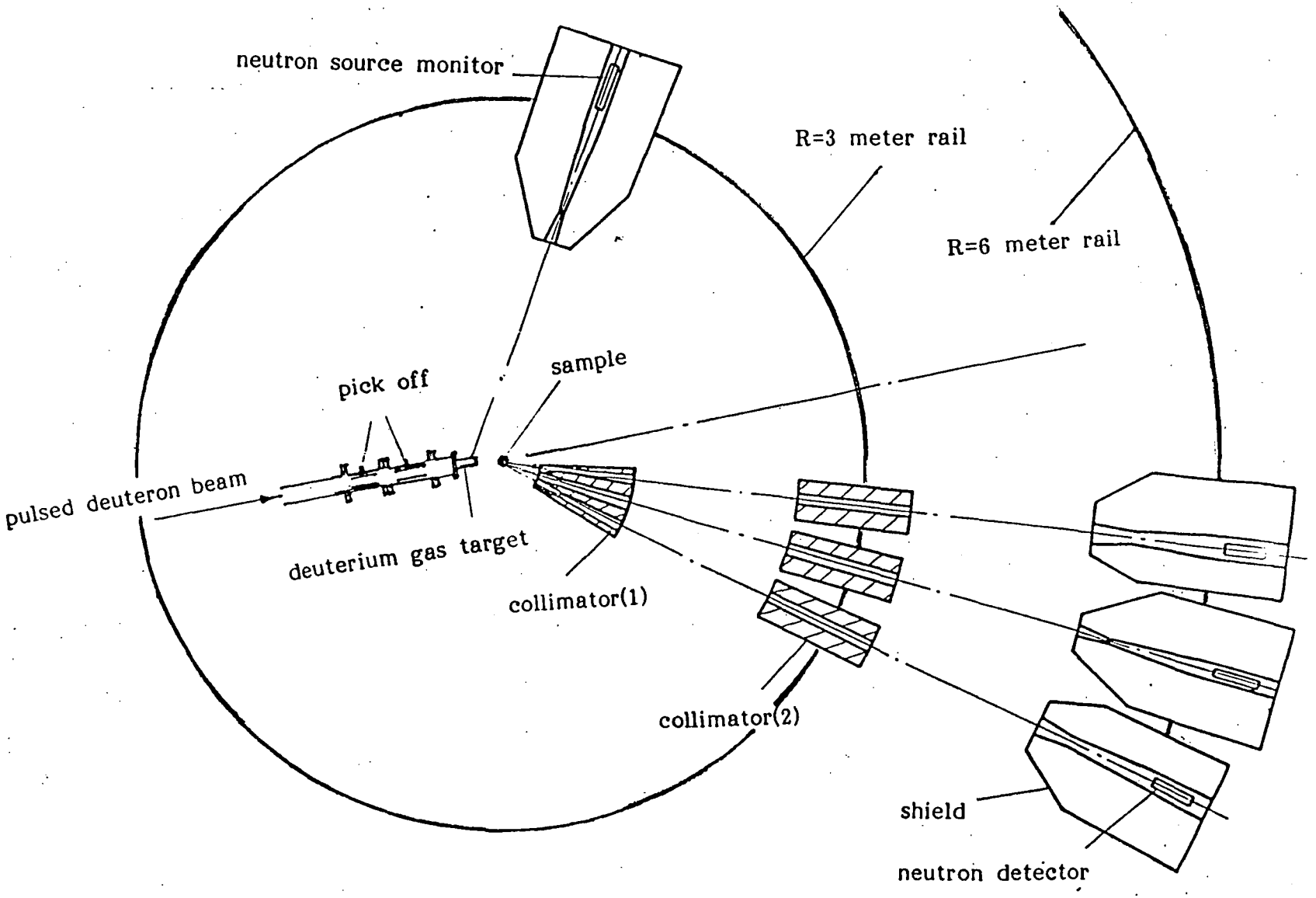

Fig.17 Three-detector fast neutron TOF facility at the HI-13 tandem accelerator

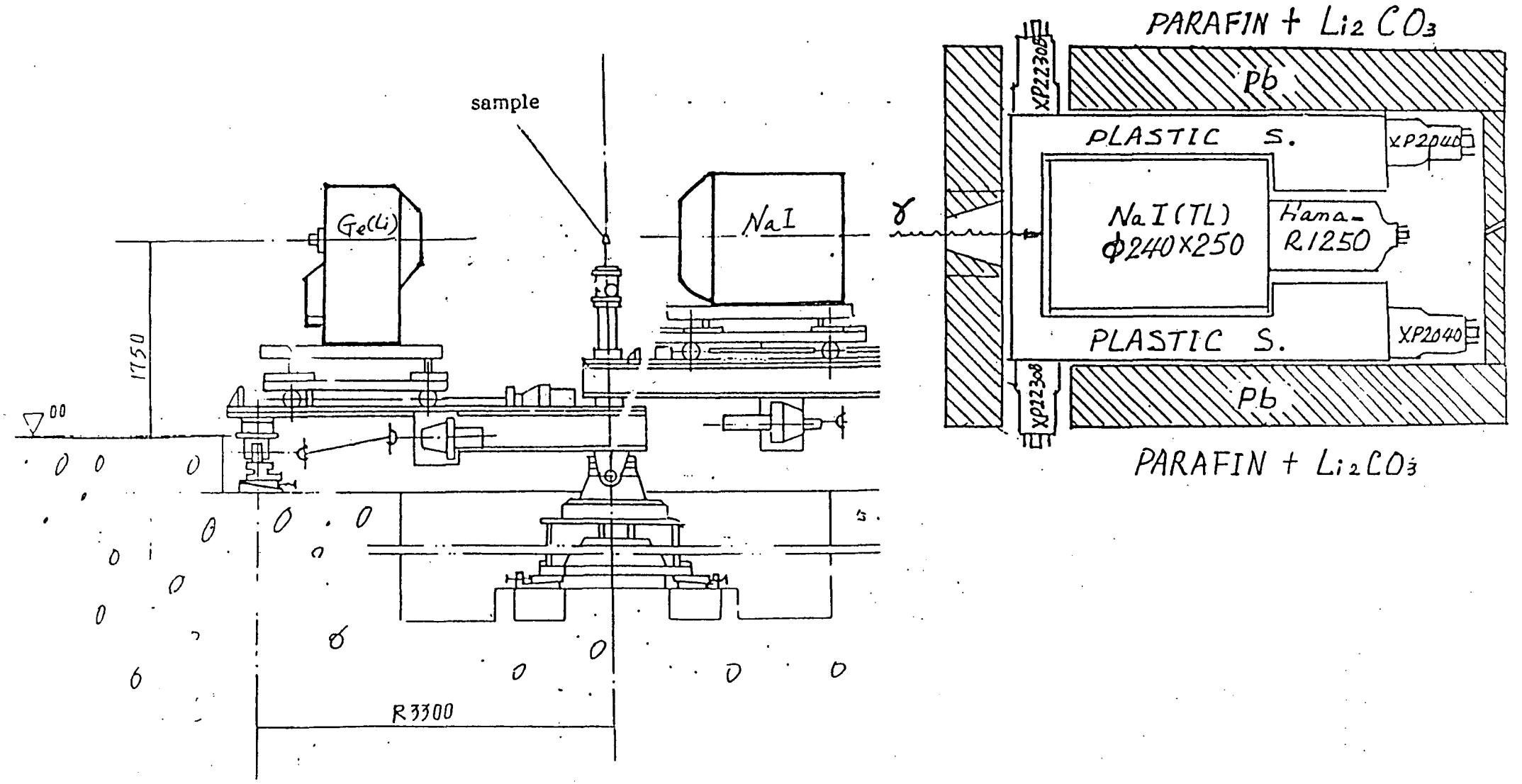

Fig. 18 Gamma-ray goniometer at the HI-13 tandem accelerator

MEASUREMENT OF DOUBLE DIFFERENTIAL NEUTRON EMISSION CROSS SECTIONS OF ^{238}U INDUCED BY 14.2 MeV NEUTRONS

Sep. 10, 1987

Shen Guanren, Huang Tangzi, Tang Hongqing, Yu Chunying,
Li Anli, Sui Qingchang, Sa Jun, Zhuang Youxiang and Liu Tingjin
Institute of Atomic Energy, P.O.Box 275, Beijing

Abstract Double differential neutron emission cross sections of ^{238}U at 14.2 MeV have been measured by means of associated particle time of flight technique. The neutron flight path is 3.055m. The neutron detector consists of a ST-451 liquid scintillator (Φ105x50mm) and a XP-2041 photomultiplier tube. The time resolution of the TOF spectrometer is about 1.2 ns. The double differential cross sections in the effective energy range 2 to 12 MeV are obtained at 13 angles between 15 to 155 degrees with an overall error of 5 to 15%. The data are corrected for neutron flux attenuation, multiple scattering and finite geometry with a Monte-Carlo code. The experimental results are compared with theoretical calculations and good agreement is achieved.

1. Introduction

^{238}U is a very important fuel material in fast neutron breed reactors and fission-fusion hybrid reactors. Because of rapid change of the fission cross sections of ^{238}U with neutron energy, an accurate measurement of the secondary neutron spectrum of ^{238}U is of importance both for calculation of fission rate and for check of nuclear models.

Double differential neutron emission cross sections of ^{238}U at 14 MeV have been measured in a few laboratories. Bertrand[1] and Voignier[2] in Geel made spectrum measurements in the lower neutron energy region of 0.1 to 8 MeV. Kammerdiener et al.[3] in Lawrence Livemore Laboratory performed a measurement with Livemore multi-angle fast neutron TOF facility. The energy range of the measured spectra is wide. However, because of a long flight path (10.5 meters), the statistical error in the higher energy part of the spectrum (8-12 MeV) is rather poor. At the same time, there exist some discrepancies between these two laboratories in the overlapped energy region. Degtyarev et al. at Kiev State Un-iversity [4] made a spectrum measurement on ^{238}U at 14 MeV. However, the measurement was performed only at five angles. For clarifying the discrepancy and obtaining more accurate data, especially in the higher energy part of the spectrum, a measurement is made in our institute.

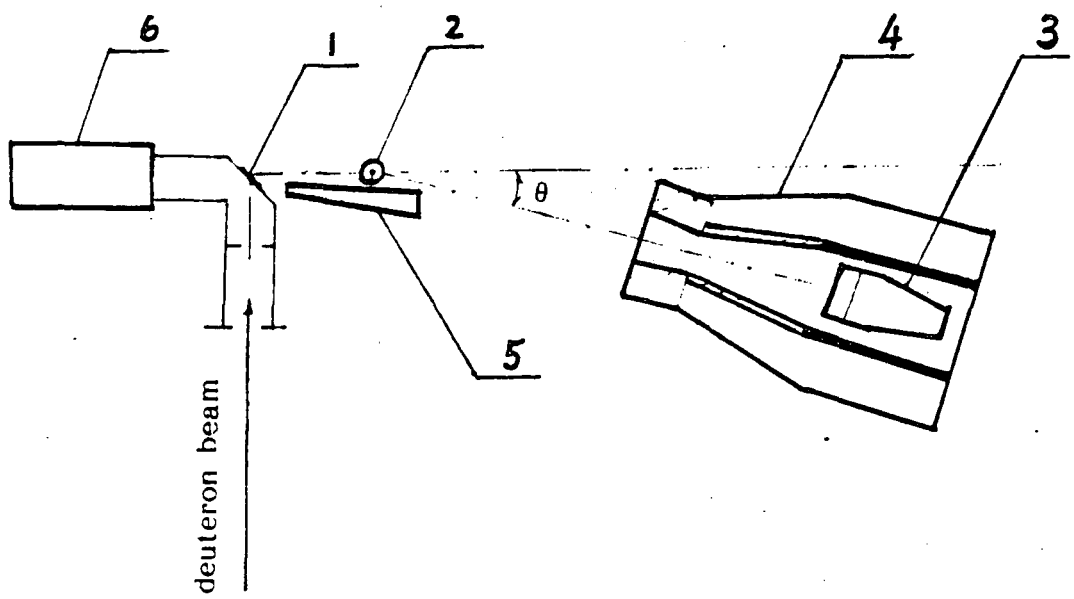

Fig.1 Experimental arrangement
1-tritium target(TTi), 2-^{238}U sample,
3-neutron detector, 4-shield,
5-shadow bar, 6- α-detector

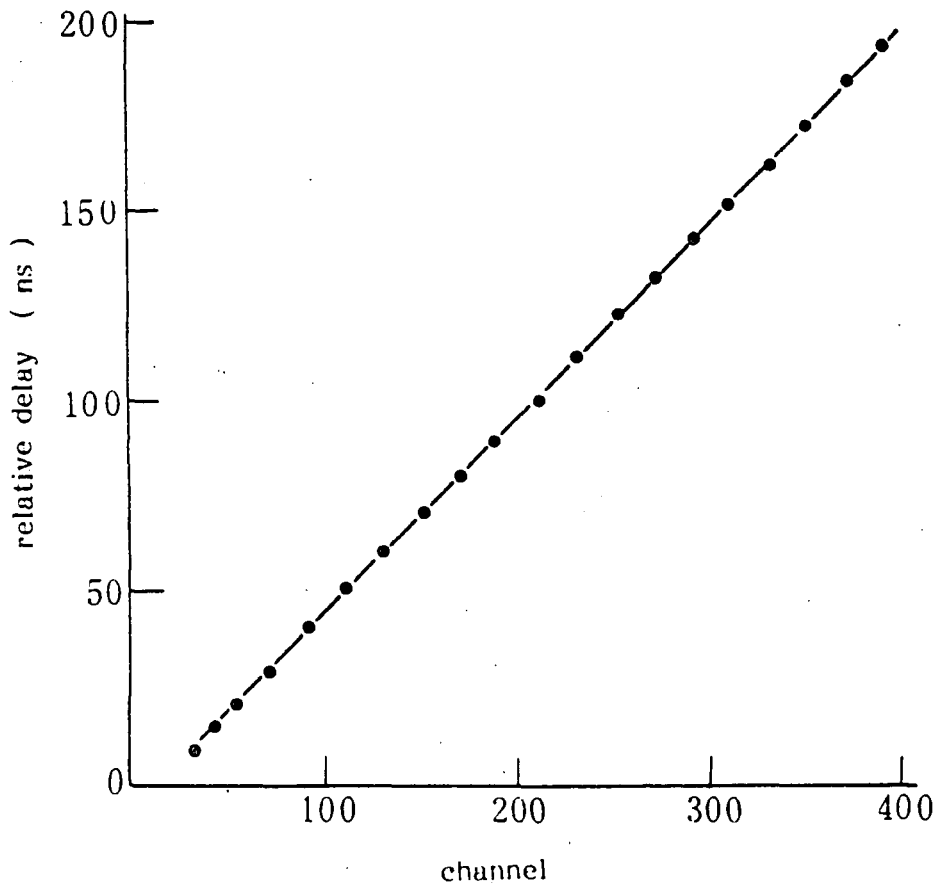

Fig.2 Linearity of the spectrometer

2. Experimental procedure

The details of the α-particle associated TOF spectrometer have been described previously[4]. Here a brief introduction is given only. Fig. 1 shows the experimental arrangement. 14.2 MeV neutron is produced at the Cochcroft-Walton accelerator through the $T(d,n)^4He$ reaction in the 90 degrees with respect to the deuteron beam. The ^{238}U sample is a hollow cylinder of depleted uranium metal with an outside diameter of 3 cm and an inside diameter of 1 cm and a height of 3 cm. The neutron detector is composed of an ST-451 liquid scintillator (ϕ105x50mm) and an XP-2041 photomultiplier tube. The detector bias is 1.75MeV. γ—produced background is reduced by exploiting a pulse shape analyzer. The distance between the neutron detector and the sample is 3.055 meters. The time resolution of the spectrometer is 1.2 nanoseconds.

The linearity of the spectrometer is shown in fig.2. The integral linearity is better than 1% and the differential one better than 2%. the neutron detector efficiency is calibrated by measuring the n-p scattering angular distribution and shown in fig.3. The measured efficiency is fitted with orthogonal polynomials. Its uncertainty is about 1%(except for two points near the threshold).

To obtain the neutron energy spectrum in 4π space, the measurement is performed at 13 angles in a rather wide angular range 15 to 155 degrees. For comparing with nuclear theoretical calculations, the measurement is focused on the spectra at 25, 45, 60, 75, 120 and 145 degrees, of which the uncertainty of 5% (for the lower part of the spectrum, i.e. E_n<8 MeV) or 10% (for the higher

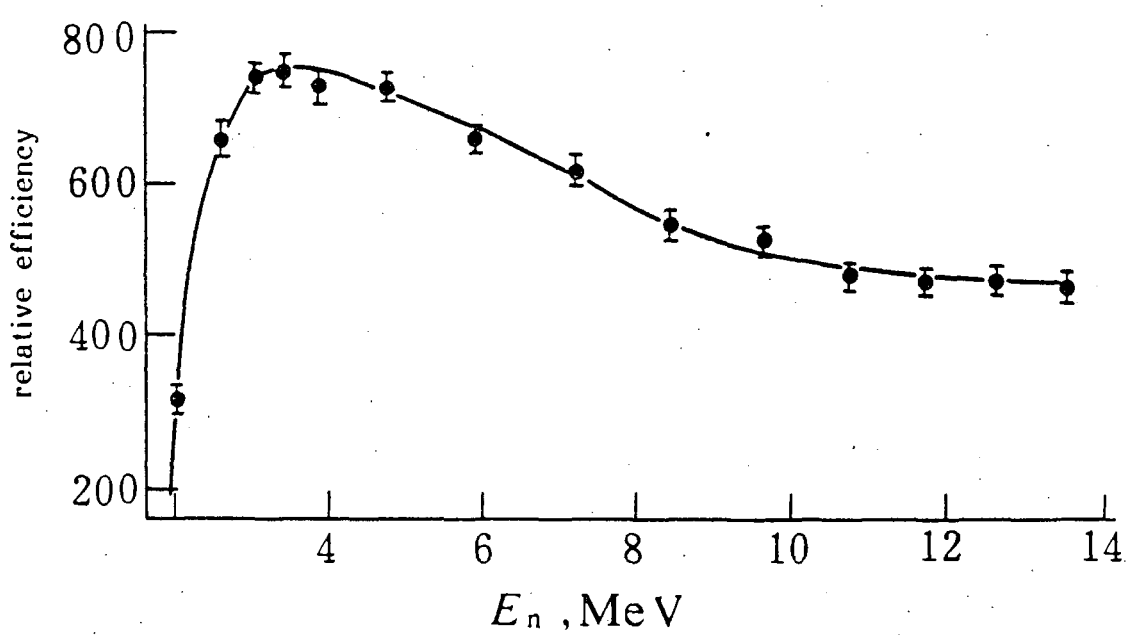

Fig.3 Neutron detector efficiency

•--measured value,

——--fitted curve with orthogonal polynomials

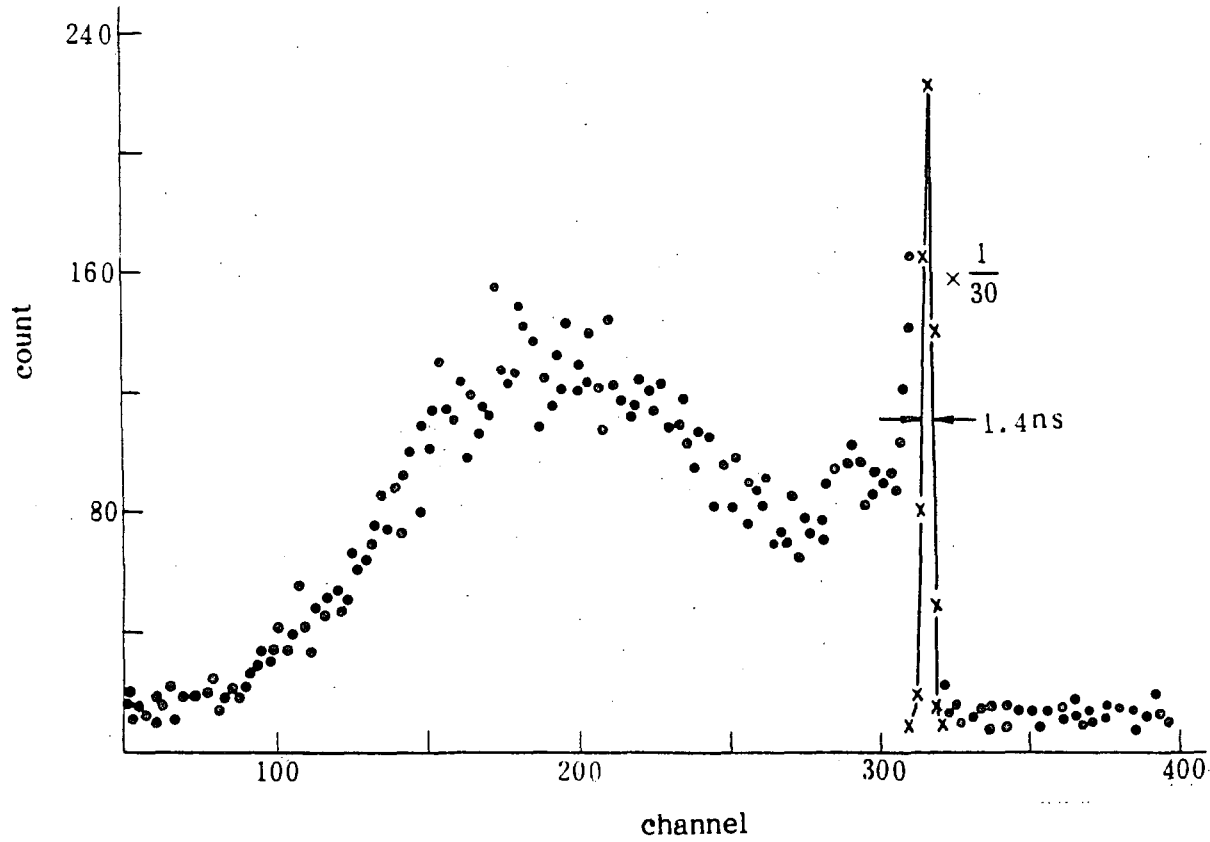

Fig. 4 Neutron TOF spectrum of ^{238}U induced by 14.2 MeV neutrons

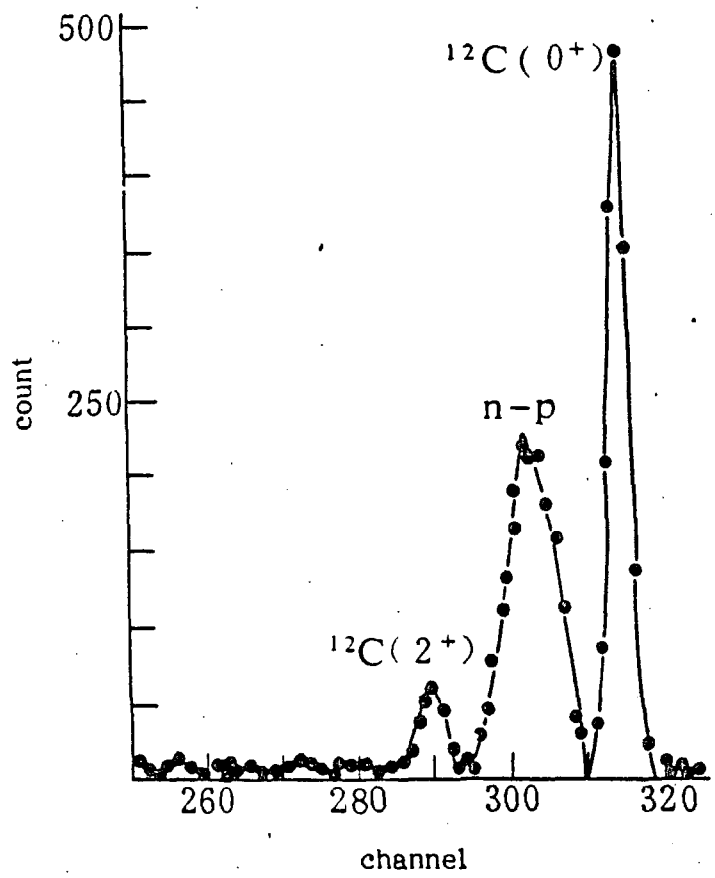

Fig.5
Neutron TOF spectrum scattered from polythene sample by 14.2 MeV neutrons

part, i.e. 8 MeV$<E_n<$12.5 MeV) is required. Fig. 4 shows a measured neutron TOF spectrum of ^{238}U at 35 degrees. During the measurement, the stability of the instruments is monitored, the detector bias is frequently checked and the alpha-particle counting rate is kept as constant as possible.

To get the absolute value of the double differential cross sections of ^{238}U, the n-p scattering differential cross section at 25 degrees is used as a reference standard. Fig.5 shows a neutron TOF spectrum at 25 degrees measured with a polythene sample being of the same size as ^{238}U sample and under the same experimental condition as the ^{238}U measurement. From fig.5 it can be obviously seen that the n-p scattering peak is completely seperated with elastic and inelastic peaks of ^{12}C.

3. Data reduction

After subtraction of the background and the "tail" of the elastic scattering peak, the net neutron TOF spectrum of ^{238}U is obtained. For the measurements at angles which are greater than 35 degrees, the average counts on the right hand side of the elastic peak is used as the background. For the measurements at angles which are less than or equal to 35 degrees, time—correlated background, which decreases with the increase of the angle, should be considered. Sample-out measurements are required. Fig.6 shows a background TOF spectrum measured at 20 degrees.

The incident neutron TOF spectrum is used for elastic "tail" subtraction.

The net neutron TOF spectrum is converted into neutron energy spectrum. Considering the time resolution of the spectrometer, a 0.2 MeV energy interval is chosen in the 2—5 MeV region of the spectrum, a 0.25 MeV in the 5—8 MeV region and a 0.5 MeV in the 8—12.5 MeV region.

The double differential cross sections of ^{238}U is obtained by the following expression

$$\sigma(E_i,\theta)=\frac{N_u(E_i,\theta)}{N_H(25^o)}\cdot\frac{n_H}{n_u}\cdot\frac{\varepsilon_H(E_H)}{\varepsilon_u(E_i)}\ \sigma_H(25^o)$$

where θ is the scattering angle in the laboartory system, n_H and n_u are the numbers of hydrogen nuclei in the polythene sample and of ^{238}U nuclei in the ^{238}U sample respectively, $\varepsilon_H(E_H)$ and $\varepsilon_u(E_i)$ are the neutron detection efficiencies respectively for n-p scattering neutrons at 25 degrees and neutrons with energy of E_i, $N_H(25^o)$ is the total counts of the n-p scattering peak at 25 degrees. $N_u(E_i,\theta)$ is the counts in the energy interval between E_i and $E_i+\Delta E$ of the spectrum at the angle of θ, $\sigma_H(25^o)$ is the n-p scattering differential cross section at 25 degrees, for present work $\sigma_H(25^o)$=192.1 mb/sr.

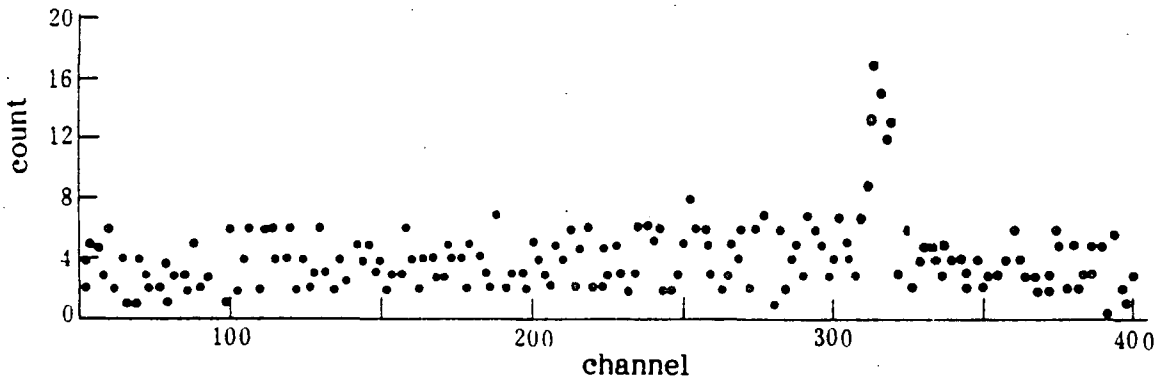

Fig.6 Sample--out TOF spectrum $\theta_L=20^o$

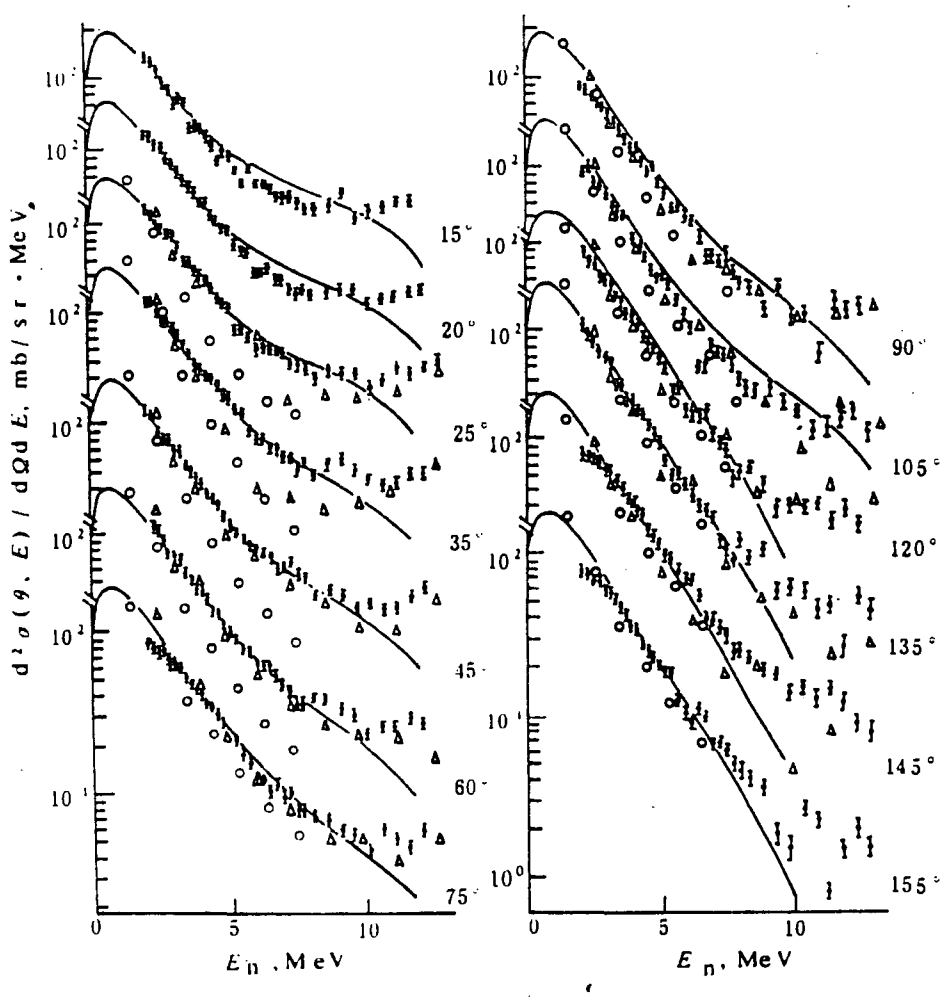

Fig.7 double differential neutron emission spectra of ^{238}U induced by 14.2 MeV neutrons

●—present work, △—Kammerdiener,

○—Voignier, solid curve—evaporation model calculation

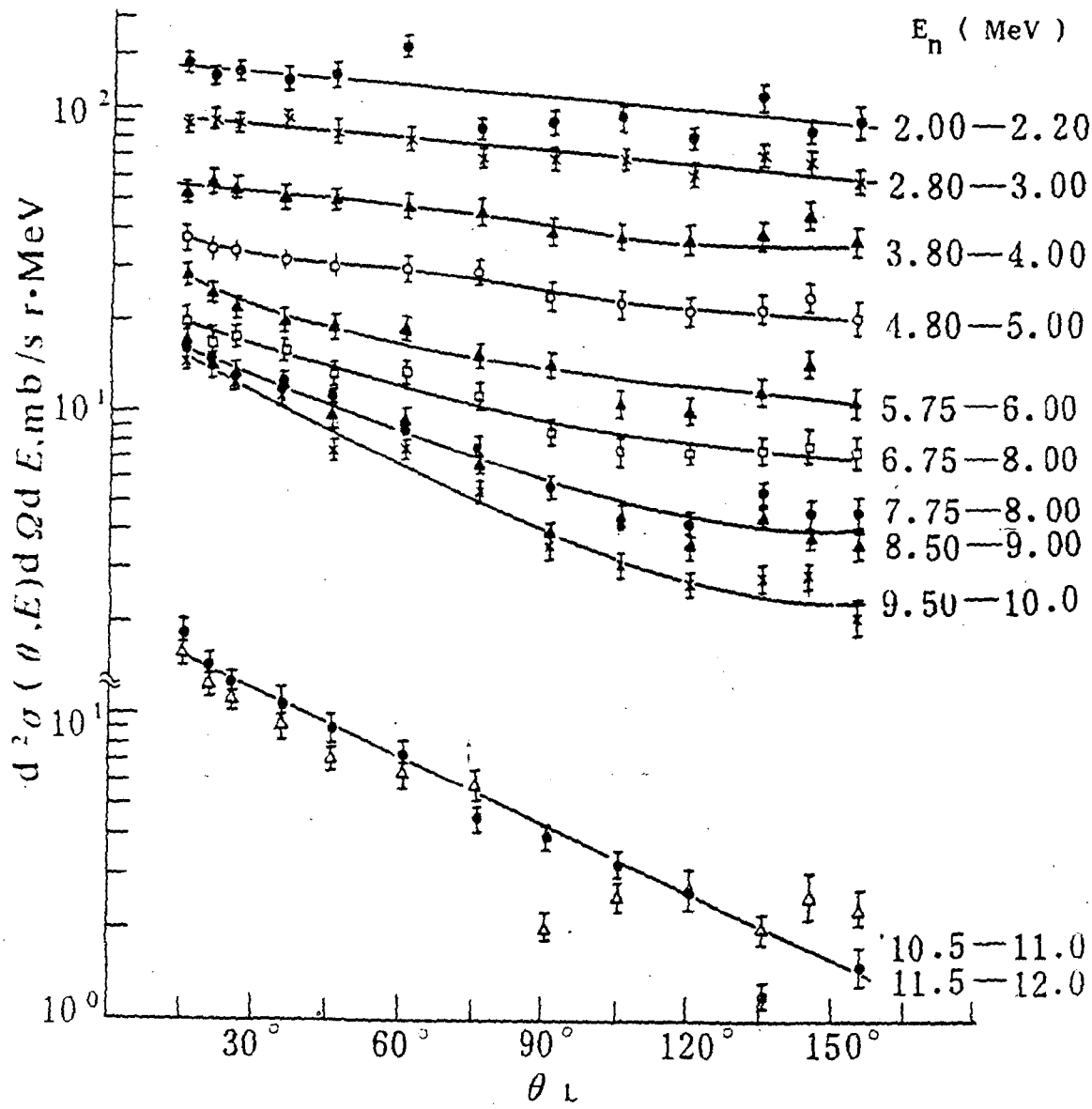

Fig.8 Double differential cross section angular distributions of ^{238}U measured by present work

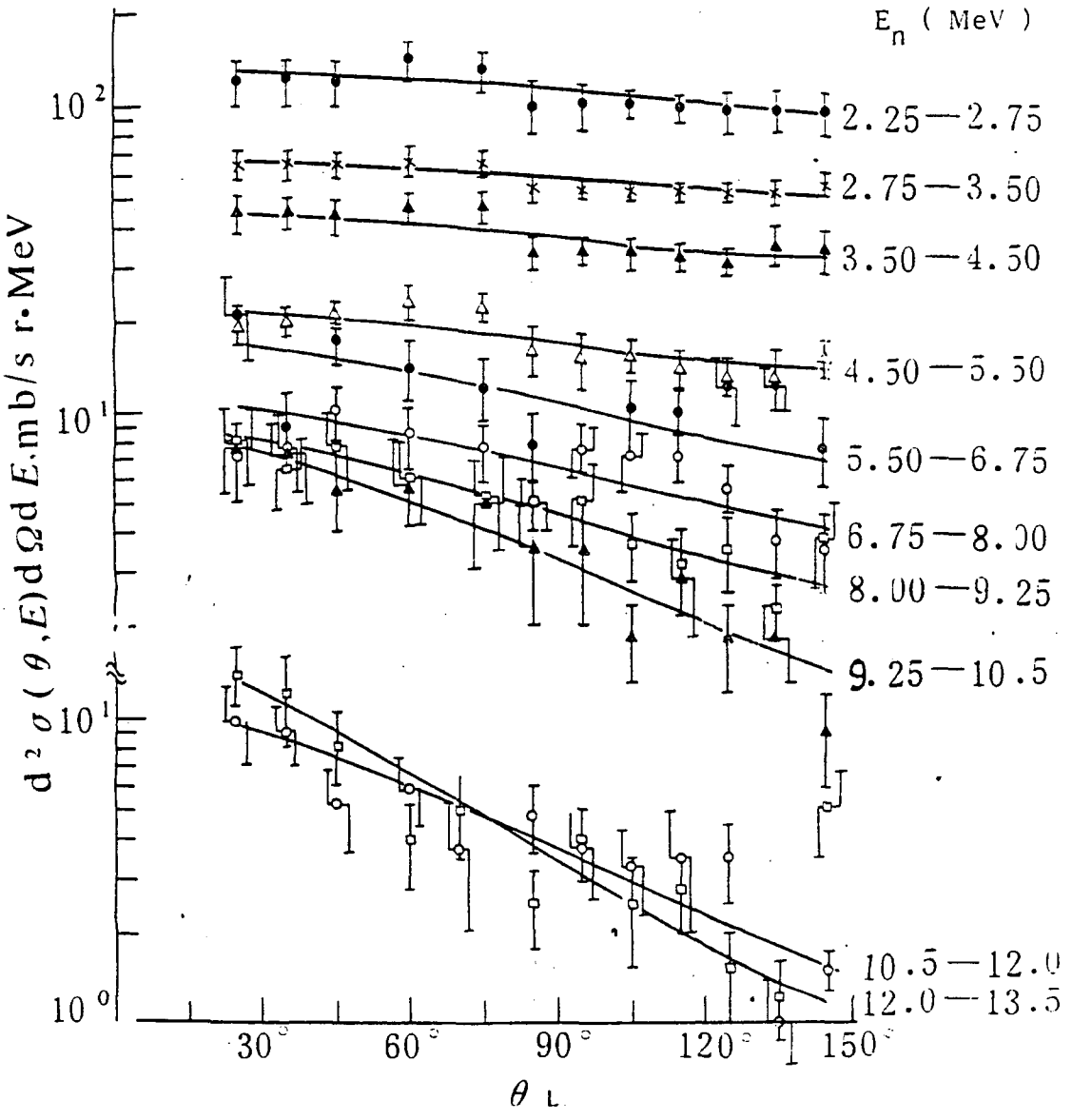

Fig.9 Double differential cross section angular distributions of ^{238}U measured by Kammerdiener et al.

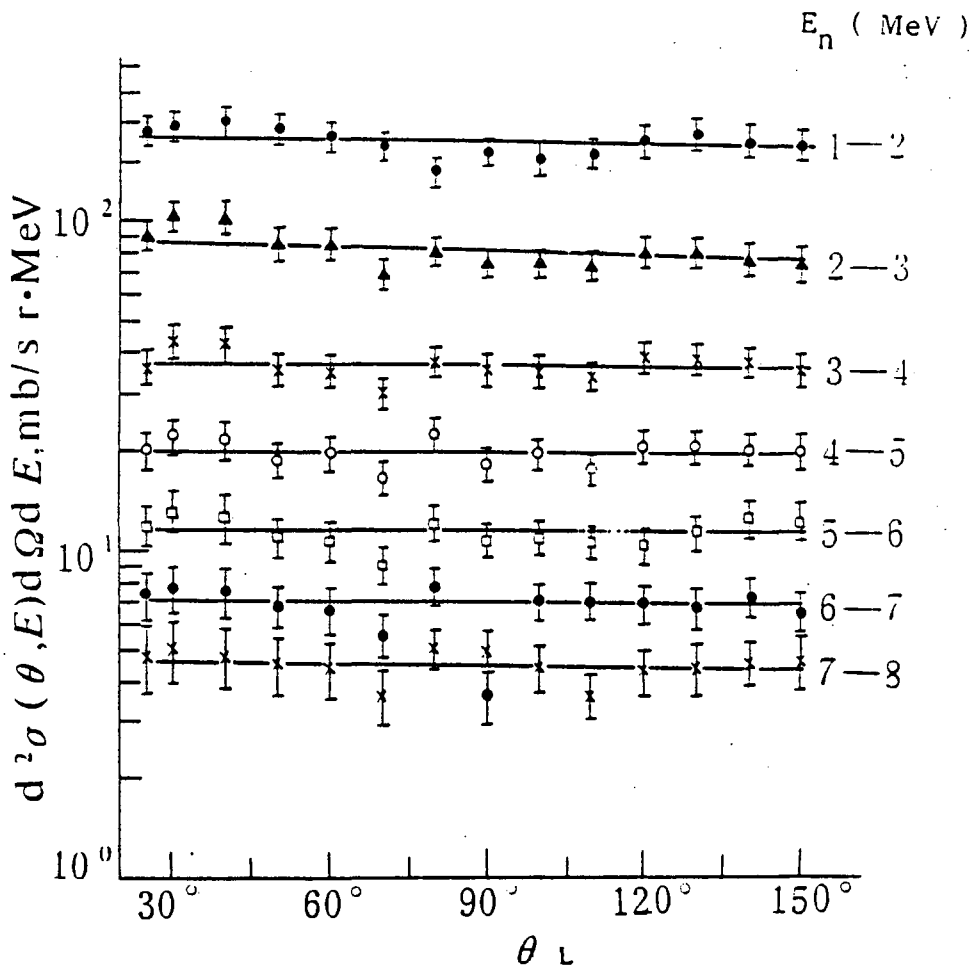

Fig.10 Double differential cross section angular distributions of ^{238}U Measured by Voignier et al.

4. Results

The measured double differential neutron emission cross sections at different angles together with the results of Voignier and Kammerdiener are shown in fig.7. Generally, present data and Kammerdiener's results are in agreement within the experimental error. The count statistics of the present work is better than the two others, especially in the greater than 8 MeV region. The experimental result is compared with theoretical calculations of the evaporation model with preequilibrium emission mechanism. A good agreement is achieved for the region of less than 10 MeV. For the higher part of the spectrum, the calculation is much lower than the measurement, because direct inelastic scattering is not included in the calculation.(5).

The angular distribution of double differential cross sections is shown in fig.8. For comparison, the results of references (2) and (3) are in figs.9 and 10 respectively. It can be seen from figs.8 and 9 that when $E_n \geq 5$ MeV, the angular distributions are forward peaked. For the angular distribution of 11-13 MeV energy neutrons, the cross section at the small angle is an order of magnitude higher than that at large angles.

TABLE 1 ERRORS AND THEIR SOURCES

error source	E_n(MeV)	2—4	4—6	6—8		8—10		10—12					>12				
	θ(degree)	15—155	15—155	<75	≧90	<75	≧90	15	20	25	30—75	≧90	15	20	25	30—75	≧90
count statistics (%)		2—5	3—7	4.5—9	6—12	5—8	9—13	8.2-9	6-6.5	6.9-7	6—9	10-14	4-6.5	4-6.3	4-6.7	2—7	6—15
$\sigma_{n-p}(25^o)$		3% for the whole energy region															
count of n-p scattering peak		3% for the whole energy region															
detector efficiency		1% for the whole energy region															
Monte-carlo correction		0.1--0.5% for the whole energy region															
dead time correction		0.3% for the whole energy region															
number of ^{238}U nuclei		less than 10^{-5}, neglected															
time-correlated background								1%	1%	1%			1.5%	1.5%	1.5%		
subtraction of the elastic peak								6%	1.5%	0.5%			9%	5%	1%		
overall error, %		4.8-6.7	5.3-8.3	6.3-10	7.4-13	6.7-9.1	10-13	11-12	7.7-8.1	8-8.5	6.7-10	11-14.7	11-12	7.9-9.3	6.3-8	4.8-8.3	7.4-15.6

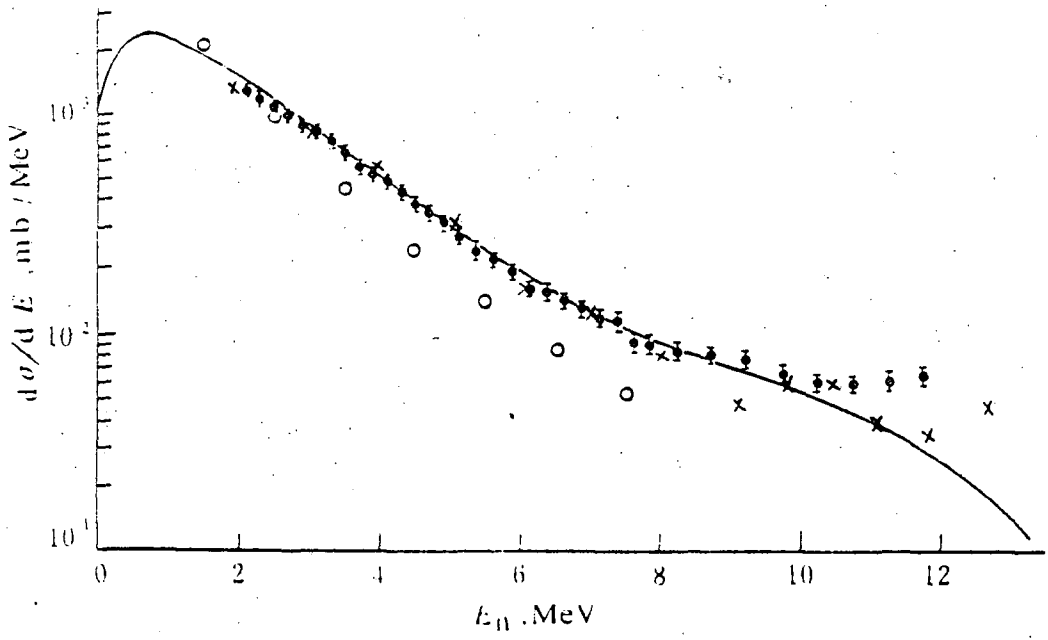

Fig.11 The integral spectrum over the whole space
● --present work, O-- Voignier's data
x -- Degtyarev's data, obtained by averaging over the emission angles in the forward semisphere
solid curve --calculations of the evaporation model with preequilibrium emission mechanism

The integral spectrum of ^{238}U over the whole space is shown in fig.11.

The error varies with the angle and spectrum neutron energy. The typical value and sources of the errors are listed in table 1. The major error sources come from count statistics and n-p scattering differential cross section. The error due to subtraction of the "tail" of the elastic scattering peak is decreased with the increase of scattering angles in the small angle region. At the angles which are greater than 25 degrees, it can be neglected.

References

1. Bertrand,F. et al.,CEA-R-4132,1971.
2. Voignier,J.J. et al., CEA-R-3503, 1968.
3. Kammerdiener,J.L. et al., UCRL-51232, 1972.
4. A.P.Degtyarev et al., Sov. J. Nucl. Phys. 34(2), Aug. 1981
5. Shen Guanren et al., Chinese Journal of Nuclear Physics,6,193(1984)
6. Shi Xiangjun et al., Chinese Journal of Nuclear Physics,9,16(1987)

The Research of Isomeric Cross-sections for In(n,n') Reactions at 14 MeV

Lu Hanlin, Ke Wai, Zhao Wenrong, Yu Weixiang, Yuan Xialin
(Institute of Atomic Energy, P.O.Box 275(3), Beijing, China)

1. Introduction

The In(n,n') reactions are very useful in the measurement of fast neutron spectra in fission and fusion reactors for its low threshold and high cross-section. It seems easy to determine the activities of the metastable states quite accurately, however, contrary to this expectation, there is a large scatter in the results at E_n=14 MeV.

As H.Vonach has once said, "Our knowledge of cross-sections for formation of metastable states in (n,n') reactions at E_n=14 MeV is still very poor. Most measurements suffer from large systematic errors due to the 'contamination' of the used 14 MeV neutrons with low energy and an accurate absolute calculation of such cross-sections is not possible at present."

In(n,n') reactions were once measured by us in 1978[1]. But systematic errors were found with the recent Monte-Carlo calculation to determine the effects of neutron scattering in the sample and the target system. Therefore effort was made to determine, and try to reduce, the correction of lower energy neutrons in our laboratory.

2. Experimental Procedure

The $^{115}In(n,n')^{115m}In$, $^{113}In(n,n')^{113m}In$ and $^{115}In(n,2n)^{114m}In$ reaction cross-sections were measured by activation method. The neutron source was the $T(d,n)^4He$ reaction produced by 200-keV deuterons at the IAE Cockcroft-Walton accelerator and 1.75-MeV deuterons at the IAE Van der Graaff accelerator on a solid T-Ti target (0.3-1.9 mg/cm^2 Ti).

The samples to be irradiated were natural metal foils of 15-mm diameter in the absolute measurements with a purity better than 99.9%; in the relative measurements the samples were 15mm x 5mm wide and 0.5 mm thick.

The neutron flux was determined by associated particle counting, with an accuracy +- 1.0% at 14.58 MeV. The sample employed for the absolute measurement was placed at 7-10 cm from the target and at 45° with respect to the deuteron beam. Irradiation usually lasted ten hours for (n,2n) reaction.

Because the neutron flux was rather weak for the activity measurement of product nuclei of short-lived, such as ^{115m}In, it's necessary, then, to irradiate the samples at distance as close to the target as possible to obtain the enough

activities. In our case, the distance was 3 cm. However, this measurements only provided with the ratio of cross-sections for (n,n') and (n,2n) reactions occured in the samples.

The γ-activities of the irradiated samples were measured with a well calibrated Ge(Li) spectromater. The energies of γ-rays of the product nuclei of interest and their half-lives and intensities were given in Table 1.

Table 1: Nuclear data

Isotope	Half-life	r-ray (keV)	Intensity (%)
^{113m}In	(1.658+-0.001)h	391	64.89+-0.17
^{114m}In	(49.51+-0.01)d	190	15.70+-0.18
^{115m}In	(4.486+-0.004)h	336	45.9 +-0.1

3. Corrections

The main corrections of (n,n') reaction are on the impurity of neutron field. The neutron field of $T(d,n)^4He$ reaction is always contaminated by d-D and evaporation neutrons which are produced in the vicinity of neutron source and the samples.

The cross section of (n,n') reaction at $E_n \sim 2$ MeV is several (3 - 6) times higher than at 14 MeV, so the contributions of lower energy neutrons are quite large and should be corrected appropriately.

A. Corrections for d-D neutrons

d-D neutrons in 14-MeV neutron field are produced by the incident d beam on the accumulated D on the target.

Deuterons were accumulated in the magnetic analyzer, collimator of beam and the target by the bombardment of D beam. The contributions of former two were rather weak, since the sample was placed far away from them. Those geometrical arrangements for the irradiation of sample leaded to the d-D source of target foil only, which must be determined carefully.

In the measurements of (n,n') reaction cross section, new T-Ti target was used to reduce the presence of d-D neutrons. At the other hand, under the same experimental condition the associated porticle method and activate method (target without T) were employed to measure the ratio of neutron flueuce of d-D and D-T. Geometrical arrangement was shown in Fig.1.

The 90° tube relative to the deuteron beam was used to measure the fluence of 14-MeV neutrons produced on the T-Ti target by D-T reaction (ϕ_T); 135° to measure the fluence of 3-MeV neutrons by D-D reaction. (ϕ_D)

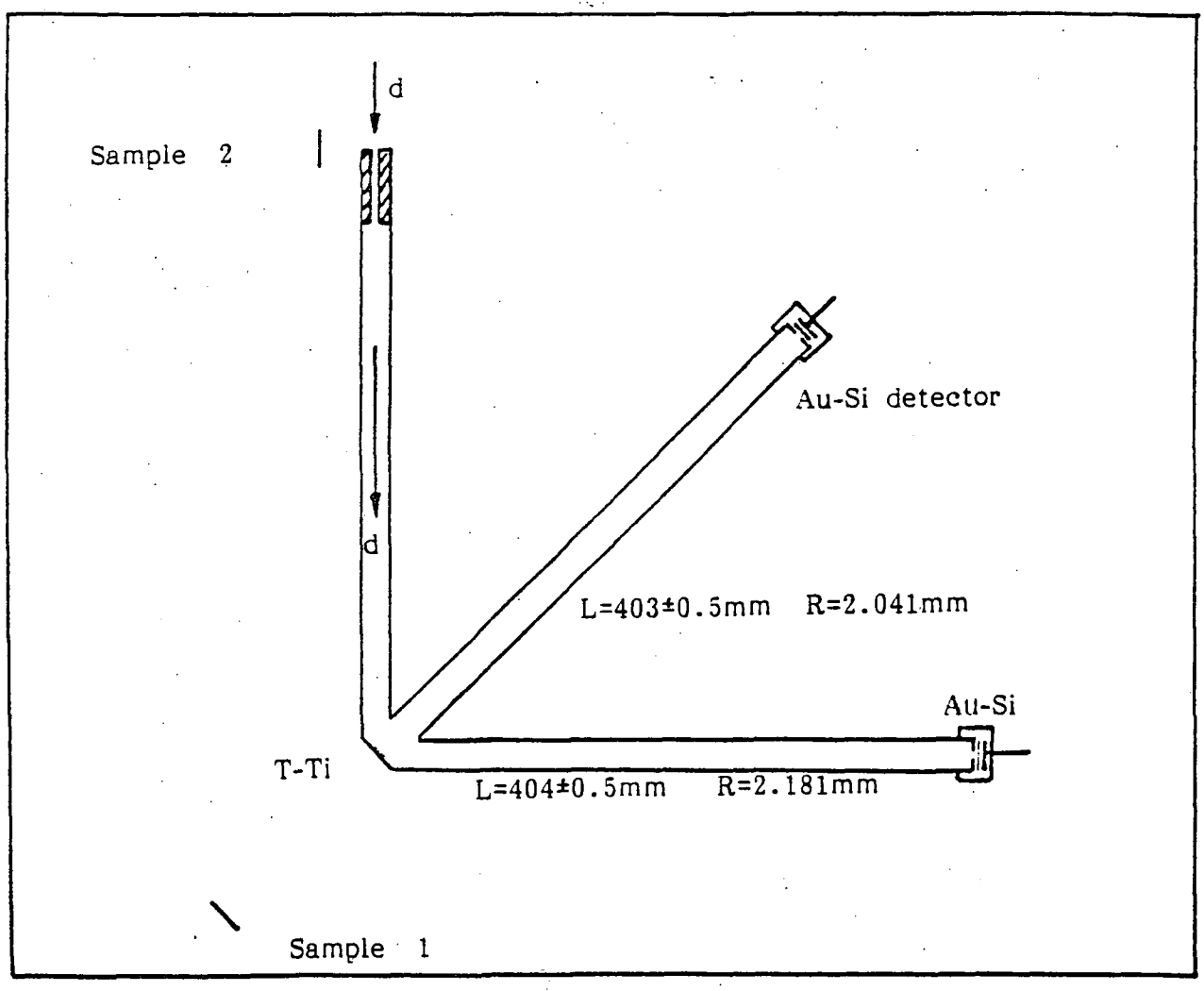

Fig. 1. Geometrical arragement for determination of D-D reaction

$$\phi_T = \frac{N_\alpha}{\Delta\Omega_\alpha} A_\alpha \quad \ldots\ldots\ldots\ldots (1)$$

$$\phi_D = \frac{N_p}{\Delta\Omega_p} A_p \quad \ldots\ldots\ldots\ldots (2)$$

where N_α and N_p denote the count rates of α particles and protons detected; $\Delta\Omega_\alpha$ and $\Delta\Omega_p$ are solid angles of two detectors with respect to the neutron source; A_α and A_p, factors of anisotropy of α particles and protons. From eqns (1) and (2), we get

$$\phi_D / \phi_T = \Delta\Omega_\alpha A_p N_p / \Delta\Omega_p A_\alpha N_\alpha$$

Fig.2 shows the proton spectra after a new target is used for two hours and five hours respectively, with the background of Si(n,x) reaction at neutron energy 14 MeV. With the incessant accumulation of deuterons ϕ_D / ϕ_T will vary with the time as shown in Fig.3.

The results show that in the first five hours of irradiation of a target, the contribution of D-D neutrons in (n,n') reactions is about 0.27%. The experiment

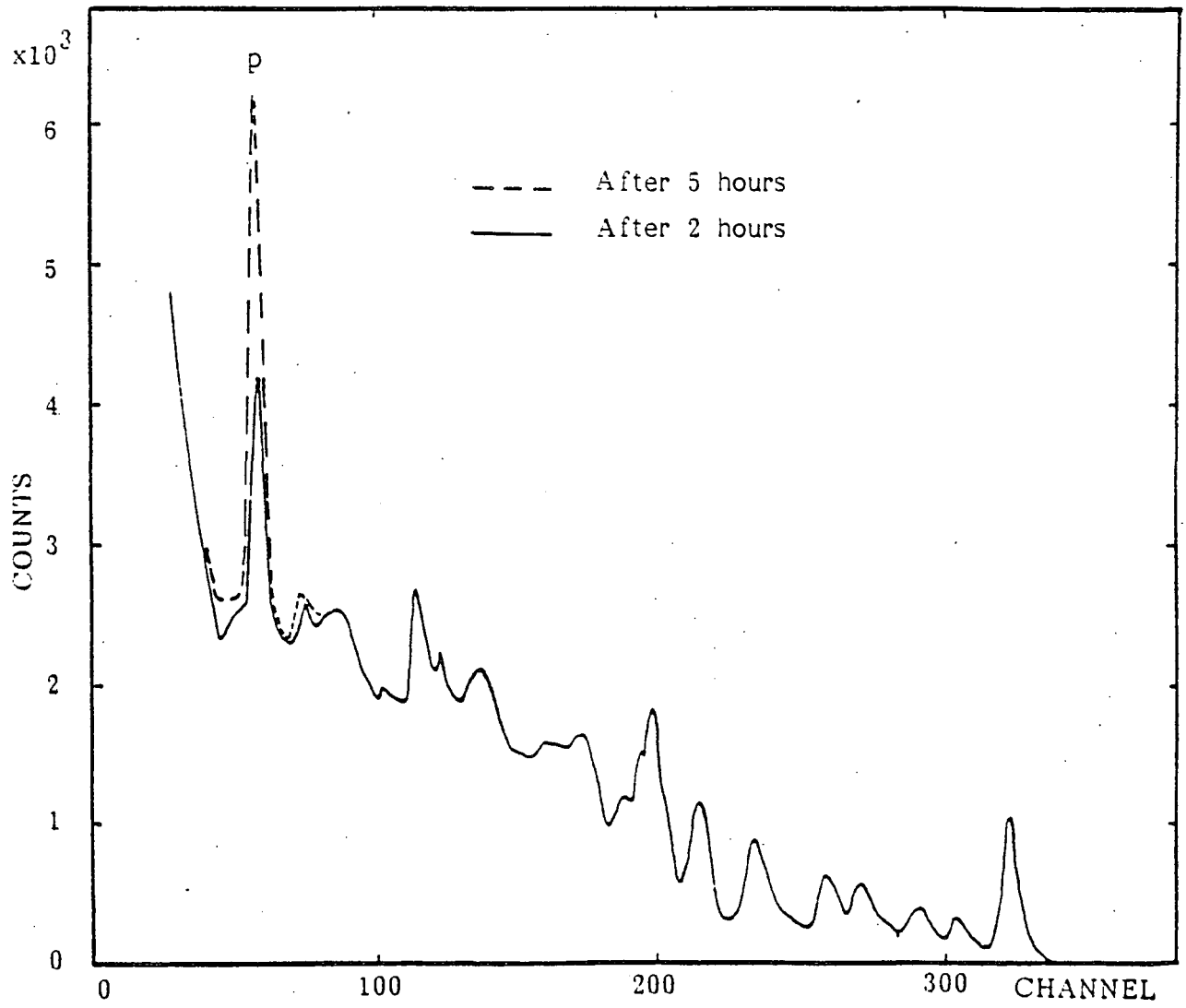

Fig. 2. A typical proton spectra of D-D reaction ofter a new target is used for two and five hours

using no-tritium-targets shows an effect of 0.2%. Under our experimental conditions, corrections could amount up to (8+-4)%, so we should limit the beam time of irradiating a target. The value of corrections for a five hours of irradiation is (0.25+-0.05)%.

Ryves (83)[3] estimated that corrections for these neutrons would reduce the measured (n,n') cross sections by (2.5+-1.5)%. This effect has been previously observed by Decowski (73). The reason that their corrections were larger than ours was they used rather old T-Ti targets.

B. Corrections for neutron scattering at target assemblies and activation sample

Another important source of contamination of the 14-MeV neutron field comes from the interaction between the incident neutrons and the target assemblies. The lower energy neutrons are produced by (n,n') and (n,2n) reactions. We try to reduce the mass of the target assemblies and samples to reduce the contaminations.

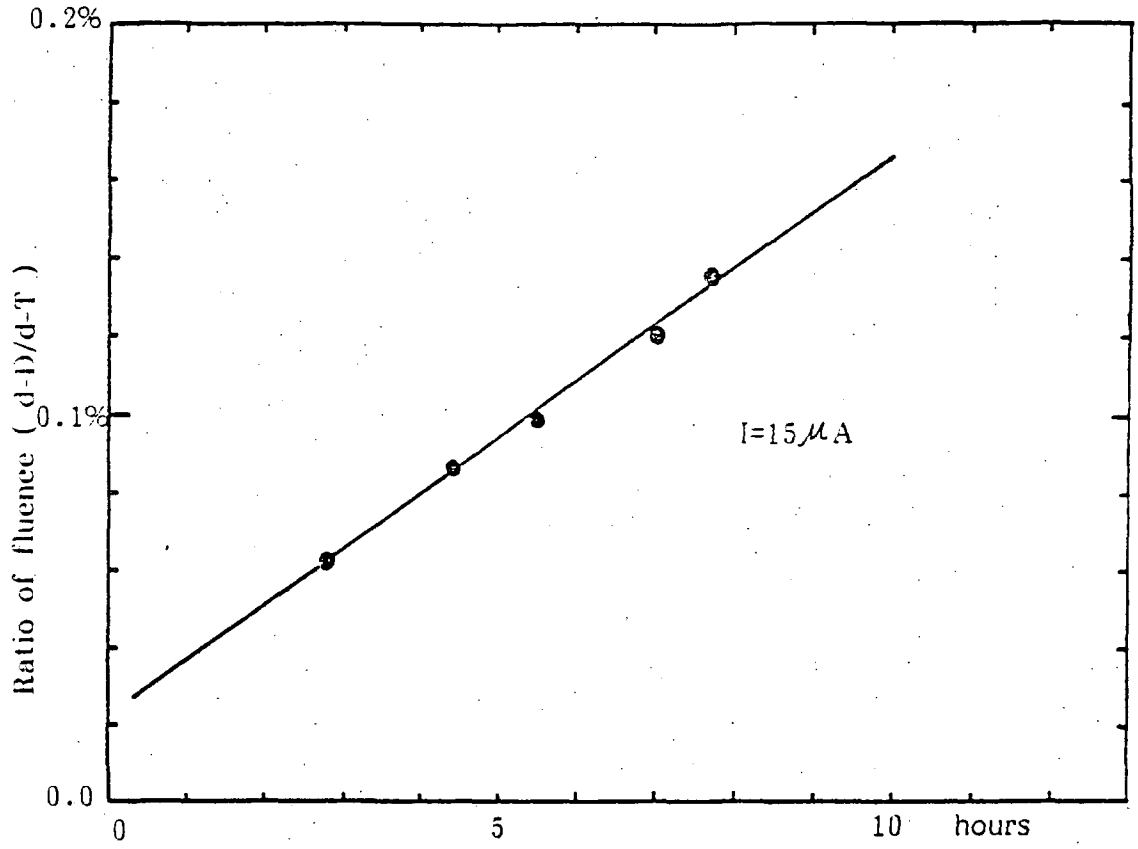

Fig. 3 Ratio of fluence with time of irradiation

The T-Ti target foil with Mo backing (0.3mm in thickness) was fitted on to a thin-walled Cu beam tube (0.2-0.25mm in thickness, 23mm in diameter). But even 1% of the low energy neutrons would make the cross sections larger by 5%. Therefore corrections should be made very carefully. We simulated the experimental process by Monte-Carlo method and the calculation results showed that the effects of low energy neutrons on the high-thresholded $^{115}In(n,2n)^{114m}In$ reaction were small while those on the (n,n') reaction quite large.

Because of the different situations at all laboratories, scattering corrections for the target assemblies are difficult to compare to each other directly, though scattering corrections for the samples, which have something to do with the thickness of the samples, could be compared. The results given by Anderson[7] were 2.5% for a sample of 1 mm thick whereas 1.5% for a sample of 0.25 mm thick given by Ryves. Our calculations show a 0.8% correction for a sample of 0.5 mm thick. We can see that the discrepancies are large, to decrease the errors of this correction thin samples should be used. The results of Monte-Carlo scattering correction are given in Table 2.

Those neutrons that are scattered many times in the experimental hall distribute evenly with their energies becoming very low. Generally we place samples far from the neutron source to measure the effect of background neutrons. Another method is using the fact that neutron source intensity is inversely proportional to the square of distance. Both measurements showed

Table 2 : Corrections and Uncertainties

Source	Correction (%)			Uncertainty (%)		
	^{115m}In	^{114m}In	^{113m}In	^{115m}In	^{114m}In	^{113m}In
1, Neutron from $D(d,n)^3He$ reaction	0.25		0.2	0.05		0.05
2, Neutron scattering effects due to target system	7.2	1.2	5.5	2.2	0.3	1.8
3, Neutron scattering by sample	0.8	0.3	0.6	0.4	0.1	0.3
4, Neutron absorption in the target backing		1.6			0.2	
5, Gamma ray self-absorption in sample	4.0	7.2	3.4	0.4	1.0	0.4
6, Sample area effect	0.6	1.0	0.6	0.1	0.3	0.1
7, Variation of neutron yield		0.1----3.5		0.2	0.1	0.2
8, Detector efficiency or activity ratio				1.5	1.7	1.5
9, Neutron fluence or standard cross section				2.4	1.2	2.4
10, Angular distribution of neutron				1.0	1--3	1.0
Total				3.6	2.4	3.4
Excitation curve				3.7	3.8	3.6

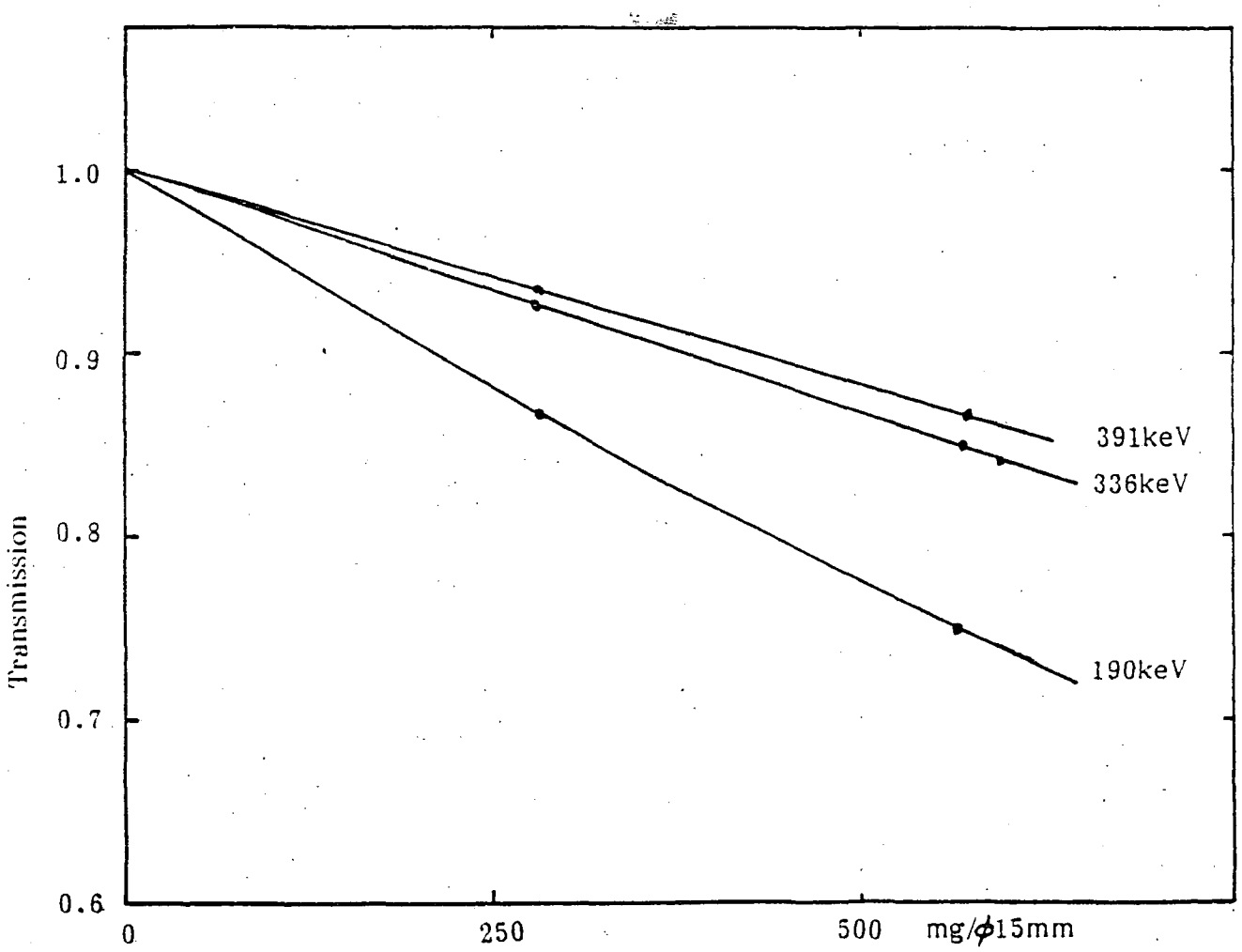

Fig. 4. The transmission for the indium source v.s. thickness of sample

within the precision of the experiment no obvious interference of these neutrons existed, so this term of corrections was negligible.

C. Other Corrections

The corrections for the fluctuation of neutron fluence during irradiation were made. These corrections amount to (0.1-3.5)%. Corrections were also made for the sample's finite area and self absorption. The curve of relative photopeak efficiency off the centrial axial was measured with an indium sample of 3 mm in diameter, and the corrections thus obtained for a sample of 15 cm were 1.0% and 0.6%, for ^{114m}In and ^{115m}In respectively. The transmission measurements were performed using absorption method to determine the sample-thickness dependence of the detector efficiency for different γ-rays and these corrections amount to 3.4% through 7.2% as shown in Fig.4.

All corrections and errors considered in the measurements of In(n,n') and (n,2n) cross section were listed in Table 2.

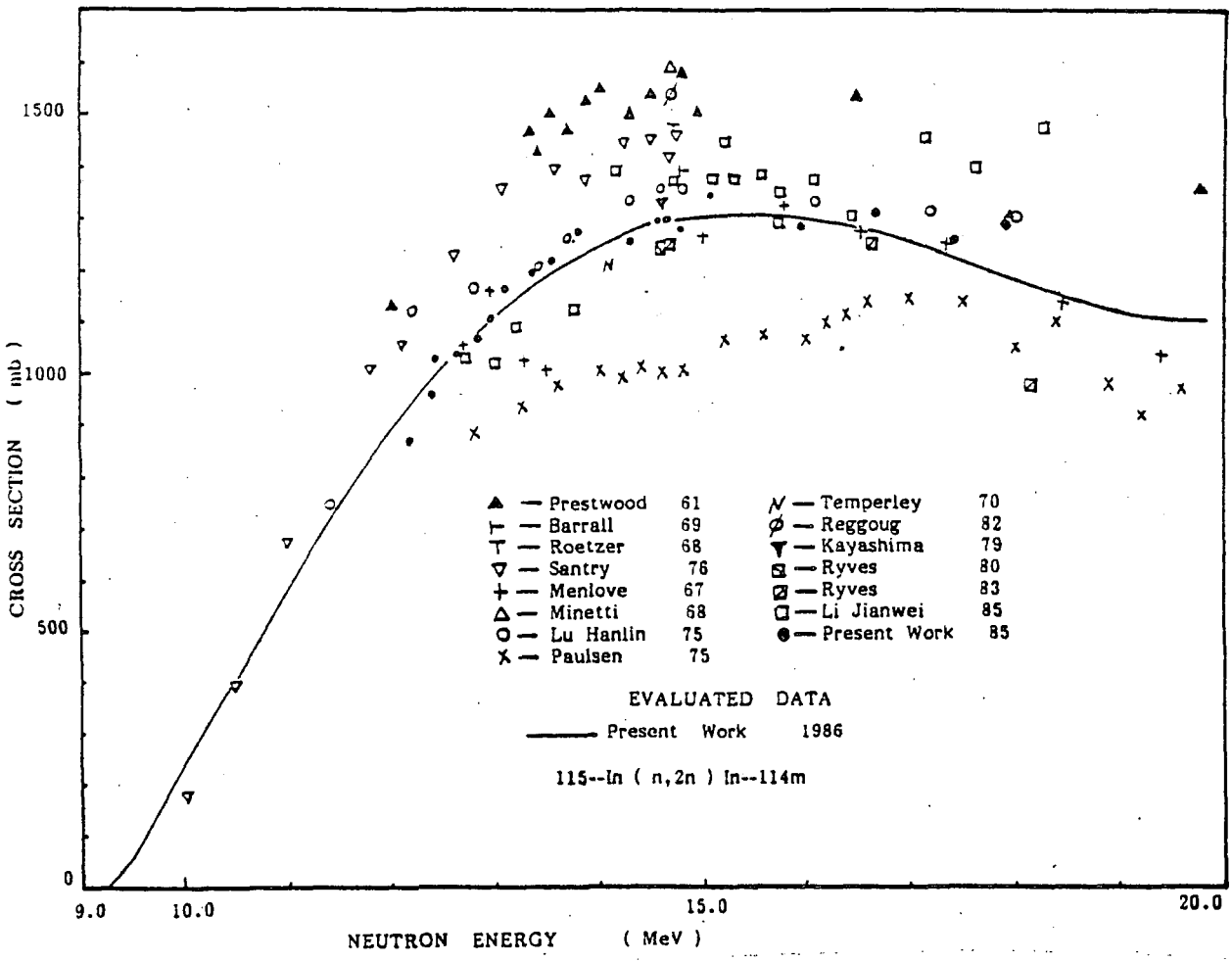

Fig. 5. The cross section for ^{115}In (n,2n) ^{114m}In reaction

4. Results and Discussions

First, we consider the (n,2n) reaction which serves as the flux standard for the (n,n') reactions in our measurements. From Fig.5 we can see a large scatter in the results of different investigators. If we renomalize the results of Prestwood,(25) Santry,(14) Menlove,(6) Lu Hanlin(26) and this work with the same cross section value, we can get the results quite consistent with each other at 9-20 MeV. (Fig.6) So the large discrepancies between the existing (n,2n) data were due to the measurement of absolute cross sections. The standard cross sections and decay data used in the calculation of cross sections could be adjusted, however, even done so, large discrepancies still existed. The principal reason was the errors in the ^{114m}In activity measurement (especially by NaI(Tl) spectrometer). There are two measurements with high accuracy, Ryves's and our work. (Errors less than 3%) Our results are 1296+-32 mb at neutron energy 14.57+-0.23 MeV.

(n,n') reaction

The cross sections of $^{115}In(n,n')^{115m}In$ and $^{113}In(n,n')^{113m}In$ were shown in Fig.7 and 8 and Table 3 through 5. We can see even after adjustment to the standard cross sections and to the decay data, discrepancies still exist.

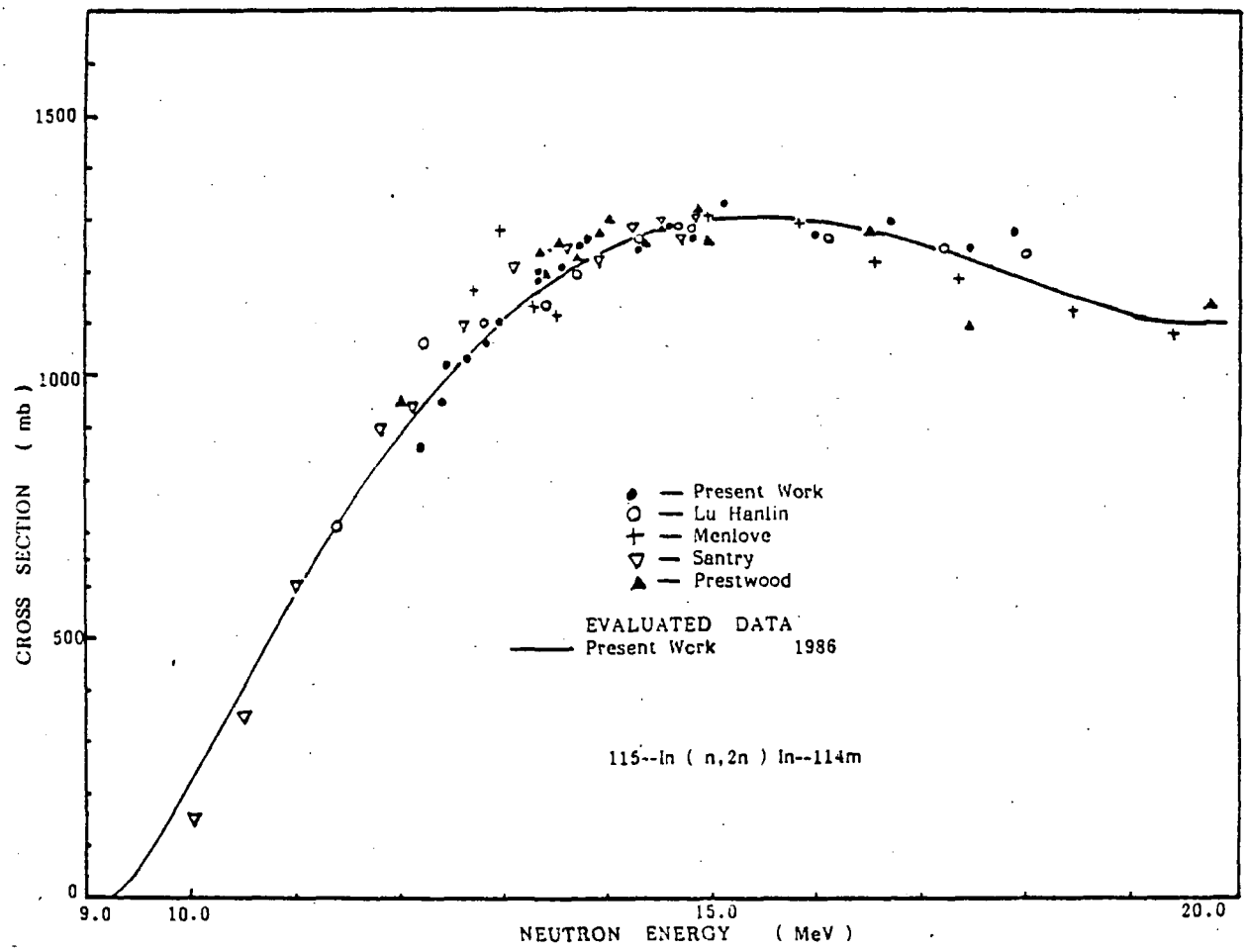

Fig. 6. The cross section renormalize with 1288mb at 14.6MeV

Table 3: Cross section results (mb)

En (MeV)	$^{115}In(n,n')^{115m}In$	$^{113}In(n,n')^{113m}In$
13.54+-0.11	67.2+-2.5	63.4+-2.4
13.72+-0.05	64.1+-2.3	62.2+-2.3
14.10+-0.30	54.4+-2.0	51.5+-1.9
14.31+-0.13	55.1+-2.0	54.3+-2.1
14.50+-0.30	54.3+-2.9	51.1+-2.4
14.58+-0.15	53.8+-2.0	51.0+-1.9
14.78+-0.15	50.8+-1.9	44.8+-1.7
14.80+-0.30	50.8+-1.8	49.7+-1.8

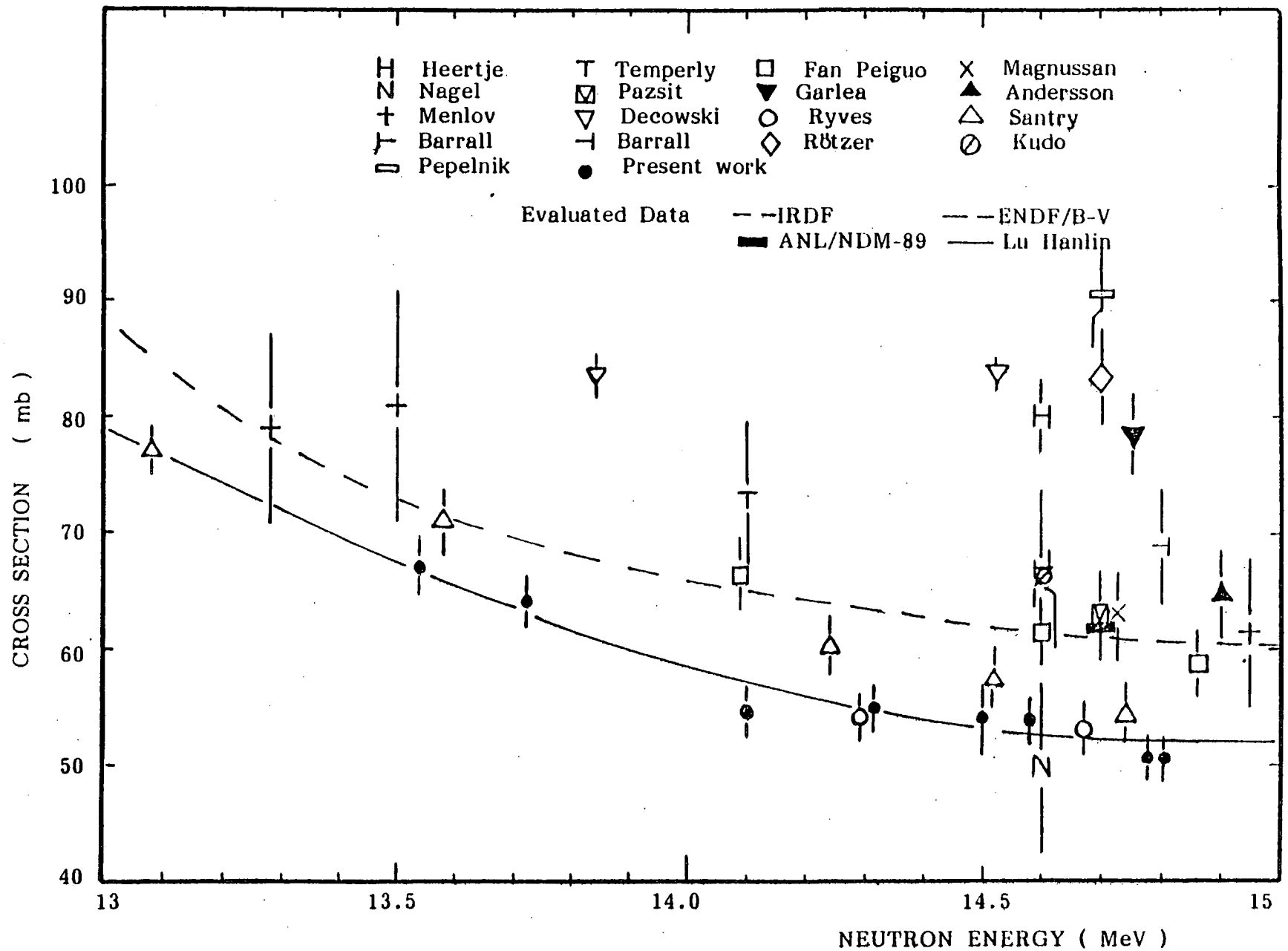

Fig. 7. The cross section for 115-In(n,n')115m-In reaction

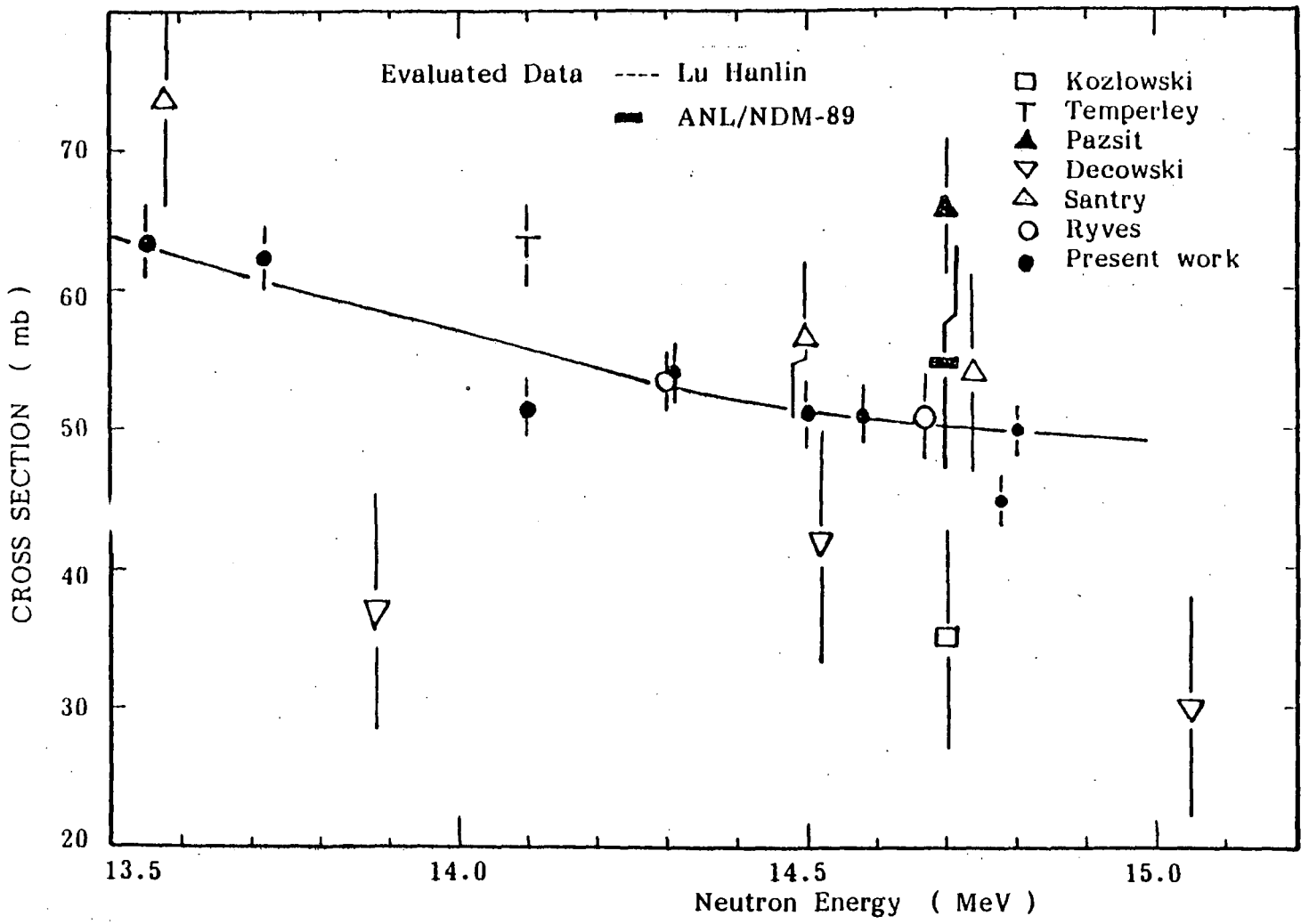

Fig. 8. The cross section for 113-In (n,n') 113m-In reaction

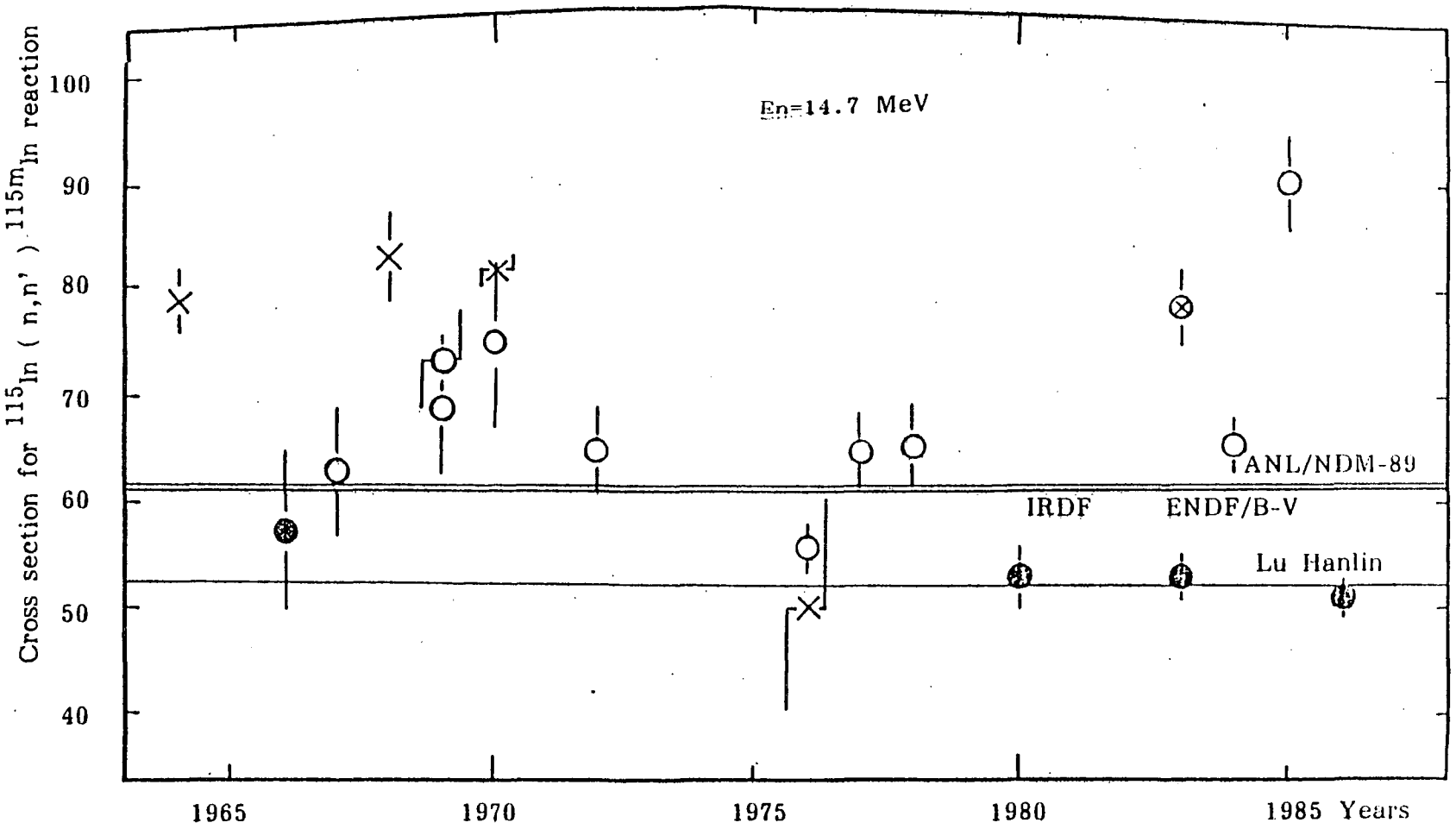

Fig. 9. The values of cross section for ^{115}In (n,n') ^{115m}In reaction with times of publication

Correction for low energy neutron	Adjusted for I_r and reference cross sections
● yes	yes
⊗ yes	no
○ no	yes
× no	no

Table 4: Cross section of $^{115}In(n,n')^{115m}In$ at 14 MeV

Authors		Ref.	En (MeV)	Cross section (mb) Publiched	Adjusted	Fluence method	Correction for low energy neutrons
Heertje	64	/ 4/	14.6	80 +-3			
Nagel	66	/ 5/	14.6	50 +-7.8	*57.42	Fe	yes
Menlove	67	/ 6/	14.96	61.6+-6.3	63.17	U-238	no
Minetti	68	/ 7/	14.70	125 +-10		A	no
Rötzer	68	/ 8/	14.70	83.5+-4.2		Al	no
Barrall	69	/ 9/	14.60	76 +-7	*69.14	Al	no
Barrall	69	/10/	14.80	69 +-5	*73.59	Al	no
Temperley	70	/11/	14.10	73 +-8	*75.17	Fe	no
Decowski	70	/12/	14.52	83.8+-1.2		Zn-64	no
Pazsit	72	/13/	14.70	63 +-4	*65.21	Al	no
Santry	76	/14/	14.74	54.5+-2.2	*55.75	S	no
Hudson	76	/15/	15.2	50 +-10			no
Magnusson	77	/16/	14.7	63 +-4	*64.90	Al	no
Andersson	78	/17/	14.90	65 +-4	*65.49	A	no
Fan Peiguo	80	/ 1/	14.63	60.4+-3.1	53.06	Al	yes
Garlea	83	/18/	14.75	78.6+-3.6			yes
Ryves	83	/ 2/	14.67	53.1+-2.2	52.06	Fe	yes
Kudo	84	/19/	14.60	66.2+-2.3			no
Pepelnik	85	/20/	14.70	90.5+-4.5			no
Present work			14. 8	50.8+-1.8	51.11	In	yes
EVALUATED DATA							
IRDF		/23/		61.2+-22%			
ENDF/B-V			14.70	61.2			
ANL/NDM-89		/21/		61.75+-2.92			
Lu Hanlin				52.4 +-1.5			

* From ANL/NDM-89

Table 5: Cross section of $^{113}In(n,n')^{113m}In$ at 14 MeV

Authors		Ref.	En (MeV)	Cross section (mb) Publiched	Adjusted	Fluence method	Correction for low energy neutrons
Kozlowski	68	/22/	14.7	35 +-8	*35.75		no
Minetti	68	/ 7/	14.70	680 +-50		A	no
Temperley	70	/11/	14.10	63 +-3	*64.51	Fe	no
Pazsit	72	/13/	14.70	66 +-5	*67.23	Al	no
Decowski	73	/ 3/	14.52	42 +-9	*44.31		no
Santry	76	/14/	14.74	53.9+-7.1	53.07	S	no
Ryves	80	/24/	14.67	51 +-3	50.85		yes
Ryves	83	/ 2/	14.3	53.4+-2.1	49.38	In	yes
Present work			14.8	49.7+-1.8	51.28	In	yes
EVALUATED DATA							
ANL/NDM-89	85	/21/	14.7	54.69+-7.98			
Lu Hanlin				50.5 +-1.5			

* From ANL/NDM-89

We divided the cross section data of $^{115}In(n,n')^{115m}In$ from 1964 into four groups, each with a kind of notation. (Fig.9) We can see discrepancies don't decrease with the development of modern detecting technology. Those data which have no lower energy neutron corrections are generally larger and have a large scatter; Those which apply lower energy corrections are well agree with each other within experimental accuracies. We made the scattering corrections to our previous work published in 1980 and at the same time we made some adjustments to the decay data and standard cross sections. The results were consistent with our present work.

There are lately on $^{115}In(n,n')^{115m}In$ reaction three evaluated data, ENDF/B-V, IRDF(1982) and ANL/NDM-89, which give approximately the same value (61 mb). On the basis of the work of Ryves and ours, we also give an evaluation datum, 52.4+-1.5 mb at En= 14.70 MeV. This value deviated 17% from the results of the former three, as a result of low energy neutron corrections being made.

The natural isotopic abundance of ^{113}In is very small (4.16%), and its reaction character is similar to that of ^{115}In. Because of this, it has not caught people's much attention. Our results on this reaction well agree with Ryves's, too.

In short, it is very difficult to measure the isomeric cross sections for the (n,n') reaction at 14 MeV precisely because of its high sensitivity to the lower energy neutrons, and in the Monte-Carlo calculations for the scattering corrections there are many approximations and interpolations, which increase the uncertainties. So we should lower the composition of lower energy neutrons in the experimental arrangements. So far the reliable data have only been on indium, and a large amount of wrok is urgently desirable.

References

(1) Fan Peiguo et al., C.J.Nucl. Phys. 2 (1980) 337.

(2) T.B.Ryves et al., J.Phys. G: Nucl. Phys. 9 (1983) 1549.

(3) P.Decowski et al., Nucl. Phys. A204 (1973) 121.

(4) I.Heertje et al., JR, Some nuclear reactions induced by D+T neutron, J,Phy, 30,775, 64 (1964).

(5) W.Nagel, Physica 31, 1091 (1965).

(6) H.O.Menlove et al., Phys. Rev. 163 (1967) 1308.

(7) B.Minetti et al., Z. Phys. 217 (1968) 83.

(8) H.Rötzer, Nucl. Phys. A109 (1968) 694.

(9) R.C.Barrall et al., Report AFWL-TR-68-134 (1969).

(10) R.C.Barrall et al., Nucl. Phys. A138 (1969) 387.

(11) J.K.Temperley et al., Report BRL-1491 (1970)
(12) P.Decowski et al., Institut Baden Jadrowych Report INR 1197 p18 1969.
(13) A.Pazsit et al., Sov. J.Nucl. Phys. 15 (1972) 232.
(14) D.C.Santry et al., Can J.Phys. 54 (1976) 757.
(15) C.G.Hudson et al., J. BAP-21-188 (DB5) 7602 (1976).
(16) G.Magnusson et al., Nucl. Technol. 34 (1977) 114.
(17) P.Andersson et al., Report LUNF-DG-3021 (1978).
(18) I.Garlea et al., Report INDC (ROM)-15 (1983).
(19) K.Kudo et al., Prog. Report NEANDC (J)-106/J 1 (1984).
(20) R.Pepelnik et al., Prog. Report NEANDC (E)-262U 32 (1985).
(21) B.P.Evain, D.L.Smith and P.Lucchese, ANL/NDM-89 (1985).
(22) T.Kozlowski et al., Acta Phys. Pol. 33 (1968) 409.
(23) D.E.Cullen et al., Report IAEA-NDS-48 (1982).
(24) T.B.Ryves et al., From (2).
(25) R.J.Prestwood et al., Phys. Rev. 121 (1961) 1438.
(26) Lu Hanlin et al., A.E.Sci. and Technol., China, 2 (1975) 113.

Measurement of fission product yields

Li Ze Cui anzhi Liu Conggui Liu Yonghui
Tang Peijia Qi Linkun Wang Xiuzhi Chang Chunhua

(Institute of Atomic Energy, P. O. Box 275, Beijing)

1, Introduction

Fission product yield is one of important nuclear data, it is widely used to evaluate the burnup fraction for various nuclear devices. A survey of the literature reveals a lack of fast neutron data or too large spread in data values for the application. Some measurements of fission product yields were performed in IAE. Radiochemistry and γ-ray spectrometry methods were set up for these measurements successively. The fission rate was determined accurately with double fission chamber. So we can obtain absolute fission product yield data. Nevertheless, for Cf-252 measurement, the absolute fission rate was obtained with catcher foil technique for the first time.

Following fission systems were determined during past several years: the fission of U-235 induced by thermal, fission spectrum, and 14.9MeV neutrons, the fission of U-238 induced by 3.0 5.0 8.3 and 14.9MeV neutrons and Cf-252 spontaneous fission.

2, Experimental methods

(1) Determination of fission rate

A, Catcher foil technique. Fission products were collected with catcher foil. The collecting efficiency was calibrated accurately. So we can obtain absolute fission rate. This technique was used to measure Cf-252 and the device was shown in Fig. 1.

B, Double fission chamber. A sandwich of standard-irradiation-standard was put in a double fission chamber as shown in Fig. 2., when it was used in measurement of fission of U-238 + 8.3MeV neutron. The fission rate in each standard target was directly determined and absolute fission rate in the irradiation target was calculated from those in two standard targets.

(2) Determination of fission products

A, Radiochemistry method. Fission product elements were separated from uranium target irradiated and then purified by different chemical proceedures. For some products it was necessary to employ the more sensitive β-counting method, while for the others γ-ray counting was used. These detectors were calibrated precisely with the standard sources.

B, γ-ray spectrometry method. In our laboratory, 130cm^3 Ge(Li) detector was used to determine γ-ray spectra of fission products. Its resolution (FWHM) was 1.85keV for the 1.33MeV γ-ray of Co-60. The spectra were acquired with SCORPIO-3000 multichannel-computer system. The detector efficiency was calibrated with a set of standard γ-ray sources.

3. Results

Comparing with similar work we obtained more absolute yields and more complete mass distribution curve. We also obtained some mass distribution characteristics. The results were shown in Table 1 and Fig. 3. for Cf-252 spontaneous fission, Table 2 and Fig. 4. for U-238 + 8.3MeV neutron and Table 3 and Fig. 5. for U-235 + fission spectrum neutron. The precision of yield data was 3% to 10% for peak yields and 5% to 25% for valley yields. The most absolute yields (fourty four mass chains from Kr-85^m to Eu-157) were obtained for Cf-252 spontaneous fission. Nine of fourty five yield values were obtained, for the first time, for fission of U-235 induced by fission spectrum neutron.

References

1. H. W. Schmitt et al., Phys. Rev. 137(1965) B837
2. H. Thierens et al., Nucl. Instrum. Methods 134(1976) 299
3. W. E. Nervik, Phys. Rev. 119(1960) 1685
4. K. F. Flynn et al., J. Inorg. Nucl. Chem. 37(1975) 881
5. J. Bbaehot et al., Rendments de Fission Cumulafits du Cf-252, Internal Report, C. E. A. Grenoble
6. S. Nagy et al., Phys. Rev. C17(1978) 163
7. K. F. Flynn et al., Trans. Am. Nucl. Soc. 22(1975) 677
8. T. C. Chapman et al., Phys. Rev. C17(1978) 1089
9. Group of Fission Yield, J. Nucl. Radiochem, (in chinese) 2(1980) 1
10. A. Ferrieu et al., AERA-R-8753(1977)
11. K. Debertin. IAEA-208 2(1978) 261
12. K. A. petrzhak et al., AEC-Tr-4696 (1960)
13. Li Ze et al., Chinese Journal Nuclear Physics 5(1983) 226
14. Li Ze et al., Chinese Journal Nuclear Physics 7(1985) 97

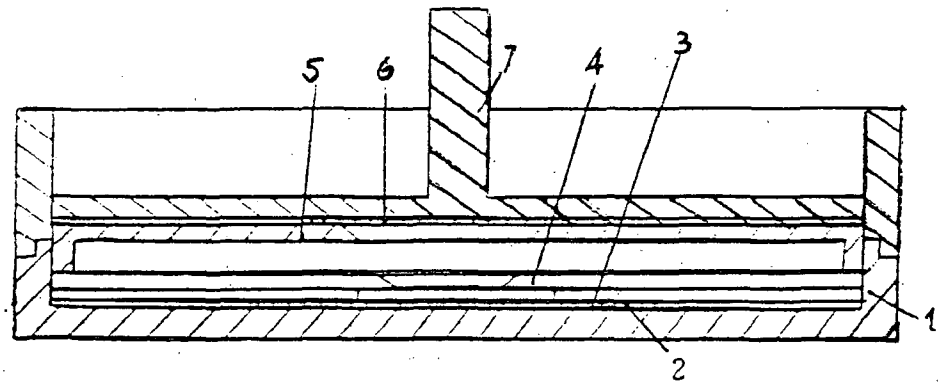

Fig. 1. Experimental device for catcher foil technique
1--hull, 2--backing of Cf-252 source, 3--spacer,
4,5--aperture, 6--catcher foil, 7--backing of catcher foil

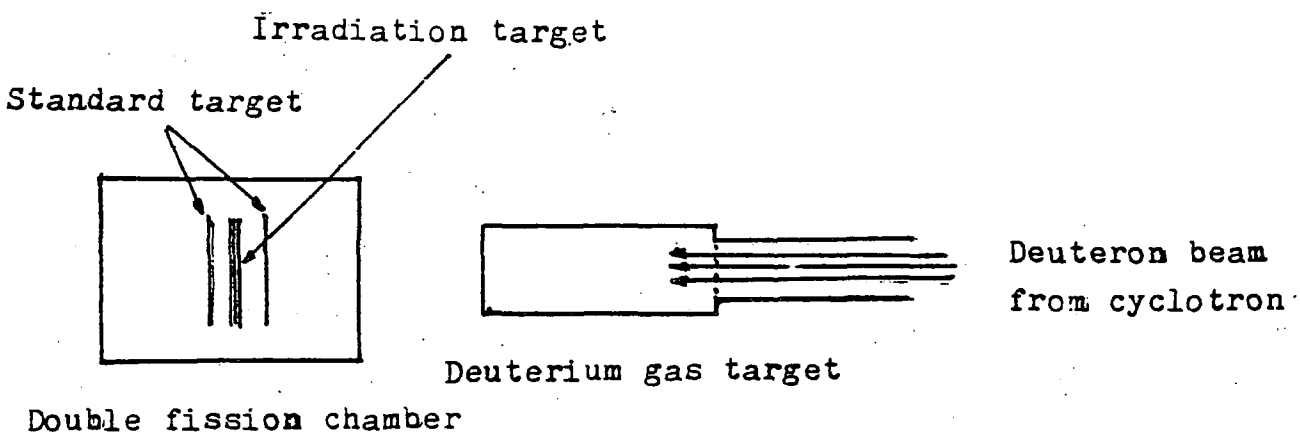

Fig. 2. Experimental arrangement for double fission chamber.

Table 1. Yields of Cf-252 spontaneous fission

Mass number	Nuclide	Yields, %					
		Present work[13]	Schmitt[1]	Thierens[2]	Nervik[3]	Flynn[4]	Bbaehot[5]
85	^{85m}Kr	0.111±0.007	0.156	0.11±0.02		0.078±0.008	
88	^{88}Kr	0.296±0.042	0.281	0.30±0.03			
91	^{91m}Y	0.535±0.06	0.477	0.48±0.03	0.59±0.06	0.58±0.06	0.41±0.06
92	^{92}Sr	0.604±0.026	0.727	0.71±0.07			0.57±0.12
94	^{94}Y	1.049±0.080	1.029	1.06±0.12			
95	^{95}Zr	1.175±0.035	1.219	1.19±0.04	1.37	1.24±0.12	1.28±0.06
97	^{97}Zr	1.683±0.054	1.747	1.61±0.06	1.54±0.15	1.81±0.18	1.58±0.08
99	^{99}Mo	2.55±0.11	3.098	2.78±0.12	2.57±0.03	2.48±0.13	2.28±0.09
101	^{101}Tc	3.91±0.13	4.394	4.00±0.21			
103	^{103}Ru	5.59±0.16	5.556	5.21±0.26		4.62±0.46	5.90±0.23
104	^{104}Tc	5.45±0.20	5.916	5.57±0.29			
105	^{105}Ru	5.92±0.27	5.935	6.13±0.15	5.99±0.21	5.53±0.55	6.77±0.24
106	^{106}Rh	6.06±0.25	5.742	5.93±0.36		5.75±0.58	7.01±0.30
107	^{107}Rh	6.63±0.22	6.536	6.61±0.37			
109	^{109}Pd	5.89±0.32	5.348	6.00±0.49	5.69±0.59	5.60±0.56	
111	^{111}Ag	5.29±0.23	4.931	5.17±0.32	5.19±0.29	5.04±0.25	4.78±0.14
112	^{112}Ag	5.31±0.18	4.327	4.69±0.24	3.65±0.18	4.21±0.42	5.49±0.36
113	^{113g}Ag	4.61±0.16	3.805	4.88±0.30	4.23±0.38		
115	^{115m}In	2.97±0.09	2.810	2.98±0.18	2.28±0.13	2.33±0.23	3.12±0.20
117	^{117}Cd	1.35±0.13	1.419	1.56±0.13			1.13±0.15
127	^{127}Sb	0.148±0.030	0.171	0.138±0.013	0.130±0.008	0.072±0.007	0.12±0.05
128	^{128m}Sb	0.293±0.032	0.393	0.260±0.0027			

Table 1. (Continued)

Mass number	Nuclide	Yields, %					
		Present work[15]	Schmitt[1]	Thierens[2]	Nervik[3]	Flynn[4]	Bbaehot[5]
129	^{129}Sb	0.527±0.054	0.557	0.57±0.07	0.615±0.017	0.317±0.032	0.74±0.12
131	^{131}I	1.77±0.06	1.718	1.61±0.09	1.27±0.18	1.64±0.16	1.73±0.07
132	^{132}Te	2.36±0.11	2.329	2.13±0.16	1.75±0.03	2.17±0.11	2.27±0.12
133	^{133}I	3.16±0.11	2.843	3.09±0.16	2.77±0.20	3.03±0.30	
134	^{134}I	3.66±0.23	3.493	3.65±0.15			
135	^{135}Xe	4.23±0.17	4.031	4.50±0.14	4.33±0.03	3.86±0.39	3.75±0.36
137	^{137}Cs	5.43±0.17	5.465	5.42±0.36	4.40		4.51±0.30
138	^{138}Cs	5.10±0.23	5.266	5.25±0.19	4.94		
139	^{139}Ba	5.62±0.25	5.564		5.73±0.16	5.75±0.58	
140	^{140}Ba	5.76±0.18	5.806	5.50±0.22	6.32±0.54	5.50±0.28	6.05
141	^{141}Ce	5.78±0.26	5.859	6.13±0.36	5.9±0.3	6.08±0.61	6.33±0.12
142	^{142}La	6.15±0.24	5.621	6.19±0.52			
143	^{143}Ce	6.30±0.23	5.685	6.13±0.31	5.94±0.35	5.66±0.28	6.29±0.30
144	^{144}Ce	6.16±0.28	5.590	6.21±0.38		5.98±0.30	
146	^{146}Ce	5.53±0.16	4.612	5.18±0.32			
147	^{147}Nd	4.03±0.18	4.471	4.10±0.21	4.69±0.08	3.99±0.40	4.80±0.30
149	^{149}Nd	2.87±0.18	2.751	2.74±0.20	2.65	2.81±0.28	3.90±0.30
151	^{151}Pm	2.17±0.11	2.107	1.99±0.13	2.18	1.60±0.16	1.77±0.20
153	^{153}Sm	1.405± 066	1.510	1.31±0.08	1.41±0.03	1.12±0.11	1.51±0.18
155	^{155}Sm	0.701±0.039	0.868	0.838±0.035			
156	^{156}Sm	0.696±0.043	0.758	0.614±0.039	0.703±0.008	0.69±0.07	
157	^{157}Eu	0.523±0.12	0.559	0.56±0.06			0.43±0.05

Table 2. Yields of U-238 + 8.3MeV neutron

Mass number	Nuclide	Yields, %							
		Present work (8.3MeV) (5)		Nagy (7.7MeV) (6)		Flynn (8MeV) (7)		Chapman (8.1MeV) (8)	
		γS	RC	γS	RC	γS	RC	γS	γS, RC
83	^{83}Br		0.51±0.04		0.74±0.04	0.80	0.62		
84	^{84}Br		0.98±0.06					1.1102±0.44	
85	^{85m}Kr	0.79±0.05		0.74±0.04					
87	^{87}Kr	1.80±0.06		1.82±0.09		2.00		1.7395±0.32	
88	^{88}Kr	2.08±0.11		2.32±0.15		2.28			
89	^{89}Rb	2.77±0.09	3.33±0.10	2.68±0.33		2.64	2.49		2.6125±0.22
91	^{91}Sr	4.14±0.13	4.54±0.16	4.04±0.23		4.40	3.70		3.7717±0.38
92	^{92}Sr	4.20±0.13		4.23±0.27		4.83			
93	^{93}Y	5.41±0.22		5.05±0.34		5.33			
94	^{94}Y	4.29±0.15		4.51±0.38		5.01			
95	^{95}Zr	5.42±0.16	5.68±0.16	5.36±0.19		5.96	5.91		4.9810±0.40
97	^{97}Nb(Zr)	5.73±0.18	6.01±0.21	5.62±0.16		6.28			5.3968±0.54
99	^{99}Mo	6.23±0.20	6.22±0.19	5.96±0.25		6.82	7.68		6.0623±0.49
101	^{101}Tc	6.13±0.20		6.79±0.46		7.34			
103	^{103}Ru	6.01±0.18	5.19±0.34	6.22±0.27		6.45	5.12		5.2195±0.48
104	^{104}Tc	3.74±0.13		4.44±0.31				4.5611±1.25	
105	^{105}Ru	3.71±0.12		3.75±0.21		3.96			3.5643±0.39
106	^{106}Ru		2.68±0.18		3.02±0.30		3.11		
107	^{107}Rh	1.83±0.07		0.71±0.18		2.36			
109	^{109}Pd		0.523±0.028		0.32±0.03		0.32		
111	^{111}Ag		0.346±0.03		0.26±0.03		0.24		0.1945±0.017
112	^{112}Pd		0.257±0.011		0.20±0.04		0.20		0.1688±0.015
113	^{113}Ag		0.25±0.01						
115	^{115}Cd		0.227±0.009		0.191±0.032		0.16		0.1352±0.0097
121	^{121}Sb		0.263±0.025		0.176±0.024		0.16		
125	^{125}Sn		0.076±0.003		0.091±0.022		0.16		
127	^{127}Sb	0.56±0.02	0.728±0.027	0.53±0.06	0.047±0.07	0.57	0.37		0.5390±0.28

Mass number	Nuclide	Yields, %							
		Present work (8.3MeV)(14)		Nagy (7.7MeV)(6)		Flynn (8MeV)(7)		Chapman (8.1MeV)(8)	
		γS	RC	γS	RC	γS	RC	γS	γS, RC
128	^{128}Sn	0.70±0.03						0.4604±0.96	
129	^{129}Sb	1.32±0.05		1.23±0.08	1.16±0.13	1.29	0.79		
130	^{130}Sb	0.66±0.04						0.7326±0.14	
131	^{131}I	3.29±0.11	3.16±0.10	3.89±0.14		4.33	2.30		
132	^{132}Te	5.13±0.24	4.61±0.12	5.22±0.13		5.06	4.35		4.6612±0.28
133	^{133}I	7.21±0.22		7.04±0.20		7.33	8.07		6.7132±0.98
134	^{134}I	6.55±0.23		7.02±0.43					
135	^{135}Xe	6.75±0.34		6.79±0.20		6.28	7.61		
136	^{136}Cs								0.0105±0.003
137	^{137}Cs								3.8[illegible]48±0.77
138	^{138}Cs	5.87±0.16		5.16±0.21		5.52			
139	^{139}Ba	4.89±0.30		4.54±0.35		4.91			
140	^{140}Ba	5.71±0.17	5.64±0.16	5.69±0.14		5.82	5.71		5.1455±0.42
141	^{141}Ba, Ce	4.68±0.24	5.49±0.16	5.51±0.33		5.92	5.39		4.6197±0.44
142	^{142}La	4.21±0.15		4.35±0.26		4.43		4.6722±1.76	
143	^{143}Ce	4.66±0.14		4.58±0.27		4.61	4.35		4.7749±0.[illegible]8
144	^{144}Ce		4.06±0.12						4.3396±0.42
146	^{146}Pr	3.62±0.15		3.19±0.25		3.40			
147	^{147}Nd	2.70±0.13	2.58±0.07	2.66±0.24		2.85			2.6285±0.26
149	^{149}Pm,Nd			1.91±0.19		2.03	0.69		
151	^{151}Pm	0.704±0.024				0.70	0.54		0.8208±0.11
153	^{153}Sm		0.434±0.013				0.19		
156	^{156}Eu		0.0905±0.0066						0.0770±0.011
161	^{161}Tb		0.0040±0.0003						

Where γS -- γ-ray spectrum method | RC -- Radiochemistry method

Table 3. Yields of U-235 + fission spectrum neutron

Mass number	Nuclide	Yields, %					
		Present work		Group of fission yield (9)	Ferrieu (10)	Debertin (11)	Petrzhok (12)
		γS	RC	RC	γS	γS	RC
84	^{84}Br	1.097±0.067					
85	^{85}Kr	1.345±0.092			1.52±0.05		
87	^{87}Kr	2.470±0.194			2.59±0.07		
88	^{88}Kr	3.675±0.087			3.35±0.04		
89	^{89}Rb	4.072±0.188					5.6±0.4
91	^{91}Y	5.392±0.183			3.01±0.05		
92	^{92}Sr	5.413±0.148			5.32±0.19		
93	^{93}Y	5.790±0.176			5.93±0.08		
94	^{94}Y	5.948±0.171					
95	^{95}Zr	6.418±0.198	6.46±0.30	6.53±0.27	6.52±0.07	6.40±0.07	7.7±0.6
97	^{97}Zr	6.120±0.166	6.04±0.46		6.33±0.09	6.09±0.04	
99	^{99}Mo	6.365±0.196	6.36±0.17	6.38±0.18	6.08±0.08	6.22±0.15	6.4±0.4
101	^{101}Tc	4.626±0.188					
103	^{103}Ru	3.46±0.03		3.36±0.18	3.25±0.04	3.46±0.03	
104	^{104}Tc	1.77±0.05					
105	^{105}Ru	1.25±0.07			1.33±0.06		
111	^{111}Ag		0.0254±0.0057		0.03±0.01		0.031±0.002
112	^{112}Pd		0.0558±0.0053				
113	^{113}Ag		0.0194±0.0086				
115	^{115}Cd		0.019±0.004		0.06±0.01		0.022±0.002

125	^{125}Sn		0.048±0.015		0.11±0.04		
127	^{127}Sb		0.297±0.028		0.19±0.03		
128	^{128}Sn	0.592±0.013					
129	^{129}Sb	0.940±0.035			0.89±0.05		
131	^{131}I	3.06±0.10			3.23±0.06	3.58±0.04	
132	^{132}Te	4.69±0.16	4.31±0.16		4.35±0.07	4.82±0.04	
133	^{133}I	6.67±0.23			6.96±0.10		
134	^{134}Te	7.47±0.27			6.53±0.05		
135	^{135}Xe	6.21±0.20			6.03±0.04		
138	^{138}Cs	6.48±0.22					
139	^{139}Ba	5.82±0.40					
140	^{140}Ba	6.00±0.22			6.22	6.09±0.07	6.0±0.5
141	^{141}Ce		5.67±0.32		6.40±0.05		
142	^{142}La	5.05±0.15			6.42±0.09		
143	^{143}Ce	5.61±0.18			5.89±0.07	5.37±0.04	
144	^{144}Ce		5.12±0.16	5.28±0.24	5.91±0.06		
146	^{146}Pr	3.51±0.18					
147	^{147}Nd	2.32±0.08	2.33±0.08	2.36±0.11	1.95±0.06		
149	^{149}Nd	1.014±0.07			1.23±0.09		
151	^{151}Pm	0.381±0.002			0.37±0.05		
153	^{153}Sm		0.154±0.007		0.16±0.05		
156	^{156}Eu		0.0186±0.0017				
161	^{161}Tb		0.00069±0.00006				

Where γS -- γ-ray spectrum method RC -- Radiochemistry method

Table 4. Mass distribution characteristics

Fission system	Mean mass (amu) L-group	Mean mass (amu) H-group	Peak-to-Valley ratio	$\bar{\nu}_{cal}$	$\bar{\nu}_{exp}$
$^{235}U+FSn$	95.04	138.43	366	2.53	2.56±0.07
$^{238}U+8.3MeVn$	97.3	138.3	30	3.4	3.543±0.015
^{252}Cf S.F.	106.6	141.8		3.56	3.732±0.008

Where $\bar{\nu}$ is the average number of neutrons emitted per fission. Subscript 'cal' represets the values calculated on mass conservation from the data of present work. 'exp' represents experimental values based on direct measurement by fission-coincident neutron counting.

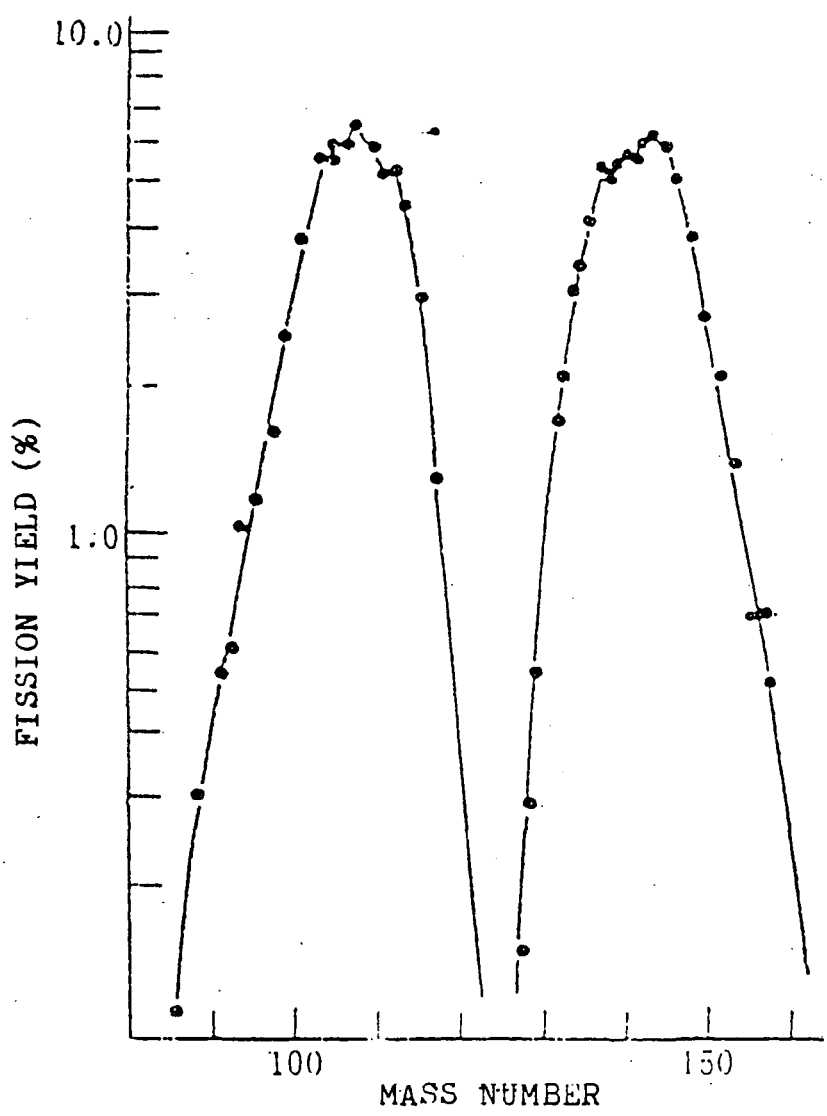

Fig. 3. Cf-252 spontaneous fission

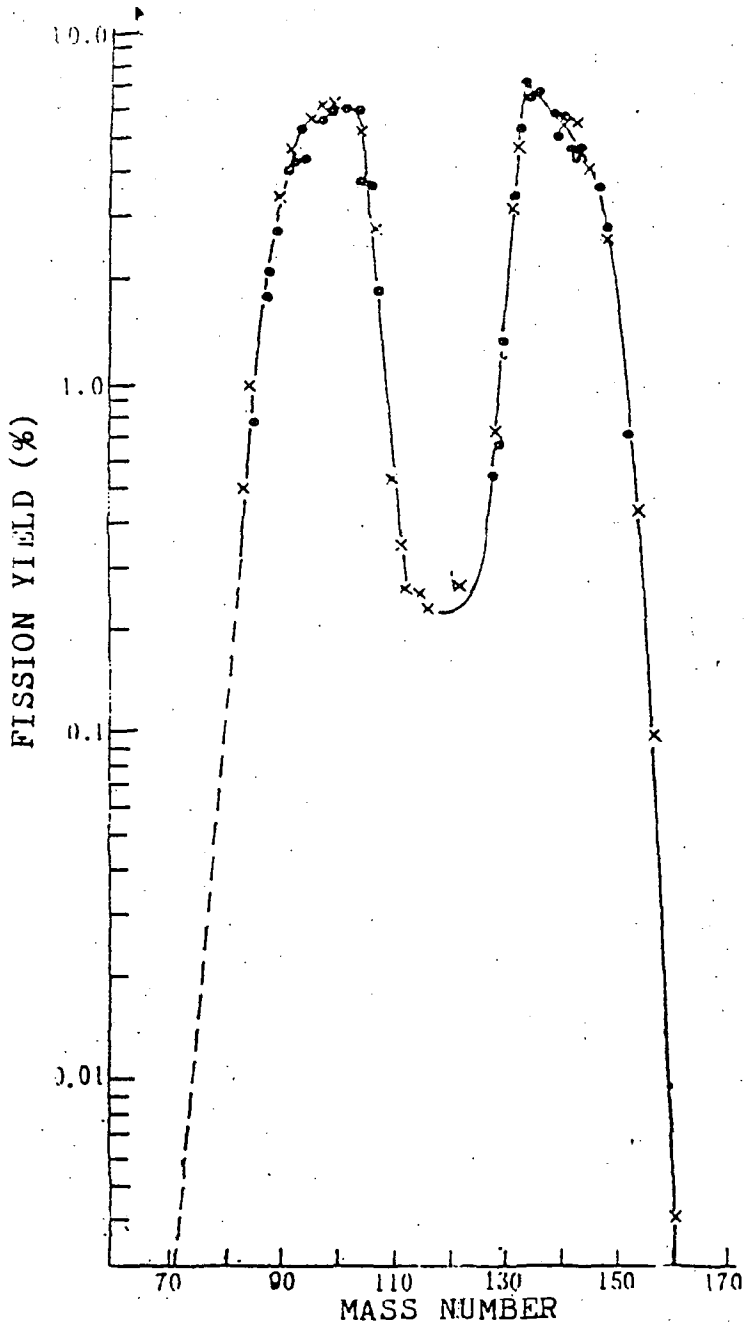

Fig. 4. Fission of U-238 induced by 8.3MeV neutron

● -- γ-ray spectrum X -- Radiochemistry

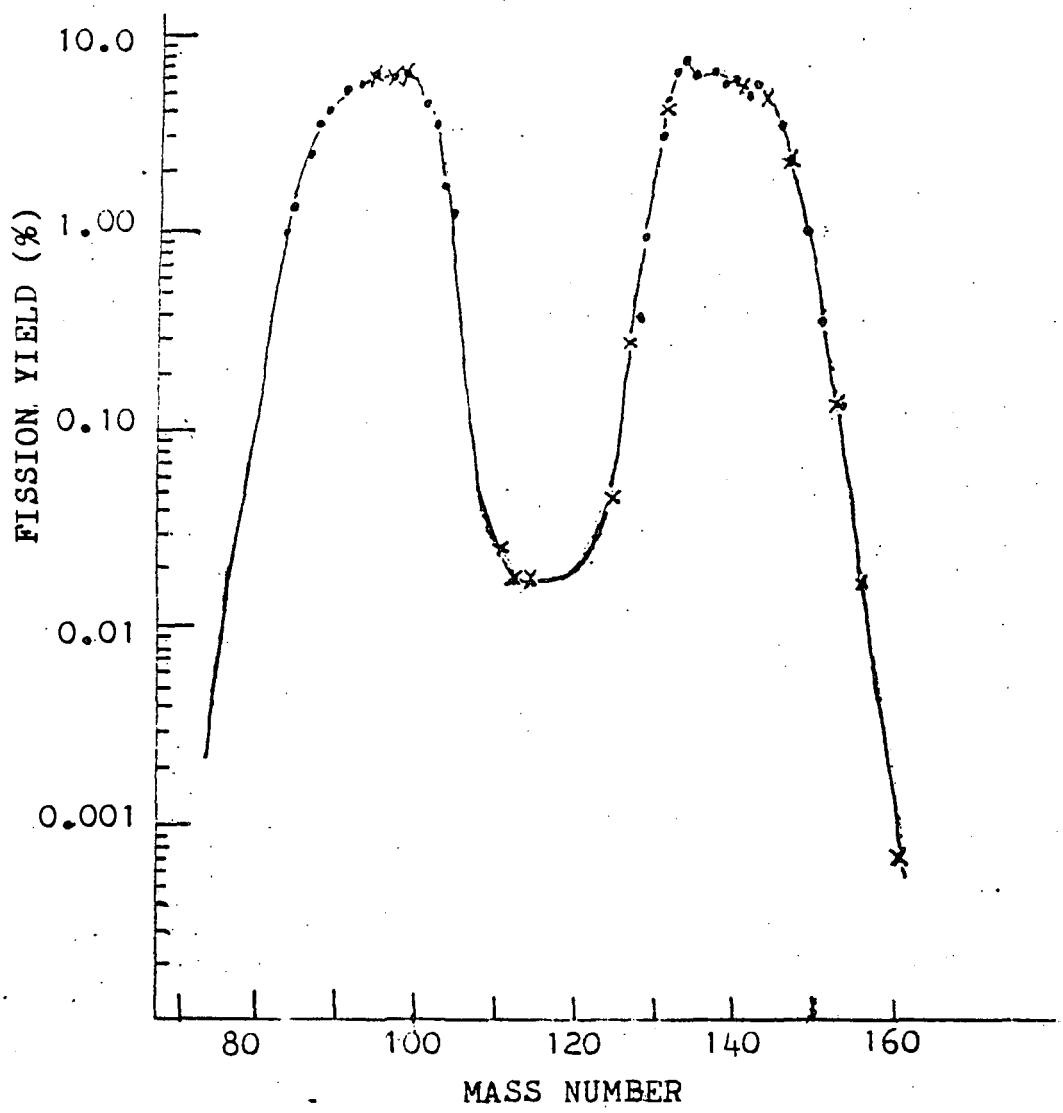

Fig. 5. Fission of U-235 induced by fission spectrum neutron

• -- γ-ray spectrum method

X -- Radiochemistry method

An Experimental Study of the Prompt Neutron Spectrum of 235-U Fission Induced by Thermal Neutrons

Yu-feng WANG, Xi-xiang BAI, Xiao-zhong WANG, An-li LI,
Jing-wen LI, Jiang-chen MENG and Zong-yu BAO
INSTITUTE OF ATOMIC ENERGY
BEIJING , CHINA

Abstract

The prompt neutron spectrum of 235-U fission induced by thermal neutrons has been measured in the 0.6-16 MeV energy range using a TOF spectroscopy consisting of a multilayer-multisection fast fission chamber and a ST-451 liquid scintillation neutron detector. The γ -ray background was suppressed by applying an efficient pulse shape n/γ discrimination.

The several systematical influences upon the measured TOF spectra were corrected in detail. Especially, the correction for the distortion resulting from non-correlated fission signals have been carried out meticulously.

The experimental result demonstrates the measured spectrum cannot be described by Maxwellian distribution in the energy range given above. However, Madland-Nix model (MNM) calculation fairly corresponds to the data in quite a wide energy range.

1. Introduction

The prompt fission neutron spectrum occupied a key position among the nuclear data required for application in reactor design, meanwhile a detailed knowledge of fission spectra is also important for other applications. The increasing use of integral data measurements with critical assemblies for adjustment of evaluated data is one factor that focuses the interst on fission spectra. There are several cases of discrepancies between differential data and integral data measured as averages over fission spectra. More reliable and accurate fission spectrum data are necessary for clarifying the discrepancies. As for application, 235-U fission spectrum could be used as standard for several categories of nuclear data. On the other hand, accurate data of fission spectra are significative for verifying the theoretical model and studying fission mechanism further.

The existing data on prompt neutron spectra of 235-U fission induced by thermal neutrons are listed in table 1. Most of them cover only a narrow energy range (1-10 MeV) and the data in higher energy range are very rare. In addition,

Table 1. Summary of the Results of Neutron Spectra Measurements of 235-U Fission Induced by Thermal Neutrons

Ref.	Year	Incident energy (MeV)	Secondary energy range (MeV)	Fitted function	Results E(mean) (MeV)	Results Tm (MeV)	Menthod	Sample	Detector	Comments
(1)	1972	Thermal	0.1-9.5	Numeric integral & Maxwell	1.946±0.12 1.932±0.13	(1.298) (1.293)	Proton recoil	93% U-235 enrich	Prop. counter	Preliminary possibly over-estimate systematic error.
(2)	1971	Thermal		Maxwell	2.010±0.060	(1.340)	Li-6 spectr.		Li-glass	
(3)	1969	Thermal	2-11	Maxwell	(1.987)	1.318 ±0.005	TOF	Neal-crili sphere	Li-glass	Spectr was consid pure fission above 2 or 3 MeV
(4)	1965	Thermal	0.7-6.0	Wall	1.980	(1.321)	TOF at 90°		Stibene crystal	Scantly information on experiment details & on correcti
(5)	1984	Thermal	0.03-4.00	Maxwell	1.973	1.315	TOF		Li-Glass & Fission-chamber	
Present 1986-1987		Thermal	0.9-15.6	Maxwell & Madland + Nix	1.976	1.317	TOF	93% 235-U enrich	Liquid scintill. & fission-chamber	Number of correct-ions.

Table 2. The Summary of Experimental Condition

Energy Range	0.6 - 16 MeV
High bias	5 - 16 MeV
Middle bias	1.0 - 9 MeV
Low bias	0.6 -3.2 MeV
Flight Path	3.17 m
Timing Resolution	1.82 ns
Neutron Beam	High purity thermal neutron beam
Cd-ratio	18000
Neutron flux	$7.5 \cdot 10^6$
Neutron Detector	A 10 cm diam. by 5 cm thick ST-451 liquid scintillator
n/γ discrimination	Zero-crossing
Calibration of efficience	1.Experimental method 2.Monte Carlo calculation
Fission Chamber	Multilayer-multisection fast fission chamber
Sample	Enrich Uranium, 21mg
Fission rate	$7.6 - 5.3 \cdot 10^4$ /s

the methods used by these measurements are usually obsolescent.The discrepancies among these measurement results are greater than the errors given by authors. It is clear,there exist some systematic errors.In view of the above-mentioned facts,a more accurate measurement of this spectrum is necessary.

2.Experimental Set-up and Method

The essentials of the experimental arrangement are summarized in Table 2. The experimental set-up is shown schematically in Fig.1.The neutron detector was installed in a massive collimator/shielding consisting of Pb,Fe and paraffin.

The high purity thermal neutron beam(6) was suplied by thermal column at the heavy water reactor of IAE.A collimator and a single crystal silicon filter are utilized for upgrading the beam quality.

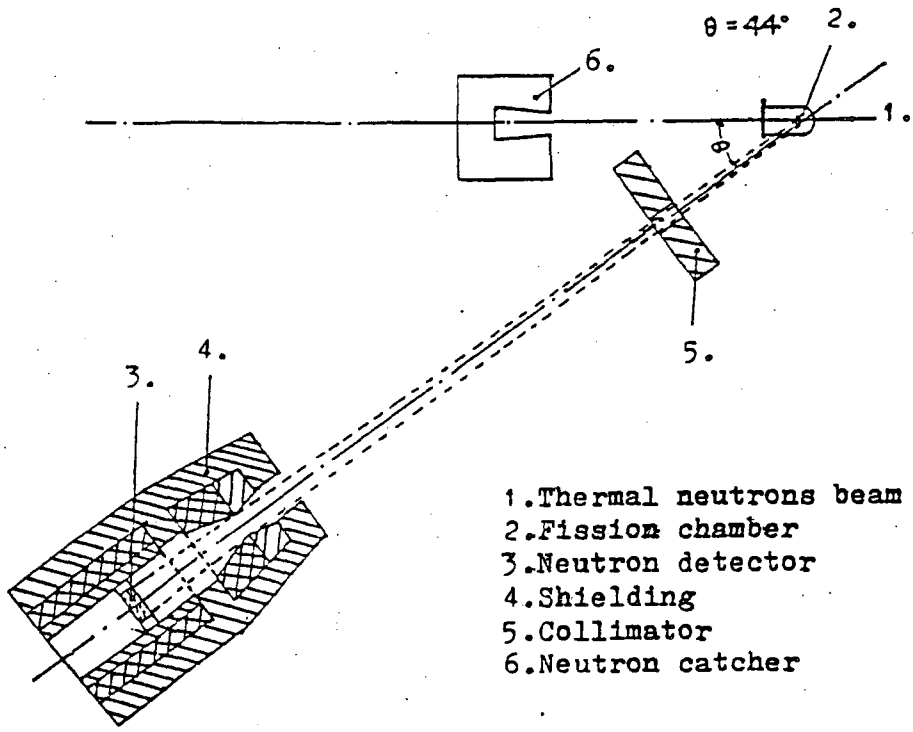

Fig. 1 Scheme of the experimental set-up

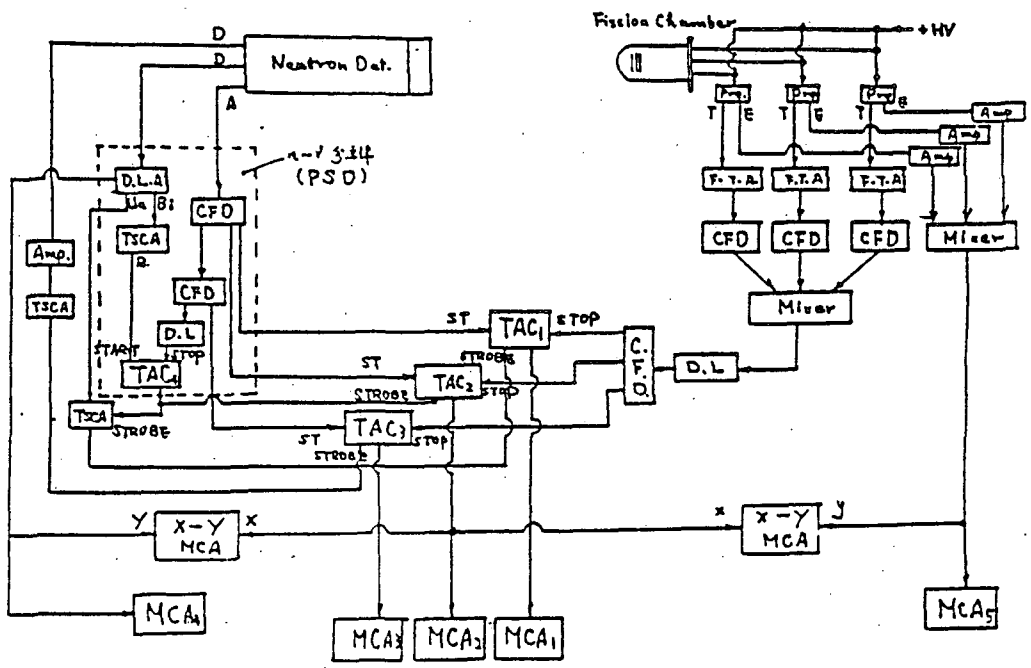

Fig. 2 Schematic representation of electronics of the TOF spectroscopy.

The block-diagram of the electronics is shown in Fig.2.

A multilayer-multisection fission chamber of 235-U was used as timing-detector of fission fragments.The structure of the chamber is illustrated in Fig.3.

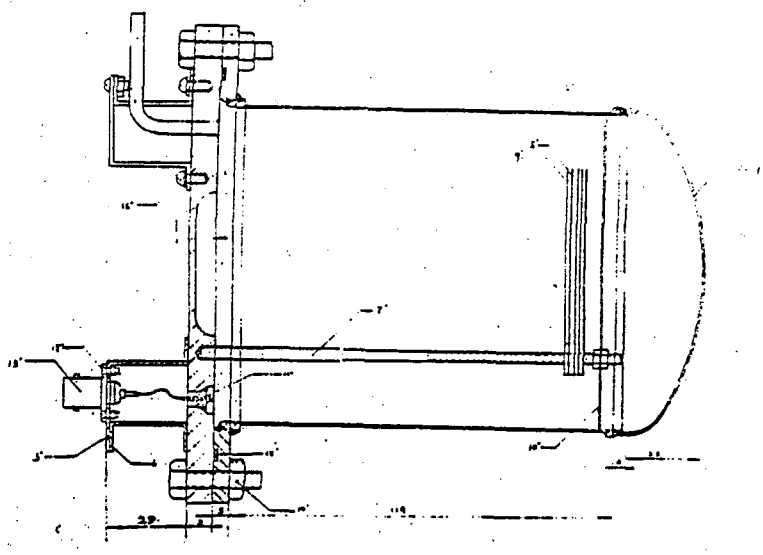

Fig. 3 The structure of fission chamber.

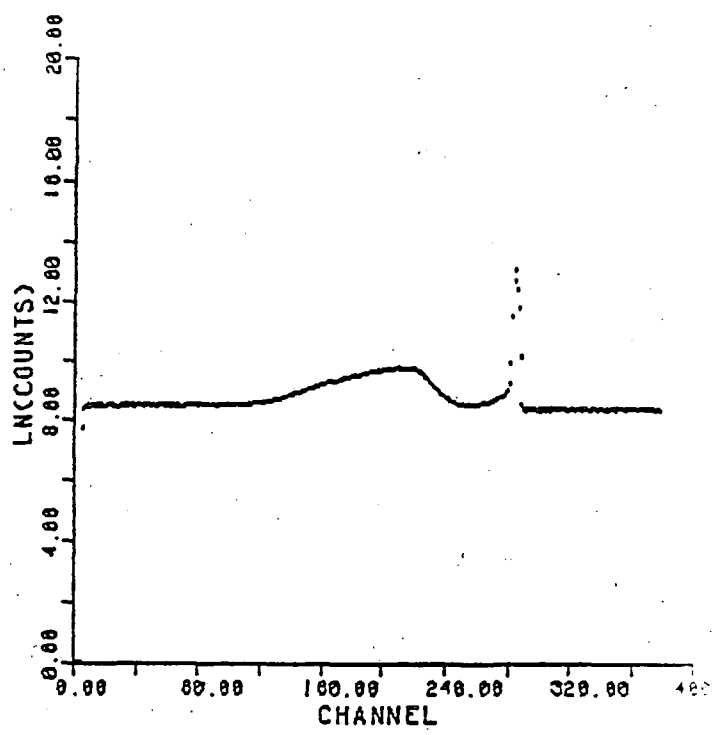

Fig. 4 The TOF spectrum of low bias

The neutron detector has consisted of a ST-451 liquid scintillator and a 58AVP photo-multiplier. Pulse shape discrimination was applied to suppress gamma-ray background efficiently.

Three channels of fission signals taken from the separated sections of the fission chamber were fed into three Ortec 142B preampliliers respectively, and the timing output of each 142B was fed into a corresponding constant-fraction discriminator. Then three channels of timing signals were mixed togther by a Mixer.

The mixing output delayed properly was used as stopping-signal of TAC.The timing output from the neutron detector was used as starting-signal.

For obtaining suitable effect-background ratio in higher energy ranges, three different biases of neutron detector were set as listed in Table 2 and the corresponding TOF spectra were measured by using three MACs simultaneously.

Typical TOF spectra are shown in figures 4-6.

The accuracy of the shape of spectrum is restricted by the accuracy of neutron detection efficiency response to a great extent.The detection efficiency of ST-451 liquid scintillator was determined by two independent methods. One is (n,p) scattering experiment using 14.8 MeV neutron source,and another is Monte Carlo calculation using the standard code of NEFF4(7).The results of two different methods accorded with each other in suitable accuracy.

3.Corrections

We have made a number of corrections for the measured TOF spectra.Since the corrections on this spectrum have not been discussed in detail in previous papers listed in Table 1,we discussed them within more careful cosideration.

A.The disturbances from non-correlated timing signals(8)

The effects of these disturbances have been corrected in two steps.The first,having deducted the background due to the random coincidences of n/γ events non-correlated to fission events and stopping signals.Both the statistical analysis and the measurements have indicated this background was channel-dependent,and can be determined in full range by fitting the distribution beyond the prompt gamma-peak of TOF spectrum with a proper exponential form.The second,having removed the distortions due to random coincidences of the true fission n/γ signals and the stochastic fission signals arriving before the related ones.This correction has been carried out by means of probability analysis and iterative treatment.

B.Scattered neutron background

The scattered neutron background,coming from the fission neutron which was emitted into 4π space except neutron detector direction scattered by the surrounding materials around the fission chamber,has been measured with a shadow bar and corrected in the same way as mentioned above.Finally,it has been deducted from the total TOF spectrum measured without the shadow bar.

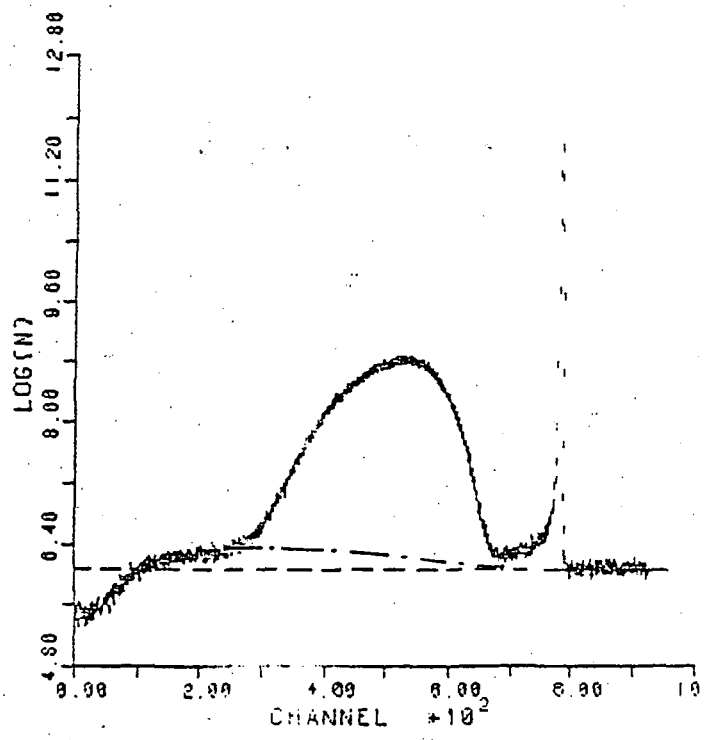

Fig. 5 The TOF spectrum of middle bias

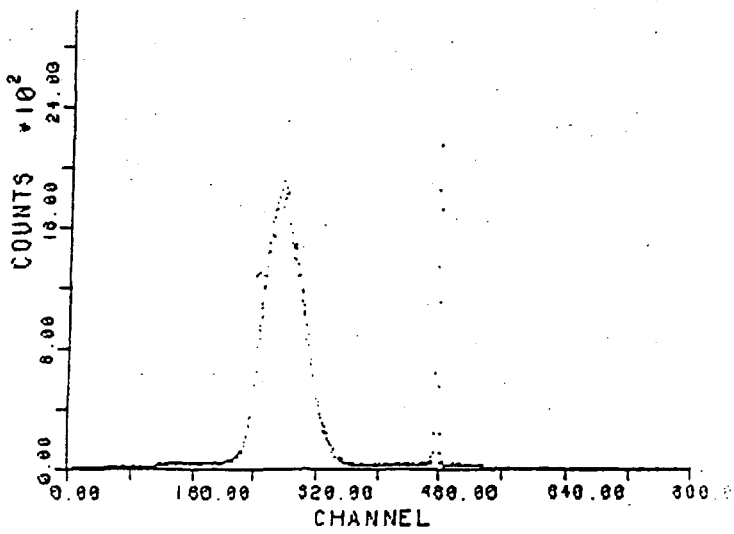

Fig. 6 The TOF spectrum of high bias

C.Attenuation in Air

It is not always negligible for fission neutron intensity attenuation due to the absorption and scattering of the oxygen and nitrogen components of the air in the flight path,even the correction is usually small.Specifically,it becomes signification for low energy resonances in nitrogen and oxygen.

Other influences to the TOF spectrum,such as incomplete thermalized neutrons, delayed gamma-rays and delayed neutrons following fission are negligible.

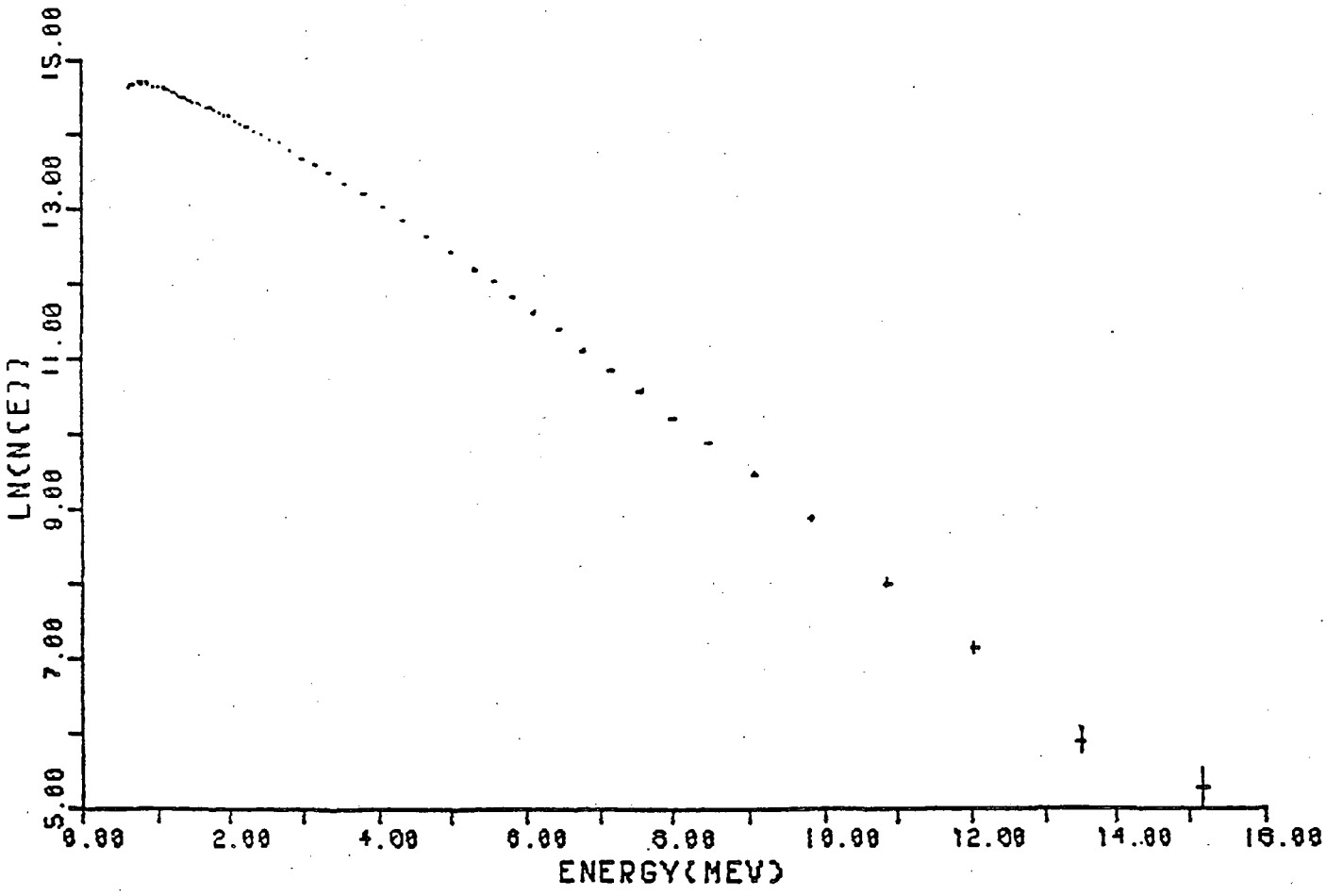

Fig. 7 The neutron energy spectrum in the measured energy range.

Having finished above procedures, the three different bias spectra have been merged into a wide energy range spectrum using the method of normalization in the same energy interval in which the conterminous spectra have the same shape. The final neutron energy spectrum is shown in Fig.7.

4. Results and Discussion

The measured spectrum cannot be fairly described by Maxwellian distribution in the full energy range of the measurement. For the optimum fitting, Maxwellian temperature T=1.321 MeV, the ratio of data to Maxwellian distribution is shown in Fig.8. In the energy range bellow 6 MeV, the spectrum approches Maxwellian distribution. However, in the energy range beyond 6 MeV, the spectrum deviates down from Maxwellian distribution nearly 50%.

We have preliminarily compared the experimental results with MNM(9) calculation. The ratio of the experimental spectrum to the calculated one using a constant cross section in the model is shown in Fig.9. In the lower energy range of 1.0-15 MeV, the experimental data accord with MNM calculation roughly. But the data are 20% higher than those of the calculation in the lower energy range. A more rigorous MNM calculation seems to be necessary for the comparison.

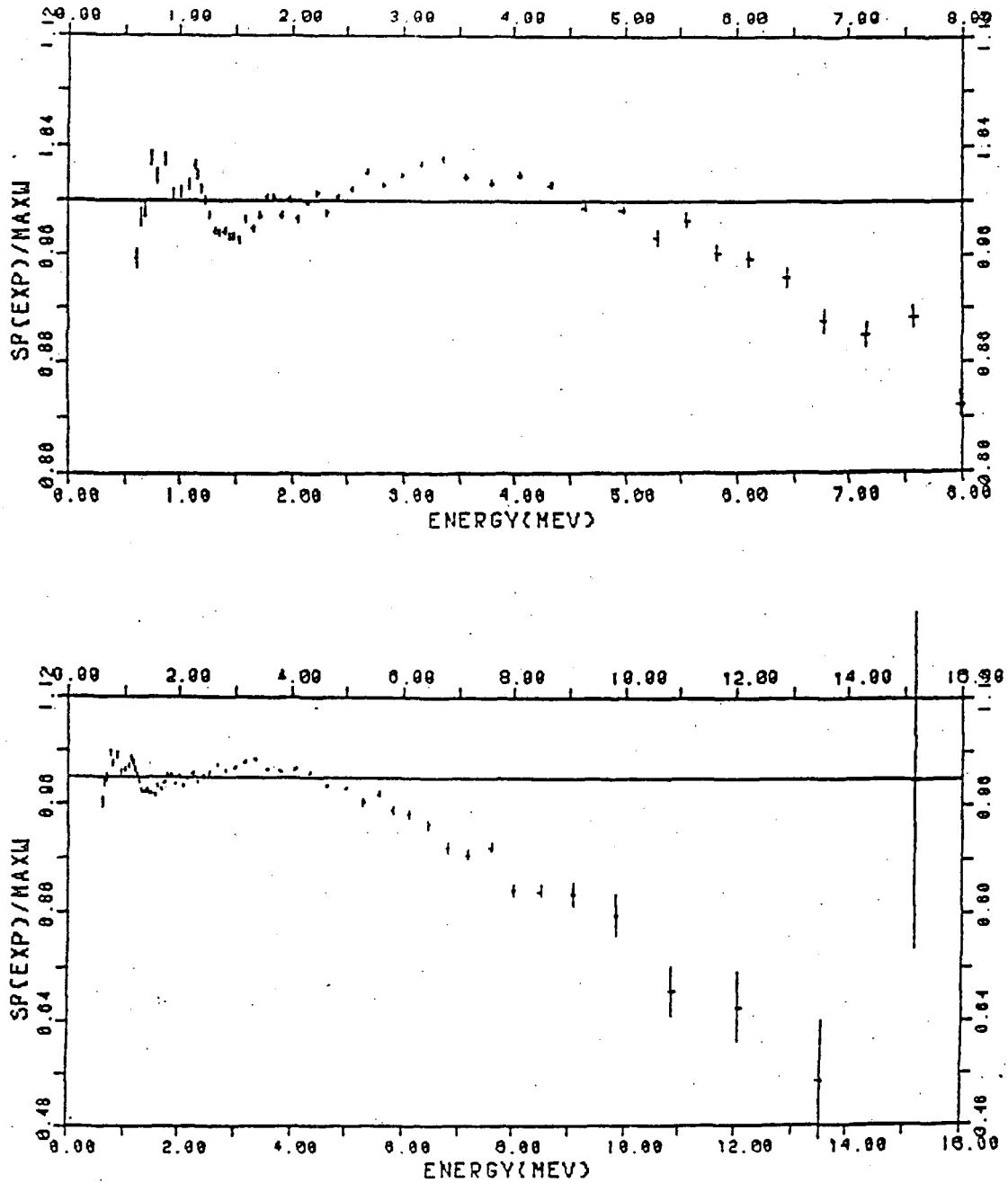

Fig.8 Ratio of the experimental spectrum and the spectrum calculated using Maxwellian distribution. The Maxwellian temperature T_M=1.321 MeV.

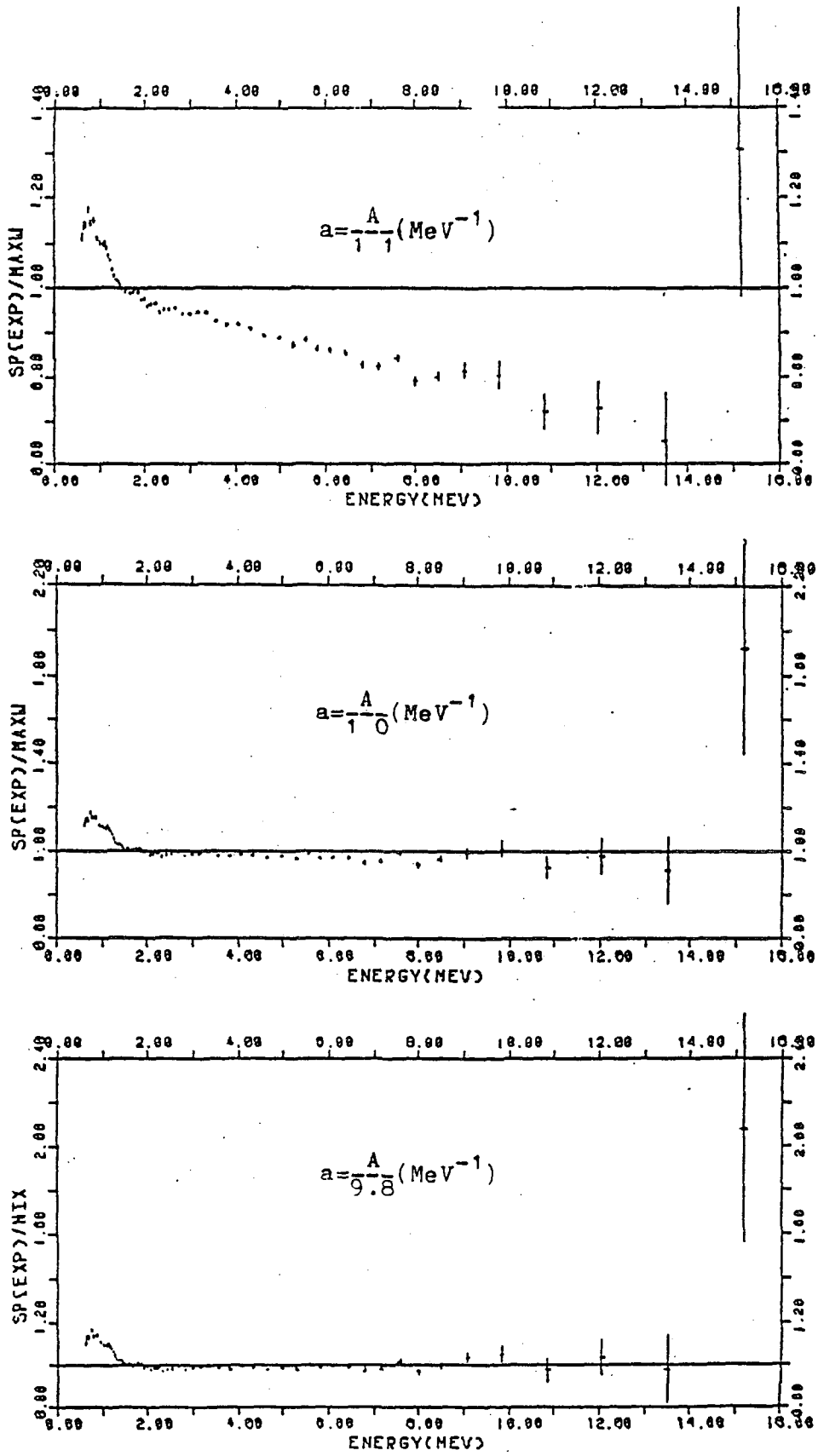

Fig.9 Ratio of experimental spectrum and MNM calculation spectrum with a constant cross-section, the level-density parameter a as a variable parameter in the calculations.

Acknowledgements

We are grateful to Shi Zong-ren, Cao Zhong and Yu Chun-ying for their technical assistances. Further acknowledgement for valuable suggestions goes to Prof. Huang Sheng-nian and Prof. Wang Da-hai. We would also like to thank Dr. G. Dietze for his help in supplying the Monte Carlo code NEFF4.

References

(1) H. Werle, et.al., J. Nucl. Eng., 1972, V26, p165, Data given in "Prompt fission neutron spectra", Vienna, IAEA, 1972

(2) I. C. Richards, Thesis, Uniersity of London(1971)

(3) L. Neill, Rep. GA-9753(1969)

(4) V. N. Nefedov, et.al., Atomn. Energ. 20(1966)342

(5) a. Lajtai, et.al., IAEA-TECDOC-355(Nuclear Standard Reference Data, Geel, 12-16 Nov, 1984, p312.

(6) Shi Zong-ren, et.al., A facility and design of high purity thermal neutron beam, to be published.

(7) G. Dietze and H. Klein, PTB-ND-22

(8) H. Klein, et.al., INDC(NDS)-146, p191

(9) D. Madland and J. Nix, NEW CALCULATION OF PROMPT FISSION NEUTRON SPECTRA AND AVERAGE PROMPT NEUTRON MULTIPLICITIES, Preprint LA-UR-81-2968.

AN INTENSITY GAMMA SOURCE AND IT'S APPLICATIONS

Ye Zongyuan (Institute of Atomic Energy, beijing)

An intense gamma source based on thermal neutron capture reaction has been installed at the swimming pool reactor of the Institute of Atomic Energy, Beijing. The possible energy range of this gamma source is 4--11 MeV. The typical gamma intensity is about 5×10^{13}/s at the source position and 10^{6}/s.cm^{2} outside the reactor shielding. Besides, this gamma source is characterized by high energy resolution, small angular divergency and low neutron background. Some experiments have been done with this facility.

1) Gamma source facility: The facility is shown schematically in Fig. 1. The radiator material which is used to produce special gamma ray is located near the active zone of the reactor. The produced capture gamma rays are extracted passing through a horizontal chanell of reactor.

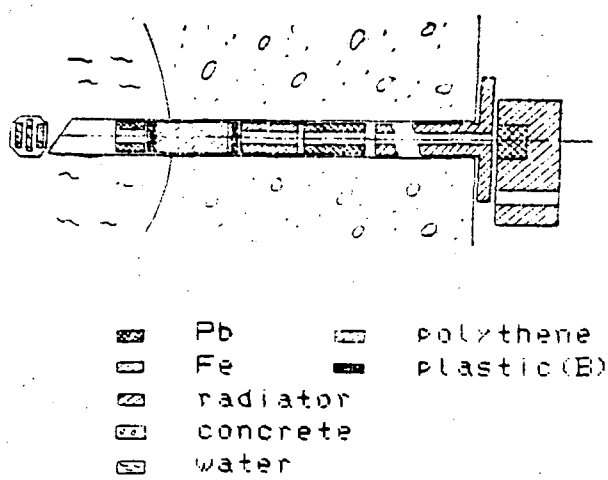

Fig. 1 The schematical arrangement of the facility

In order to reduce the strong background of low energy photons and neutrons produced in the reactor. a collimator system was used. The system consists of two parts. The inner

part includes: a Pb cylinder with inner diameter 3 cm and outer diameter 10 cm and 3 cm long; a 1 cm thick boric plastic layer; a 30 cm long polythene bar; again a boric plastic layer of 1 cm thikness; then a 30 cm long polythene cylinder and another Pb cylinder also 30 cm long. The outer part of the collimator consists of a 130 cm long iron cylinder with inner diamter 3 cm and outer diamter 10 cm. The total length of the collimator is about 240 cm. In addition, an iron cylinder with inner diamter 1 cm and outer diamter 3 cm could be added into the channel to reduce further the size of the beam. In result, a parallel gamma beam with angular divergency 45' and 30' could be obtained.

The radiator material was contained in an aluminium box and could be changed from the top of reactor conveniently and safely.

2) Determination of energy and intensity of the gamma lines:

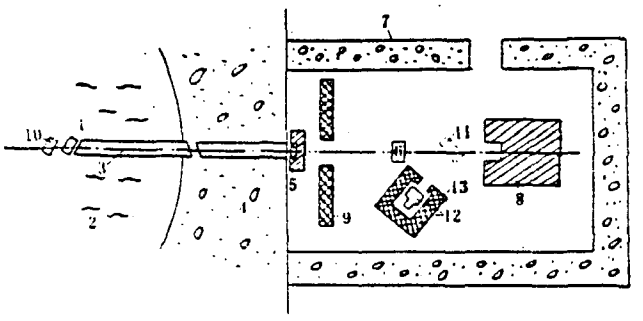

Fig. 2 The scheme of experimental arrangement
1. Radiator; 2. water;
3. Horizontal channel;
4. Ractor shielding;
5. Gate(Fe+Pb);
6. Detector;
7. concrete wall;
8. Beam catcher;
9. Pb shielding; 10. Bi
11. Scatterer;
12. detector;
13. Pb shielding for detector.

The experimental arrangement is shown schematically in Fig. 2. In order to measure the energy and intensity of gamma lines, a detector is put on the position 6. A Pb block of 2--3 cm thickness was put in front of the gate 5 to eliminate the

strong low energy gamma background; in the same time the intensity of the special gamma lines was reduced to an acceptable level. The energy spectrum of gamma rays was measured by using a 60 cm Ge(Li) detector. Fig. 3 and 4 show the gamma spectra for Fe and Ni rediators, respectively.

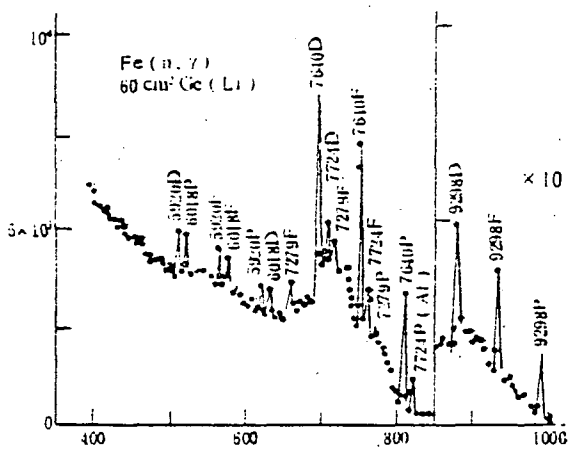

Fig. 3 The gamma spectrum produced in the thermal neutron capture reaction of Fe

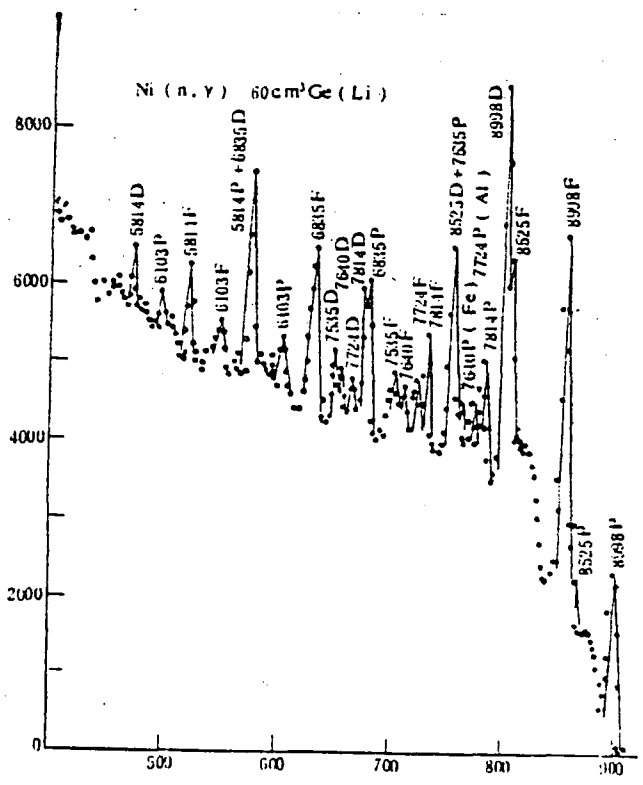

Fig. 4 The gamma spectrum produced by Ni radiator

The intensity of the gamma lines was measured by using scintillation detector of NaI(Tl) with diamter 100 mm and 100 mm high. The efficiency of the NaI(Tl) detector was calculated by Monte-Carlo methed. Fig.5 shows the calculated values of the efficiency versus E_γ for some energy points.

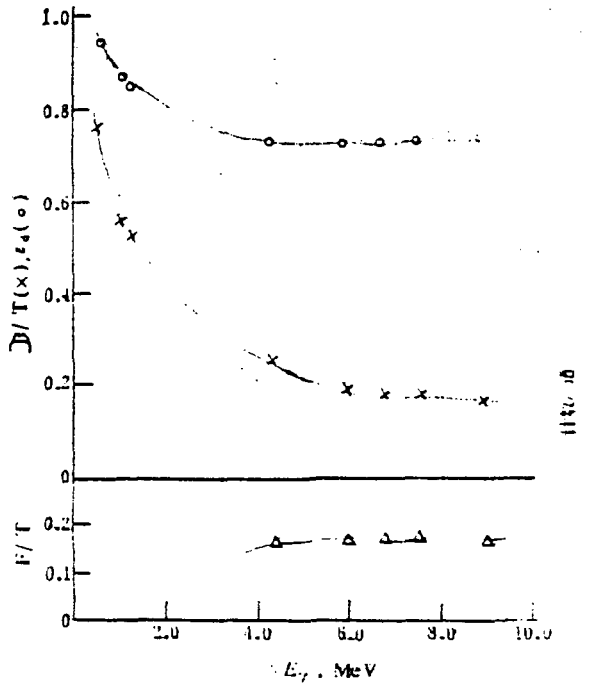

Fig.5 The efficiency of NaI(Tl) gamma detector

o —— ε_d (intrinsic efficiency for incident γ)

X —— D/T the ratio of total energy peak to intrinsic value

Δ —— F/T the ratio of single escape peak to intrinsic value

The energies and intensities of γ lines for some radiators are shown in Table 1 for the case when the reactor power is 3MW.

Table 1: The measured energies and intensities of γ rays

radiator	E (keV)	Rel. intensity	Abs. intensity
Fe	9298	3.9	
	7643+7629	49	$1.1*10^6$ /s.cm
	7279	5.3	
	6018	8.5	
	5920	8.3	
Ni	8998	26	$6*10^5$ /s.cm
	8525	13	
	7814	6.1	
	7535	3.4	
	6832	4.5	
	5814	2.1	
Be	6820		$1.6*10^5$ /s.cm

Some experiments have been done after installation of this facility:

a) Resonance scattering of gamma rays: In this kind of experiment the scatterer sample was put in position 11 and the detector was put in position 12(see Fig.2). Fig.6 shows the $^{74}Ge(\gamma,\gamma')$ resonce scattering spectrum at 6018 keV when

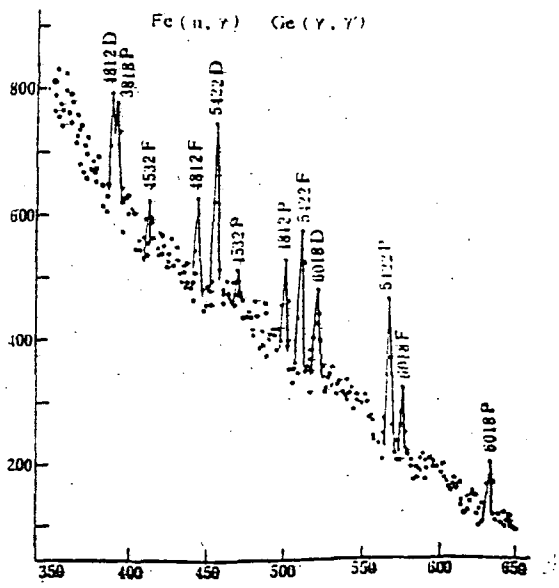

Fig.6 The ^{74}Ge(γ,γ') reaonance spectrum

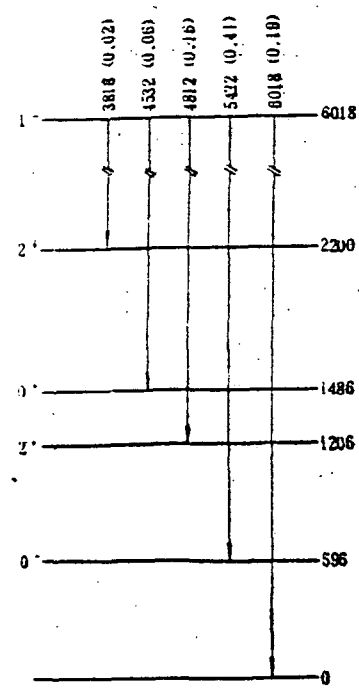

Fig.7 The level scheme of Ge-74

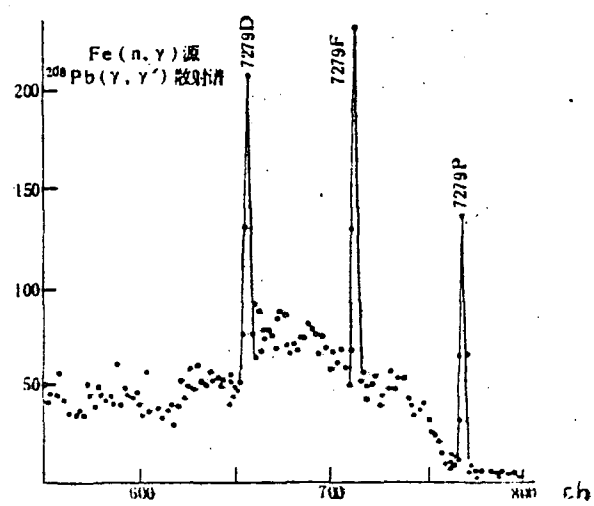

Fig.8 The ^{208}Pb(γ,γ') resonance scattering spectrum

Fe radiator was used. Fig.7 shows the measured level scheme for Ge-74. Fig.8 shows the ^{208}Pb(γ,γ') resonance scattering spectrum, when the same Fe rediator was used. We can see from Fig.8 that a quiet pure monochromatical 7.28 MeV gamma line was obtained which could be used as a convenince

high energy gamma source for the total cross section measurements and energy calibration of some gamma detectors.

b) Total photo cross section measurement for some metals at E =7.28 MeV (see attachd paper);

c) Cross section of ^{209}Bi(γ,n) reaction induced by thermal neutron eapture gamma ray on Fe: (FAST NEUTRON PHYSICS, Proceeding of the International Conference on Fast Neutron Phyeics, Dubrovnik, May 26-31 1985, p.292);

d) Fission product yields of Th-232 photo--fission at 7.64 MeV (to be published);

e) Energy and relative efficiency calibration for some gamma detectors;

f) Test of the effectiveness of some shielding materials: We have tested three bunches of shielding materials. Data obtained have been used as references for some production of shielding materials.

PROGRESS ON THE APPLICATION OF STATISTICAL THEORY TO NUCLEAR DATA EVALUATION

WANG Shu Nuan

Institute of Atomic Energy, P.O.Box 275-41, Beijing, China

Abstract

The double differential cross section, spectrum, angular distribution and cross section of all more important reaction channels in the energy range between 3 and 20 MeV for both structural and fissionable nuclides are described simultaneously and consistently. The systematic behavior of level density on saddle point has been obtained by means of the approximation of effective single hump fission barries.

1. Introduction

The nuclear data of reactions induced by neutron in the energy range of 1 keV - 20 MeV have been described by different theoretical models, namely optical model, Hauser-Feshbach statistical theory with width fluctuation correction, exciton model and evaporation model. The pre-equilibrium statistical theory has been proved to be very successful in the description of light projectiles inducing reactions in the energy range of several tens of MeV. We have first derived an exact closed form solution for the time-integrated master equation of exciton model with emphasis of the importance by taking into account the influence of both the Fermi motion and the Pauli princeple[1] in the energy range of several tens of MeV, which is comparable with or less than Fermi energy. The calculated results[1] show that the theory can explain the presently existing experimental[2] data, especially solve the problem of double differential cross section for emitted neutrons with high energy at backward angles. The theory has been using for the calculation of FM-6 in ENDF/B-VI for both of structural and fissionable nuclides and analysing new experimental data.[3-4] By using the unified or combined approach of those theory models mentioned above, the double differential cross section, spectrum, angular ditribution

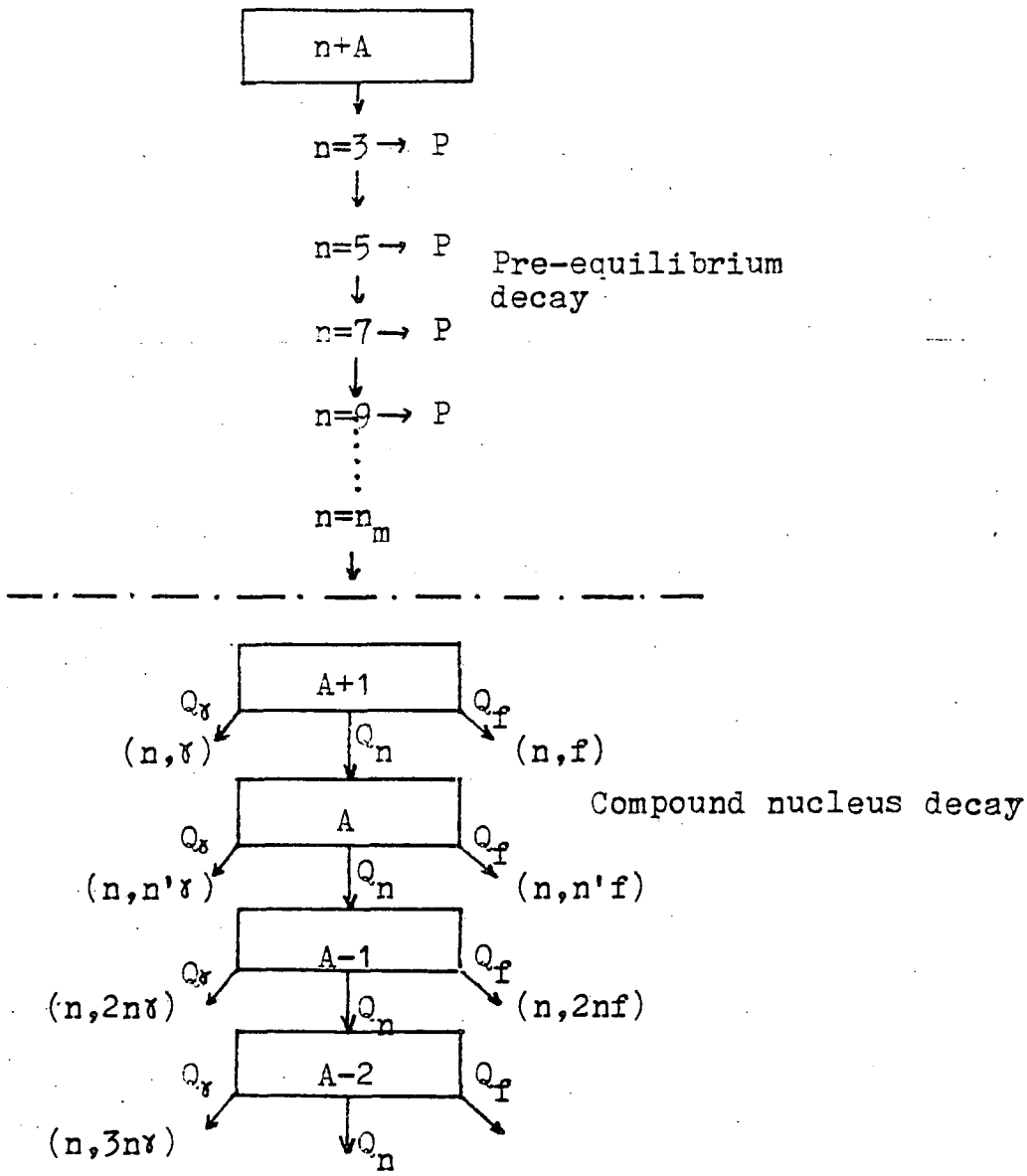

Fig.1 scheme of reaction

and cross section of each reaction channel for multi-particle emission processes can be expressed simultaneously and consistently. In this respect we have been working for years and making the unified standard codes for theoretical fitting, interpolation and extrapolation of the nuclear data as well as for the data calculation of non-stable isotopes. The main lines of the description are given in Sec.2.

For actinede nuclei bombarded by neutron with energy in the range of 3-20 MeV, the unified evaporation and exciton models to calculate the whole set of reaction data for multi-neutron emission process have been used satisfactorily. (5) The systematic behavior of level density on saddle point has been obtained by means of the approximation of effective single hump fission bar-

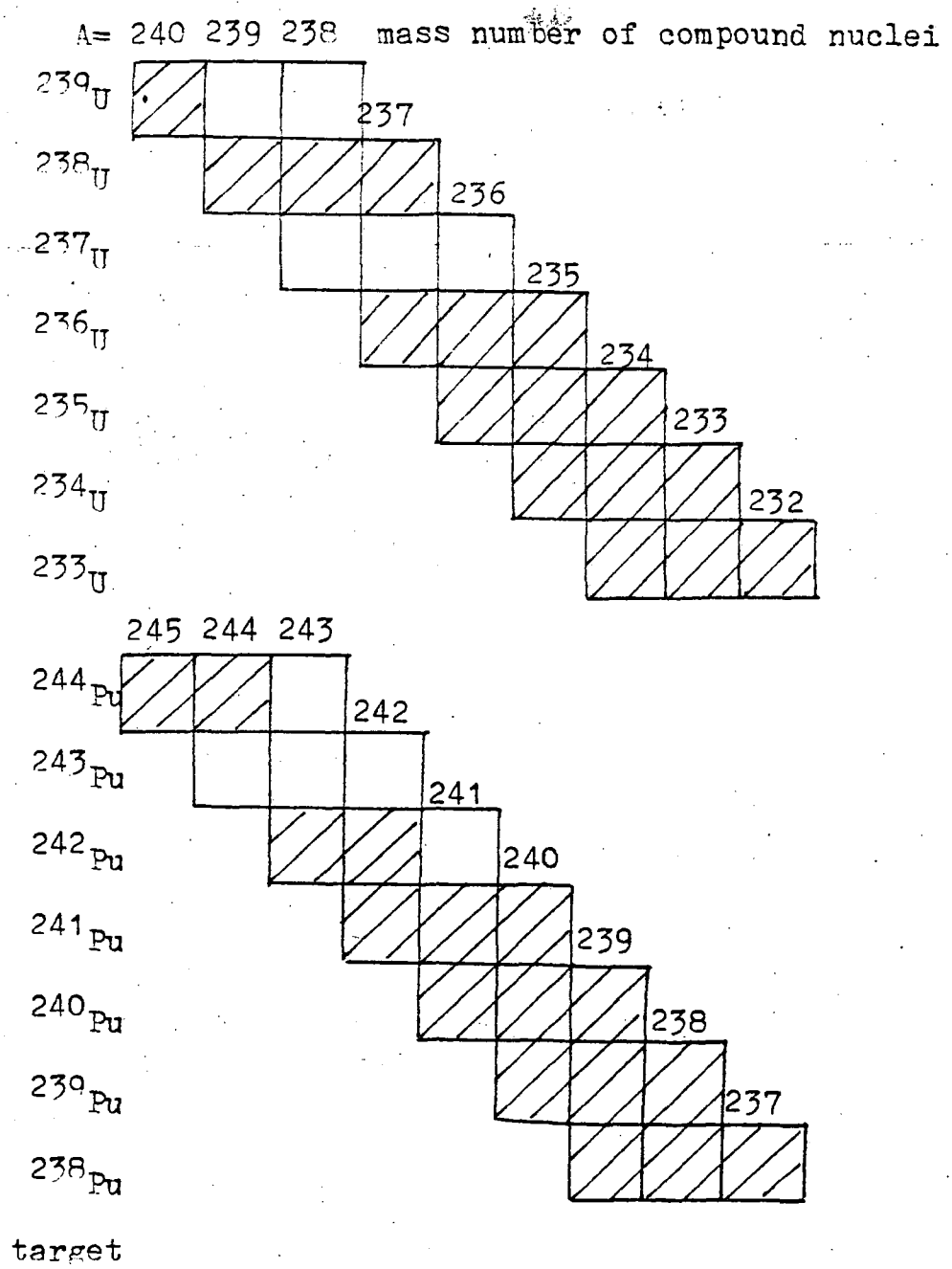

Fig.2 scheme of the situation for U,Pu elements
//// There are some exp. fission cross section data.

ries, [5] which is in good agrement with the one given by J.E.Lynn in the same energy range. [6] The systematic behavior of level density on saddle point and the shape of normalized spectrum for (n,nγ), (n,n'f), (n,2nγ), (n,2nf), (n,3n) reaction channels of U, Pu elements are discussed in Sec.3.

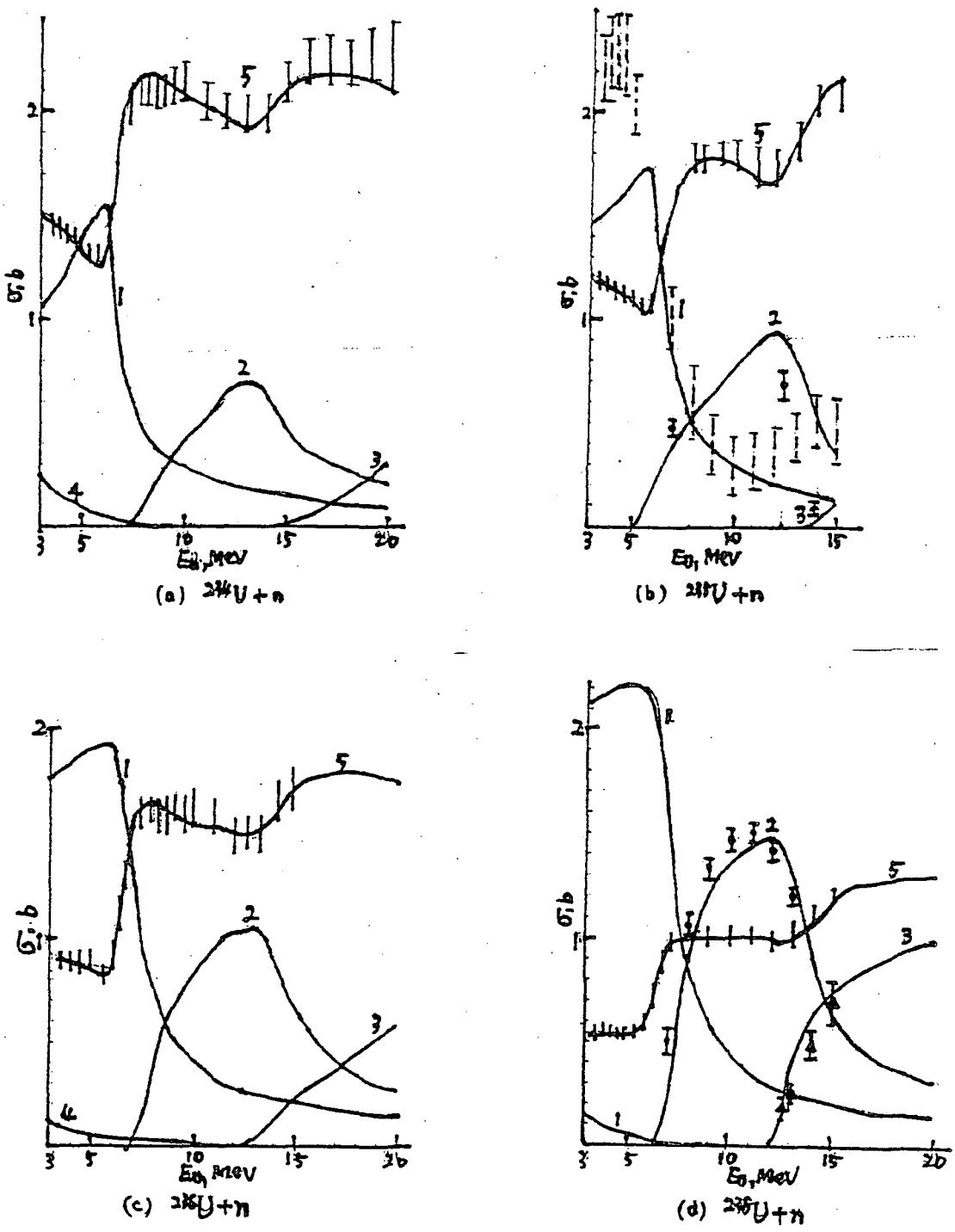

Fig. 3

2. The Model for Multi-Particle Emission Process in the Energy Range of 3-20 MeV

As mentioned in Sec.1, we have unified optical model, exciton model and evaporation model consistently to calculate FM3, 4,5,6 of ENDF/B for both structural and fissionable nuclides. We assume that for the former, the charged particle, such as p,d, ^{3}He, T, α can be emitted, but the fission channel is no opened; for the latter, fission channel is opened instead of charged

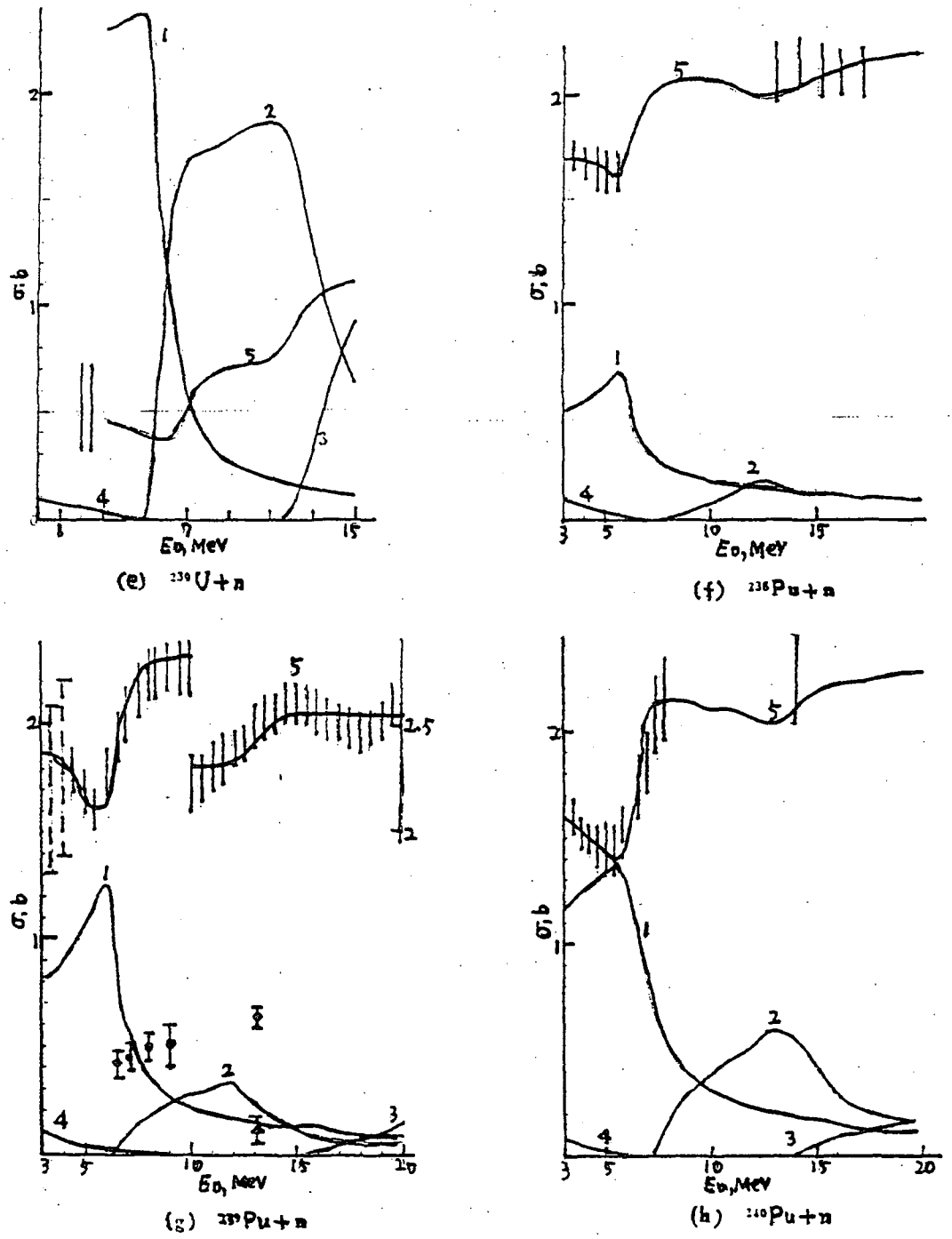

Fig. 4

particle emissions. In the model direct reaction mechanism is ignored. In generalized master equation of exciton model the Fermi gas model has been adopted for nucleon-nucleon interaction inside the nucleus for the derivation of the kernel, thus the effects of Paule principle and Fermi motion are properly taken into account as proposed in ref. (1). The effects of the finite nuclear size and the refraction of the incident wave at the nuclear surface underling the exciton model are also properly taken into account by cutting l values and considering refraction kernel. We sup-

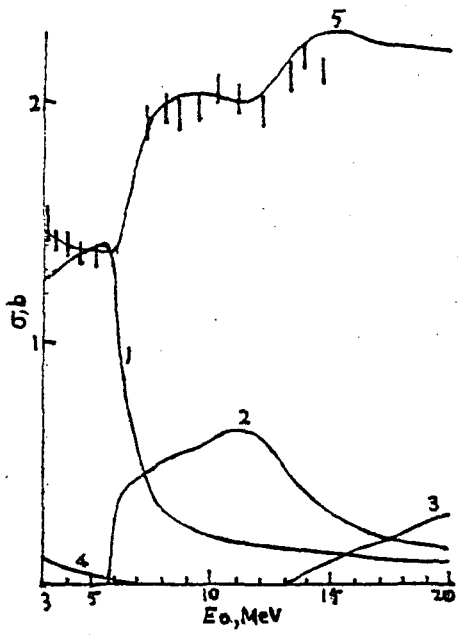

(i) $^{241}Pu+n$

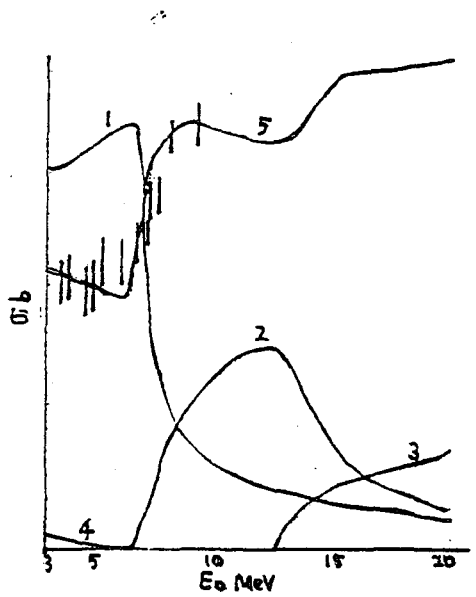

(j) $^{242}Pu+n$

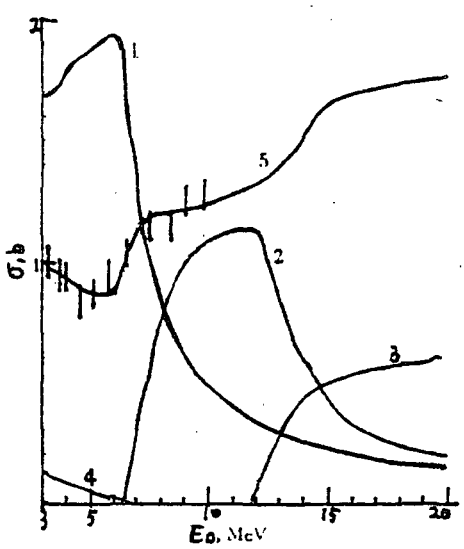

(k) $^{244}Pu+n$

Fig.5

Fig. 3-5 cross sections of U,Pu elements

1-5 are for $\sigma_{n,n'\gamma}$, $\sigma_{n,2n\gamma}$, $\sigma_{n,3n}$, $\sigma_{n,\gamma}$, $\sigma_{n,F}$

$\sigma_{n,n'\gamma}$ exp. data

$\sigma_{n,F}$ exp. data

$\sigma_{n,2n\gamma}$ exp. data

$\sigma_{n,3n}$ exp. data

pose only considering the first and second pre-equilibrium emissions in the calculations.

First of all, we define the tending to equilibrium probability from exciton number n_1 to n_2 by λ_{+2} transition of the composite system with mass number A, atomic number Z, excitation energy U for k-th emission process as the following

$$D_k(n_1, n_2, Z, A, U) = \prod_{\substack{n=n_1 \\ \Delta n=2}}^{n_2-2} \frac{\lambda_+(Z, A, U, n)}{(\lambda_+(\,''\,) + \lambda_-(\,''\,) + \lambda_0(\,''\,) + W_k(\,''\,))}$$

here, $\lambda_{\pm,0}$ are the exciton transition rate for $\Delta n=\pm 2,0$ processes. $W_k(Z,A,U,n)$ is the k-th total emission rate of the n-th exciton state.

Another definition is the probability of emitting particle with mass number A_ν, atomic number Z_ν, energy E_ν in direction Ω_k at the composite system state with mass number A, atomic number Z, excitation energy U after from exciton number n_1 to n_2 by λ_+ transition for k-th emission process as bellow

$$P_k(Z, A, U, n_1, n_2; Z_\nu, A_\nu, E_\nu, \Omega_k) = t_k(Z, A, U, n_2, \Omega_k) \cdot \omega_{\nu_k}(Z, A, U, n_2; Z_\nu, A_\nu, E_\nu)$$

with

$$t_k(Z, A, U, n_2, \Omega_k) = \sum_l \tau_l(Z, A, U, n_2) P_l(\cos\theta_k)$$

here, t_k, ω_{ν_k} are the life time and the total emission rate of per MeV, respectively. τ_l is the exact closed form solution to the time-integrated master equation in the form of partial wave,[1] in which the effects of the finite nuclear size and the refraction of the incident wave at the nuclear surface have been included by cutting l values [1] and calculating the refraction kernel as given in ref. (7).

We take (n,2nγ) reaction as an example to give the formulas of double differential cross section $\sigma_{n,2n\gamma}(E_0,E_n,\theta)$, normalized spectrum $N_{n,2n\gamma}(E_0,E_n)$, angular distribution $\sigma_{n,2n\gamma}(E_0,\theta)$ and cross section $\sigma_{n,2n\gamma}(E_0)$ as follows

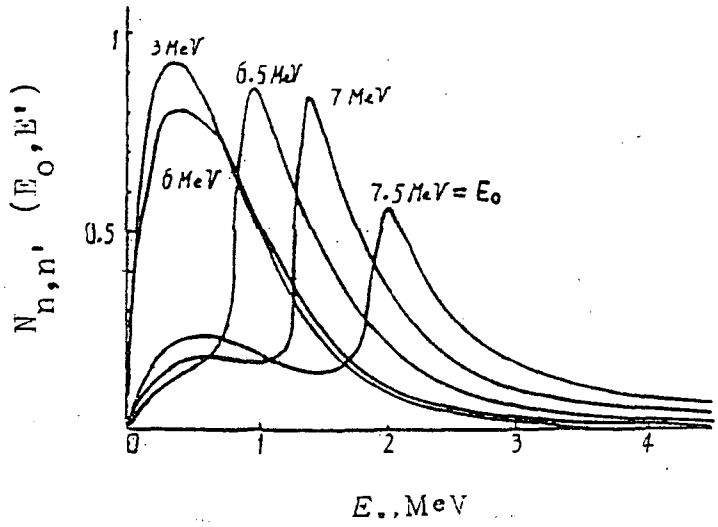

Fig.6 n+^{235}U(n,n') normalized spectrum

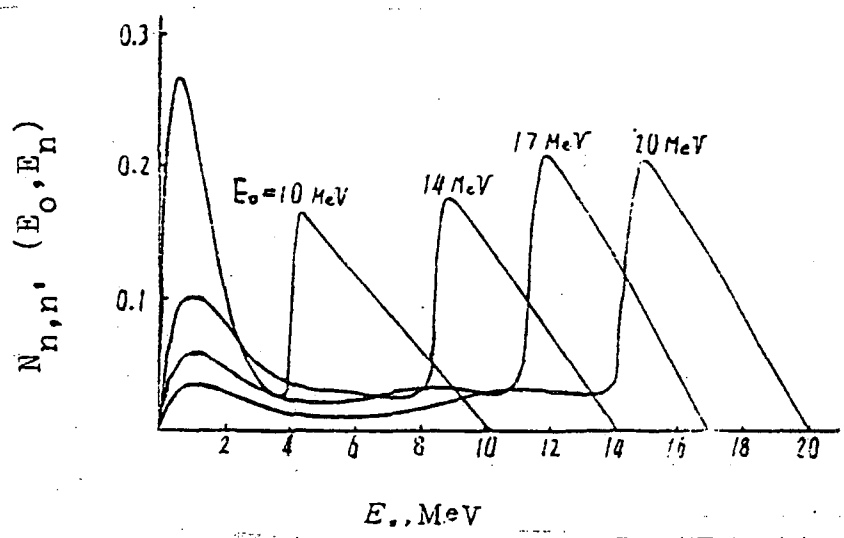

Fig.7 n+^{233}U(n,n') normalized spectrum

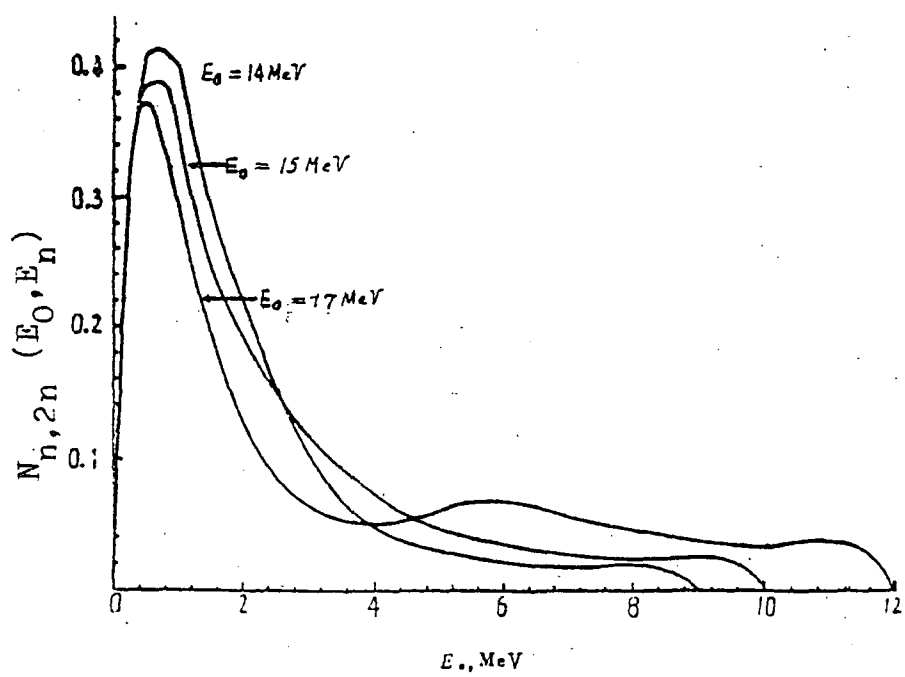

Fig.8 n+^{237}U(n,2n) normalized spectrum

$$\sigma_{n,2n\gamma}(E_0) = \sigma_a(E_0)\int_0^{E_0-B_{n_2}} dE_{n_1}\int_0^{E_0-B_{n_2}-E_{n_1}} dE_{n_2}\int d\Omega_1\int d\Omega_2$$

$$\cdot\left\{\sum_{\substack{n=n_0\\ \Delta n=2}}^{\bar{n}} P_1(Z, A+1, E_0+B_{n_1}, n_0, n; 0, 1, E_{n_1}, \Omega_1)\right.$$

$$\cdot\left[\sum_{\substack{m=n-1\\ \Delta m=2}}^{\bar{n}} P_2(Z, A, E_0-E_{n_1}, n-1, m; 0, 1, E_{n_2}, \Omega_2)\right.$$

$$\left.\cdot q_2(Z, A, E_0-E_{n_1}, 0, 1, E_{n_2})\right]$$

$$+ D_1(n_0, \bar{n}, Z, A+1, E_0+B_{n_1})\cdot q_1(Z, A+1, E_0+B_{n_1}, 0, 1, E_{n_1})$$

$$\left.\cdot q_2(Z, A, E_0-E_{n_1}, 0, 1, E_{n_2})\right\}$$

$$\cdot Q_\gamma(Z, A-1, E_0-E_{n_1}-B_{n_2}-E_{n_2})$$

here, E_0 is the energy of incident neutron. B_{n1}, B_{n2}, E_{n1}, E_{n2} are the binding energy and the emission energy of the first and second emitted neutrons, respectively. q_1, q_2 are the probabilities of the evaporated first and second neutron per unit of MeV. Sr. Q_γ is the γ-ray emission probability after two neutrons emitting. $\sigma_a(E_0)$ is the formation cross section of the compound system. Thus we have

$$\sigma_{n,2n\gamma}(E_0, E_n, \theta) = \frac{1}{2}\left(\int \sigma_{n,2n\gamma}(E_0)\, dE_{n_1} d\Omega_1 + \int \sigma_{n,2n\gamma}(E_0)\, dE_{n_2} d\Omega_2\right)$$

$$\sigma_{n,2n\gamma}(E_0, \theta) = \frac{1}{2}\left(\int \sigma_{n,2n\gamma}(E_0)\, dE_{n_1} dE_{n_2} d\Omega_1 + \sigma_{n,2n\gamma}(E_0)\, dE_{n_1} dE_{n_2} d\Omega_2\right)$$

$$N_{n,2n\gamma}(E_0, E_n) = \left(\int \sigma_{n,2n\gamma}(E_0)\, d\Omega_1 d\Omega_2 dE_{n_1} + \int \sigma_{n,2n\gamma}(E_0)\, d\Omega_1 d\Omega_2 dE_{n_2}\right) \Big/ 2\sigma_{n,2n\gamma}(E_0)$$

3. Systematics of Level Density on Saddle Point

We have used the unified evaporation model and exciton model presented by probability of finding the system in the state of exciton number n at time t with never come back assumption to calculate cross sections and spectrum of (n,n'γ), (n,n'f), (n,2nγ),

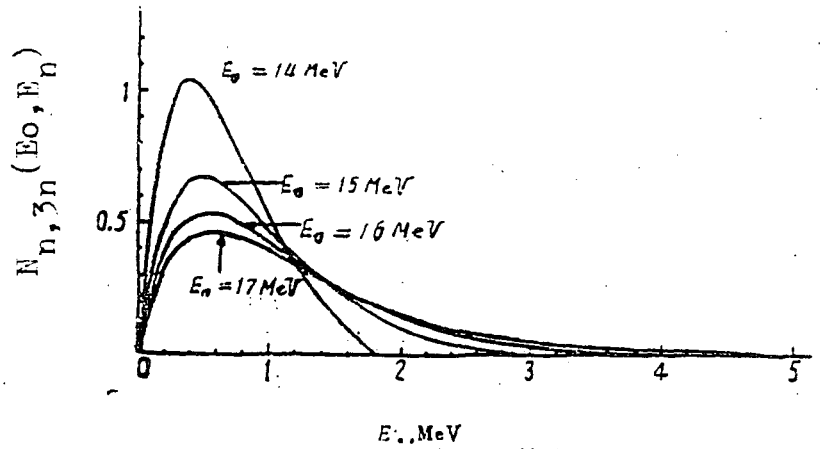

Fig.9 n+^{237}U(n,3n) normalized spectrum

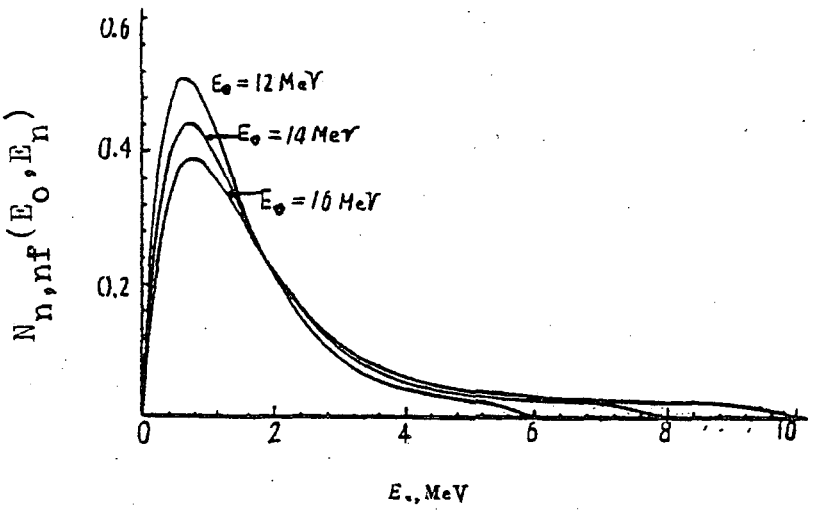

Fig.10 n+^{237}U(n,n'f) normalized spectrum

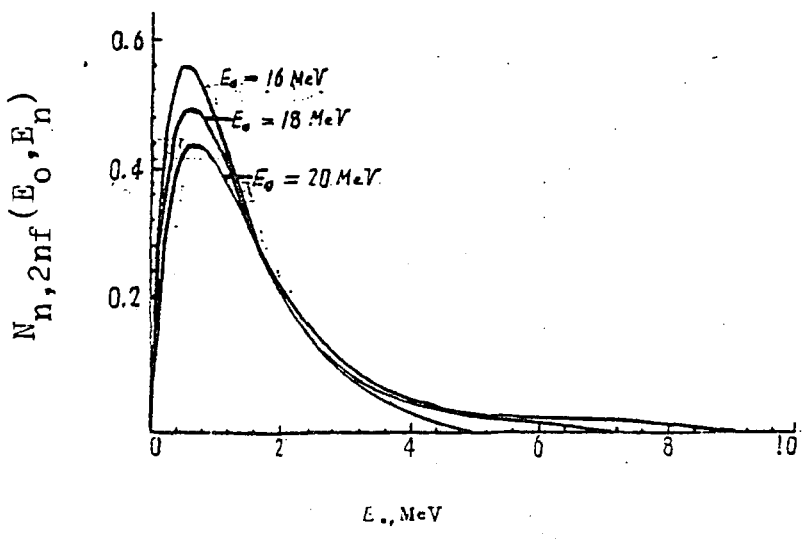

Fig.11 n+^{237}U(n,2nf) normalized spectrum

(n,2nf), (n,3n) reactions for U,Pu elements. (see fig. 1) In the calculations the compound and residual nucleus level densities are adopted in the form of Gilbert-Cameron.[8] The saddle point state density is adopted in the same form, but the level parameter a_f is no longer constant for a large deformation nucleus as below

$$a_{f/a} = 1 + \frac{K_2}{E-\Delta}$$

here K_2 is a fitting parameter.

The constant temperature factor is

$$T_f = \left(\sqrt{\frac{a}{E_T - K_2 - \Delta}} - \frac{1}{E_T - \Delta} - \frac{1}{2(E_T + K_2 - \Delta)} \right)^{-1}$$

The saddle point state level density is written as

$$\rho_f(E) = \begin{cases} \dfrac{K_1 \sqrt{\pi} \exp\left(2\sqrt{a(V_T + K_2)} + (E - E_T)/T\right)}{12\sqrt{a(E + K_2 - \Delta)}\,(E - \Delta)}, & (E \leq E_T) \\[2ex] \dfrac{K_1 \sqrt{\pi} \exp\left(2\sqrt{E + K_2 - \Delta}\right)}{12\sqrt{a(E + K_2 - \Delta)}\,(E - \Delta)}, & E > E_T \end{cases}$$

with $$V_T = E_T - \Delta$$

here, K_1 is another fitting parameter. The K_1, K_2 for U, Pu elements are obtained by fitting known experimental fission cross section shown in fig. 2 based on the approximation of effective single hump fission barries assumption.

The systematic behavior of level density on saddle point are shown as

$$\eta = \begin{cases} 1.675 & \text{for e-e nuclei} \\ 4.624 & \text{for odd nuclei} \end{cases}$$

with $$\eta = \rho_f(E, K_1, K_2) / \rho(E, K_1 = 1, K_2 = 0)$$

The values of $\rho_f(E, K_1, K_2)$ which we have obtained is the same as the one proposed by J.E.Lynn[6] in the same energy range of E = 3-4 MeV. The calculated cross sections are shown in fig.3-5, the normalized spectrum results are shown in fig. 6-11.

From the calculated results presented in this paper we can conclude that the model described above and the systematic behavior of level density on saddle point are very satisfactorily. Based on the models described in Sec.2 and combined with Hauser-Feshbach formula with width fluctuation correction, we have made more useful codes of FM4-5 in form ENDF/B named MUP1, 2, FUP1 for both of structural and fissionable nuclides from 1 keV to 20 MeV successfully. The codes to calculate the FM3,4,5,6, from 1 keV to 20 MeV for both structural and fissionable nuclides are just on the way.

References

1. Sun Ziyang et al., Z. Phys. A-Atoms and Nuclei 305, 61 (1982); Commun. in Theor. Phys., 1, 581 (1982).
2. D. Hermsdorf et al., ZfK-277 (1974).
3. H. Gruppelaar and J. M. Akkermans, ECN-85-090; ECN-164.
4. WANG Shu Nuan, Yan Shi Wei, Chinese Journal of Nuclear Phys., Vol. 7, 2, 189 (1985).
5. Zhang Jing Shang and WANG Shu Nuan, Atomic Energy Science and Technology, 1, 631 (1983).
6. J. E. Lynn, AERA-R 7468.
7. H. Gruppelaar et al., International Conf. on Nuclear Data for Science and Technology, Antwerp, 1982.
8. A. Gilbert, A. G. W. Cameron, Can. J. Phys., 43, 1446 (1965).

DIFFERENTIAL ELASTIC SCATTERING CROSS SECTIONS OF THE FAST NEUTRONS FROM Mo,Nb AND W

Cao Jianhua Li Jingde Wang Chunhao Dai Yunsheng
Ja Jing Li Yiexang Xie Daquan Wan Dairong
Liang Xuecai Wan Hongsheng Zhang Di Wang Shiming

Institute of Nuclear Science and Technology
Sichuan University,Chengdu,Sichuan
The People's Republic of China

In the interaction of neutron with material,the neutron elastic scattering from nucleus is a fundamental physical process,so the neutron elastic scattering cross sections are important for nuclear theory and nuclear engineering design.

The 14.2MeV neutron elastic scattering cross sections of Mo and Nb have been measured for angles between 5 and 150 degree.The 14.7MeV neutron elastic scattering cross sections of W have been measured for angles between 45 and 150 degree.

The associated particle time-of-flight method was used to select 14.2MeV neutrons which originated from the $T(d,n)^4He$ reaction at angle near 83 degree with respect to 200KeV deuteron beam.For 14.7MeV neutrons---at angle near 40 degree.

A thin ST-401 plastic scintillator served as a-particle detector.The neutron detector used was a ST-451 Liquid scintillator.The time resolution was about 1 ns. Pulse-shape discrimination was used to eliminate r-ray events.

Data were recorded as the net number of true coincidences in the time window of a time-to-pulse height converter(TAC) gated by a-particle.The data,after substracting background,were normalized by moving the detector to 0 degree with the scaterer removed,and corrected for the dead-time,finite angular geometry,neutron-flux attenuation and multiple scattering.The results were given in table 1 and fig. 1--3.

The measured data shown in fig. 1 for Mo agree well with the results published by Strizak(1).The data in fig. 2 for Nb are in good agreement with results of Western(2) and Kammerdiener(3).The data in fig. 3 for W agree fairly well with the results of Nauto(4).

It is noted that present data are extended into the smaller or larger angle range where no data were available in previous works.

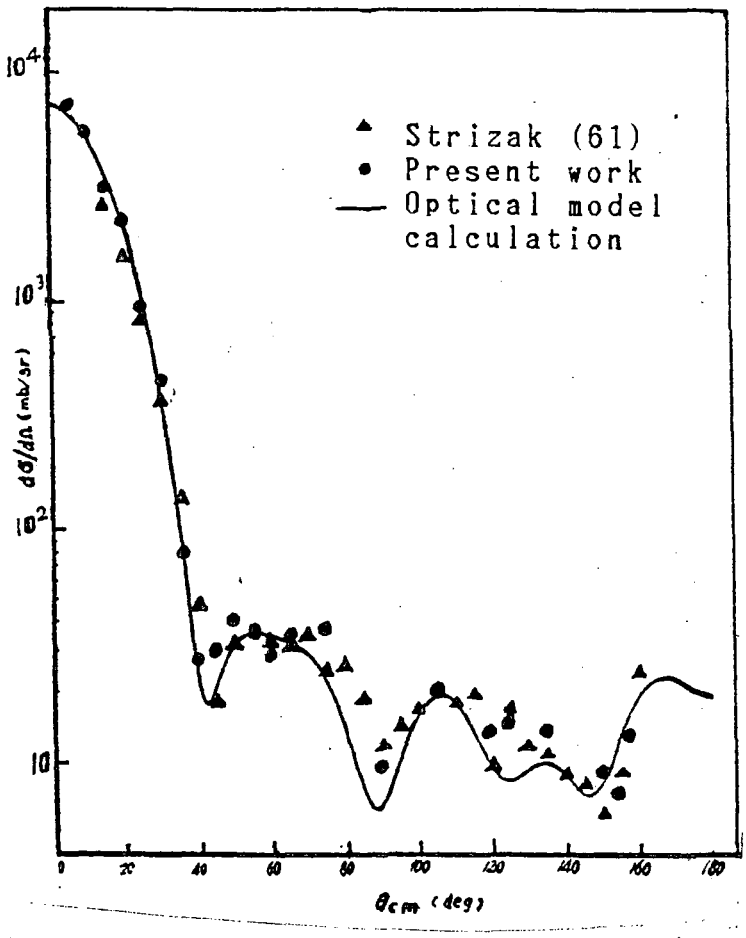

Fig.1. The differential elastic scattering cross sections for 14.2 MeV neutrons on Mo.

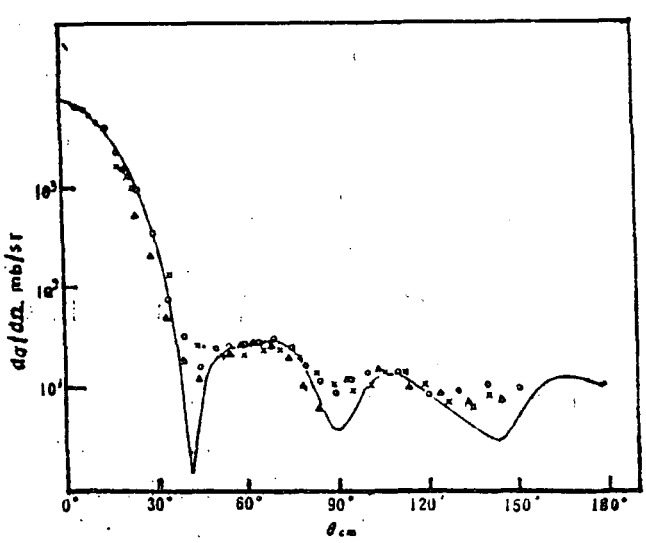

Fig.2. The differential elastic scattering cross sections for 14.2 MeV neutrons on Nb. x--ref.2, ▲--ref.3, o--this work. The solid line is optical model calculation.

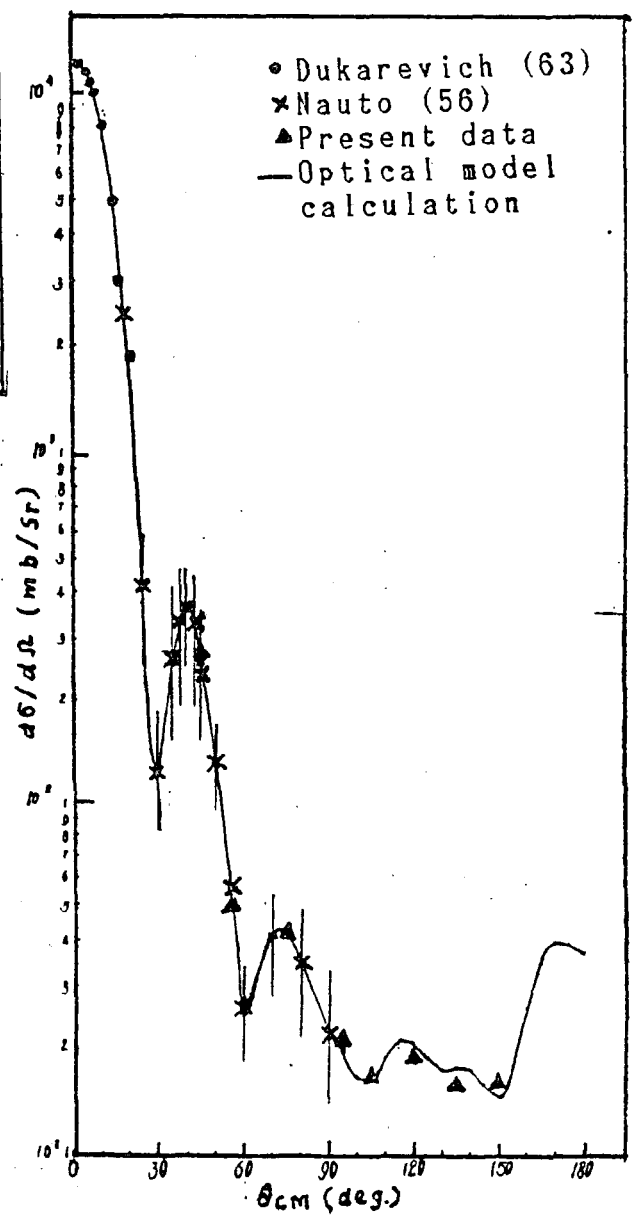

Fig.3. The differential elastic scattering cross sections for 14.7 MeV neutrons W.

Table 1. The differential elastic scattering cross sections of the fast neutrons from Mo,Nb and W

Mo			Nb			W		
θcm (deg)	dσ/dΩ (mb/sr)	Δdσ/dΩ (mb/sr)	θcm (deg)	dσ/dΩ (mb/sr)	Δdσ/dΩ (mb/sr)	θcm (deg)	dσ/dΩ (mb/sr)	Δdσ/dΩ (mb/sr)
5.05	7459	248	6.07	5850	235	45.22	274	20
10.10	5704	189	8.09	5843	284	55.26	54	4
15.15	3095	103	10.11	5036	238	75.30	43	3
20.20	2333	77	12.63	4102	176	95.31	22	2
25.26	959	42	15.16	3783	177	105.30	16	2
30.30	460	20	17.69	2103	100	120.27	20	2
35.34	82	5	20.21	1438	73	135.22	17	2
40.38	28	2	25.26	968	18	150.16	16	2
45.42	32	2	30.29	321	16			
50.46	43	3	35.26	74	5			
55.49	38	2	40.40	34	2			
60.52	29	2	45.44	17	1			
65.54	35	2	50.48	24	1			
75.58	40	3	55.51	25	2			
90.60	10	1	60.54	26	2			
105.58	21	2	65.56	26	2			
120.52	15	1	70.58	30	3			
135.42	14	1	75.60	24	2			
150.30	9	1	80.61	16	1			
155.25	7	1	85.62	11	1			
157.73	13	1	90.62	9	1			
			95.62	12	1			
			100.61	14	1			
			110.58	14	1			
			120.54	8	1			
			130.48	9	1			
			140.40	10	1			
			150.30	10	1			

Reference

(1)Strizak;ZET, V.41, N.2, P.313 (1961).
(2)Western, G.T., et al.; CONF-660303, 2, P.675 (1966).
(3)Kammerdiener, J.L.; UCRL-51232 (1971).
(4)Nauto, H.; Nucl.Phys. V.2, P.124 (1956/57).
(5)Dukarevich, Yu.V., et al.; Zh.Eksp.Teor., 44, P.130 (1963).

DIFFERENTIAL ELASTIC SCATTERING CROSS SECTIONS OF 1 MEV NEUTRONS ON NICKEL

Li Jingde Zhan Di Xie Daquan Li Yiexiang
Wang Siming Liang Xuecai Zhou Yiming Cao Jianhua

Institute of Nuclear Science and Technology
Sichuan University,Chengdu,Sichuan
The People's Republic of China

The measurement was carried out at the 2.5 MeV Van de Graaff accelerator oprated in the pulsed and bunched beam.The pulse duration was 1.7ns,repeat rate was 2 MHz and the average proton beam intensity was 2--4uA.

The $T(p,n)^3He$ reaction was used as neutron source. The neutron detector was shielded by a big tank filled with lithium carbonate and paraffin,and a lead ring was set inside the tank.The pulse-shape discrimination was applied to reduce the r-ray contamination.The total time resolution was 3ns.

The differential cross sections were measured in the interval 20--150 degree with use of time-of-flight method ,and normalized to C-12,ref.(1).

The results were given in table 1 and fig.1.The data shown in fig.1 are in good agreement with the results of Cox(2) and Darden(3),but somewhat larger than results of Wallt(4) in the small angle range.

Table 1. the differential elastic scattering cross sections of 1 MeV neutrons on Ni

Cosθcm	dσ/dΩ (mb/sr)	Δdσ/dΩ (mb/sr)
0.938	555	35
0.862	518	32
0.698	284	18
0.487	201	13
0.243	160	10
-0.017	141	9
-0.275	139	10
-0.513	154	11
-0.716	222	16
-0.870	238	17

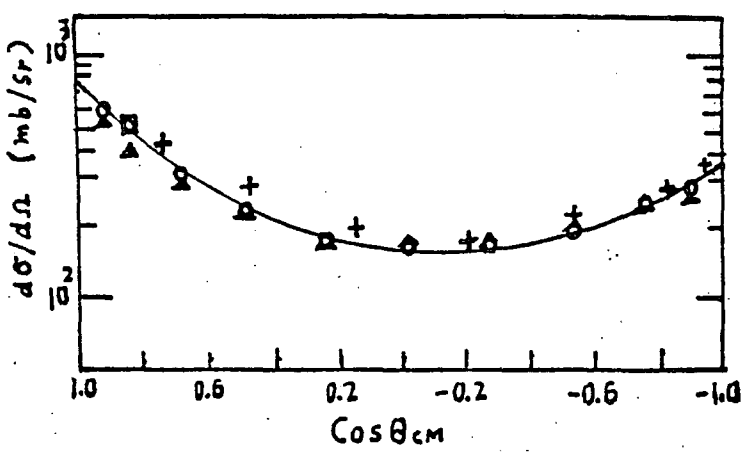

Fig.1.The differential elastic scattering cross sections for 1 MeV neutrons on Ni. +--ref.2, []--ref.3,▲--ref.4,o--this work.

Reference

(1)Carber,D.L.,et al.;BNL-400 3-rd ed.1 (1970).
(2)cox,S.A.,et al.;Bull.Am.Phys.Soc.,8,P.478 (1963).
(3)Darden,D.T.,et al.;BNL-325 3-rd ed.2, (1976).
(4)Wallt,M.,et al.,Phys.Rev.,93,P.1602 (1954).

SMALL-ANGLE SCATTERING OF 14.7 MEV NEUTRONS

Cao Jianhua Wan Dairong Dai Yunsheng
Liang Xuecai Wang Chunhuao

Institute of Nuclear Science and Technology
Sichuan University,Chengdu,Sichuan
The People's Republic of China

The elastic scattering of fast neutrons into angles below 10 degree is the subject of both theoretical and experimental stydies.As neutron elastic differential cross section measurements are extended downward in angle toward 0 degree,the dominant interaction is predicted to change from nuclear to electromagnetic,that has been verified by observing the scattering of neutron on heavy nuclei(1).However,about the existence of anomalously strong scattering at small angles,there is contention among different investigators(2--6).

The present experiment was undertaken to investigate the behaviour of fast neutron elastic scattering on the heavy,medium-weight and light nuclei at the small angles.

The 14.7 MeV neutron elastic scattering differential cross sections of U, Pb, Fe, Al, C and Be have been measured in the angles 2.7--9.9 degree by use of a fast neutron position-sensitive spectrometer and associated particle time-of-flight method.The detector consists of a ST-1701 liquid scintillator filled in a glass cylinder, 80cm in length and 5cm in diameter,with both end-faces in optical contact with two photomultiplies.The time difference between both output signals of the phototubes,owing to the different optical paths,may be well approximated by a linear function of position of the light-producing region. An important feature of this method is that data might be taken simultaneously at the total angle of acceptance of the scintillator.The time resolution of the system is 0.87 ns.The pulse shape discrimination was applied to reduce the r-ray backgrounds.

The experimental equipment is basically a shielded-source geometry. The associated particle time-of-flight method was used to select 14.7 MeV neutrons which originated from the $T(d,n)^4He$ reaction at angles near 40 degree with respect to a 200KeV deuteron beam.The electronically collimated neutron cone passed through an iron-polyethylene collimator,120cm in length.The profile of the neutron beam was about 1.1 degree.

Each sample was a cylinder,the diameter was larger than the size of the collimated neutron beam ,and the thickness was chosen to give a transmition of approximately 0.6. The position-sensitive spectrometer was symmetrically placed with respect to the neutron beam direction in the horizontal plane.

The scattering measurements were alternated with background measurements, by replacing the scatterer from the back aperture of collimator to the front. The differential cross sections were normalized by moving each counter-element of the positional spectrometer

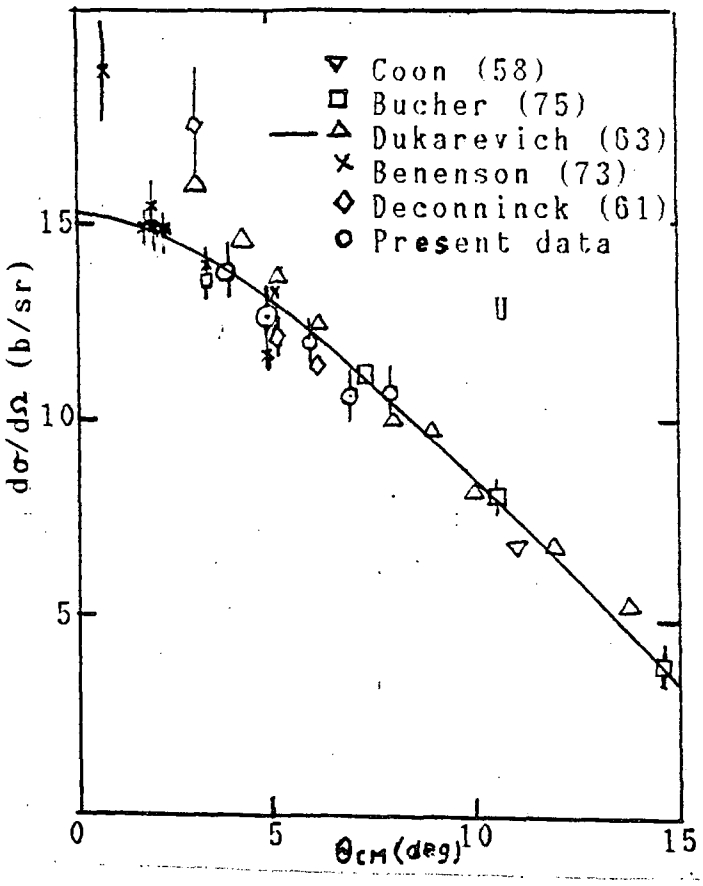

Fig.1. The 14.7 MeV neutron elastic scattering from U

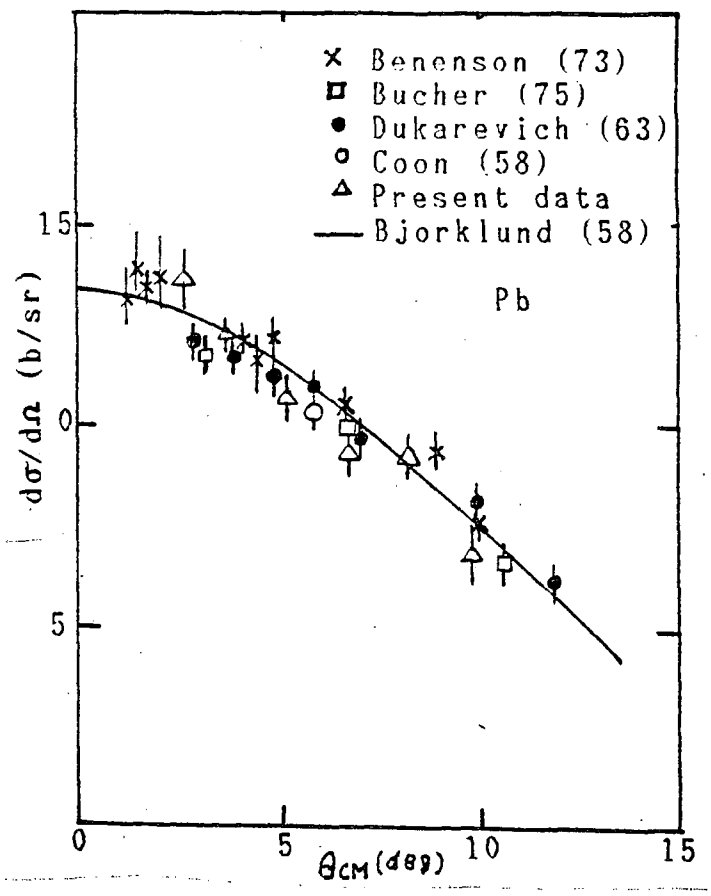

Fig.2. The 14.7 MeV neutron elastic scattering from Pb

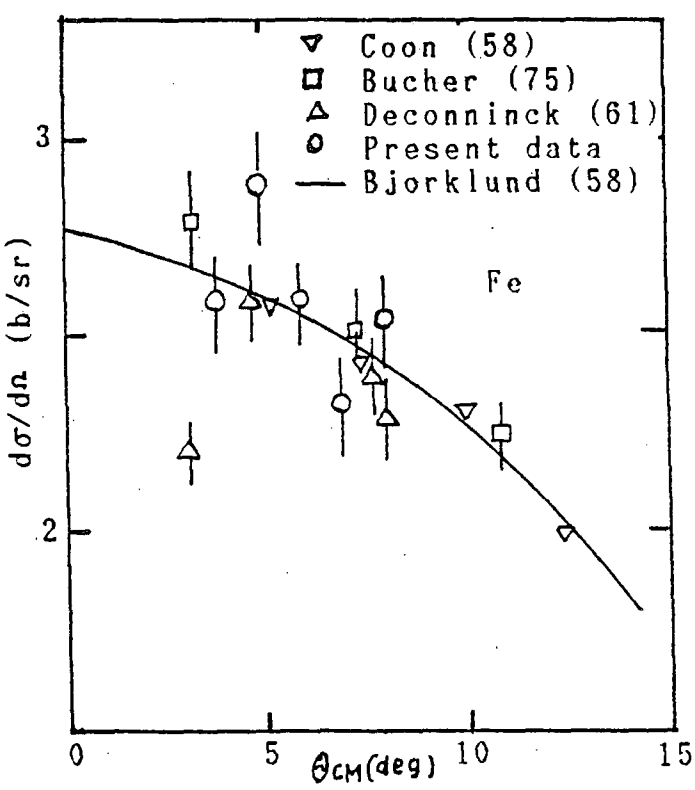

Fig.3. The 14.7 MeV neutron elastic scattering from Fe

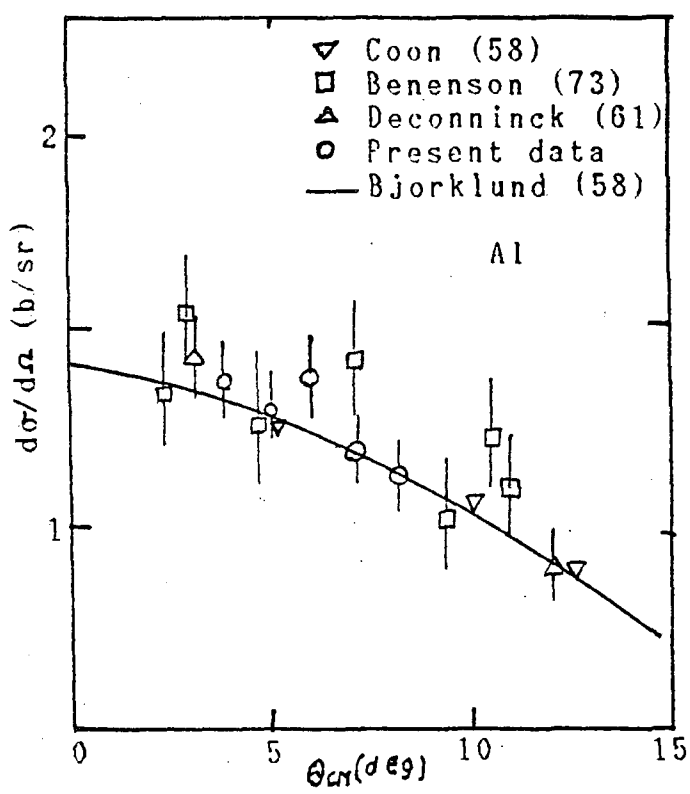

Fig.4. The 14.7 MeV neutron elastic scattering from Al

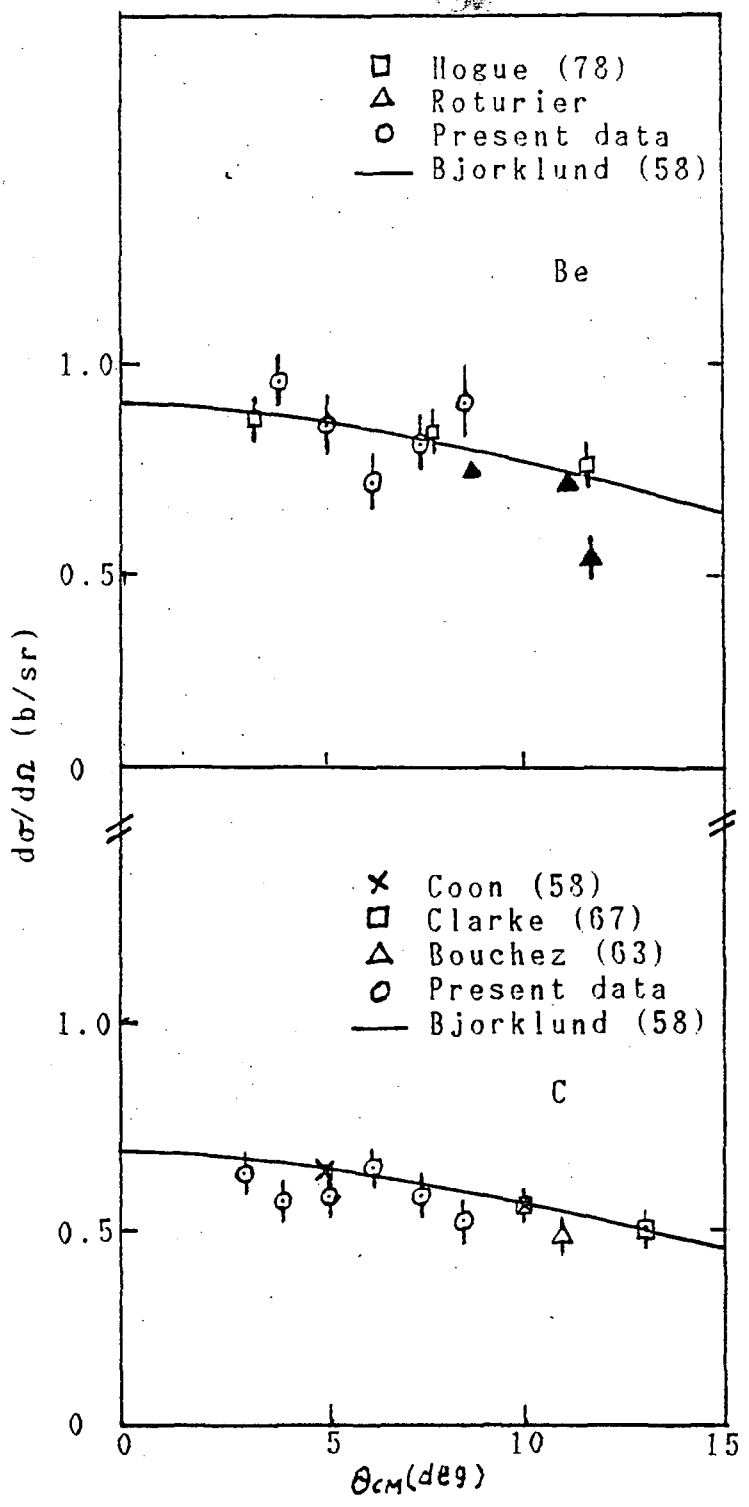

Fig.5. The 14.7 MeV neutron elastic scattering from C and Be

to 0 degree with the scatterer removed. The results were corrected for dead time, and corrected for finite angular geometry, neutron flux attenuation and multiple scattering in the samples using a Monte-Carlo method.

The experimental results, subtracted Schwinger scattering, are shown in table 1 and fig. 1--5.

The present data in fig.1 for U agree well with the data of Benenson(5), Bucher(6), and Coon(8), but are lower than the data of Dukarevich(2) in the smaller angle region. The data in fig.2 for Pb are in fair

Table 1. The 14.7 MeV neutron elastic scattering differential cross sections of U,Pb,Fe,Al,C,and Be in the angles 2.7-9.9

U			Pb			Fe		
θcm (deg)	dσ/dΩ (mb/sr)	Δdσ/dΩ (mb/sr)	θcm (deg)	dσ/dΩ (mb/sr)	Δdσ/dΩ (mb/sr)	θcm (deg)	dσ/dΩ (mb/sr)	Δdσ/dΩ (mb/sr)
3.70	13777	964	2.66	13594	952	3.76	2632	184
4.72	12631	884	3.87	12059	844	4.78	2924	205
5.75	11931	835	5.30	10517	736	5.83	2619	183
6.81	10451	732	6.83	9313	652	6.90	2329	163
7.87	10611	743	8.34	9237	647	7.98	2559	174
			9.88	6819	477			

Al			C			Be		
θcm (deg)	dσ/dΩ (mb/sr)	Δdσ/dΩ (mb/sr)	θcm (deg)	dσ/dΩ (mb/sr)	Δdσ/dΩ (mb/sr)	θcm (deg)	dσ/dΩ (mb/sr)	Δdσ/dΩ (mb/sr)
3.83	1366	96	2.98	644	45	4.10	959	67
4.87	1285	90	4.01	566	40	5.22	847	59
5.94	1382	97	5.09	585	41	6.36	711	50
7.03	1175	82	6.21	664	46	7.53	797	56
8.13	1119	78	7.34	578	40	8.71	912	64
			8.49	519	36			

agreement with result of Benenson(5), Bucher(6), Dukarevich(2) and Coon(8). The data in fig.3 for Fe agree with the data of Bucher(6) and coon(8) in uncertainties.The data in fig.4 for Al agree well with data of coon(8),Deconninck(7) and Benenson(5).The data in fig. 5 for C are in excellent agreement with the data of coon(8) ,Clarke(9) and Bouchez(10).The data in fig.5 for Be agree well with the data of Hogue(11) and Roturier(12).

Cconclusions: No evidence of anomalies has been found at the small-angle range.Previous results of anomalous scattering could be attributed to insufficient accuracy in measurements.

Reference

(1) Schwinger, I.;Phys.Rev., 73,P.407 (1984).
(2) Dukarevich, Yu.V., et al.; Zh.Eksp.Teor.Fiz., 44, P.130 (1963).
(3) Anikin, G.V.; Yad.Fiz., 12,P.1121 (1970).
(4) Giordano, V., et al.; Nucl.Phys. A302, P.83 1978.
(5) Benenson, R.E., et al.; Nucl.Phys. A212,P.147 (1973).
(6) Bucher, W.P., et al.; Phys.Rev.Lett., 35, P.1419 (1975); Phys.Lett., 58, P.277 (1975).
(7) Deconninck, G.; J.ASS., 75, P.102 (1961).
(8) Coon, J.H., et al.; Phys.Rev., 111, P.250 (1958).
(9) Clarke, R.L.; Nucl.Phys., A95, P320 (1967).
(10) Bouchez, R.; Nucl.Phys., 43, P.628 (1963).
(11) Hogue, H.H.;Nucl.sci.Eng., 68, P.38 (1978).
(12) Roturier, J.;
(13) Bjorklund, F., et al.; Phys.Rev., 109, P.1295 (1958) and UCRL-4926T (1957).

FAST NEUTRON SMALL-ANGLE ELASTIC SCATTERING RESEARCHES

Ma Gonggui, Zou Yiming, Wang Shiming,
Li Jingde, Xie Daquan and Chen Shuying

Institute of Nuclear Science and Technology of
Sichuan University, Chengdu, Sichuan, China

The small-angle elastic scattering of fast neutrons is the common interesting subject of both theoretical and experimental studies.The interaction of the magnetic moment of neutrons with the Coulomb field of the nucleus has been verified by many experimental studies. The possibility of an interaction between the induced electric dipole moment of the neutron and the Coulomb field of the nucleus is still controversial. In order to do further studies a lot of nuclide over a wide mass range have been measured and the experimental results have been compared with the related theory.

The elastic scattering differential cross sections of Al,Ti,Fe,Cu,Mo,Cd,W,Pb,Bi and U-238 for 14.2 Mev neutron at angles from 1.7° to 25° have been measured by the associated particle time-of-flight method and the shielded source-neutron beam collimation arrangement[1]. Monoenergetic neutrons were produced by the reaction $T(d,n)^4He$. A thin ST401 plastic scintillator was used to detect the associated α-particles. The neutron detector was an 5cm diameter, 5cm thick ST451 scintillator optically coupled to an 56AVP photomultiplier. Pulse shape discrimination against γ-rays was also employed. Detector threshold was set at neutron energy of 3Mev. The resolution time of the facility was about 0.94ns for 14.2MeV neutron. The scattering neutrons were measured at ten angles in the interval 1.7° to 25°. The differential cross sections were normalized by moving the detector to 0° with the scattering sample removed and measured the incident neutron flux per monitor count of associated-αparticles. Backgrounds were measured by the filter arrangement. The extracted elastic yields, obtained after subtracting the background,were corrected for dead time. The corrections for neutron flux attenuation, multiple scattering and finite geometry are performed using Monte-Carlo method. The total uncertainty is about 7%. The exeperimental results, from which Schwinger[2]scattering has been subtracted are compared with the available data from other work[3,4,5] and the theoretical calculation [6,7,8,9,10]. The theoretical curve at the region of small angles is sensitive to the choice of the optical potential. The good agreement is obtanined between the present results of Al,Ti,Fe,Cu, Mo, Cd, W, Pb,Bi and the theoretical curve of Rapaport [9].The basic agreement is obrained between the present results of U-238 and theoretical curve for β=0.24 of Palla[8] which takes into account the effect of nuclear deforation[see Fig. and Table].

It is concluded that the optical model and Schwinger scattering can make better description of the small-

Table 1. Small-angle elastic scattering differential cross section

element	θc.m(deg)	dσ/d (mb/sr)	Δdσ/d (mb/sr)
Al	4.15	1370.1	+-95.1
	6.22	1287.1	+-89.5
	8.30	1201.1	+-84.3
	10.37	1148.4	+-80.1
	15.55	853.3	+-59.0
	20.73	592.6	+-41.1
	25.91	334.9	+-23.5
Ti	4.08	2275.2	+-158.5
	6.13	2210.7	+-154.4
	8.17	1997.5	+-139.7
	10.21	1868.4	+-128.1
	15.31	1302.4	+-89.3
	20.41	761.6	+-50.1
	25.50	364.3	+-25.6
Fe	1.73	3233.5	+-220.7
	2.55	3174.2	+-213.8
	4.07	3078.0	+-205.5
	6.11	2895.6	+-208.1
	8.14	2746.4	+-191.3
	10.18	2499.0	+-174.8
	15.27	1777.4	+-124.4
	20.35	1172.2	+-82.0
	25.44	491.7	+-34.6
Cu	1.73	3896.6	+-248.1
	2.54	3864.1	+-247.5
	4.06	3772.5	+-244.3
	6.10	3625.7	+-227.9
	8.13	3411.2	+-214.6
	10.16	3063.8	+-196.1
	15.24	2202.1	+-143.0
	20.31	1325.1	+-86.1
	25.38	667.9	+-48.2
Mo	1.72	7258.0	+-391.9
	2.53	7074.0	+-378.2
	5.05	6359.0	+-356.1
	7.58	5967.4	+-358.5
	10.10	5274.8	+-327.0
Cd	1.72	8669.7	+-507.3
	2.52	8560.9	+-484.1
	4.02	8408.0	+-497.2
	6.05	7884.1	+-517.0
	8.07	7032.8	+-419.6
	10.09	6604.7	+-394.1
	15.13	4132.9	+-288.6
	20.18	2187.9	+-152.8
	25.22	1047.4	+-75.5

Table 1. Small-angle elastic scattering differential cross section

element	θc.m(deg)	dσ/d (mb/sr)	Δdσ/d (mb/sr)
W	1.71	13237.0	+-762.2
	2.51	13123.0	+-816.3
	5.03	11885.0	+-756.6
	7.54	10145.0	+-665.8
	10.05	8341.9	+-568.2
Pb	1.71	13837.0	+-819.6
	2.51	12958.0	+-807.9
	4.02	12699.0	+-830.2
	5.02	11415.0	+-737.0
	6.03	11806.0	+-786.5
	8.04	9974.0	+-646.4
	10.05	8118.6	+-550.0
	15.07	3689.9	+-250.0
	20.10	1040.5	+-72.5
	25.10	43.5	+-3.2
Bi	1.71	14091.0	+-806.5
	2.51	13074.0	+-620.3
	5.02	11618.0	+-752.4
	7.54	9613.9	+-701.5
	10.05	7813.3	+-553.6
U-238	1.71	16191.0	+-733.7
	2.44	14867.7	+-660.1
	3.54	13997.3	+-668.8
	6.25	12417.0	+-613.2
	10.04	8300.5	+-470.1
	15.04	4028.8	+-275.2

Table 2. Integrated elastic scattering cross section

element	σel(mb)	Δσel(mb)
Al	746.95	+-13.05
Ti	1079.13	+-21.70
Fe	1225.35	+-25.94
Cu	1551.52	+-21.52
Mo	2056.60	+-96.90
Cd	2575.49	+-57.95
Pb	2859.43	+-96.30
Bi	2860.48	+-23.99
U-238	3052.99	+-136.52

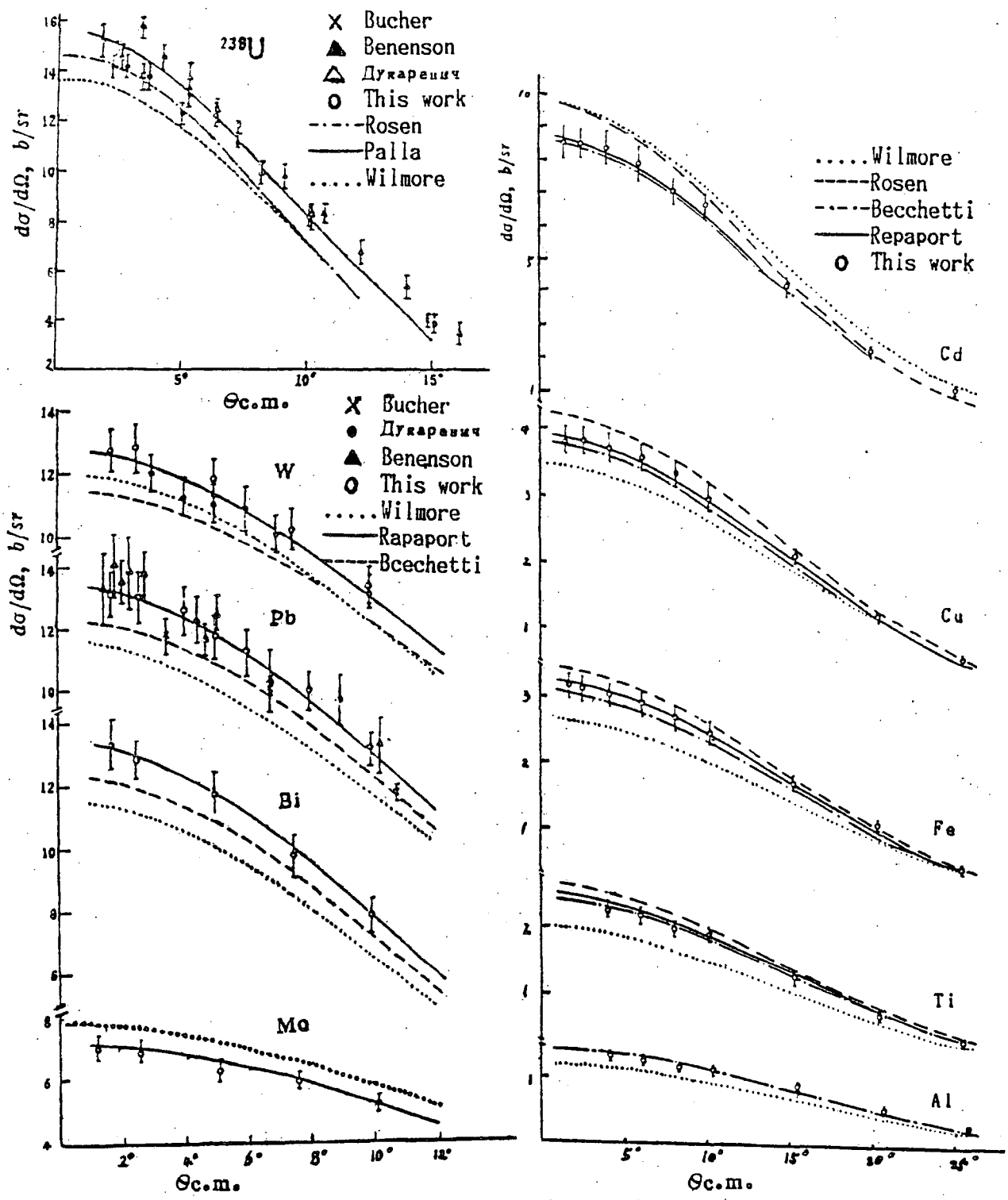

Fig. small-angle elastic scattering differential cross section of Al,Ti,Fe,Cu,Cd,W,Pb,Bi,Mo,U-238.

angle elastic scattering results. There may be deformation effect on W and U-238, but small-angle anomalous scattering phenomenon is not observed. There is no evidence which can show exist of non-nuclear scattering mechanism, except for Schwinger scattering. It is important to adjust and choose the best optical model parameters. The measurement have supported scientific foundation to do so.

References

[1] Li Jingde et al.,Chinese Journal of Nucl. Phys., 8, 245 (1986).

[2] J.Schwinger, Phys. Rev., 73, 407(1948).

[3] W. P. Bucher et al., Phys. Rev. Lett., 35, 1419 (1975).

[4] R. E. Benenson et al.,Nucl. Phys., A212, 147 (1973).

[5] Ю.В. Дукаревич, и др.,ЖЭТФ,44,130(1963).

[6] D. Wilmore et al., Nucl. Phys., 55, 673(1964).

[7] L. Rosen et al., Ann. Phys.(N.Y.) (US), 34, 96 (1965).

[8] G.Palla, Phys. Lett.,35B, 477(1971).

[9] J. Rapaport et al., Nucl. Phys.,A330, 15 (1979).

[10] F. D. Becchetti et al., Phys. Rev., 182, 1190(1969).

[11] Li Jingde et al., Chinese Journal of Nucl. Phys.,7, 106 (1985).

[12] Li Jingde et al., Chinese Journal of Nucl. Phys.,9, 97 (1987).

[13] Li Jingde et al.,Journal of Sichuan University Natural Science Edition, 24, 194 (1987).

Fast Neutron Capture Cross Sections of Tm-169 and Ta-181 from 1.0 to 1.5 MeV

Xu Haishan Xiang Zhengyu Mu Yunshan
Chen Yaoshun Liu Jinrong Li Yexiang
Institute of Nuclear Science and
Technology of Sichuan University, Chengdu

Introduction

Capture cross sections for fast neutron are important data in nuclear reaction theory and reactor design. Seeing from the published experimental data, those in the 1.0-3.0 MeV energy range are not ideal. Particularly for some nuclides, there are very few data and some disagreements exist between these data.

There are three works for capture cross section measurements of Tm-169 above 0.7 MeV. Joly et al.[1] measured capture cross section in 0.5-3.0 MeV by detecting the prompt capture r-ray with NaI. Jiang Songsheng et al.[2] measured capture cross section in 0.1-1.5 MeV using activation. The nonhydrous scintillator and TOF method were used to measure capture cross section in 2.6 KeV-2.0 MeV by Macklin et al.[3]. In 0.5-3.0 MeV energy range there are seven works for Ta-181. In which Miskel[4],Cox [5]; Brzoska[6] and Linduer[7] measured by using activation.Diven [8]; Fricke[9] and Hellstrom[10] measured by determining prompt r-ray, only Hellstrom[10] did above 1.0 MeV energy range but there is only one experiment point.

Experiment

Fast neutron capture cross sections have been measured for Tm-169 and Ta-181 from 1.0 to 1.5 MeV. The prompt gamma-ray

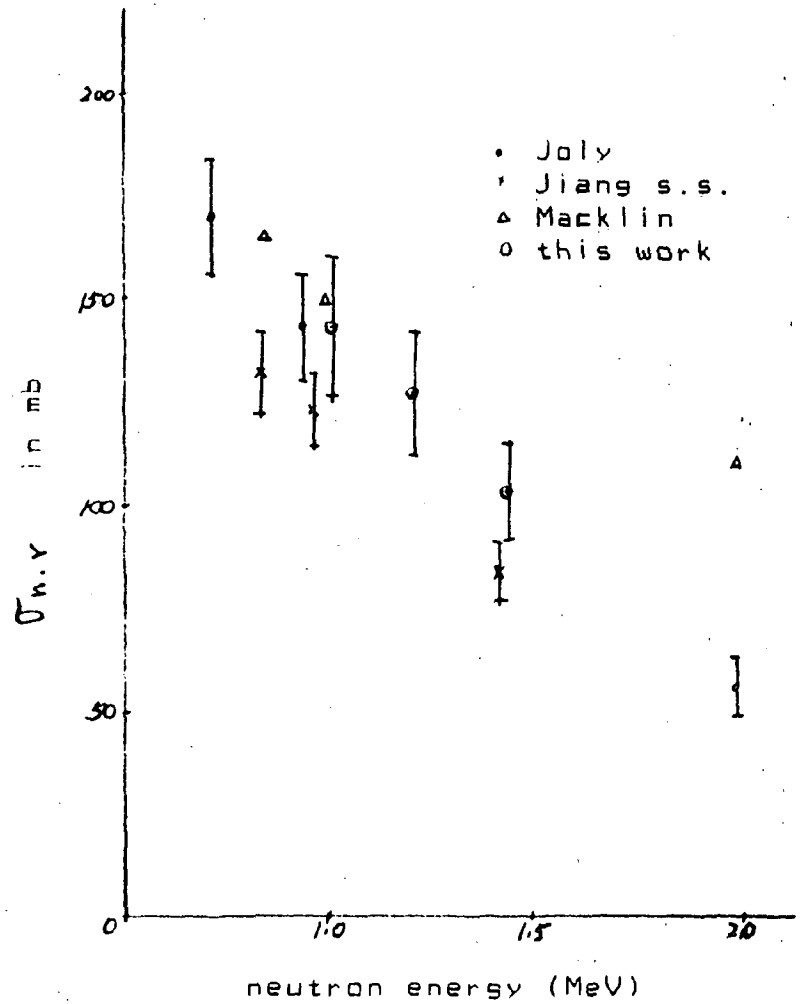

Fig.1 neutron capture cross section for Tm-169 as functions of neutron energy

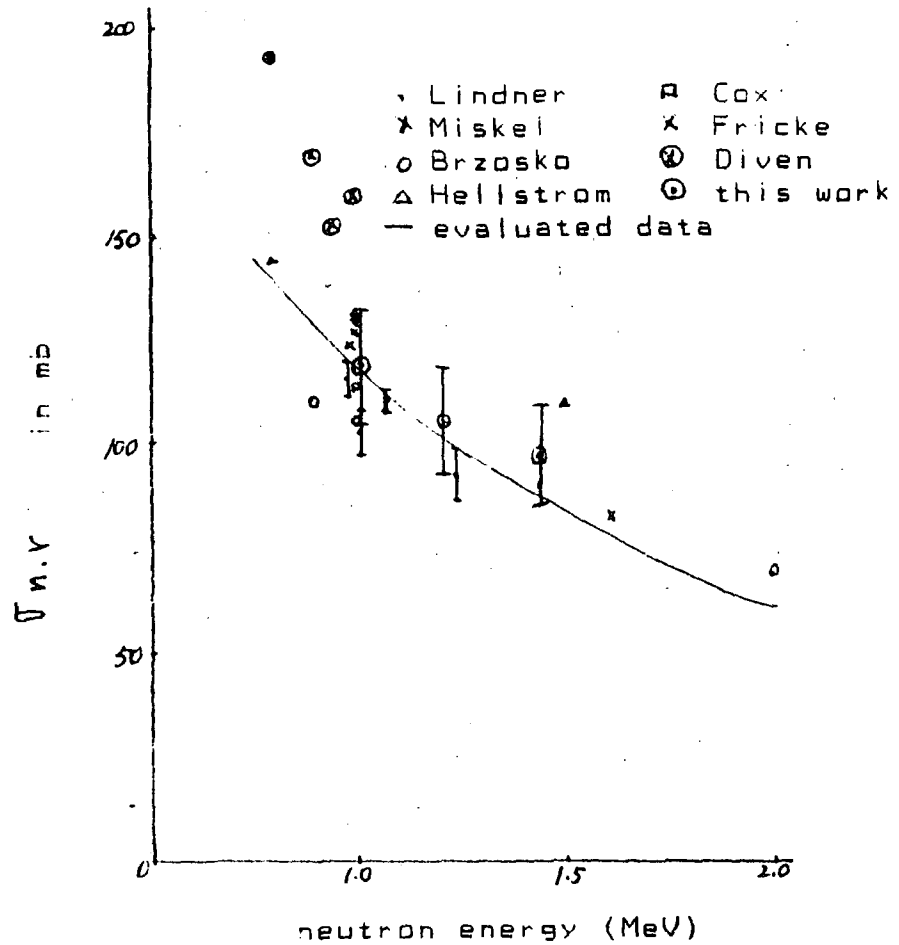

Fig.2 neutron capture cross section for Ta-181 as functions of neutron energy

Table 1. Neutron capture Cross Sections

(in mb)

neutron energy (MeV)	1.01+0.15	1.21+0.14	1.44+0.11
Tm-169	143+17	127+15	103+12
Ta-181	119+14	106+13	97+12

were detected by a one-meter-diameter liquid scintillation tank and TOF technique. The experimental sample was placed at the center of the tank for irradiation by a pulsed neutron beam which was produced at 2.5 MeV Van de Graaff through T (p.n)^{3}He. The duration of pulsed beam is 10 ns and the average proton currents is 3-4 μa.

The Tm_2O_3 and metal Ta-181 foil90 x 1mm were used as samples. purity of samples is better than 99.9% . relative cross section have been determined by Au-197 as a standard model.The measured sample and Au-197 was measured alternatively many times.

Discussion

These results are shown in Figs. 1 and 2 as a function of neutron energy. It can be observed that for Tm-169, our results are higher than the measurement of Jiang Songsheng et al.[2], but agree well with those of Joly et al.[1] and Macklin et al . [3]. For Ta-181 the present values are lower than those of Diven et al.[8], but agree well with those of other works.

References:

[1] S. Joly et al., Nucl. Sci. Eng., 70, 53 (1979)

[2] Jiang Songsheng et al., Chinese Jour. of Nucl. Phys. 4, 2, 136-139 (1982)

[3] R.Macklin et al.,Nucl. Sci. Eng., 82,143 (1982)

[4] J. A. Miskel et al., Phys. Rev.,128, 2717 (1962)

[5] S. A. Cox, Phys. Rev., B133, 378 (1964)

[6] L. S. Brzosko et al., Nucl. Phys., A123, 603 (1969)

[7] M. Lindner et al.,Nucl. Sci. Eng., 59, 381 (1976)

[8] B. C. Diven et al., Phys. Rev., 120,556 (1960)

[9] M. P. Fricke et al., Nucl. Data for Reactors, 2,265(1970)

[10] J. Hellstrom, J. Nucl. Energy, 27, 71 (1973)

THE NEUTRON CAPTURE CROSS SECTIONS OF ^{93}NB, ^{169}TM AND ^{181}TA IN THE ENERGY RANGE FROM 10 TO 100KeV

Xia Yijun Yang Jingfu Guo Huachong Wang Minghua
Xie Bizhen Yang Zhihua Wang Shiming
(Institute of Nuclear Science and Technology Sichuan University, p.o.Box 390-1, Chengdu, China)

*Zhao Wengrong *Yu Weixiang
(Institute of Atomic Energy, Academica Sinica, P.O.Box 275-3, Beijing, China)

The capture cross sections of ^{93}Nb, ^{169}Tm and ^{181}Ta were measured in the 10 to 100keV neutron energy range,using ^{197}Au as a standard. Kinematically cllimated neutrons were produced Via the ^{7}Li(p,n)^{7}Be reaction with the 2.5 Mv pulsed Van De Graff accelerator at Sichuan University.Capture events were detected by two Moxon-Rae detectors with graphite converter. The results are compared with recent data of other authors.

Introduction

The knowledge of neutron capture cross section in kev region is of fundamental importance for designing reactors, for nuclear reaction theories and for astrophysical theories. The isotop ^{93}Nb is fission product and its capture cross section are therefore of general importance for fast reactor calculation. Because of its superconductivity,niobium is also of interest as a structural material in fusion research. The capture cross section of ^{169}Tm is required for radiochemical diagnostic studies. The capture cross section of ^{181}Ta is mostly required for fast breeder control and burnup calculations. This cross section may also serve as a standard.

In the present work,the neutron capture cross sections of ^{93}Nb, ^{169}Tm and ^{181}Ta have been measured in the neutron energy range from 10 to 100keV, using ^{197}Au as a standard. The reasults are compared with recent data of other authors.

Experimental method

Similar to recent work by Wisshak et al[1],the principle of the experimental method is to use ^{7}Li(p,n)^{7}Be reaction for neutron production at proton energies just above the eaction threshold. In this case the neutrons are kinematically collimated by the center mass motion of the compound nucleus ^{8}Be. All neutrons are emitted within a cone in a forward direction, the opening angle

*Only attended the measurement of the neutron capture cross section of ^{169}Tm.

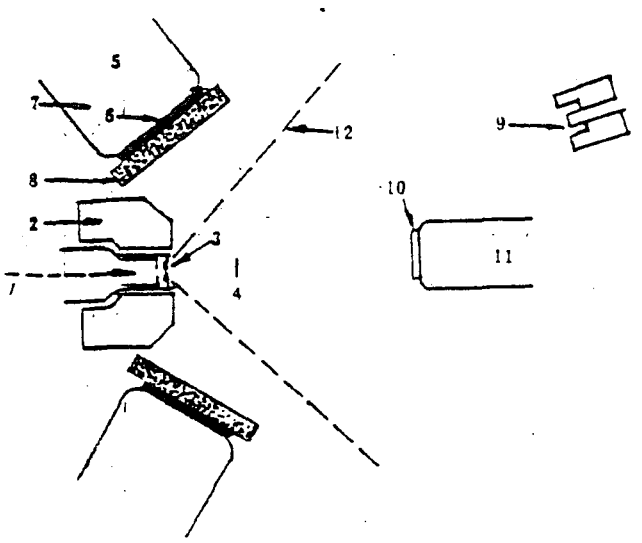

Fig. 1. Experimental setup

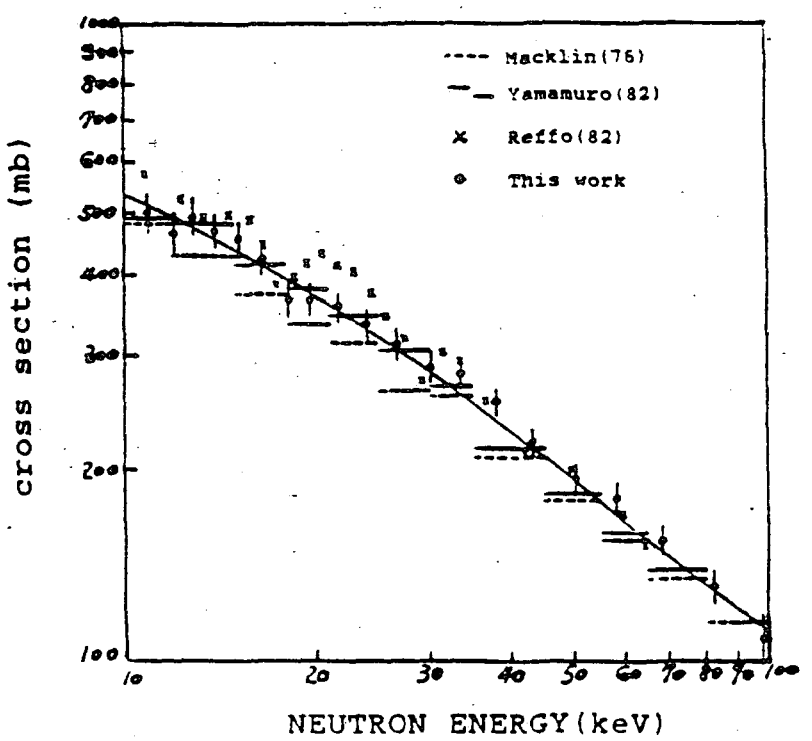

Fig. 2. The neutron capture cross section of ^{93}Nb

of which is determined by the proton energy. The capture events can be observed by detector placed at backward angles completely outside the neutron cone.

A detailed description of the experimental set-up, block diagram of the electronics, and data analysis is given in Ref[2] and[3]. Therefore, only a brief description is given here.

The scheme of the experimental setup is shown in fig.1. The pulsed proton beam hits a water-cooled metallic lithium target producing kinematically collimated neutrons. The proton energy was adjusted only 20 keV above the

reaction threshold in order to obtain a kinematically collimated beam and a continuous neutron spectrum in the energy range from 10 to 100 keV.

Two Moxon-Rae detectors with graphite outside the neutron cone at a backward angle of 120 deg with respect to the proton beam axis served for the detection of capture gamma-rays. The neutron energy was determined by time-of-flight(TOF). With a flight path of only 7 cm, the overall experimental time resolution was 1.7ns, and consequently the energy resolution was 24ns/m.

A ^{6}Li-glass detecor was positioned at 0 deg with respect to the proton beam axis as a transmission detector. The ^{6}Li-glass detector was used to record transmitted neutron spectra which monitored changes of incident neutron spectra during the experiment.

Neutron flux was monitored with a long counter placed at 20 deg to the beam direction and the distance of 1.7m from the target.

The samples of niobium, tantalum and glod are metal disk. The sample of Tm was prepared by pressing 99.99% pure Tm_2O_3 powder into thin disk. All samples are 4cm in diameter. In table 1, all sample masses, thicknesses, chemical composition and the neutron binding energy of the compound nucleus are listed in detail.

Table 1. compilation of the relevant sample data

sample	chemical composition	weight (g)	thickness (mm)	thickness (atom/b)	binding energy(keV)
^{93}Nb	metal	5.7457	0.5	2.963×10^{-3}	7228
^{181}Ta	metal	6.3572	0.3	1.683×10^{-3}	6063
^{197}Au	metal	4.7607	0.25	1.158×10^{-3}	6513
^{169}Tm	Tm_2O_3	5.8130	1.25	1.444×10^{-3}	6593
C	graphite	2.3834	1.4	9.524×10^{-3}	____

The data acqutsition was carried out by an on-line micro computer. The TOF spectrum recorded by the Moxon-Rae detector and the Li-glass detector were all stored on magnetic disks.

Data analysis and results

The data analysis has been described in detail in Ref [3]. The ratios of the capture cross section of niobium, thulium, tantalum, and gold were determined according to the relation:

$$\frac{\sigma_r(x)}{\sigma_r(Au)} = \frac{Cx}{CAu} \cdot \frac{NAu}{Nx} \cdot \frac{BAu}{Bx} \cdot \frac{(MS.SS)Au}{(MS.SS)x} \cdot \frac{SAu}{Sx} \cdot \Delta\varepsilon$$

where

C is the background corrected counting rate in the TOF spectrum.

N is the sample thickness.

B is the neutron binding energy.

MS.SS and S are the correction factors for multiple

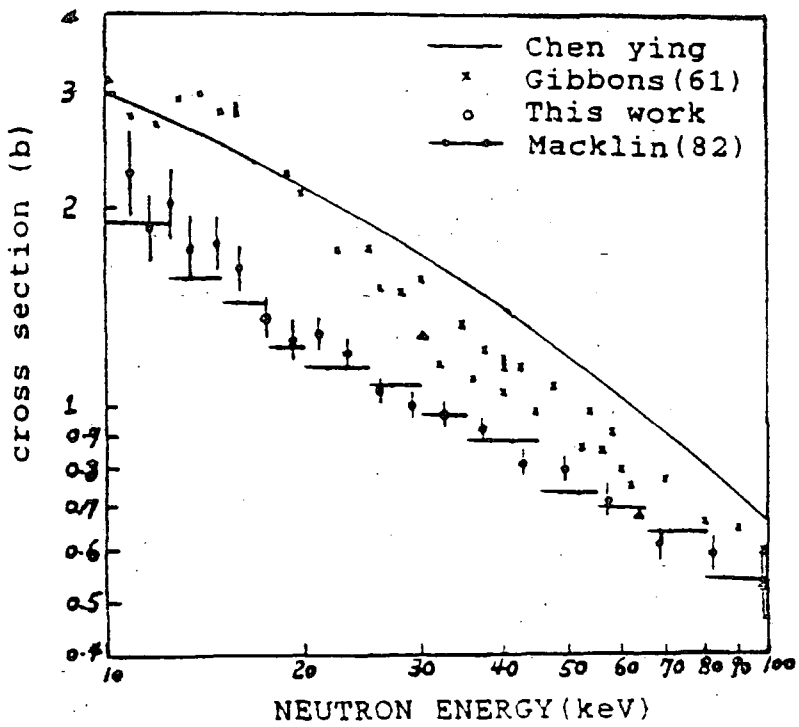

Fig. 3. The neutron capture cross section of ^{169}Tm

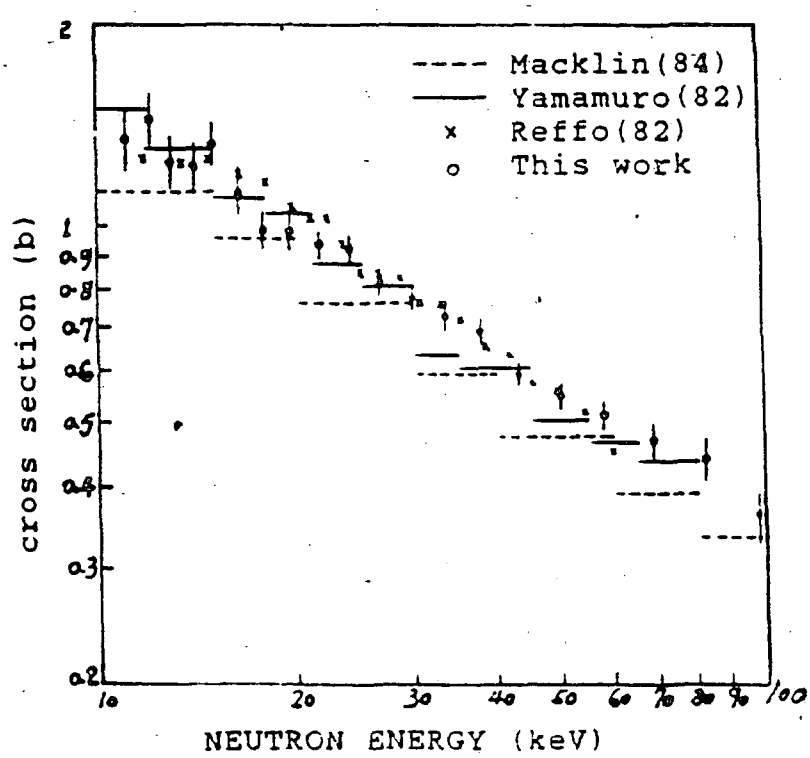

Fig. 4. The neutron capture cross section of ^{181}Ta

scattering, selfshielding and gamma-ray self-absorption, respectively.

$\Delta\varepsilon$ is the correction factor for the deviation of the detector efficiency from a linear relation with gamma-ray energies.

X is the index for ^{93}Nb, ^{169}Tm, and ^{181}Ta.

The correction factors Ms and SS were calcuated by the "SESH" Monte Carlo[4] programme. The correction factor S

Table 2. Experimental results of neutron capture cross section of ^{93}Nb

En±ΔEn (Kev)	$\sigma_r(^{93}Nb)/\sigma_r(^{197}Au)$	$\sigma_r(^{93}Nb)$ (mb)	uncertainty(%) statistical	systematic	total
11.2±0.36	0.447	496	8.3	5.6	10
12.0±0.40	0.442	464	7.6	5.1	9.2
12.9±0.45	o.492	492	7.0	5.0	8.6
14.0±0.5	0.499	470	6.1	5.1	8.0
15.1±0.56	0.496	454	5.2	4.8	7.1
15.4±0.64	0.497	439	4.5	5.0	6.7
17.9±0.73	0.460	368	4.3	5.2	6.7
19.6±0.84	0.470	354	4.0	4.5	6.0
21.6±0.96	0.501	356	3.4	4.2	5.4
23.9±1.1	0.499	333	3.2	4.3	5.4
26.5±1.3	0.487	306	3.0	4.0	5.0
29.6±1.6	0.477	282	2.6	4.1	4.9
33.3±1.9	0.504	279	2.5	4.7	5.3
37.8±2.2	0.495	256	2.4	4.6	5.2
43.2±2.7	0.448	216	2.1	4.4	4.9
49.8±3.4	0.430	193	2.1	4.2	4.7
58.1±4.3	0.436	181	2.0	4.0	4.5
68.6±5.5	0.404	155	1.9	4.0	4.4
82.3±7.2	0.370	132	1.9	5.6	5.9
100±9.82	0.339	109	3.9	10.	10.5

Table 3. Experimental results of neutron capture cross section of ^{169}Tm.

En±ΔEn (Kev)	$\sigma_r(^{169}Tm)/\sigma_r(^{197}Au)$	$\sigma_r(^{169}Tm)$ (mb)	uncertainty(%) statistical	systematic	total
11.2±0.36	2.26	2509	14	7.2	12.3
12.9±0.45	2.13	2132	12	5.0	13
14.0±0.5	1.82	1713	12	5.6	13.2
15.1±0.56	1.91	1749	10	5.0	11
16.4±0.64	1.82	1593	8.3	5.4	9.9
17.9±0.73	1.66	1328	6.5	5.3	8.4
19.6±0.84	1.65	1244	5.6	5.3	7.9
21.6±0.96	1.82	1291	5.3	4.4	6.9
23.9±1.1	1.80	1236	4.3	4.3	6.1
26.5±1.3	1.69	1062	3.8	4.3	5.7
29.6±1.6	1.71	1010	3.4	4.3	5.5
33.3±1.9	1.77	979	3.0	4.2	5.2
37.8±2.2	1.79	925	2.9	4.4	5.3
43.2±2.7	1.72	830	2.6	4.9	5.5
49.8±3.4	1.83	802	2.5	4.3	5.0
58.1±4.3	1.76	732	2.2	4.3	4.8
68.6±5.6	1.65	632	2.0	4.2	4.8
82.3±7.2	1.71	609	2.2	5.1	5.6
100±9.8	1.72	552	3.2	11.3	11.7

Table 4. Experimental results of neutron capture cross section of ^{181}Ta.

En±ΔEn (Kev)	$\sigma_r(^{181}Ta)/\sigma_r(^{197}Au)$	$\sigma_r(^{181}Ta)$ (mb)	uncertainty(%) statistical	systematic	total
11.2±0.36	1.22	1354	8.9	6	11
12.0±0.40	1.38	1449	8.2	5.6	9.9
12.9±0.45	1.25	1251	7.9	5.6	9.7
14.0±0.50	1.31	1233	7.1	5.5	9.0
15.1±0.56	1.44	1319	7.1	5.4	8.9
16.4±0.64	1.27	1111	6.2	5.4	8.2
17.9±0.73	1.23	984	5.4	5.2	7.5
19.6±0.84	1.31	988	4.5	4.5	6.4
21.6±0.96	1.33	944	4.4	4.4	6.2
23.9±1.1	1.40	935	3.8	4.5	5.9
25.6±1.3	1.28	804	3.2	4.4	5.4
29.6±1.6	1.30	768	3.0	4.4	5.3
33.3±1.9	1.31	725	2.6	4.3	5.1
37.8±2.2	1.35	697	2.5	4.4	5.1
43.2±2.7	1.24	598	2.2	4.4	4.9
49.8±3.4	1.24	557	2.0	4.2	4.7
58.1±4.3	1.25	520	1.9	4.0	4.4
68.6±5.5	1.23	471	1.8	4.4	4.8
82.3±7.2	1.23	438	1.8	6.1	6.4
100±9.8	1.13	363	3.1	10.6	11

was calculated with the mass absorption coefficient given by Hubbell[5]. The correction factor $\Delta\varepsilon$ was determined using the shape of efficiency curve given in Ref[6] and the shape of capture gamma-ray spectrum of ^{93}Nb, ^{181}Ta and ^{197}Au given in Ref[8].

The experimental result for the capture cross section of ^{93}Nb, ^{169}Tm and ^{181}Ta are compiled in table 2`3 and 4. To compare our results with recent measurements of other authors, the experimental ratios have been converted to absolute cross section by using the gold cross section evaluated by Ref[7]. To avoid the difference of the gold cross section used, the experimental ratios of Ref[8] for ^{93}Nb and ^{181}Ta have also been converted to absolute cross section by using the gold cross section evaluated by Ref [7]. The results are shown in Fig.2,3 and 4 together with recent measurements of other authors.

In the case of ^{93}Nb, excellent agreement is found with the data published recently by Reffo et al [8], Yamamuro et al [9], and Macklin [10]. The evaluation of Ref[11] is a good representation of the experimental results.

Our values for the capture cross sections of ^{169}Tm are in good agreement with the result of Macklin [12], while the results of Gibbons [13] are systematically higher.

For ^{181}Ta,our capture cross section are in good agreement with the results of Reffo et al. and Yamamuroet al. The data of Macklin[14] are systematically lower.In the 10 to 20keV, our average cross section are higher by 6%. In the energy range from 20 to 80keV, our data are higher by 15%.

References

1) K.Wisshak et al., Nucl. Sci. Eng., 66, 363(1978)
2) Xia Yijun et al., China. Jour. of Nucl. Phys., to be published
3) Xia Yijun et al., China. Jour. of Atomic Energy Science and Technology., to be published
4) F.H.Frohner, GA-8380 (1968)
5) J.H.Hubbell, Int. J. Appl. Radial. Isot., 33,126(1982)
6) S.S.Malik, Nucl. Instrum. Method., 125,45(1975)
7) Jiang Sonsheng "Evatuated neutron capture cross section for ^{197}Au" hsj-77141 (1978) (bp)
8) G.Reffo et al., Nucl. Sci. Eng., 80, 630(1982)
9) N.Yamamuro et al., J.Nucl. Technol., 59,12(1980)
10) R.L.Macklin, Nucl. Sci. Eng., 59, 12(1976)
11) Zhou Hongyu, "Evaluated neutron Capture cross section for ^{93}Nb unpublished
12) R.L.Macklin, Nucl. Sci. Eng., 82, 143(1982)
13) J.H.Gibbons et al, Phys. Rev., 122, 182(1961)
14) R.L.Macklin, Nucl. Sci. Eng., 86, 362(1984)
15) J.H.Gibbons et al, Phys. Rev., 122, 182(1961)

MEASUREMENT OF THE NEUTRON CAPTURE CROSS SECTIONS OF WOLFRAM AND GADOLINIUM BETWEEN 560 AND 1610 KEV

Xiang Zhengyu Mu Yunshan Li Yexiang

Wang Shiming Xu Haishan

Institute of Nuclear Science and Technology

of Sichuan University,Chengdu,China

The capture cross sections of W and Gd were measured relative to that of Au at six neutron energy points: 0.56±0.06, o.77±0.06, 0.98±0.09, 1.16±0.09, 1.34±0.08 and 1.61±0.07 MeV.

The $T(p,n)^3He$ reaction was used as a neutron source. A pulsed and bunched proton beam was accelerated by the 2.5 MV Van de Graaff accelerator.The repetition rates were 2 MHz and the pulse width was 10 ns.The average proton beam intensity was from 2 to 4 μa. The tritium targets were all of the Ti-T type.Tow long-counters were used for monitoring the neutron flux.

The capture gamma-ray detector was a 680-liter tank filled with a liquid scintillator formulated in this laboratory. The tank has the shape of sphere approximately with a diameter of 100 cm and has a central channel with a diameter of 20 cm .It was shielded by 10 cm lead and 40 cm Li-paraffin.

In order to reduce background the time-of-flight technique and the coincidence between the two half-spheres of the detector have been used.

The present results for the measured capture cross section of W and Gd are given in Table 1.These data are

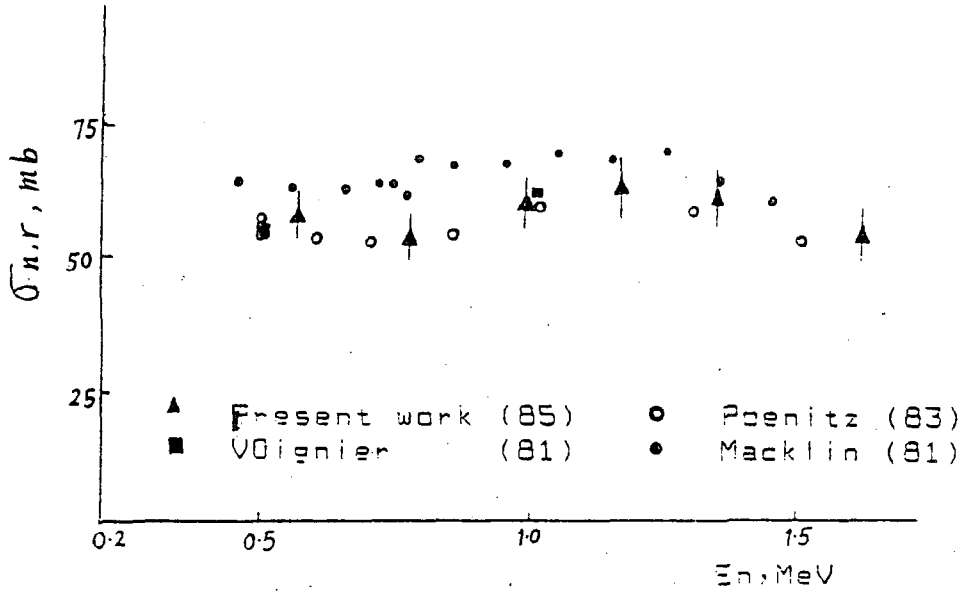

Fig.1.Comparison of the neutron capture cross sections of W obtained in the present work with those of other experiments.

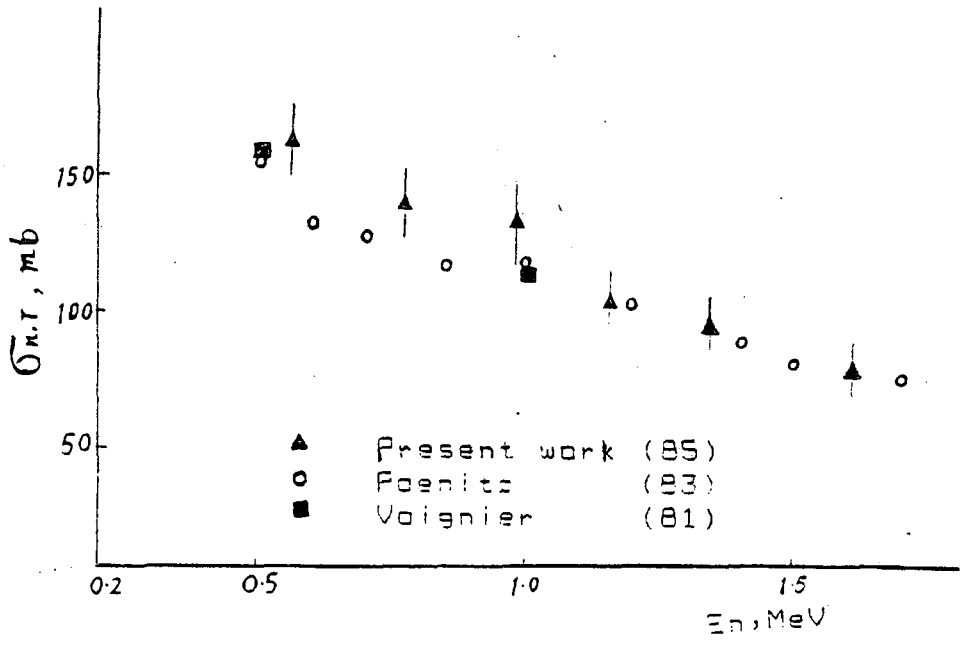

Fig2.Comparison of the neutron capture cross sections of Gd obtained in the present work with those of other experiments.

shown in Fig.1 and Fig.2.The present measurements agree well with recent measurements by Poenitz [1],Macklin [2] and Voignier [3] in uncertainty range (see Fig.1 and Fig.2).

Table 1. Present results for the measured capture cross sections of W and Gd

En (MeV)	±ΔEn	σ (W) (mb)	±Δσ	σ (Gd) (mb)	±Δσ
0.56	0.06	59.1	7	164	19
0.77	0.06	55.4	6	142.6	17
0.98	0.09	62.7	7	136.6	16
1.16	0.09	66.9	8	108.5	13
1.34	0.08	65.1	8	102.5	12
1.61	0.07	59.0	7	86.4	10

Reference

[1].W.P.Poenitz, ANL-83-4,239 (1983)

[2].R.L.Macklin, Nucl.Sci.Eng.,84,98 (1981)

[3].J.Voignier, CEA-R-5089 (1981)

Neutron-capture Cross section Measurments of Neodymium, Samarium, Dysprosium, and Ytterbium between 0.34 and 1.68MeV

Li yexiang Xiang zhengyu Xu haishan
Mu yunshan Wang shiming
Institute of N-uclear Science and
Technology of Sichuang University, Chengdu

1. Introduction

The measurments of neutron capture cross section of $_{60}$Nd, $_{62}$Sm, $_{66}$Dy and $_{70}$Yb relative to capture cross section of ^{197}Au were carried out from 0.34 to 1.68MeV using a large liquid scintillator detector (680Liter) and time-of-flight technique. For these nuclei, there were very few experimental data.

2. Apparatus and technique

The large liquid scintillator detector and the target chamber were placed in two halls seperated by 1.4m concrete wall. The distance from the target to center of the detector was 2.54M. There is a 10° opening angle between the beam line and the centrical channel of detector. The $T(p,n)^{3}He$ reaction with a pulsed and bunched proton beam(10 ns width, 2-Mhz-repetition rate and average proton currents of 2-4μa) was used as a neutron source. The detector was shielded by 10cm of Lead and 40cm of Li-paraffin. In order to reduce background a tricoincidence of three group signals from 12 photomultiplier and time-of-flight technique were used. two long counters, one in the first hall and another in the second were used for monitoring neutron flux. The threshould

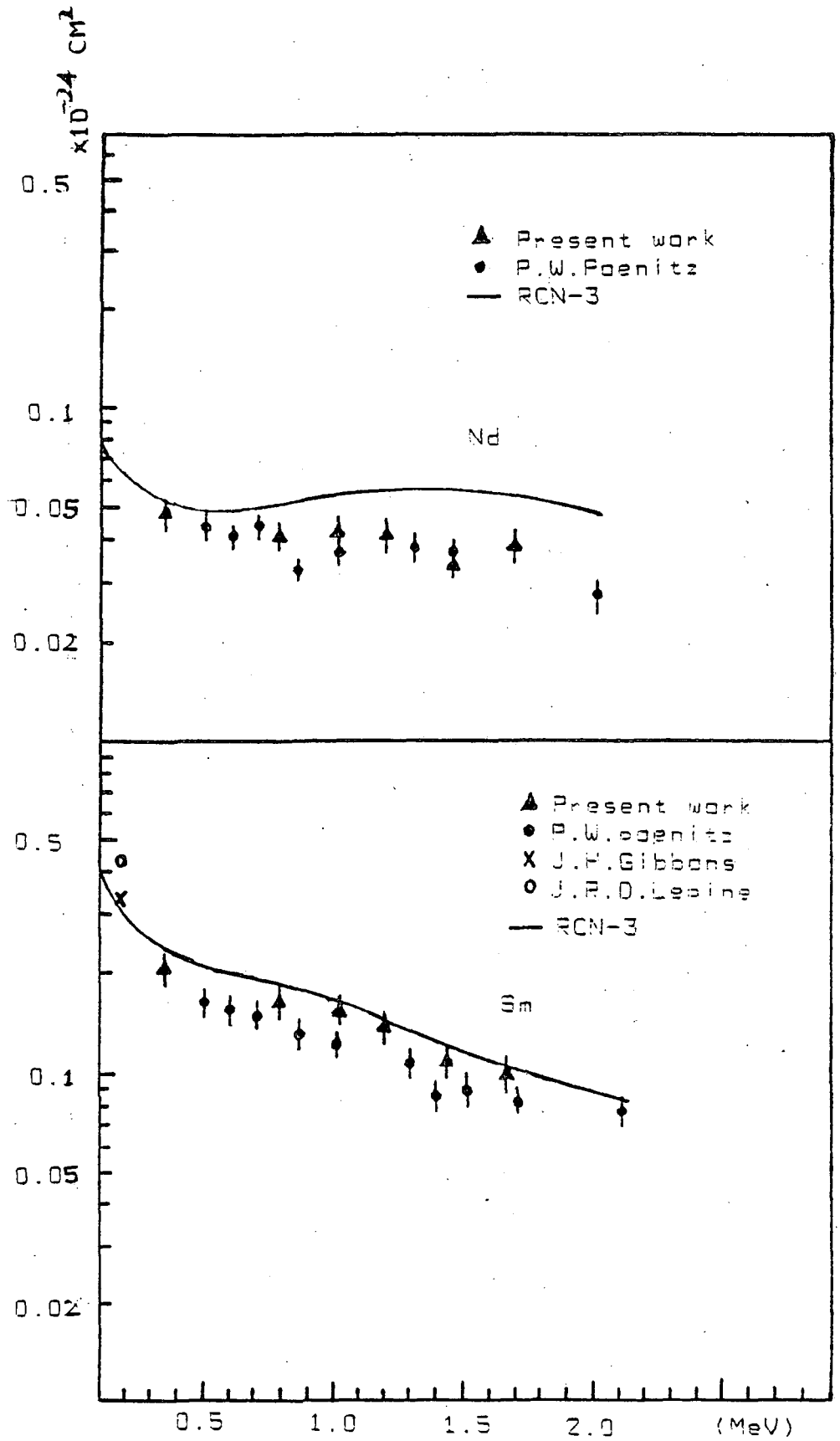

Fig. 1-1. Comparison of the Present Results with Other Data

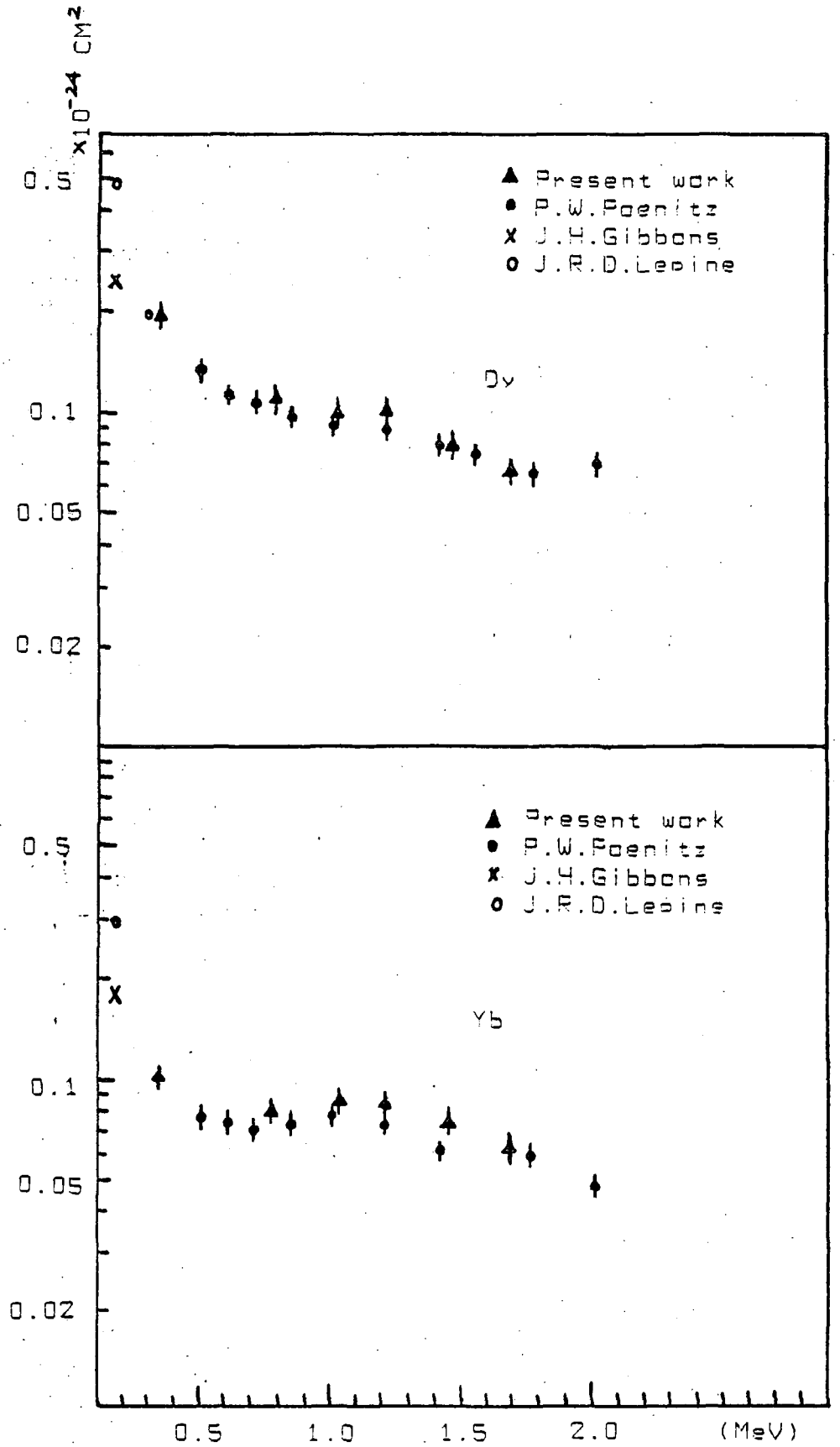

Fig. 1-2. Comparison of the Present Results with Other Data

value corresponding to r-ray energy set up at 1.58MeV. Measurments were made relative to the standard capture cross section of ^{197}Au over the entire energy range.

3. Results and discussion

The cross section measured are illustrated in fig.1. The standard capture cross section of ^{197}Au quoted from evaluation of Jiang songsheng. From fig.1. we can see that:

a) Our results are little higher than that of W.P.Poenitz [3] except the point of Nd of 1.34MeV.

B) The shape of the excitation function of every element is tha same as of Poenitz.

c) For Nd and Sm, our results and the Poenitz's all are less than the RCN-3 evaluation.

The total error is estimated to be about 9-14%. The error of standard cross section is 5-7%.

References

[1] J.H.Gibbons, Phys. Rev. vol.122 182 (1961)

[2] J.R.D.Lepine Nucl. Phys. vol.A133 513 (1969)

[3] W.P.Poenitz Conf. 79 BØlongna 85 (1979)

[4] W.P.Poenitz ANL-83-4 239 (1983)

[5] RCN-3

MEASUREMENTS OF THE FAST NEUTRON RADIATIVE CAPTURE CROSS SECTIONS OF NATURAL Tb AND Hf

Mu Yunshan Li Yexiang Wang Shiming
Xiang Zhengyu Xu Haishan
Institute of Nuclear Science and Technology of
Sichuan University,Chengdu

1.Introduction

Fast neutron capture cross sections of Tb and Hf were unavailable above a few hundred KeV until the data of W.P.Poenitz[1] and J.Voignier[2] were available.

The radiative neutron capture cross sections of Tb and Hf are measured relative to that of Au in the energy range from 0.8 to 1.6 MeV by using of a large liquid scintillator detector and time-of-flight method.The $T(P,N)^3He$ reaction is used as neutron source at a pulsed 2.5 MeV Van de Graaff(10 nsec width and a 2MHz repetition frequency).The samples are disks with diameter of 9 cm, and the thickness of Tb is 5.7×10^{21} atoms/cm^2,Hf 4.4×10^{21} atoms/cm^2,Au 5.7×10^{21} atoms/cm^2.

The uncertainty of the required extropolation to zero-pulse hight is estimated to be about 8%.With the addition of other uncertainties(7% for the standard cross section, 2% for the correction for capture of scattered neutrons in the samples,2% for the capture-event-detection efficiency,3-4% for the statistical uncertainty)we obtained cross section data with 11-12% uncertainties.

The scattering correction is calculated by using of the Mote Caro method.

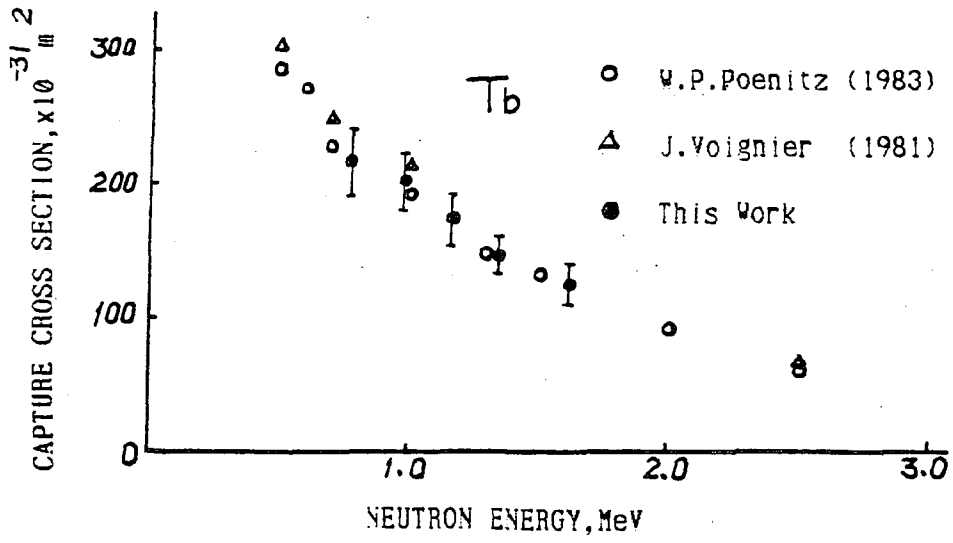

Fig.1 Present Data for Tb, and Comparison With Others' Results.

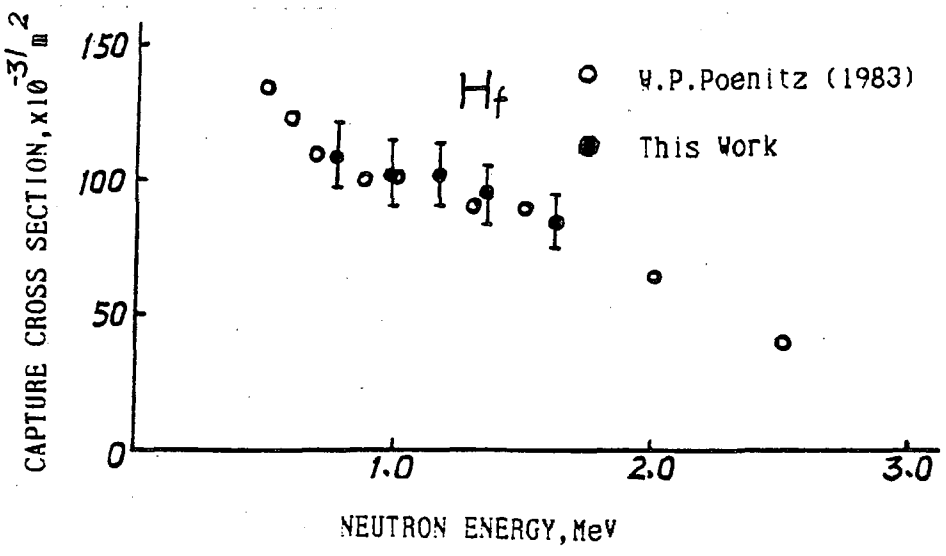

Fig.2 Present Data For Hf, and Comparison With The Data of W.P.Poenitz.

2. Results and discussions

The present data are listed in following table:

En, MeV	σ_{Tb}, x10^{-31} m^2	σ_{Hf}, x10^{-31} m^2
0.77±0.06	216±25	110±13
0.98±0.09	203±23	103±12
1.16±0.09	174±20	103±12
1.34±0.08	148±17	95±11
1.61±0.07	126±15	86±10

and a comparison with others' results are shown in figs. 1-2.

The present results for Tb agree very well with the results of reference[1],and agree with the results of reference[2] within the uncertainty though these data are systematically higher.The present results for Hf agree well with the results of reference[1].

References

[1] W.P.Poenitz,ANL-83-4,239(1983).

[2] J.Voignier et al.,Neutron-Capture Gamma-Ray Spectroscopy and Related Topics 1981,The Institute of Physics,Bristal and London,England,P516-517.

ON SOME RESULTS OF THE MEASUREMENTS OF THE ANGULAR DISTRIBUTIONS OF SEPARATED γ-RAY PRODUCTION CROSS SECTIONS FROM REACTIONS (n,xγ) FOR ^{51}V INDUCED BY 14.9MeV NEUTRONS

Yan Yiming, Zhou Hongyu, Tang Lin, Fan Guoying
Lan Liqiao, Sun Suxu, Wang Qi, Wen Senlin
Hua Ming, Liu Shuzhen, Rong Yaning
(Institute of Low Energy Nuclear Physics,
Beijing Normal University)

A. Introduction

In order to do some researches in the field of fast neutron physics, a fast neutron time-of-flight facility based on the cockcroft-Walton accelerator is built in the Institute of Low Energy Nuclear Physics at Beijing Normal University(1).

The vanadium is one of the constituent of the fusion reactor structural materials, so the cross-section data are necessary for reactor designing. ^{51}V is a neutron closed-shell nucleus, it can be considered as consisting of ^{48}Ca core plus three protons at $f_{7/2}$ subshell. Analysis of the nuclear structure of ^{51}V is useful for understanding the residual interaction in the $f_{7/2}$ subshell.

There are some articles related to the interactions of fast neutrons with ^{51}V. (2-7) But all these papers are related to neutrons with energies less than 4MeV. No measurement of separated γ-ray production cross-sections of ^{51}V from(n,xγ) reactions with 14 MeV neutrons is published yet. So our measurements of such interaction are first.

B. Experimental Procedure

The experiments were performed at the t-o-f facility in the Institute of Low Energy Nuclear Physics. The general arrangment of this facility is shown in Fig.1. The deuteron beam accelerated to 300 KeV was deflected by deflecting magnet and pulsed by beam pulsing system, consisting of a high frequency and high voltage chopper and a spiral loaded wave guide buncher. The repetition frequency was 3.16 MHz. The FWHM of neutron pulses were 1-1.5 ns, and the FW 2% M is 3-4 ns. The average intensities of the ion beams are 3-6 μA, which gave the neutron yield $\approx 5\times10^{8}$n/s. The target-sample distance was 13.5 cm and the distance between sample and detector was 140cm. A

shadow bar was used for attenuating the direct neutron fluence emitted from Ti-T target. The scattered neutrons and γ-photons emitted by the sample in the process of interaction of ^{51}V with neutrons were detected by a Ge(Li) detector placed inside the large 4π shield. The detector has a sensitive volume of 110.7cm^3 and a resolution of 2 KeV for ^{60}Co 1332.5KeV γ-peak. A careful absolute efficiency calibration was made using a series of standard γ-photon sources and understandard (6-10 MeV) multiline sources. The range of calibration was runing from 20 KeV to 10.8 MeV. The accuracy of calibration was 2.5 - 3% for 200 KeV -4 MeV γ-rays, 3 - 6% for 30 - 200 KeV and 4 - 8 MeV γ-rays and 6 - 10% for 8 - 10 MeV γ-rays. A careful adjustment gave good time resolution of this detector. It was 2.4ns (FWHM) and 13.8ns (FWTM) for γ-lines of ^{60}Co. A online time-of-flight spectrum of γ-rays and neutrons produced by $^{51}V(n,x\gamma)$ reactions is shown in Fig.2.

In our measurements, the time-of-flight technique was used for selecting the signals corresponding γ emission. Coincident measurements of signals from Ge(Li) spectrometer with these selected signals could significantly reduce the background caused by primary and scattered neutrons. The background of surrounding objects independent on the time was suppressed by monitor-normalized subtraction of counts measured without the sample from counts measured with the sample.

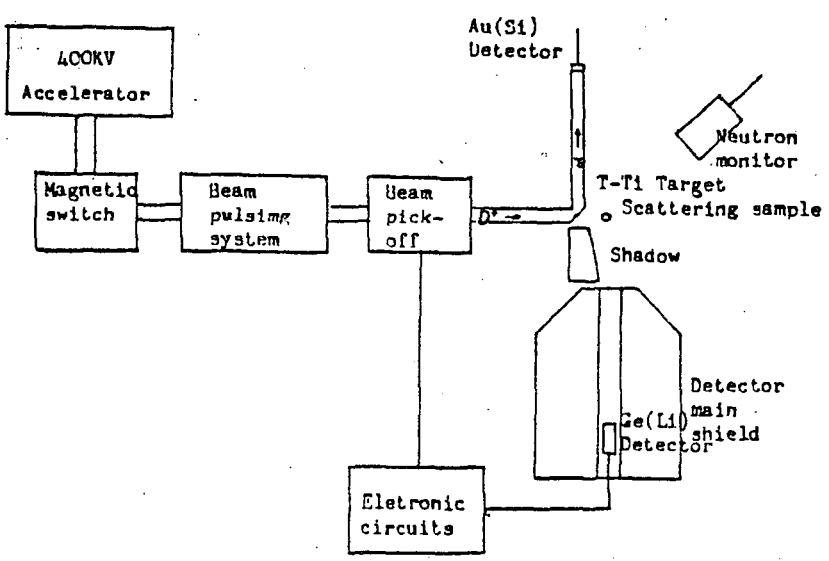

Fig.1. General View of the Experimental Set-up.

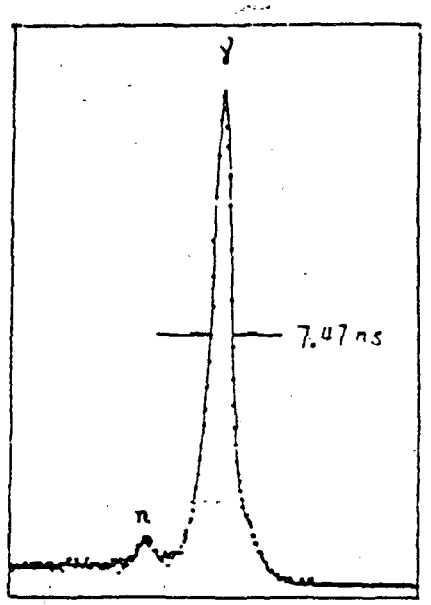

Fig.2. The γ-ray time-of-flight spectrum of ^{51}V

Neutron fluence was determined by associated α-particle counting with a Si(Au) detector placed at 90° angle to the deuteron beam

axis. The counts of Si(Au) detector were also used for the normalization. A liquid scintillator neutron detector was used as an additional neutron fluence monitor. A time-of-flight technique and PSD were used for neutron measurements.

The block scheme of electronic circuits is shown in Fig.3.

For testing the performance of this facility, the γ-ray production cross-sections of Fe(n,xγ) were measured more than ten times at 90°, particularly for 847 KeV γ-rays. Two different sizes samples were used. The diameters, hights and weights are 1.00cm, 1.40cm; 2.04cm, 2.98cm and 49.146g, 139.85g respectively. Some corrected values of cross-sections are shown in Table 1.

Table 1 Some results of measurements of 847KeV γ-ray* production cross-sections from ^{56}Fe(n,n'γ) reaction at 90°($10^{-31}m^2/sr$)

Data of measurements(1985)	23-May	24-May	30-May	17-July	18-July	weighted Average value
Samples	big	big	big	big	small	
Cross-section	66.48	66.43	66.83	67.09	67.16	67.14±3.42

*About the corrections and data processing see(8).

The measurements with vanadium sample were carried out during 1985 - 1986. The sample, 3cm long, 3cm in diameter and 130.0g in mass, has 99.9% purity. Measurements were taken for seven angles: 30°, 40°, 55°, 90°, 110°, 125°, 140°. Each measurement was carried out with and without sample. The monitor-normalized subtracted spectrum measured at 40° is shown in Fig.4.

C. Data processing and results

Experimental yields were calculated by fitting program capable of resolving multiplets. The experimentally obtained values of cross-sections should be corrected by neutron fluence attenuation, multiple elastic and inelastic scattering and self absorption of γ-photons in the sample. It was also necessary to introduce the corrections of anistropy of neutron source, absorption of neutrons by target backing and cooling water, and neutron source size(8). The error of determination of neutron fluence was 4%. The minimal total uncertainty of differential cross-sections is ≈5% for the largest peaks.

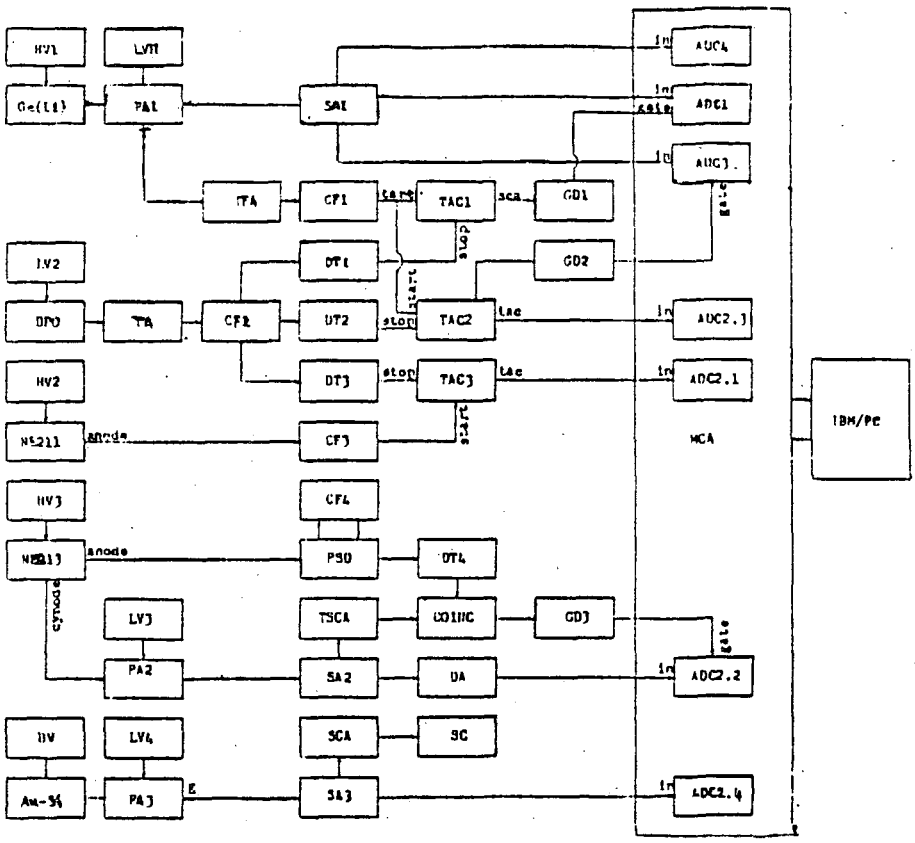

Fig.3 Electronic block diagram of data acquiprement

ADC-analogital converter, BV-bias voltage power supply, CF-constant fraction timing, DT-nsec delay, FA-fast amplifier, GD-gate and delay generator, HV-high voltage power supply, LV-low voltage power supply, MCA-multichannel analyzer, PA-preamplifier, PSD-pulse shape discriminator, SA-spectroscopy amplifier, SC-scaler, SCA-single channel analyzer, TAC-time-amplitude converter, TFA-timing filtering amplifier, BPO-beam pickoff, TSCA-timing single channel analyzer

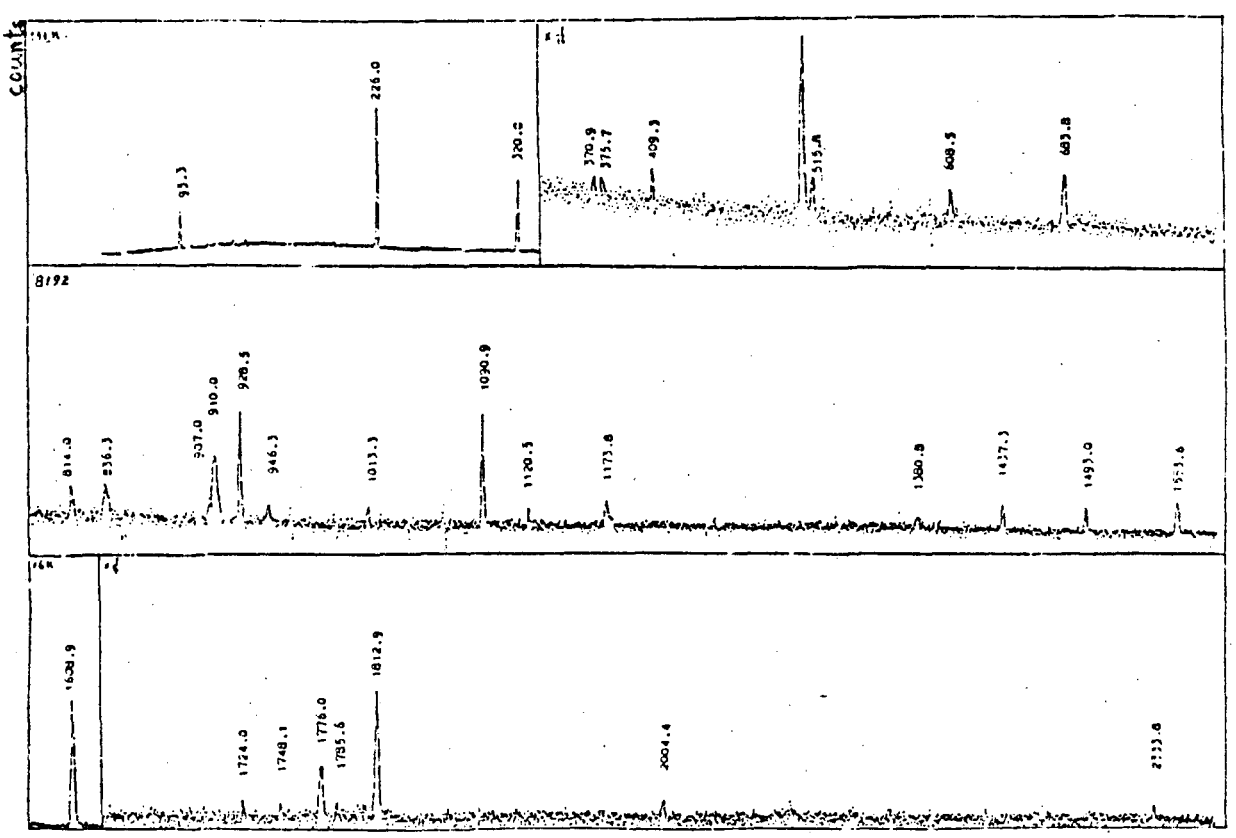

Fig.4 Spectra of ^{51}V (n,xγ) reactions with 14.9MeV neutrons

Table 2 Suggested transitions

E(KeV)	Type of reactions	Transition(KeV)	E(KeV)	Type of reactions	Transition(KeV)
93.3	(n,2n)	320.0--226.0	910.0	(n,2n)	910.00--0.0
121.0			913.3	(n,2n)	1300.7--387.9
130.0	(n,2n)	355.2--226.2	928.5	(n,n')	928.7--0.0
139.0			946.3	(n,2n)	1300.7--355.2
226.0	(n,2n)	226.2--0.0	1013.3	(n,2n)	1401.7--389.7
320.0	(n,n')	320.0--0.0	1090.1	(n,n')	2699.6--1608.9
	(n,2n)	320.0--0.0	1120.5	(n,np)	2674.9--1553.8
370.9			1173.8	(n,2n)	1700.7--320.0
375.7	(n,2n)	1676.7--1401.7	1437.3		
409.3			1493.0	(n,n')	1813.1--320.2
488.2	(n,n')	3874.0--3386.0	1553.6	(n,np)	1553.8--0.0
515.8	(n,2n)	836.4--320.0	1581.9	(n,n')	3395.6--1813.1
523.1	(n,np)	3198.7--2674.9	1608.9	(n,n')	1608.9--0.0
588.0			1724.0	(n,2n)	1725.0--0.0
608.5	(n,n')	928.7--320.2	1748.1	(n,n')	2677.6--928.7
613.2			1776.0	(n,n')	3386.0--1608.9
683.8	(n,2n)	910.0--226.2	1785.6	(n,n')	3395.6--1608.9
754.7	(n,2n)	2481.0--1725.0	1801.0	(n,n')	3614.6--1608.9
791.0	(n,2n)	1700.0--910.0	1812.9	(n,n')	1813.1--0.0
814.0	(n,2n)	1725.0--910.0	2004.4	(n,n')	3614.6--1608.9
836.3	(n,2n)	836.4--0.0	2333.8	(n,n')	3204.3--928.7
907.0					

For 14.9 MeV neutrons, the most possible(n,xγ) reactions are (n,n'γ) ^{51}V, (n,2nγ) ^{50}V, (n,pγ) ^{51}Ti, where the ^{51}Ti is radioactive($T_{\frac{1}{2}}$ = 5.8 min). In our experimental results, 42 separated γ-lines were certificated, seventeen of which were obtained for the first time in the reactions induced by fast neutrons. 35 nuclear transitions were suggested according to above mentioned types of reactions. The suggested transitions are shown in Table 2. The angular distributions of the largest 10 γ-lines were fitted by Legendre polynomials. The fitted curves and experimental results are shown in Fig. 5. All data of the cross-sections of ^{51}V are listed in table 3.

It's interested that the Doppler shifts of photopeaks of the trasitions were observed for many γ- lines.Fig.6 shows the typical energy shifts of some γ- photopeaks. It can be seen that, the shifts take place not only for the(n,n'γ) reactions, but for(n,2nγ) and(n,pγ) also.

Table 3 The measured values of cross-sections of (n,xγ) reactions induced by 14.9 MeV neutrons for ^{51}V

E(KeV)	Cross-sections (mb)						
	30°	40°	55°	90°	110°	125°	140°
93.3	19.02±2.53	16.35±2.09	16.74±2.14	18.23±2.33	16.10±2.06	17.18±2.20	15.80±2.02
121.0	0.43±0.05	0.67±0.08	0.74±0.08	0.82±0.09	0.85±0.10	0.59±0.10	0.80±0.11
130.1	1.02±0.14	1.03±0.15	1.28±0.18	1.15±0.16	1.00±0.14	0.88±0.13	0.77±0.11
139.0	0.60±0.08	0.38±0.07	0.35±0.07				0.31±0.06
226.0	3 .30±2.14	31.60±2.12	34.21±2.29	32.85±2.25	30.42±2.04	32.01±2.19	30.19±2.03
320.0	20.51±1.37	20.63±1.38	22.00±1.49	20.83±1.41	19.71±1.32	19.42±1.31	18.18±0.08
370.9	0.57±0.09	0.51±0.08	0.53±0.07	0.40±0.07	0.42±0.04	0.47±0.10	0.32±0.05
375.7		0.39±0.07	0.41±0.09	0.33±0.09	0.30±0.05	0.30±0.05	0.31±0.05
409.3	0.34±0.07	0.70±0.07	0.46±0.07	0.40±0.12	0.47±0.06	0.47±0.06	0.57±0.06
488.2	0.23±0.08	0.33±0.06		0.23±0.07		0.36±0.10	0.21±0.06
515.8	1.71±0.20	1.62±0.15	1.91±0.18	2.40±0.23	2.04±0.18	2.40±0.20	2.26±0.27
523.1	0.62±0.09	0.23±0.07	0.17±0.06	0.36±0.16	0.44±0.06	0.10±0.05	
588.0	0.16±0.04	0.15±0.05		0.38±0.06	0.19±0.06	0.31±0.05	0.43±0.07
608.5	0.82±0.10	0.84±0.08	0.82±0.10	0.95±0.11	0.77±0.07	0.79±0.07	1.01±0.09
613.2	0.68±0.10	0.57±0.08		0.26±0.05	0.33±0.05	0.50±0.07	0.37±0.05
683.8	3.17±0.24	3.18±0.23	3.28±0.25	3.16±0.22	3.05±0.23	2.78±0.20	2.72±0.32
754.7		0.23±0.07	0.27±0.07	0.44±0.07			
791.0	0.29±0.09	0.16±0.05		0.16±0.06	0.12±0.03		
814.0	1.31±0.11	1.64±0.14	1.88±0.16	1.73±0.14	1.35±0.11	1.70±0.14	1.33±0.11
836.3	2.12±0.19	2.30±0.17	2.58±0.20	2.45±0.20	2.11±0.16	2.25±0.17	2.33±0.18
907.0	1.86±0.20	1.21±0.32	1.58±0.36	1.59±0.43	2.52±0.50		
910.0	2.91±0.35	3.29±0.37	4.31±0.44	6.37±0.56	5.26±0.46	4.05±0.52	4.14±0.61
913.3	2.29±0.21	2.34±0.30	2.29±0.27				2.65±0.60
928.5	4.82±0.34	4.77±0.33	4.52±0.32	4.61±0.35	4.42±0.29	4.69±0.33	4.51±0.39

continued

E(KeV)	30°	40°	55°	90°	110°	125°	140°
946.3	1.40±0.12	1.70±0.15	1.78±0.15	1.71±0.18	1.49±0.12	1.50±0.14	1.22±0.18
1013.3	0.27±0.08	0.64±0.07	0.64±0.07	0.56±0.09	0.68±0.07	0.70±0.07	0.78±0.08
1090.1	5.38±0.31	5.81±0.32	5.95±0.34	5.65±0.32	5.41±0.31	5.40±0.30	5.10±0.28
1120.5	1.07±0.11	1.02±0.15	1.00±0.18	0.81±0.09	0.73±0.07	0.82±0.08	0.99±0.09
1173.8	1.94±0.17	1.90±0.16	1.74±0.13	1.74±0.15	1.53±0.11	1.76±0.12	1.34±0.13
1380.8	0.42±0.11	0.41±0.10	0.65±0.09	0.68±0.09	0.63±0.09	0.63±0.09	0.46±0.09
1437.3	1.78±0.14	1.62±0.11	1.53±0.12	1.49±0.17	1.69±0.12	1.40±0.12	1.56±0.13
1493.0	0.97±0.11	1.76±0.12	1.72±0.13	1.61±0.15	1.54±0.17	1.40±0.12	1.45±0.14
1553.6	2.94±0.24	2.58±0.16	2.80±0.18	2.52±0.17	2.56±0.20	2.61±0.17	2.66±0.20
1581.9	0.24±0.10		0.68±0.10	0.67±0.15	0.56±0.13	0.48±0.14	0.34±0.11
1608.9	20.05±1.14	19.20±1.10	20.45±1.10	18.46±0.99	18.73±1.05	19.61±1.05	18.69±1.00
1724.0	0.42±0.10	0.52±0.11	0.52±0.07	0.46±0.09	0.24±0.07	0.39±0.07	0.76±0.16
1776.0	1.65±0.14	1.77±0.14	2.30±0.14	2.49±0.18	1.79±0.13	2.16±0.14	1.80±0.15
1785.6		0.41±0.14	0.45±0.13	0.64±0.16		0.56±0.17	0.72±0.21
1801.0		0.21±0.13		0.36±0.08	0.21±0.07		0.20±0.11
1812.9	5.17±0.40	5.40±0.31	6.15±0.35	6.11±0.35	5.79±0.33	5.90±0.34	5.40±0.38
2004.4		0.89±0.08	0.79±0.09	0.92±0.15	0.55±0.08	0.71±0.15	0.63±0.09
2333.8		0.49±0.07	0.41±0.07	0.98±0.13	0.54±0.09	0.43±0.07	0.44±0.09

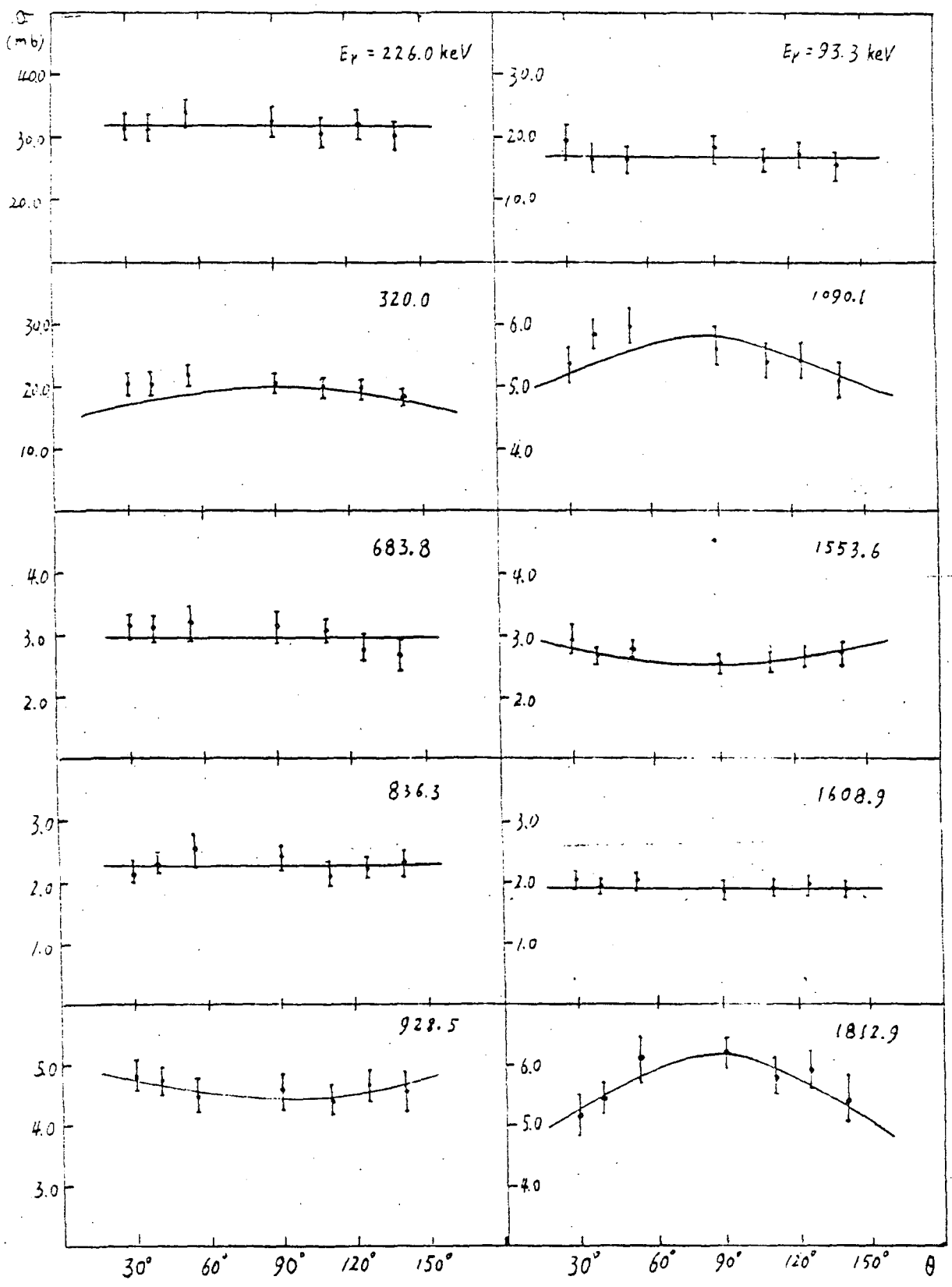

Fig.5 Fitted curves of the angular distributions of ^{51}V (n,xγ) reactions

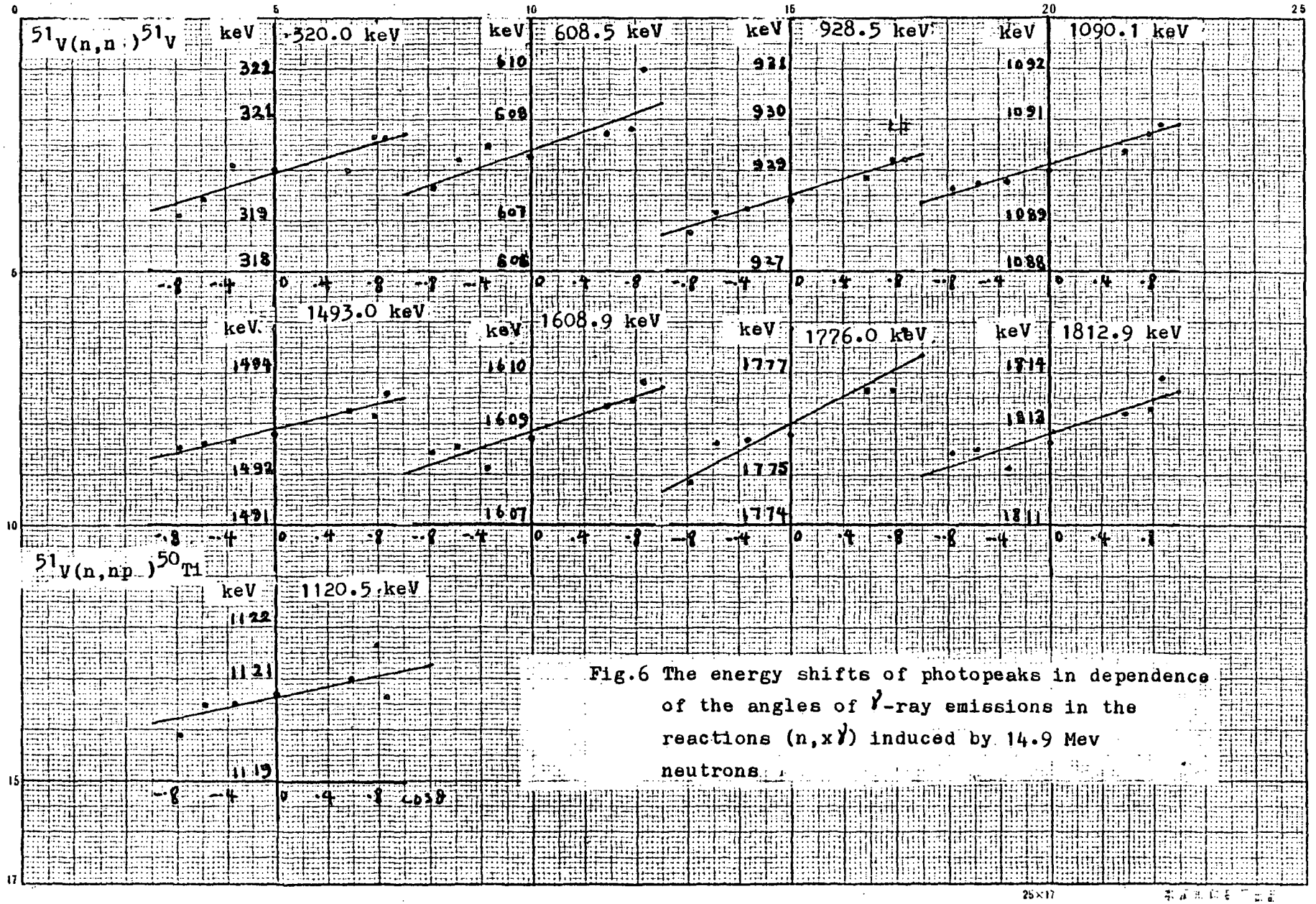

Fig.6 The energy shifts of photopeaks in dependence of the angles of γ-ray emissions in the reactions (n,xγ) induced by 14.9 Mev neutrons

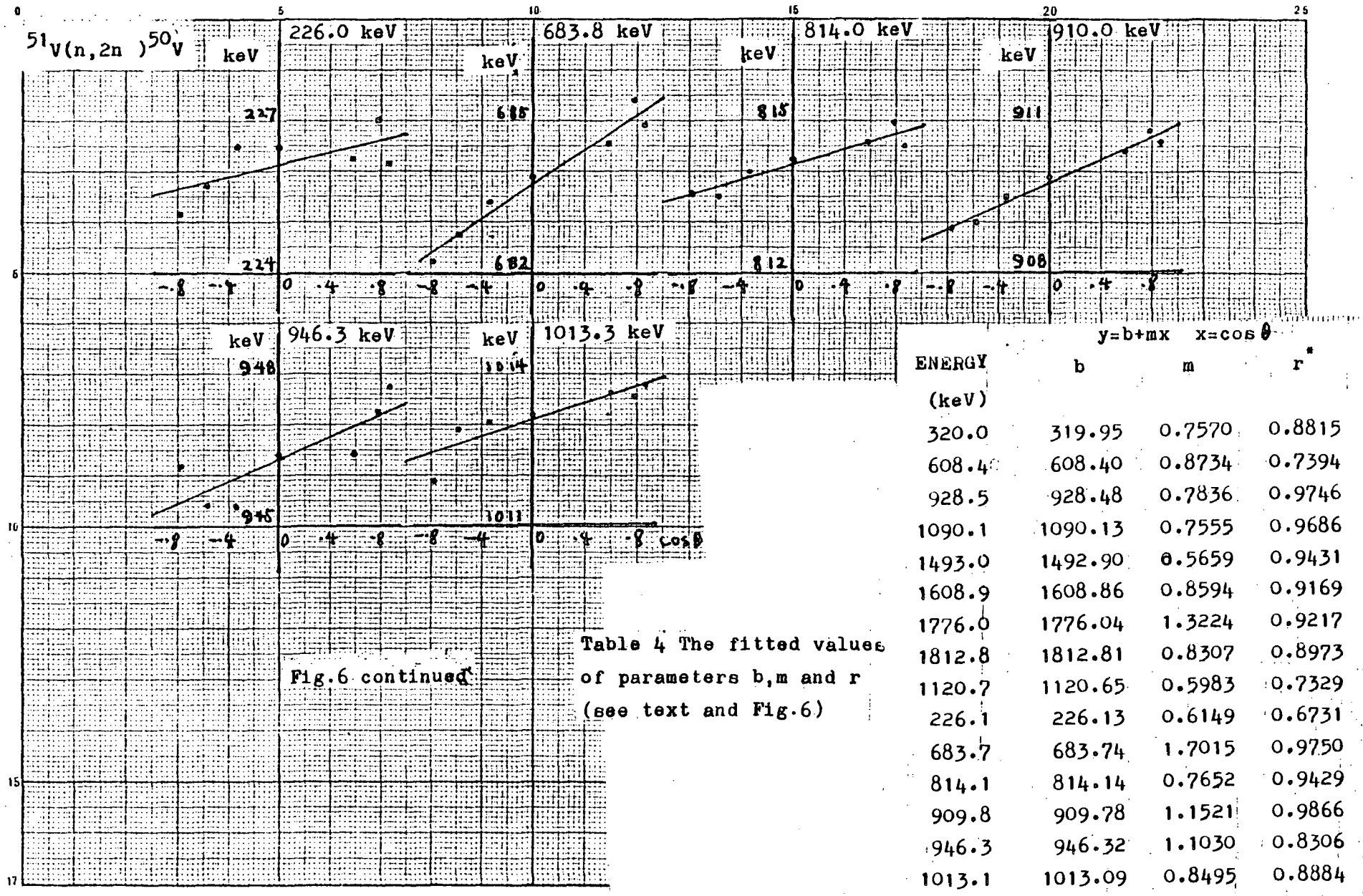

Fig.6 continued

Table 4 The fitted values of parameters b, m and r (see text and Fig.6)

y=b+mx x=cos θ

ENERGY (keV)	b	m	r*
320.0	319.95	0.7570	0.8815
608.4	608.40	0.8734	0.7394
928.5	928.48	0.7836	0.9746
1090.1	1090.13	0.7555	0.9686
1493.0	1492.90	0.5659	0.9431
1608.9	1608.86	0.8594	0.9169
1776.0	1776.04	1.3224	0.9217
1812.8	1812.81	0.8307	0.8973
1120.7	1120.65	0.5983	0.7329
226.1	226.13	0.6149	0.6731
683.7	683.74	1.7015	0.9750
814.1	814.14	0.7652	0.9429
909.8	909.78	1.1521	0.9866
946.3	946.32	1.1030	0.8306
1013.1	1013.09	0.8495	0.8884

* r is the coefficient of correlation

The experemental results of Doppler shifts can be fitted by straight lines $y = b + mx$, where the y are the values of energy shifts of γ-peaks and x are the values of angles of emission of γ-photons. The fitted values of b, m and r(coefficient of correlation) are listed in table 4.

The theortical analysis was complicated by a situation that for high energy neutrons such as 14.9 MeV neutrons there are important pre-equibrium, direct reactions in addition to the compound process. Besides, much cascade γ-ray transitions make the analysis of angular distributions difficult. The detailed analyses of Doppler shifts of γ-lines are complicated also by the situation that the decay schemes and braching ratios are unknown. So it is necessary to do further researches, for example, coincidence experiments for clear theoretical explanation.

Reference

(1) Yan Yiming et al, Ch.J.Nucl.Phys., to be published
(2) P.Guenther, Nucl.Sci.Eng. 64,733(1977)
(3) J.H.Towle, Nucl.Phys. A117.657(1968)
(4) E.Ramstrom, Nucl.Phys.A315,143(1979)
(5) A.W.Barrows, Ibid, A107,153(1968)
(6) Д.К.Капцов, Известия АН СССР,Серия Физическая 44,1877,1980
(7) U.Abbondanno, Nuovo Cimento, 72A,138(1982)
(8) Zhou Hongyu et al, to be published

*Supported by the National Natural Science Foundation of China and Ministry of Nuclear Industry of China.

Progress of Nuclear Data Work in Institute of Heavy Ion Physics, Peking University

September, 1987

Bao Shanglian

I. Introduction

Peking University is one of the earlist units which joined the work of nuclear data in China. The main group concernig nuclear data in Peking University belongs to Institute of Heavy Ion Physics and Dept. of Technical Physics. Besides, there is also a theoritical physics group on nuclear data in Physics Dept. . Nuclear data work in Peking University includes theoritical research programs, evaluation of neutron nuclear data and experiment measurements.

In our institute there are several accelerators. The characteristics of these accelerators and their further use are shown in table 1. Up to now, only the 5SDH-2 tandem Van de Graaff is ready. All others are still busy on mounting and adjusting. The own designed 4.5 MeV single Van de Graaff is mainly used for nuclear data measurements and it can be ready by the end of 1988.

II. Evaluation of neutron nuclear data of natural calcium for CENDL -1. (Tang Guoyou, Shi Zhaomin, Bao Shanglian)

Natural calcium is a component of reactor structure. Therefore the neutron nuclear data of natural calcium is important for improvement of reactor design.

Table 1. The Characteristics of Accelerators in Peking University (PU)

TYPE OF ACCELERATOR	DESIGNER & PRODUCER	HIGH VOLTAGE RANGE (M V)	ION SOURCE	BEAM INTENSITY	USER	USAGE
EN -18 VdG Tandem	HVEC EURAPA (1962)	0.5 - 6.5	Middleton Sputter He^+ Source and Neg.Soure	H^-: 20 μA C^-: 20 μA	OXford Univ. (before 1985) PU(1986)	Accelerator Mass Spettros -copy on dating Nuclear Data Research of Nuclear Structure.
4.5MV Vetical Single VdG	PU & PEEF Shanghai China	0.3 - 4.5	HF PIG	H^+: DC 10^{14}pps C^{+2}: DC 10^{13} pps AC: 1.5ns 3 MHz	PU	Neutron nuclear Data Beam Application.
5SDH -2 PeHetron Tandem	NEC, USA	0.1 - 1.7	Middel. H^+ and Meg.Source	H^-, C^- : 0.4 - 1.5 μA	PU	Beam Analysis, Material Research.
Ion Projector	PU	0.02 - 0.2	PEG	200 μA	PU	Material Research

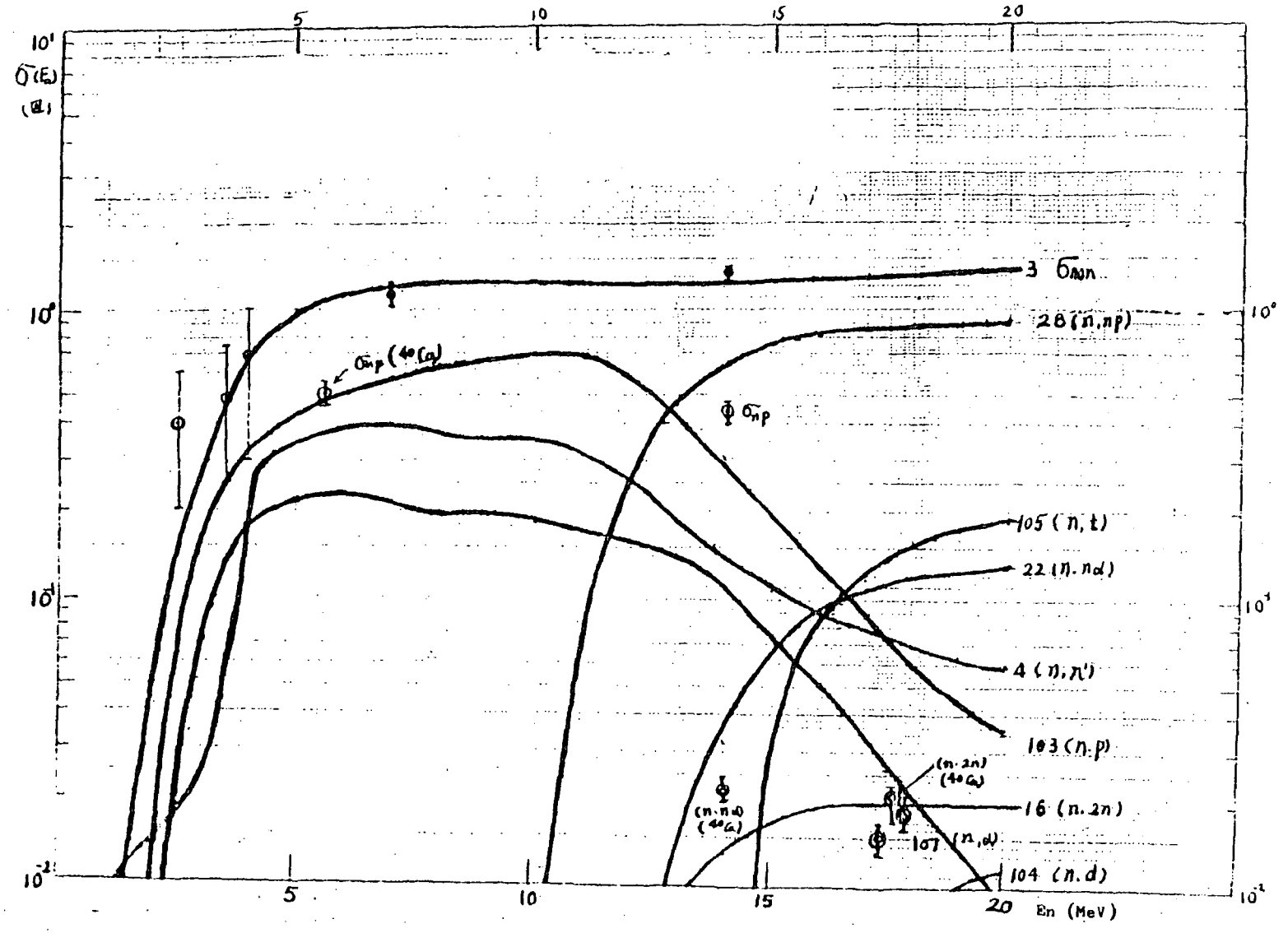

Fig. II-1 Evaluated Cross Section of Natural Calcium. The Corresponding Experimental Data are Shown on Lines Respectively.

Neutron nuclear data of natural calcium have been evaluated for CENDL -1 in the energy range of 10^{-5} eV to 20 MeV. The evaluated quantities are the total, non-elastic scattering, elastic and inelastic scattering, radiation capture, (n·P), (n,t), (n,2n), (n, α), (n,np), (n,nα) reaction cross sections, the angular distribution of elastic and inelastic cross sections, and the energy spectra of secondary neutrons. In the present evaluation the theoretical calculations were made using the program AUJP[1], which is based on the optical model and program MUP2[2], which is based on the optical model, the H - F model, and the pre - equilibrium model. These programs are made by the Nuclear Data Centre of China and a group in Nankai University.

References

1. Zhou Hongmo, Yu Zhiqiang, et al., Auto-parameter adjusting optical model calculation program AUJP, Inter. Report.

2. Yu Zhiqiang, Cai·Zhonghai, et al., Theoritical calculation program MUP2 for middel and heavy nuclei, inter. Report.

III. The Theoretical Research Programs

The theoretical research group of nuclear data in Peking University mainly works in the field of fission physics. We have proposed a macroscopic model of nucleus in 1981[1]. We also applied the Brownian motion model to study the nuclear fission probabilties[2]. In recent years using these model we have got some significant results[3-5].

1. Macroscopic Model of Nucleus.

(Hu Ji Min, Zheng Chunkai)

The macroscopic model of nucleus considers the nucleus as continuous medium of neutrons and protons with variable densities and assumed that the binding energy of a nucleus can be expessed by a simple energy function . By variation of the energy function , the densities of neutrons and protons can be obtained and the nuclear mass formula is derived. The parameters contained in the formula are determined by fitting the experimental atomic masses, rms (root-mean-square) charge radii, and the Coulomb energy differences between isobaric analog states. Using our formula and the shell corrections of Möller and Nix[6], the nuclear masses for 1500 nuclides are calculated. The rms deviation of the fitting is 0.805 MeV. The calculated charge distributions, rms charge radii, and Coulomb energy differences between isobaric analog states are also in good agreement with the experimental data.

2. The Brownian Motion Model

(Hu Ji Min, Zhong Yun Xiao)

Brownian Motion Model has been applied to study the nuclear fission probabilities. Application of Brownian motion model and The solution of Fokker-Planck equations are studied. The fission probabilities of actinide nuclei have been calculated with the Brownian motion and the results compared with others.

3. Nuclear Data Calculation

(Hu Ji Min, Wang Zhengming, Wan Guo Ji)

In recent years the fission prompt neutron spectrum of uranium and plutonium have been performed with the evaporation model. The calculated

results are satisfying [7]. The mass and charge distributions of fission fragments are also calculated by a two-mode model on nuclear fission.

References

1. Hu Ji Min, Phys. Energy Fortis Phys. Nucl., 5 244(1981).
2. Hu Ji Min, Zhong Yun Xiao, Phys. Energy Fortis Phys. Nucl. 4 368(1980).
3. Hu Ji Min, Zheng Chukai, Chinese Physics, 6 105(1986).
4. Hu Ji Min, Zhong Yun Xiao, Chinese Physics, 2 157(1982).
5. Hu Ji Min, Summer School, Chang Chun, China.
6. P. Möller and J. R. Nix, Nucl. Phys., A361 117(1981).
7. Hu Ji Min, Wang Zhengxing, Phys. Energy Fotis Phys., 3 772(1979).

IV. Calculations of Nuclear Reaction Cross Section with the Computer Code HFTT. (Huan Feizeng, Shi Zhaomin, Bao Shanglian)

1. Introduction

It is important to use theoretical models to analyse experimental data and to predict nuclear reaction cross sections which are not easy or impossible to be measured at present. The purpose of this work is to build a computer code to calculate nuclear reaction cross sections for target nuclei with mass number A $\geqslant$ 40. The code can predict the nuclear reaction cross sections induced by proton, neutron and deuteron in the energy range above a few tens of MeV. The output data are limited in the outgoing channels to proton and neutron at present. Further work will also include some other outgoing channels.

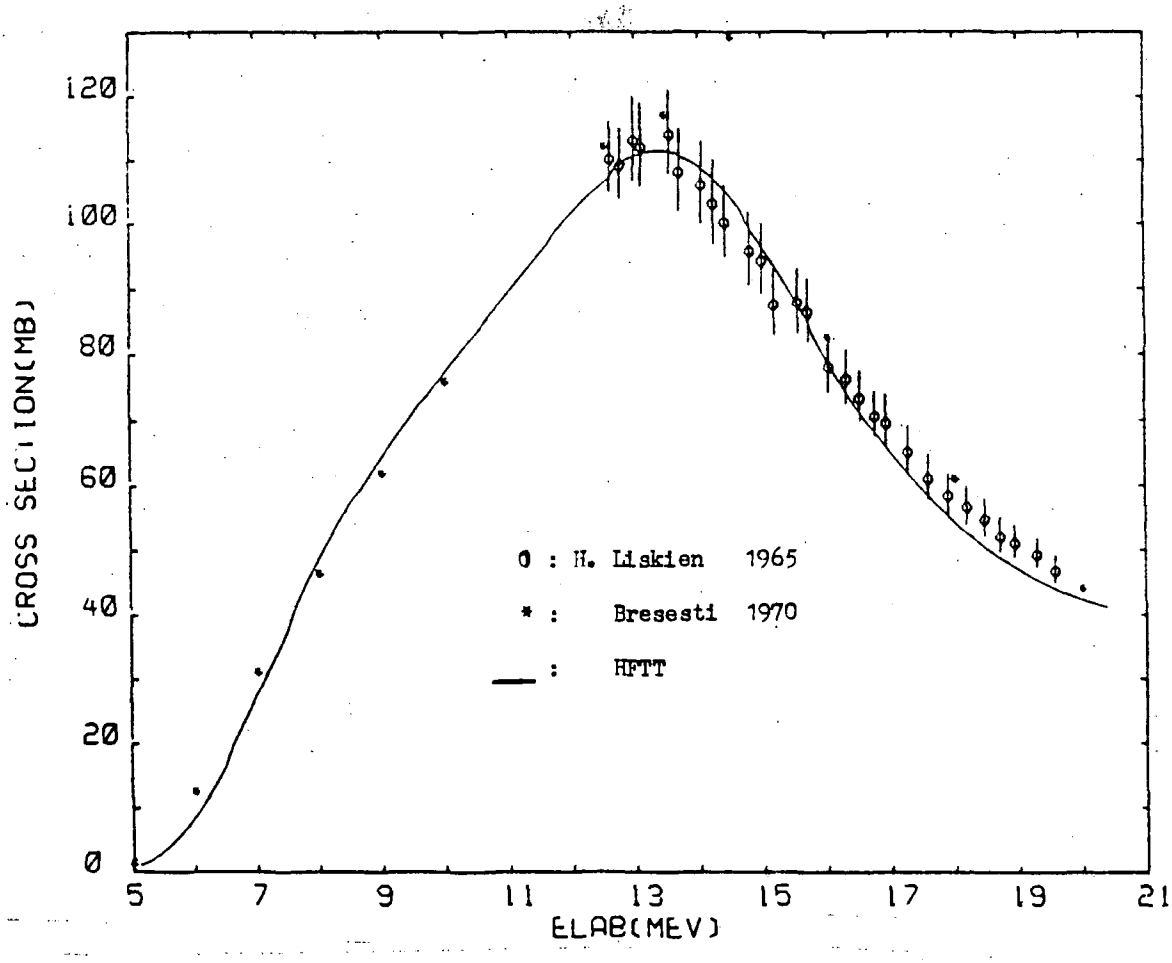

Fig. IV-1 Comparison of calculated excitation function for the $^{56}Fe(n, p)^{56}Mn$ reaction with experimental results.

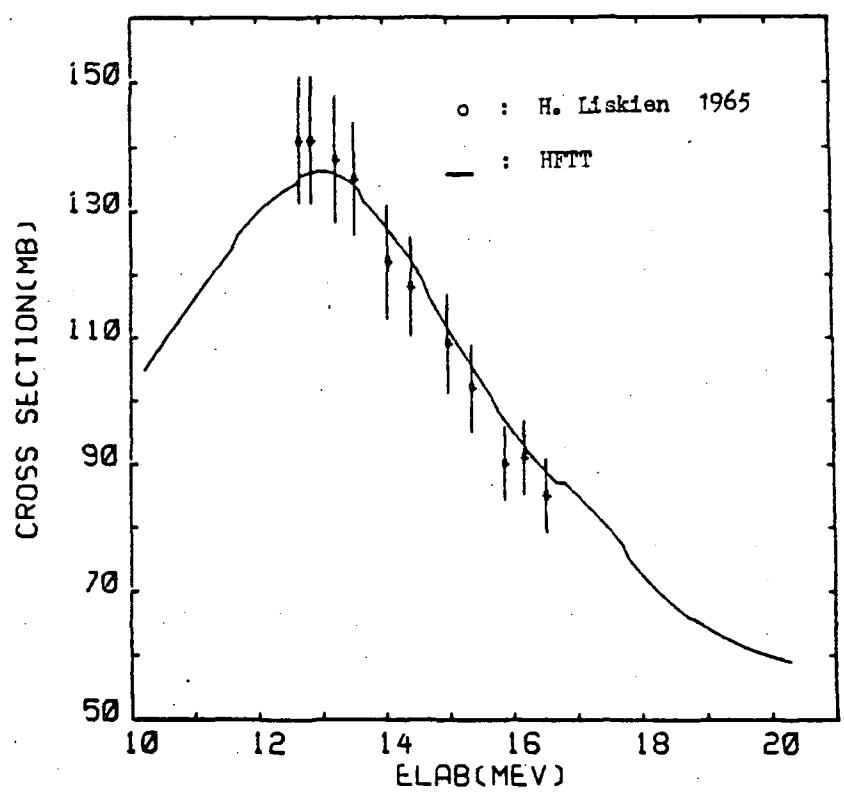

Fig. IV-2 Comparison of calculated excitation function for the $^{60}Ni(n, p)^{60}Co$ reaction with experimental result.

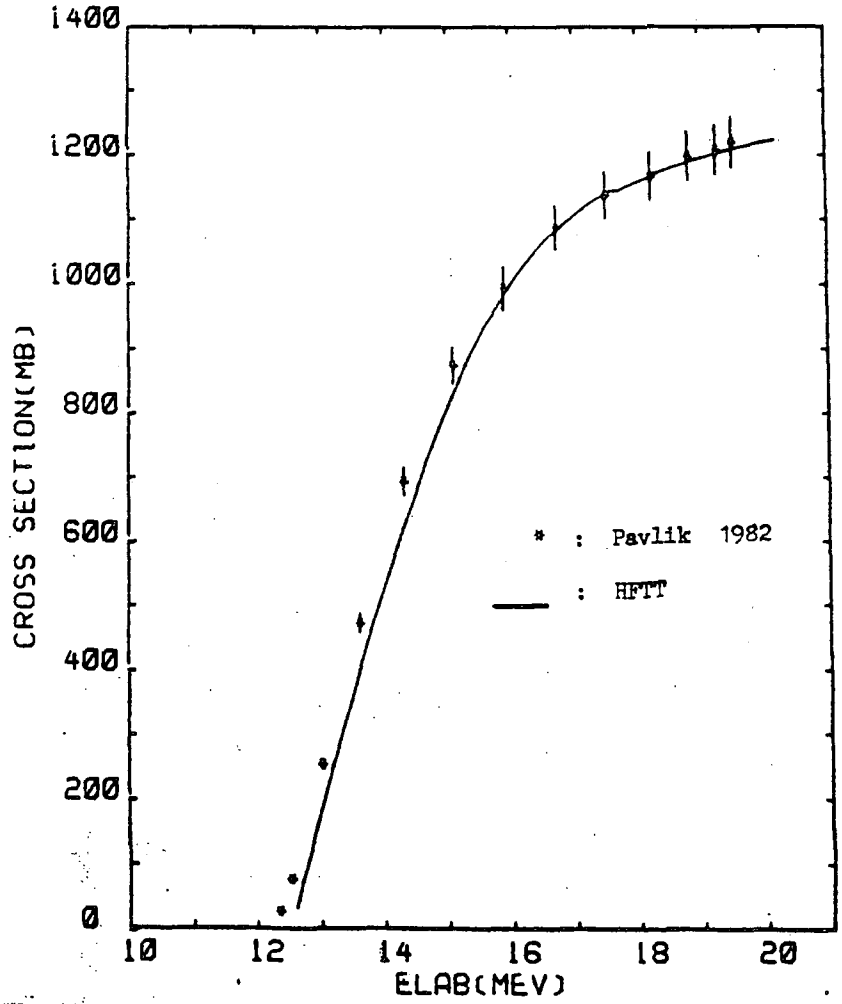

Fig. IV-3 Comparison of the calculated exitation function for the $^{90}Zr(n, 2n)^{89}Zr$ reaction with experimental result.

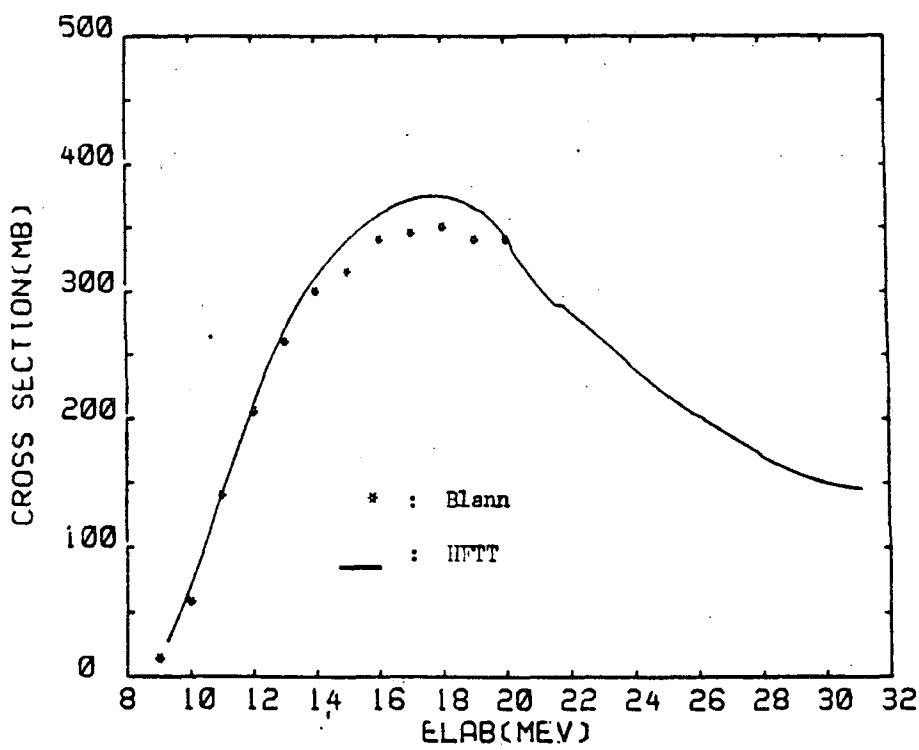

Fig. IV-4 Comparison of the calculated excitation function for the $^{52}Cr(d, 2n)^{52}Mn$ reaction with experimental result.

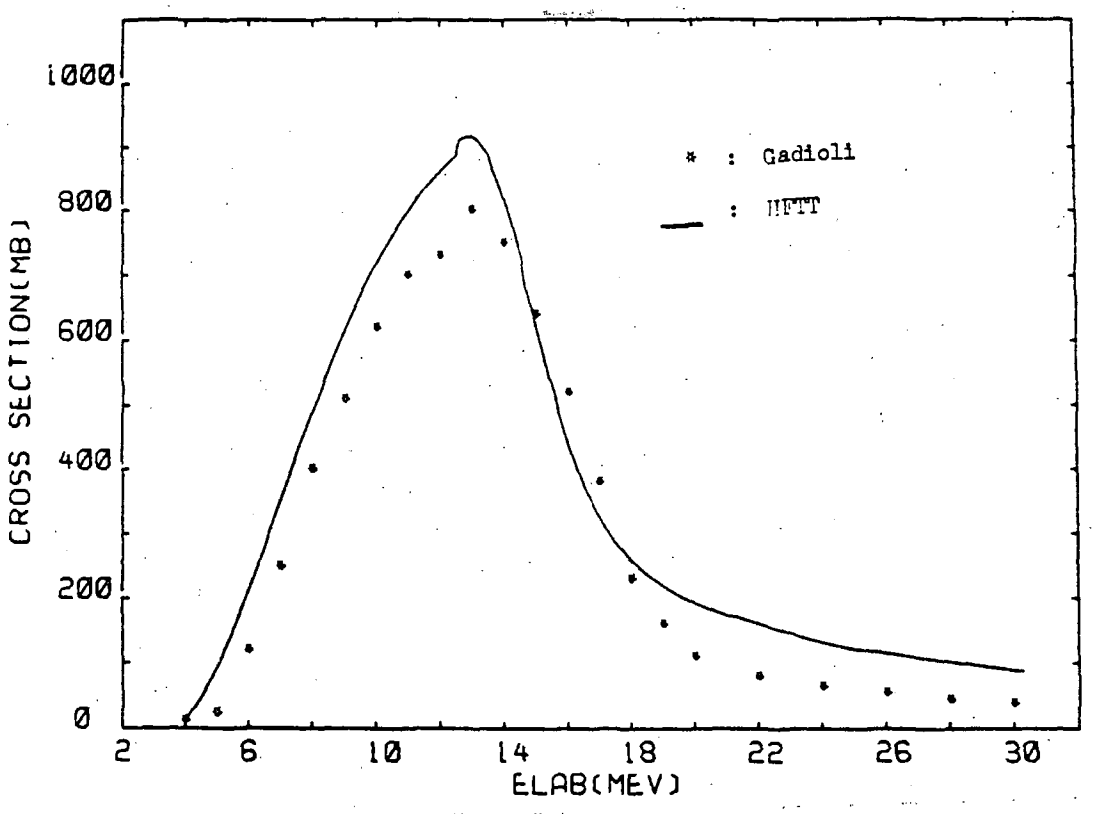

Fig. IV-5 Comparison of the calculated excitation function of the $^{89}Y(p, n)^{89}Zr$ reaction with the experimental result.

2. Brief Description of the Code

The code HFTT is based on a combination of the compound nuclear evaporation model and pre-equilibrium exciton model. The description of pre-equilibrium emission of a composite system is based on the formula of Cline [1]. The intranuclear transition rate of Oblozinsky et al. [2] and Kalbach-Cline's expression about the matrix element of the residual interaction are used in the code. The normalization constant of the matrix element is adjustable as an input parameter of the code. The first and second emission particles considered in the program are n,p,t, ^{3}He, d, ^{4}He and gamma ray. The third emission particles considered are p, n and gamma ray. We chose the initial exciton configuration of n_0=3 (2p, 1h) for nucleon induced nuclear reactions and of n_0=3(2p,1h) or n_0=4(3p,1h) for deuteron induced reactions. The level densities are calculated by the formula of

Gilbert-Gamron [3]. The optical model is used to evaluate the inverse cross sections of nuclear reactions. In order to reduce the number of adjustable input parameters which are universal suitable in some range, recommendation by Becchetti[4], Perey[5] and Mefadden[6] are used in the program.

3. Results

The excitation functions of several reactions were calculated using the code HFTT. The calculated cross sections compared with corresponding experimental results [7,8,9] are presented in Figs. IV-1 to IV-5. From the fitting we can see that calculated results are in good agreement with the experimental data.

Reference

1. C. K. Cline, Nucl. Phys. A193 417(1972).
2. P. Cblozinsky et al., Nucl. Phys. A226 347(1974).
3. A. Gilbert et al., Can. J. Phys. 43 1446(1965).
4. F. D. Becchtti et al., Phys. Rev. 182 1190(1959).
5. F. G. Perey et al., Atomic Data and Nucl. Data, V15, 4(1975).
6. Mefadden, Nucl. Phys., 84 177(1966).
7. H. Liskien et al., J. Nucl. Energy Parts A/B, V19 73(1965).
8. H. Liskien et al., Nucl. Phys., 63 393(1965).
9. Pavlik et al., J. Phys. G. Nucl. Phys. 8 1283(1982).

V. Measurement of ^{252}Cf Spontaneous Fission Prompt Neutron Spectrum In The Lower Energy Part

(Tang Guoyou, Wang Jie, Bao Shanglian, Zhong Weinguan, Shi Zhaomin: PU . Mon Jingshen, Huang Shengnian, Li Anli, Bao Zhongyu: IAE)

(Preliminary Results)

1. Introduction

The prompt neutron spectrum from the spontaneous fission of ^{252}Cf has been defined as a standard neutron spectrum[1,2]. The detailed shape of the energy spectrum is required with high precision. Californium sources are widely used for neutron detector calibration and for other applications. In recent years a number of experimental measurements have been done[3-6], and the discrepancies at low and high energy parts are still remained. Therefore, it is desirable to secure and develop the progress of the recent years both in the experimental and the theoretical directions[7].

2. Experimental Method and The Preliminary Result

Our experiment was carried out in cooperation with the Atomic Energy Institute, Beijing, using TOF method. The neutron detector in the run is NE 912 lithium glass (45 mm in diameter, 9.55 mm in thickness). A RCA 8850 PM is coupled with the detector. The rise time of the detector is about 5 ns. The fragment detector is a mini-ionization chamber, which was made by the Atomic Energy Institute, Beijing. Its weight is $\sim$1.6 g. The experiment was carried out in a 1960 m^3 neutron hall. The flight path is 10.0 cm. Data acquisition time was 100 hours. The TOF spectrum of ^{252}Cf prompt neutrons is shown in Fig. V-1. The

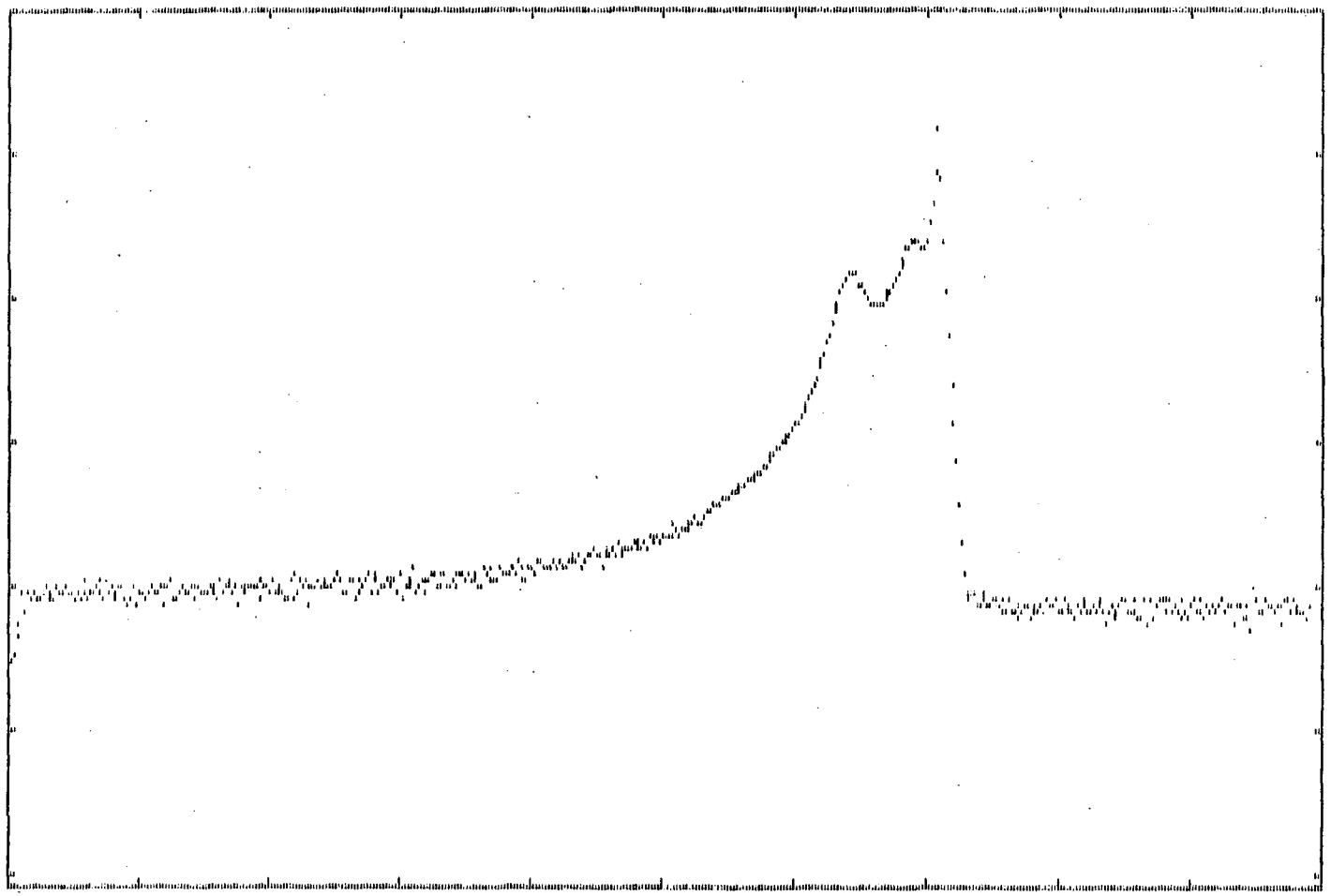

Fig. V-1 TOF of ^{252}Cf SP. The flight path: 10 cm, the neutron detector: NE912, fission fragment detector: mini-ion charmber.

intensity of the ^{252}Cf source is 4160 f/s, which was made by the Atomic Energy Institute, Beijing, by means of trasfusion in vacuum. For the second run the experiment is going on with two neutron detectors. The added neutron detector is a 2 mm thick lithium glass coupled with a XP 2020 PM positioned at 60^0 (relative to the source plane). For the data analysis we need to pay attention to the neutron scattering background and the calibration of the neutron detector efficiency. We have made a computer code to calculate the neutron detector efficiency with Monte Carlo method. But for the absolute calibration of the detector efficiency we need a suitable neutron source. Maybe we'll calibrate the detector efficiency in CBNM Geel, Belgium as a coorpration program with Geel Establishment. For further work a stronger ^{252}Cf source is needed.

References

1. Proc. IAEA Panel on Neutron Standard Reference Data, 20-40 Nov. 1972. CONF 721127, p. 362, IAEA, Vienna. (1973).

2. Proc. IAEA consultants' Meeting on Prompt Fission Neutron Spectra, Aug. 1971, P 169, IAEA, Vienna (1979).

3. A. Lajtai et al., An Absolute Measurment of ^{252}Cf Prompt Neutron Spectrum at Low Energy Range, INDC(NDS)-146, IAEA, Vienna, 1983.

4. M. V. Blinov et al., INDC(CCP) -238, IAEA, Vienna, 1984.

5. H. Märten et al., The ^{252}Cf Spontaneous Fission Neutron Spectrum in the 5 - 20 MeV Energy Range, INDC(NDS) -194, Jan. 1987.

6. J. M. Boldeman et al., Measurements of the Prompt Neutron Fission Spectrum From the Sponataneous Fission of ^{252}Cf, IAEA Advisiry Group Meeting On Nuclear Standard Reference Data, Geel, Belgium, Nov. 1984.

7. M.V. Blinov, Recent Developments In the Investigation of ^{252}Cf Spontaneous Fission Prompt Neutron Spectrum, IAEA Advisiry Group Meeting on Nuclear Standard Reference Data, Geel, Belgium, Nov. 1984.

VI. Near Future Plan For Nuclear Data

All works mentioned above will be continued.

In the field of nuclear data evaluation, the neutron nuclear data of ^{238}U will be re-evaluated. The data for ^{237}Np will be tracked. The computer system for nuclear data evaluation will be improved.

In the field of theoretical research the main interest will be in the fission Mechanism We will complete the macroscopic model and develop it into the microscopic field. The fission fragment mass distribution will be coded soon.

For theoretical analysis of the experiments and calculation of nuclear reaction cross sections the cmputer code HFTT will be modified and improved. Model calculations for light and heavy nuclei will be considered with other nuclear reaction models. For nuclear data measurements we have to wait for our acceletators to be ready. The measurements of heavy nuclei's fission parameters and activation cross sections of structural materials are the interesting fields for us.

The connection of nuclear data works with basic research is a good way for us. And some application programs will be started either.

Neutron activation cross section measurement in Fudan University

Wu Zhihua, Wu Songmao, Xu Zhizheng, Song Linggen, You Junsheng, Li Jianwei, Ding Meisong
(Department of Nuclear Science, Fudan University, Shanghai, China)

Activation cross section is very important for the application of nuclear physics. Since 1982, we have measured some neutron cross section with the method of activation. They are $^{87}Sr(n,n')^{87m}Sr$, $^{115}In(n,2n)^{114m}In$, $^{113}In(n,2n)^{112m}In$ and $^{103}Rh(n,n')^{103m}Rh$.

I. Neutron source and flux measurement

Monoenergetic neutron is produced by nuclear reaction. Deutron is accerelated in our 3 MeV Van der Graaff machine. Target is TiT or TiD. Therefore, we can get monoenergetic neutron in the range from 15 - 18 MeV or 2 - 6 MeV accordingly. Proton beam and TiT target were used to get the neutron energy lower than 2 MeV.

Neutron flux is measured by means of recoil protron telescope with semiconductor detector. A BF_3 counter located 3 meters away from target at 45 degree with beam direction was used as neutron monitor.

Neutron energy and energy spread are calculated according to reaction kinematic, the thickness of target, solid angle of sample to target and the angle of sample related to beam direction. In our case , energy spread is about tens KeV to hundred KeV. Beam energy is calibrated with the reaction $^{7}Li(p,n)^{7}Be$ and resornance reaction $^{27}Al(p,r)^{28}Si$. Beam current is 5-10 μA. Target was cooled with water or pressured air jet.

II. Sample

In and Rh are natural metal films. Its element purity was checked with PIXE method and was found 99.90% for In and 99.28% for Rh. No serious impurity could affect our measurement. ^{87}Sr is isotope pure which was offered from IAE. It

contains ^{87}Sr 52-64%. We weighed the sample using analytical balance and pressed the powder into a pellet. The size of sample is listed in table I.

Table I

chemical contain	thickness mg/cm^2	diameter mm
$Sr(NO_3)_2$	21.03 - 126.3	11.0
In	300 - 500	20.0 - 30.0
Rh	62.86	10.8

The sample is hung upon a special shelf which can be adjusted so that we can set the center coincidence with the beam direction easily.

III. Measurement of activation

According to decay mode we select different radiation to be measured. The measurement is listed in table II in detail.

Table II

nuclei	radioactivity	Energy (keV)	detector
^{87m}Sr	gamma	388	3" NaI
^{114m}In	gamma	190	Ge(Li)
^{112m}In	gamma	156	Ge(Li)
^{114m}In	Ka X ray	24.1	Si(Li)
^{103m}Rh	Ka X ray	20.17	Si(Li)&NaI
	Kb X ray	22.7	

The efficiency of the standard 3" NaI(Tl) detector was evaluated by calculation. The efficiency of the other detector was calibrated with a set of standard source. When the efficiency was calibrated, special attention had been paid to correction, such as air absorbtion, window adsorption, multi-gamma sum effect, solid angle correction and others.

IV. Result and discussion

1. As regards $^{87}Sr(n,n')^{87m}Sr$ cross section, Temerley's(3) data was the only one published prior to our experimental result. Futhermore, our experiment has compensated for the lack of data in this respect. All the data was illustrated in fig. 1.

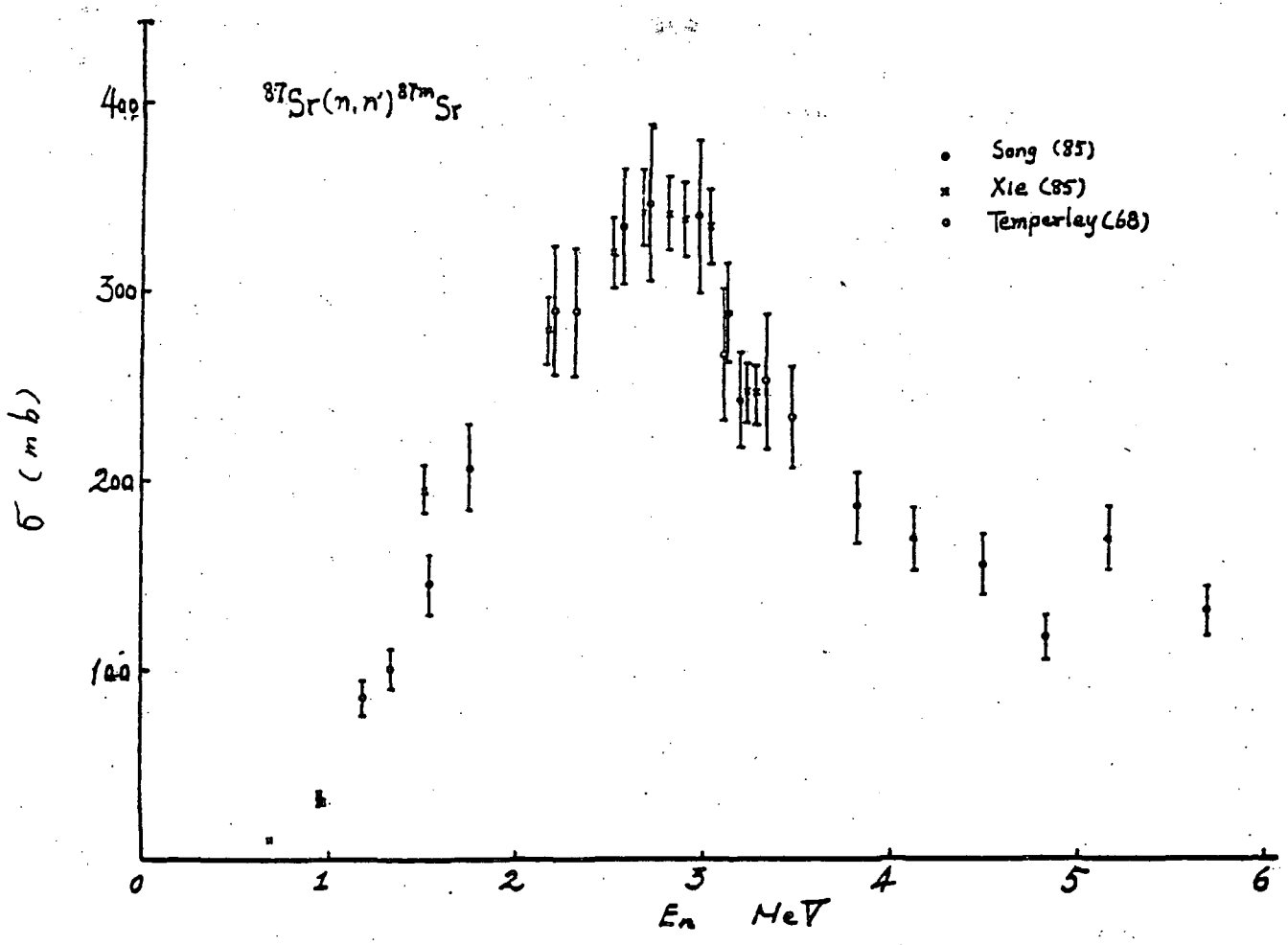

Fig. 1 $^{87}Sr(n,n')^{87m}Sr$ cross section

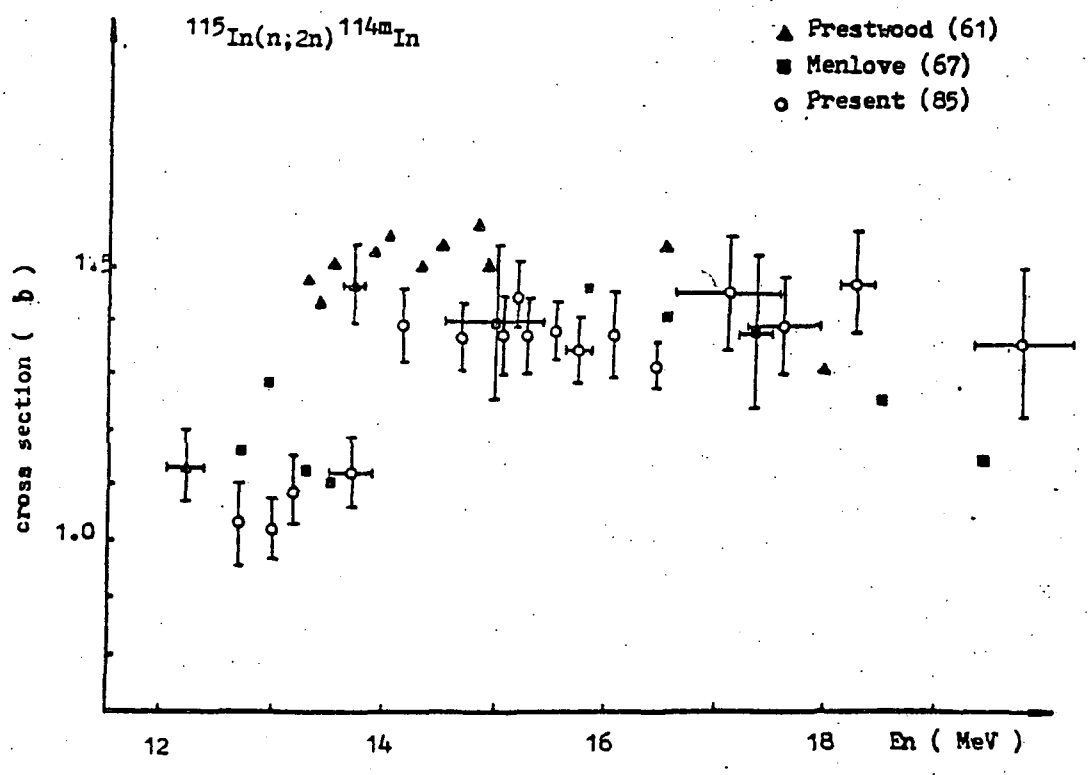

Fig. 2 $^{115}In(n,2n)^{114m}In$ cross section

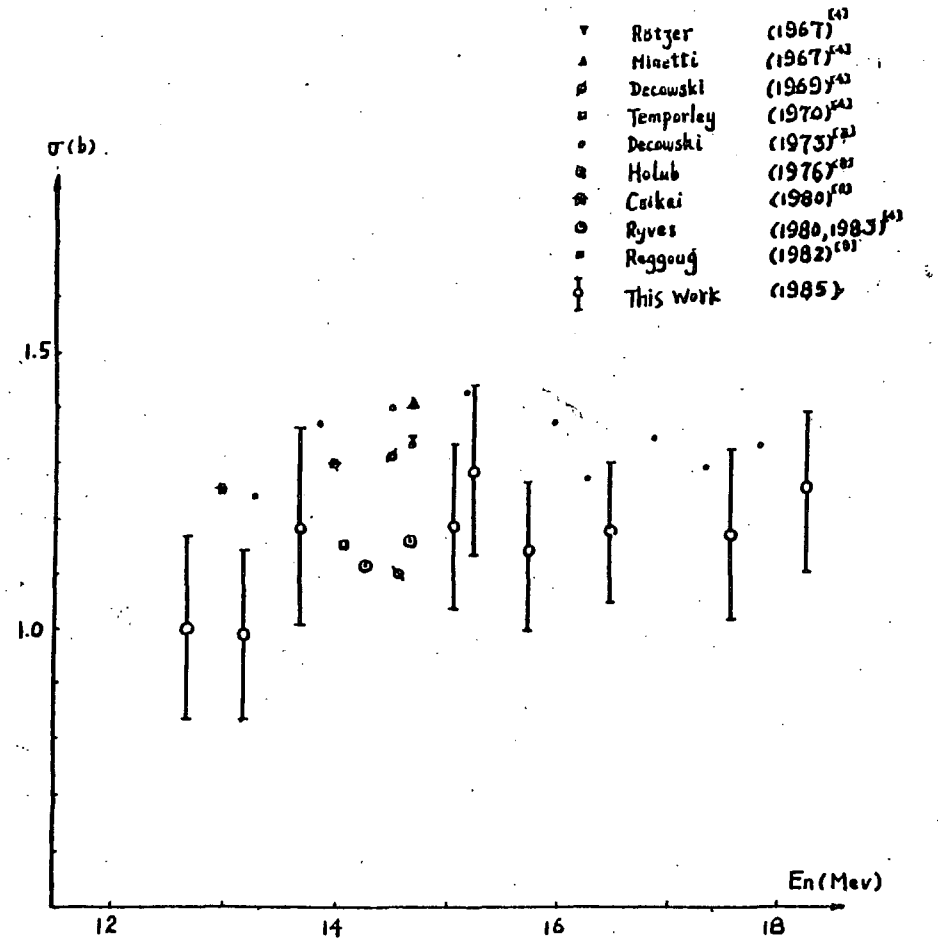

Fig. 3 $^{113}In(n,2n)^{112m}In$ cross section

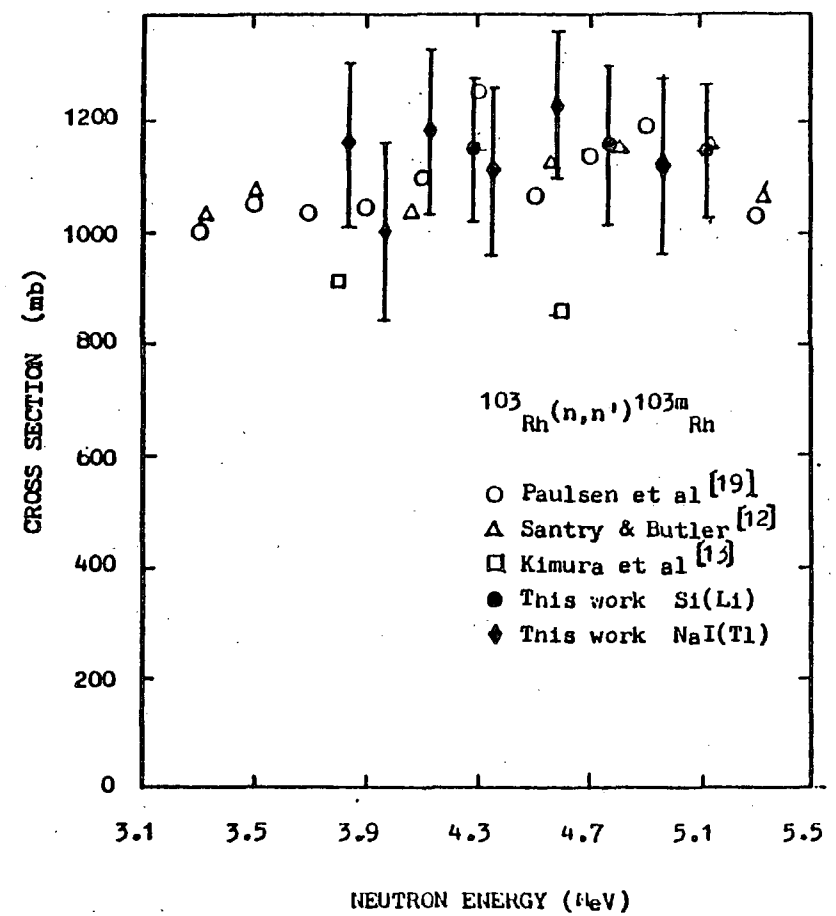

Fig. 4 $^{103}Rh(n,n')^{103m}Rh$ cross section

2. Having analysed and compared with the $^{115}In(n,n')^{114m}In$ cross section altogether, we found that the spread between the results is relevant to the measurement method of neutron flux. When Fe or Al was used as a standard sample, it was discovered that the smaller result was for Fe and the bigger result was for Al. On the other hand, when the associated particle method was used as an absolute measurement of neutron flux, the final result was deviant to bigger; while the telescope method was used to flux measurement, the result remained in the middle.

We used three different methods of measurement at some energy point, E = 15.754 MeV, in ^{115}In inelastic scattering cross section measurement. The result was given in table III.

Table III

method	cross section (mb)
Fe	1293 ± 52
Al	1349 ± 62
telescope	1345 ±108

It was proved that the systematic deviation was still exist. In order to find the reason of spread between the data, it is valuable to measure activation cross section with better precision.

3. In order to determine the $^{103}Rh(n,n')^{103m}Rh$ cross section, it's necessary to measure the intensity of low energy X radiation. Since the absolute measurement of X ray is still not good enough, it has affected the precision of the final result. The primary data is illustrated in fig 4.

References

1. Song Linggen et al. , Chinese Journal of Nuclear Physics 7 (1985) 58
2. Xie K.Z. et al.,Jour. of Applied Sciences (in Chinese) 3 (1985) 341
3. Temperley J.K. et al.,Nucl. Sci. Eng. 32 (1968) 195
4. Li J.W. et al.,Chinese Jour of Nuclear Physics, to be published.

THE PRESENT STATUS OF A+M DATA RESEARCH IN CHINA
—— THE INTRODUCTION OF CRAAMD

Du X. W.

(NUCLEAR DATA COMMITTEE OF CHINA, IAPCM, BEIJING)

Zhou E. C.

(NUCLEAR DATA COMMITTEE OF CHINA, IAE, BEIJING)

Sun Y. S.

(CRAAMD, IAPCM, BEIJING)

NOWADAYS THERE ARE GROWING REQUIREMENTS FOR ATOMIC AND MOLECULAR DATA FROM MANY FIELDS, SUCH AS:

- M C F, (Magnetic Confinement Fusion)
- I C F, (Inertia Confinement Fusion)
- L I S, (Laser Isotope Separation)
- BIOMEDICINE (RADIOBIOLOGY, RADIOTHERAPY) AND SO ON,

SO FORTH.

THERE WERE SEPARATED RESEARCH WORKS ON ATOMIC AND MOLECULAR DATA IN SOME INSTITUTIONS OF OUR COUNTRY IN PAST YEARS AND SOME RESULTS HAVE BEEN OBTAINED ALREADY. IN ORDER TO ENHANCE AND COORDINATE THESE RESEARCH WORKS, THE SORKING GROUP ON ATOMIC AND MOLECULAR DATA OF WHOLE COUNTRY HAS BEN ORGANIZED. IT HAS AN ABBRAVIATION NAME CRAAMD (CHINESE RESEARCH ASSOCIATION FOR ATOMIC AND MOLECULAR DATA).

NOW, WE WILL GIVE A BRIEF INTRODUCTION ABOUT THE STRUCTURE AND THE ACTIVITIES OF CRAAMD.

I. GENERAL SITUATION OF CRAAMD.

CRAAMD IS A WORKING GROUP OF THE WHOLE COUNTRY FOR ATOMIC AND MOLECULAR DATA. IT WAS FORMALLY ESTABLISHED IN BEIJING IN FEBRUARY THIS YEAR. CRAAMD IS SUBORDINATE TO NUCLEAR DATA COMMITTEE OF CHINA AND TO CODATA CHINESE COMMITTEE AS WELL. THERE ARE TEN RESEARCH INSTITUTIONS JOINING CRAAMD SO FAR. THEY ARE:

1. INSTITUTE OF APPLIED PHYSICS AND COMPUTATIONAL MATHEMATICS (BEIJING)
2. DEPARTMENT OF MODERN PHYSICS, FUDAN UNIVERSITY (SHINGHAI)
3. INSTITUTE OF LOW ENERGY PHYSICS AND DEPARTMENT OF PHYSICS, BEIJING NORMAL UNIVERSITY (BEIJING)
4. NUCLEAR PHYSICS DIVISION OF INSTITUTE OF ATOMIC ENERGY (BEIJING)
5. INSTITUTE OF HIGH TEMPERATURE AND HIGH PRESSURE PHYSICS, CHENGDU UNIVERSITY OF SCIENCE AND TECHNOLOGY (CHENGDU)
6. INSTITUTE OF PHYSICS, ACADEMIA SINICA (BEIJING)
7. INSTITUTE OF ATOMIC AND MOLECULAT PHYSICS,JILIN UNIVERSITY (CHANG CHUN)
8. CENTER OF BASIC PHYSICS, CHINA UNIVERSITY OF SCIENCE AND TECHNOLOGY (HE FEI)
9. INSTITUTE OF ENVIROMENTAL FEATURES (BEIJING)
10. DEPARTMENT OF APPLIED PHYSICS, CHANG SHA UNICERSITY OF SCIENCE AND TECHNOLOGY.

THERE ARE FOUR WORKING GROUPS IN CRAAMD:

A. THE GROUP OF THEORETICAL CALCULATIONS;

B. THE EXPERIMENTAL GROUP;

C. THE GROUP OF SELECTIONS AND COMPILATIONS;

D. THE DATA LIBRARY.

The Sketch of CRAAMD

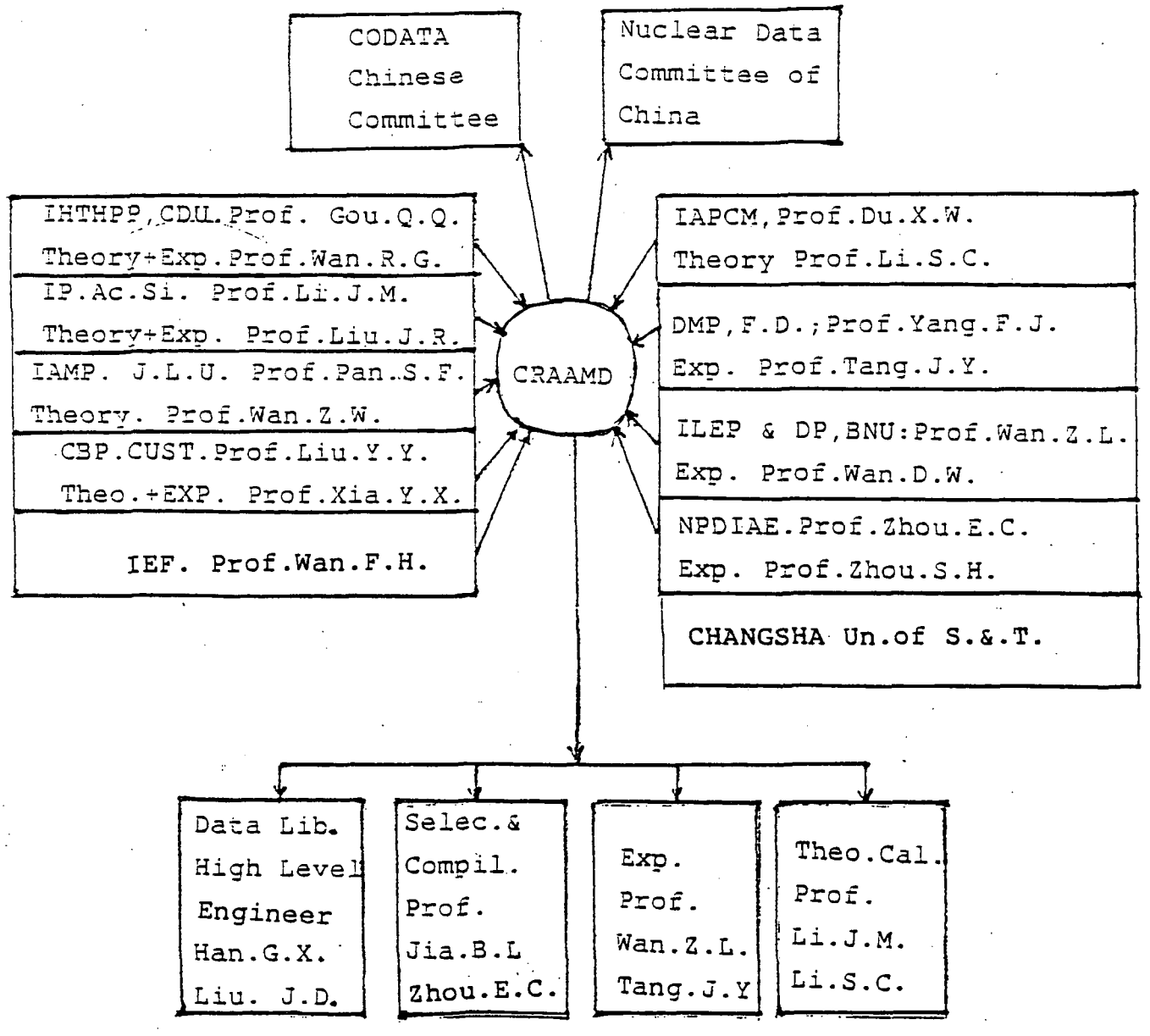

THE EXECUTIVE DUTIES OF CRAAMD ARE HANDLED BY THE LEADING GROUP OF THREE PERSONS:

SUN YONGSHENG (HEAD OF THE GROUP, IAPCM, BEIJING)

TANG JIAYONG (VICE HEAD OF THE GROUP, FUDAN UNIVERSITY)

WANG ZHONGLE (VECE HEAD OF THE GROUP, ILEP, BEIJING NORMAL UN.)

THE IAPCM IS IN CHARGE OF THE ROUTINE OF CRAAMD.THE ROUTINE WORKING BODY OF SRAAMD IS SET UP IN IAPCM.

DR. DU X. W. AND ZHOU E. C. OF NDCC ARE RESPONSIBLE FOR THE WORK OF ITS A+M WORKING GROUP —CRAAMD.

II. DUTIES OF CRAAMD

THE DUTIES OF CRAAMD ARE TO CALCULATE, MEASURE, COLLECT, COMPILE AND EVALUATE A+M DATA. OUR PURPOSE IS AS FOLLOWS: THE LIBRARY OF ATOMIC AND MOLECULAR DATA AND THE LIBRARY OF COMPUTATIONAL SOFTWARES WILL BE PROGRESSIVELY SET UP IN ORDER TO SATISFY THE NEEDS OF SOME MAJOR FIELDS OF SCIENCE AND TECHNOLOGY (FOR EXAMPLE: THE CONTROLED FUSION RESEARCH, THE LASER RESEARCH ETC.) ALL ATOMIC SCIENTISTS IN THE INSTITUTIONS JOINING CRAAMD WILL UNITEDLY MAKE THEIR PLANS AND COORDINATE THEIR RESEARCH WORKS ON ATOMIC AND MOLECULAR DATA.

AT PRESENT, WE ARE ENGAGED IN SEVERAL TOPICS SUCH AS:

(1) THE ENERGY LEVELS AND THEIR WIDTHS OF ATOMS AND IONS;

(2) ELECTRON IMPACT EXCITATION AND IONIZATION;

(3) DIELECTRONIC RECOMBINATION PROCESS;

(4) ATOMIC (ION) PHOTOELECTRIC EFFECT;

(5) CHARGE EXCHANGE PROCESS

AND SO ON.

MEANWHILE, WE ARE ALSO ENGAGED IN RESEARCH OF THE METHODS OF THEORETICAL CALCULATIONS AND OF EXPERIMENTAL MEASURMENTS, WE ALSO DEVELOP COMPUTATIONAL SOFTWARES, CALCULATE DATA, DO SOME MEASURMENTS, EXTENSIVELY COLLECT AND COMPILE A+M DATA.

III. ACADEMIC EXCHANGES

CRAAMD WOULD LIKE TO SUPPORT AND DEVELOP ACADEMIC EXCHANGES IN A+M FIELDS. RECENTLY—FROM AUGUST 26 TO SEPTEMBER 1ST WE HELD AN ACADEMIC SYMPOSIUM ON A+M DARA OF THE WHOLE COUNTRY IN QINHUANGDAO (HE BEI). MORE THAN 100 PEAPLE ATTENDED THIS SYMPO SIUM. THE PAPERS RECEIVED IN THE CONFERENCE WERE MORE THAN 80. THESE PAPERS WERE DIVIDED INTO THREE CATEGORIES:

A. THEORETICAL CALCULATIONS;

B. EXPERIMENTAL MEASUREMENTS;

C. SELECTIONS AND COMPILATIONS.

THE FAMOUS SCHOLARS—PROF. LI. Z. W, PROF. GOU. Q. Q, PROF. LI. J. W. AND OTHERS GAVE THEIR REPORTS IN CONFERENCE. THE DIGEST OF THE ABSTRACTS OF CONTRIBUTED PAPERS HAVE BEEN PUBLI SHED IN CHINESE, BUT NOT IN ENGLISH.

IN THE INTERNATIONAL ASPECT, WE HAVE ALREADY INFORMED NDS OF IAEA THAT CRAAMD WAS FORMALLY ESTABLISHED. THEY MAILED US CIAMDA, 87 AND A+M NEWSLETTER IN THE MIDDLE OF THIS YEAR.AT THE SAME TIME, WE ALSO INFORMED INTERNATIONAL CODATA THAT CRAAMD WAS ESTABLISHED.

WE WOULD LIKE TO ESTABLISH VOCATIONAL RELATIONS WITH ALL OF THE A+M RESEATCH CENTERS IN THE WORLD, AND TO TAKE PART IN THE INTERNATIONAL COOPERATIONS IN THIS AREA.

THE STUDY ON ATOMIC COLLISION IN SOLID*

Yang Baifanf, Hao Shizho, Miao Jingwe,
Jiang Zengxue and Shi Miangong

Institute of Nuclear Science and Technolog,
Sichuan University, Chengdu, China

ABSTRACT

It is the pourpose of this paper to review our group's recent works and present experimental results. These are high-resolution Coulomb explosion measurements, the transmission of molecular ions of H_2^+, D_2^+ and DH^+ passing through carbon foils and the yields of the H^-, D^- and He^- negative ions by H^+, D^+, H_2^+, D_2^+ and He^+ ions in carbon foils, respectively.

I. INTRODUCTION

Atomic collision with solid is a complex process. We look on it as the charge exchange process and velocity variation process based on experimental facts[1-4]. When high speed particle enteres into a foil, it rapidly losses many of it's electrons or capture target electrons in sudden violent collisions with target electrons. The projectile then undergoes a so-called "Coulomb explosion" as the now highly charged and monoatomic fragments repel one another apart via their mutual Coulomb forces[5] in the foil. For other entrance ion which have not any bounding electron, the electron capture will result in the bounding states as soon as it enters the foil. In the foil, the particle will either lose it's bounding electron or capture target electron in atomic collision. But in the next collision, the loss probability always larger than the capture's. At high nucleon speed the $\sigma_l >> \sigma_c$, the σ_l and σ_c are the cross sections of electron loss and electron capture respectively. So the electron loss are rapidly but the bounding states are reform little by little. The charge exchange process is a dynamic equilibrium process in beam-foil interaction from beginning to end. Except this process, both particle speed and it's moving direction will vary with collisions in every time. It will leads to energy loss and scattering of the projectile; while some target atoms will ionizd, excited, scattered or polarized in collisions. So the atomic collision process is also such process that fast ions are slowed down and scattered. In a very thin foil, the number of collisions is so few that the variation of the speed is very small. We can neglect it and only counsider the charge exchange process. Every emerge yields are resulted from the competition between the electron loss and the electron capture in the foil, while the Coulomb explosion is a particular phenomenon for molecular ions.

---

*THE PROJECTS SUPPORTED BY NATIONAL NATURAL SCIENCE FOUNDATION

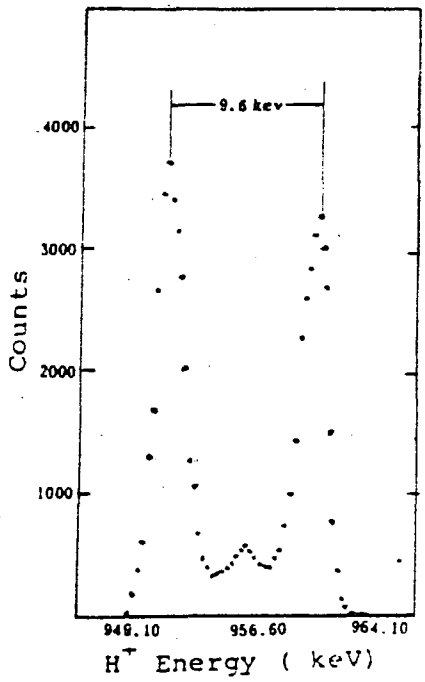

Fig. 1. Energy distribution of emergent H^+ fragments in the direction of the initial 1.915 MeV H_2^+ beam passing a ~3 $\mu g/cm^2$ carbon foil

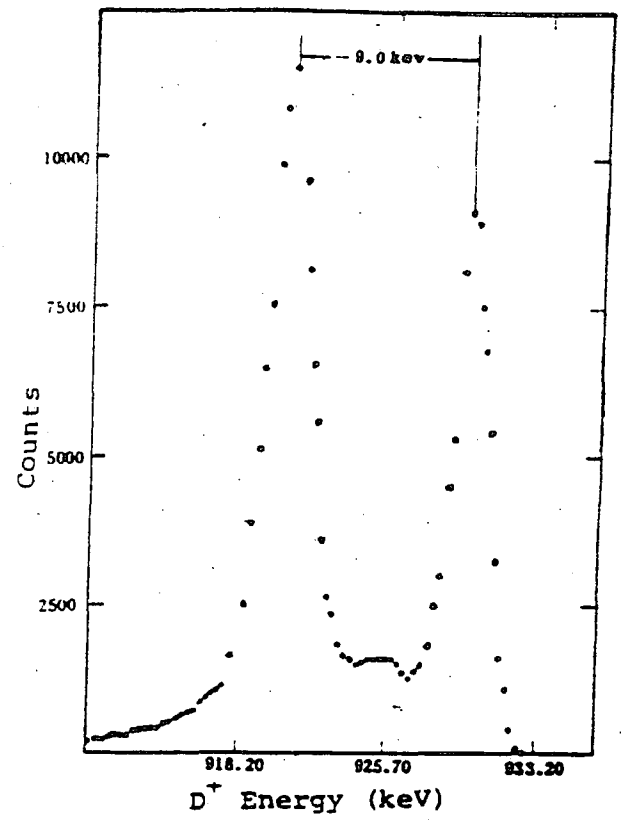

Fig. 2. The same as fig. 2 but for D^+ from 1.850 MeV D_2^+.

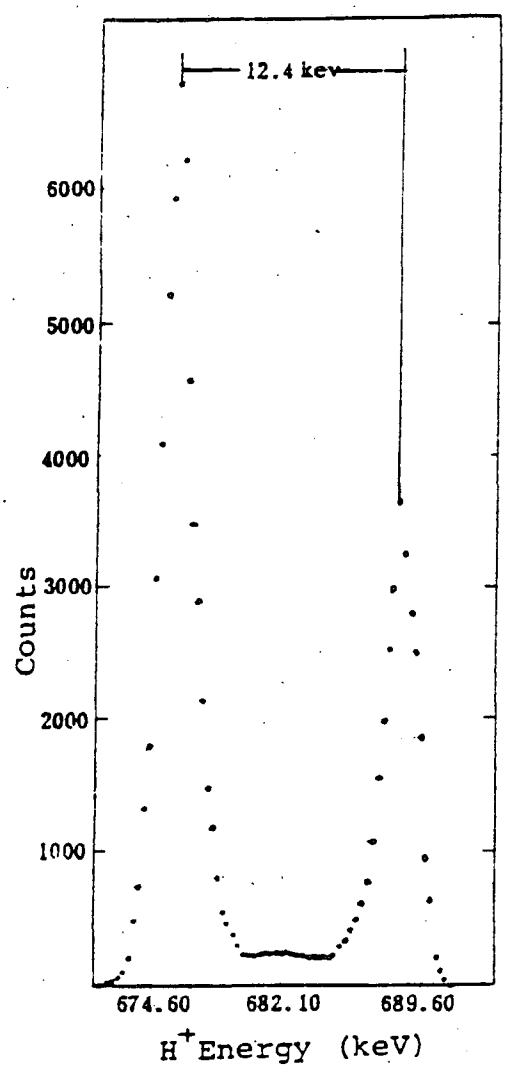

Fig. 3. The same as in fig. 2 but for H^+ from 2.060 MeV H_3^+

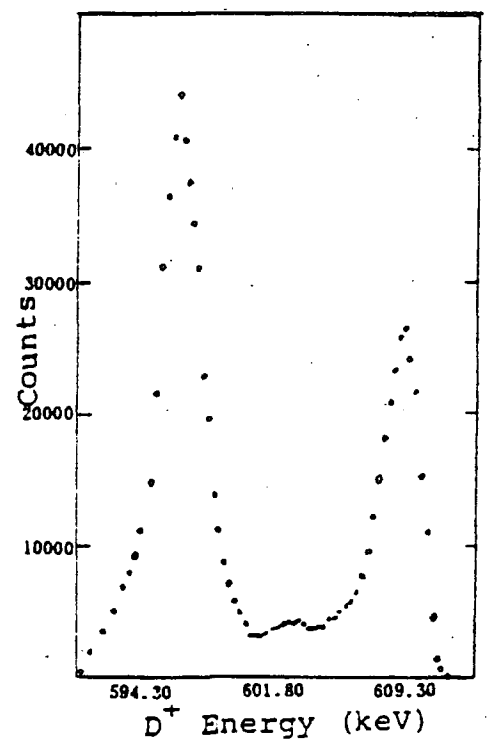

Fig. 4. The same as fig. 2 but for D^+ from 1.823 MeV D_3^+.

II. THE RESULTS OF COULOMB EXPLOSION MEASUREMENT

The coulomb explosion results in energy shifts of a few kev and angular shifts of a few mrad for the dissociation fragments. High resolution measurments of the energy distributions for these fragments offer promising possibilities for deducing the incident beam. Measured energy distribution of atomic fragments emerging co-linearly with the incident beam from the foil are shown in fig.1-4 respectively for 1.915Mev H_2^+, 1.850Mev D_2^+, 2.060Mev H_3^+ and 1.823Mev D_3^+ molcular ions. The two-peak feature in the 0° spectrum for H_3^+ is a signature of its triangular structure[6]. The same is observed for the deuterated case of D_3^+. For both the diatomic and triangular triatomic cases, the energy separation ΔE between the leading and trailing peaks is the consequence of Coulomb explosion following foil passage. The mean internuclear separation $\langle r \rangle$ of the molecular ion prior to breaking up can be obtained from ΔE. We neglect the very small corrections due to the effect of wake, differnce in the energy lost, and multiple scattering. The $\langle r \rangle$ so deduced are listed in table 1 together with the corresponding predicted g.s. values ro[7].

III. THE TRANSMISSION YIELDS OF FAST IONS

The transmission yields of H_2^+, D_2^+ and DH^+ passing through carbon foils have been measured over a range of foil thickness for 1.61Mev H_2^+, 1.5 and 1.8Mev D_2^+ and 1.8Mev DH^+ projectiles, separately. Fig.5 shown these results vary with td. The dashed lines are deduced from the expressions of the σ_i^{BS} and σ_c^{BS} [1], they are larger than corresponding observed results at same V1 separately. It may be caused by larger σ_c^{BS} or less σ_i^{BS}. The molecular ions transmitted through thin foil exhibit a strong dependnce on the velocity V1 in Bohr speed V0. Such a feature can only be reasonnably understood in terms of reconstitution process of the target electrons captured after the loss of electrons of the incident particles.

IV. THE RESULTS OF NEGATIVE IONS YIELDS

The forming process of negative ions H^- and D^- in a foil was analysed from the point of view of the charge exchange. Recently we deduced the negative ion yield ϕ^- as follows:

$$\phi^-(td)=[\sigma_c/(\sigma_c+\sigma_i)]^3/3$$

It proves that the ϕ^- depend on both σ_c and σ_i and without relation to td. This conclusion is consistent with our results. It is enough to prove that most of the emerging negative ions are produced within the rear surface of the foil.

The results of both ϕ_a^- and ϕ_m^- for various bombarding ions at various velocities are listed in table 2. The H^- and D^- yields versus td are shown in fig.6 for ϕ_a^- and fig.7 for ϕ_m^- separately. It is worth noting that ϕ_m^- depend on td at same V1 and tend to a maximum value at larger td. In fig.8 the dependence of these yields on V1 is shown. The closed circles and triagles marked ϕ_a^- and max ϕ_m^- in this figure, respectively. The ϕ^- can be deduced by the expressions of σ_i^{BS} and σ_c^{BS}, it is shown as curve a) in fig.8. These value are larger than the observed results. The reson might be that either σ_c^{BS} is larger or σ_i^{BS} is smaller. From the measured results, we had got the

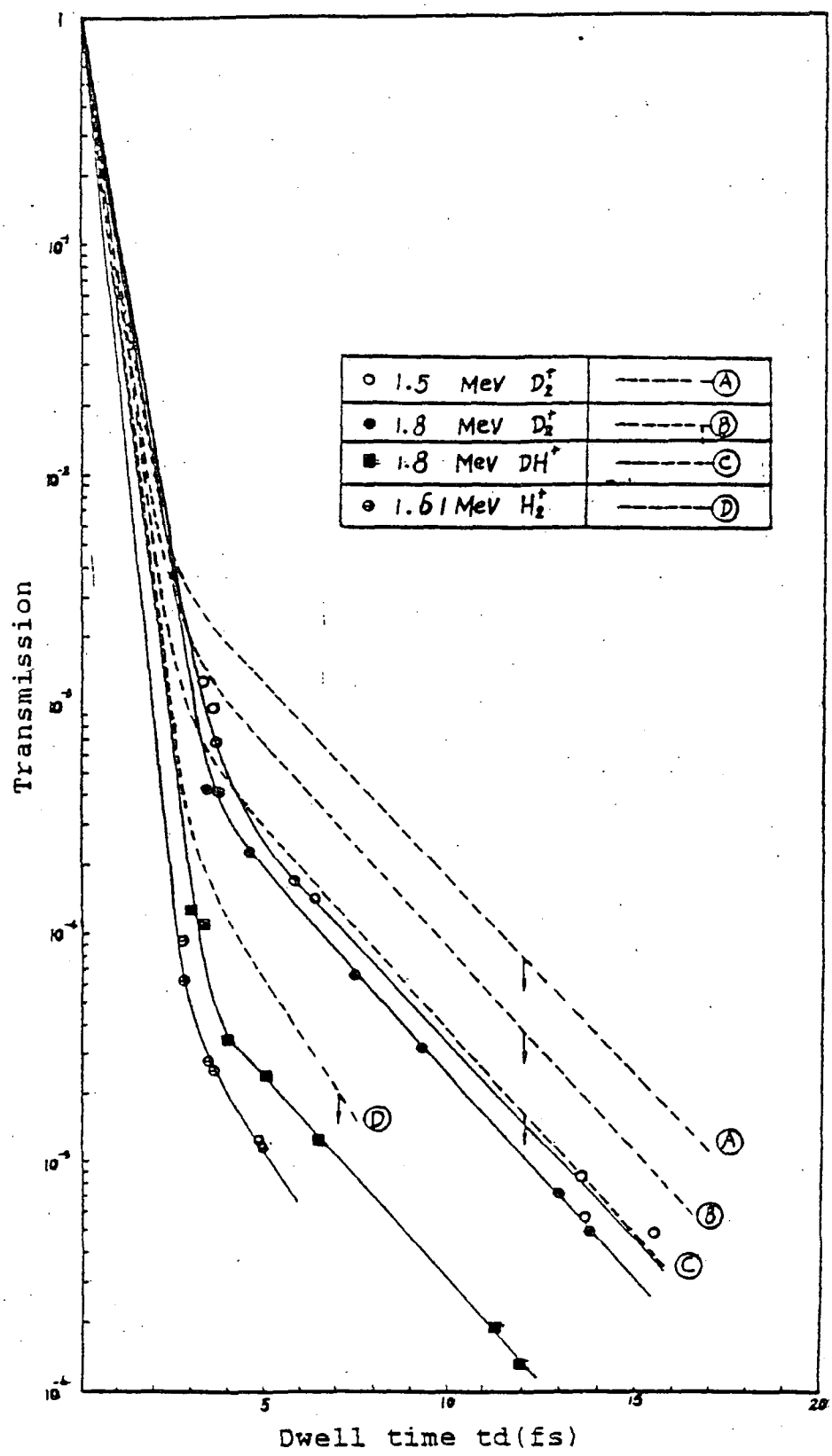

Fig.5.The transmissions of the D_2^+, DH^+ and H_2^+ passing through carbon foils.

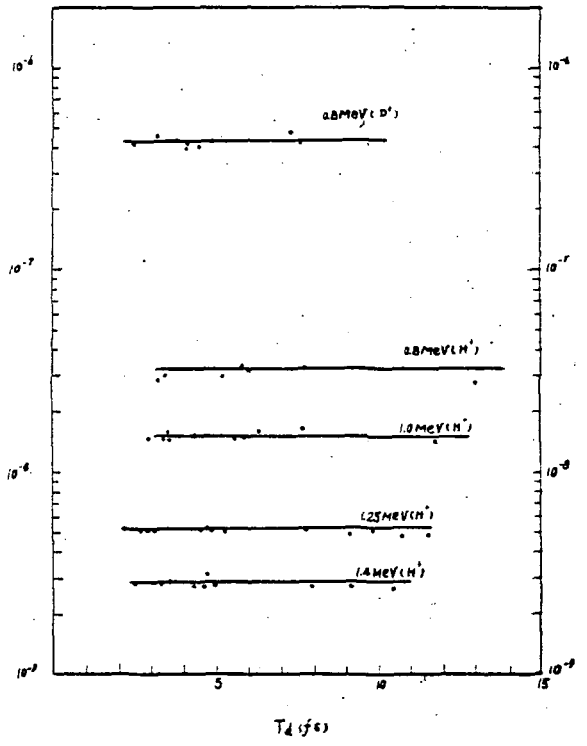

Fig.6. The curves of $\bar{\phi}a$ vary with td.

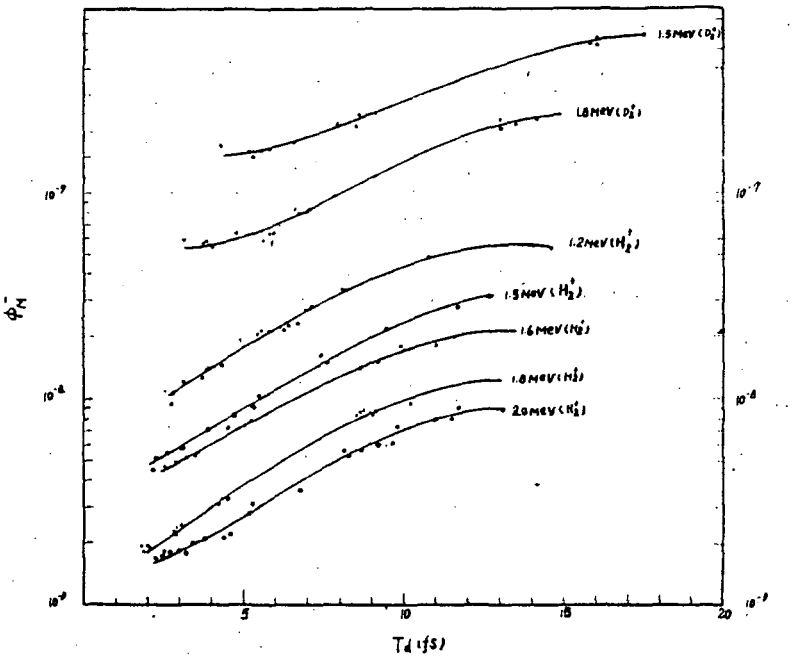

Fig.7. The curves of $\bar{\phi}m$ vary with td.

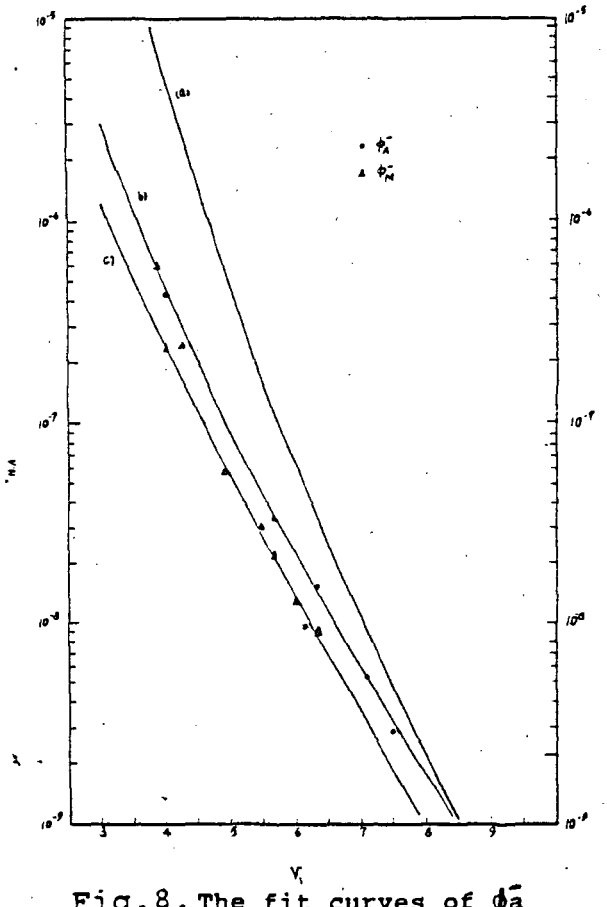

Fig.8. The fit curves of $\bar{\phi}a$ and $\bar{\phi}m$ vary with V1.

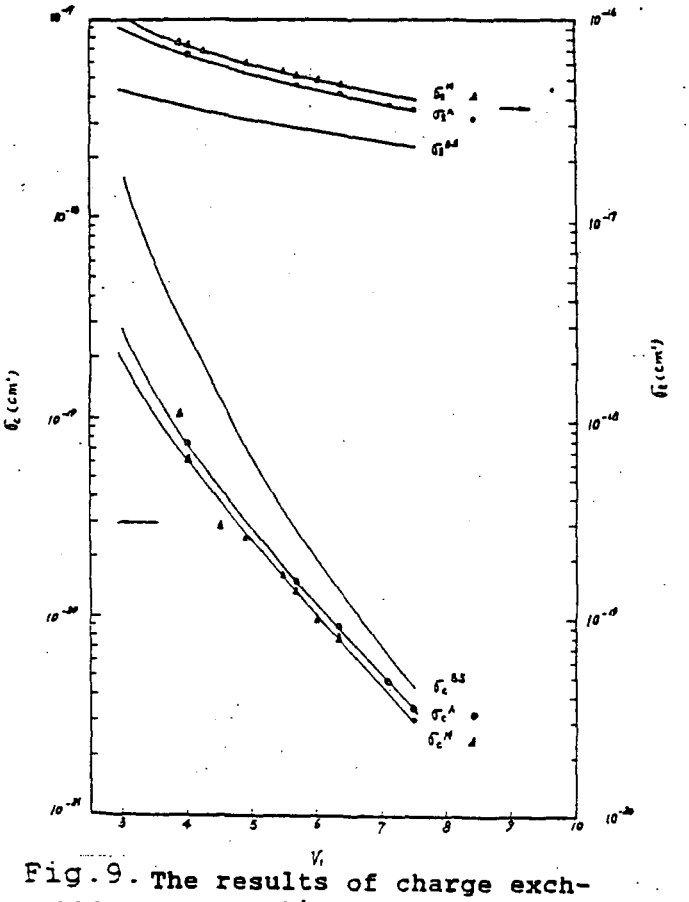

Fig.9. The results of charge exchange cross sections vary with V1.

Table 1. Internuclear separations of hydrogen molecular ions in anstroms

	Expt.	Theo.(g.s.)
H_2^+	1.19+0.03	1.052
D_2^+	1.32+0.03	1.056
H_3^+	0.98+0.02	0.873
D_3^+	0.93+0.02	--

Table 2. The results of ϕ_a^- and ϕ_m^- at various velocities.

ions	V1 in V0	ϕ_a^- $\times 10^{-7}$	ϕ_m^- $\times 10^{-7}$	note
D^+	4.00	4.3		0.8 Mev $D^+ \to D^-$
H^+	5.66	0.32		0.8 -- $H^+ \to H^-$
H^+	6.33	0.15		1.0 -- $H^+ \to H^-$
H^+	7.07	0.052		1.25-- $H^+ \to H^-$
H^+	7.49	0.028		1.4 -- $H^+ \to H^-$
D_2^+	3.87		6.0	1.5 -- $D_2^+ \to D^-$
H_2^+	4.00		2.3	0.8 -- $H_2^+ \to H^-$
D_2^+	4.24		2.4	1.8 -- $D_2^+ \to D^-$
H_2^+	4.90		0.56	1.2 -- $H_2^+ \to H^-$
DH^+	4.90		0.56	1.8 -- $DH^+ \to D^-$
H_2^+	5.48		0.30	1.5 -- $H_2^+ \to H^-$
H_2^+	5.66		0.21	1.6 -- $H_2^+ \to H^-$
H_2^+	6.00		0.125	1.8 -- $H_2^+ \to H^-$
H_2^+	6.33		0.090	2.0 -- $H_2^+ \to H^-$

Table 3. The results of charge exchange cross sections

V1 inV0	σ_1^A $\times 10^{-17}cm^2$	σ_c^A $\times 10^{-20}cm^2$	σ_1^M $\times 10^{-17}cm^2$	σ_c^M $\times 10^{-20}cm^2$	σ_1^{BS} $\times 10^{-17}cm^2$	σ_c^{BS} $\times 10^{-20}cm^2$
3.87			7.75	10.4	3.76	32.9
4.00	6.66	7.57	7.50	6.23	3.68	26.7
4.24			7.07	2.94	3.55	18.5
4.90			6.12	2.51	3.23	7.35
4.90			6.12	2.46		
5.48			5.47	1.64	2.98	3.56
5.66	4.71	1.46	5.30	1.33	2.91	3.56
6.00			5.00	0.968	2.79	1.96
6.33	4.21	0.893	4.74	0.778	2.68	1.37
7.07	3.77	0.471			2.46	0.648
7.49	3.56	0.326			2.34	0.435

curves b) for ϕ_a^- and c) for ϕ_m^- in fig.8, respectively.The bounding electron lifetime for the atomic and molecular ions are 0.207fs and 0.186fs,respectively.In other words,the cluster loses it's bounding electrons more easily than the atom does.It means that the charge exchange of molecular cluster is evidently different from one of atomic ion.

From the curve fits of ϕ_a^- and ϕ_m^-,we can get the cross sections of the charge exchange.These cross sections are plotted against V1 in fig.9.The closed circles and triangles marked the σ_1^{A},c and σ_1^{M},c respectively.The curves of the σ_c^{BS} and σ_1^{BS} are also shown in the same figure.From the figurs it could be seen that the $\sigma_1^{A,M} > \sigma_1^{BS}$ and $\sigma_c^{A,M} < \sigma_c^{BS}$ and that the measured cross sections fall on the corresponding fitting curves fairly well.

The He yields obtained is 9.5×10^{-9} and the maximum $H\mathring{e}$ yield is larger than 1.4×10^{-5} at 0.45 Mev/amu,but the D^-yield is 2.4×10^{-7}at the same V1.According to above stated the $H\mathring{e}$ or $H\bar{e}$ yields are result from the He^{++} ion capture two or three target electrons formed, repectively.So the $H\mathring{e}$ yield must be as much as the D^-'s and the $H\bar{e}$ yield must be less than the D^-'s by several orders of magnitude at the same V1.But our results shown contrary to all expectation.In order to explain the charge exchange of He^+ in foil,perhaps it is neccessary to consider the atomic structure and use different expressions of σ_c and σ_1 under different situations of electron loss and electron capture.

V.CONCLUSION

We studied the process of atomic collision and think of this is a charge exchange process and a velocity variation process.The mean value of internuclear separations were extracted as 1.19,1.32,0.98 and 0.93 angstroms respectively for H_2^+ ,D_2^+ ,H_3^+ and D_3^+ .The expression for the yields of negative ions was deduced.Some transmission of molecular ions in foils and yields of negative ions were obtained.

REFERENCES

1.M.J.Gaillard,et al,Phys.Rev.,A16,No.3,2323(1977)
2.N.Cue,et al,Phys.Rev.Letters,45,613(1980)
3.Yang Beifang,et al.Journal of Sichuan University Natural Science Edition,No.3,51(1984)
4.Miao Jingwei,et al,Jounal of Atomic and Molecular Physics,Vol.1,No.1,27(1984)
5.D.S.Gemmell,Chem.Rev.,80,301(1980)
6.M.J.Gaillard,et al,Phys.Rev.,A17,1797(1980)
7.Miao Jingwei,et al,N.I.M.,B13,181(1986)

CINDA ENTRY FOR CHINESE REPORT ON 16TH INDC MEETING

(ELEMENTS)	Quantity	Energy(eV) Min	Energy(eV) Max	Lab	Type		Documentation Ref	Vol	Page	Date	Author, comments	Data
		1.5+7	1.8+7									
$_{38}Sr^{87}$, $_{45}Rh^{103}$	Inelastic	2.0+6	6.0+6	FUD	Exp	Rept	INDC(CPR)-?			Oct.87	Wu+ ACTIVITION,TO ISOM. STA.	+
$_{49}In^{115}$, $_{49}I^{113}$	(n,2n)	"		"	"	"	"			"	"	+
$_{20}Ca$	Evaluation	1.0-5	20.+7	BJG	Eval	"	"			"	Tang+ FOR CENDL-1	+
$_{98}Cf^{252}$	Spect Fiss n			BJG	Exp	"	"			"	" TOF, PRIMARY	
$_{6}C^{12}$	Inelastic γ	1.5+7		BNU	"	"	"			"	Zhou+ 4.43MEV GAMMA,DIFF CS	+
$_{23}V^{51}$	Noelastic γ	1.5+7		"	"	"	"			"	Yan+ GAMMA SPECT. DIFF CS	+
$_{41}Nb^{93}$	"	"		"	"	"	"			"	Zhou+ " " "	+
$_{42}Mo$	Diff Elastic	1.42+7		SIU	"	"	"			"	Cao+ TOF 5-150 DEG	+
$_{41}Nb$	"	"		"	"	"	"			"	" " 45-150 DEG	+
$_{74}W$	"	1.47+7		"	"	"	"			"	" " "	+
$_{28}Ni$	"	1.0+6		"	"	"	"			"	Li+ " 20-150 DEG	+

CINDA ENTRY FOR CHINESE REPORT ON 16TH INDC MEETING

(ELEMENTS)	Quantity	Energy(eV) Min	Max	Lab	Type		Documentation Ref Vol Page	Date	Author, comments	Data
$_{41}Nb^{93}$, $_{69}Tm^{168}$, $_{73}Ta^{181}$	(n,γ)	1.0+4	1.0+5	SIU	Exp	Rept	INDCC(CPR)-?	Oct.87	Xia+ MOXON-RAE DET.STAN. AU	+
$_{92}U^{238}$	n Emission	1.42+7		IAE	"	"	"	"	Shen+ DOUBLE DIFF. 13 ANGLES	+
$_{49}In^{115}$, $_{49}I^{113}$	Tot Inelastic	1.37+7	1.48+7	"	"	"	"	"	Lu+ ACTIVITION	+
$_{98}Cf^{252}$	Fiss Yield	Spont		"	"	"	"	"	Li+ 44 MASS CHAINS MEASURED	+
$_{92}U^{238}$	"	8.3+6		"	"	"	"	"	Li+ 51 MASS CHAINS MEASURED	+
$_{92}U^{235}$	"	Fiss		"	"	"	"	"	Li+ 43 MASS CHAINS MEASURED	+
$_{92}U^{235}$	Fiss Spectra	Maxwl		"	"	"	"	"	Wang+ PROM.SPECTRA,0.6-16 MEV	+
$_{83}Bi^{209}$	(γ,n)			"	"	"	"	"	Ye GAMMA FROM THER.NEUTRON CAPTURE	+

CINDA ENTRY FOR CHINESE REPORT ON 16TH INDC MEETING

(ELEMENTS)	Quantity	Energy(eV) Min	Max	Lab	Type		Documentation Ref	Vol	Page	Date	Author, comments	Data
$_{92}U$, $_{82}Pb$, $_{26}Fe$, $_{13}Al$, $_{6}C$, $_{4}Be$	Diff Elastic	1.47+7		SIU	Exp	Rept	INDC(CPR)-?			Oct. 87	Cao+ POSITION SEN.DET.SMALL ANGLE 2.7 - 9.9 DEG	+
$_{13}Al$, $_{22}Ti$, $_{26}Fe$, $_{29}Cu$, $_{42}Mo$, $_{48}Cd$, $_{74}W$, $_{82}Pb$, $_{83}Bi$, $_{92}U^{238}$	"	1.42+7		"	"	"	"			"	Ma+ TOF,SMALL ANGLE 1.7-25 DEG	+
$_{69}Tm^{169}$, $_{73}Ta^{181}$	(n,γ)	1.0+6	1.5+6	"	"	"	"			"	Xu+ TOF,LIGUID SCIN.,STAN. AU	+
$_{74}W$, $_{64}Gd$	(n,γ)	5.6+5	1.61+6	"	"	"	"			"	Xiang+ TOF,LIGUID SCIN., STAN. AU	+
$_{65}Tb$, $_{72}Hf$	(n,γ)	8.0+5	1.60+6	"	"	"	"			"	Mu+ TOF,LIGUID SCIN., STAN. AU	+
$_{60}Nd$, $_{62}Sm$, $_{66}Dy$, $_{70}Yb$	(n,γ)	3.4+5	1.68+6	"	"	"	"			"	Li+ TOF,LIGUID SCIN.,STAN. AU	+